STABILITY AND ROBUSTNESS OF ADAPTIVE CONTROLLERS FOR UNDERACTUATED LAGRANGIAN SYSTEMS AND ROBOTIC NETWORKS

BY

KIM-DOANG NGUYEN

DISSERTATION

Submitted in partial fulfillment of the requirements
for the degree of Doctor of Philosophy in Mechanical Engineering
in the Graduate College of the
University of Illinois at Urbana-Champaign, 2015

Urbana, Illinois

Doctoral Committee:

Professor Harry Dankowicz, Chair
Professor Andrew Alleyne
Professor Daniel Liberzon
Professor Sri Namachchivaya

ABSTRACT

This dissertation studies the stability and robustness of an adaptive control framework for underactuated Lagrangian systems and robotic networks. In particular, an adaptive control framework is designed for a manipulator, which operates on an underactuated dynamic platform. The framework promotes the use of a filter in the control input to improve the system robustness. The characteristics of the controller are represented by two decoupled indicators. First, the adaptive gain determines the rate of adaptation, as well as the deviation between the adaptive control system and a nonadaptive reference system governing the ideal response. Second, the filter bandwidth determines the tracking performance, as well as the system robustness. The ability of the control scheme to tolerate time delay in the control loop, which is an indicator of robustness, is explored using numerical simulations, estimation of the time-delay margin of an equivalent linear, time-invariant system, and parameter continuation for Hopf bifurcation analysis.

This dissertation also performs theoretical study of the delay robustness of the control framework. The analysis shows that the controller has a positive lower bound for the time-delay margin by exploring a number of properties of delay systems, especially the continuity of their solutions in the delay, uniformly in time. In particular, if the input delay is below the lower bound, then the state and control input of the closed-loop system follow those of a nonadaptive, robust reference system closely. A method for computing the lower bound for the delay robustness using a Padé approximant is proposed. The results show that the minimum delay that destabilizes the system, which may also be estimated by forward simulation, is always larger than the value computed by the proposed method.

The control framework is extended to the synchronization and consensus of networked manipulators operating on an underactuated dynamic platform in the presence of communication delays. The theoretical analysis based on input-output maps of functional differential equations shows that the adaptive control system's behavior matches closely that of a nonadaptive reference system. The tracking-synchronization objective is achieved despite the effects of communication delays and unknown dynamics of the platform. When there is no desired trajectory common to the networked manipulators, a modified controller drives all

robots to a consensus configuration. A further modification is proposed that allows for the control of the constant and time-varying consensus values using a leader-follower scheme. Simulation results illustrate the performance of the proposed control algorithms.

To my parents, my wife and my brother for their love and support

ACKNOWLEDGMENTS

The research presented in this dissertation has benefited enormously from the guidance and mentoring of my advisor, Professor Harry Dankowicz. I am deeply grateful for his numerous insightful comments, suggestions and feedback throughout my years at UIUC. This dissertation would not have been possible without his encouragement and boundless patience.

I would like to thank Professor Naira Hovakimyan for introducing me to $\mathcal{L}_1$ adaptive control. She was a co-investigator on a NASA sub-award that supported a part of this work. She also co-authored an ASME conference paper with Professor Dankowicz and me. Her advice during the early stages of my study was important and valuable in shaping this research. I am also thankful for informative discussions with Ronald Choe, Dr. Evgeny Kharisov, Yang Li, Mohammad Naghnaeian and Dr. Enric Xargay on various topics in control theory.

I would like to express my gratitude to Professor Andrew Alleyne, Professor Sri Namachchivaya and Professor Daniel Liberzon for their helpful suggestions and for serving on my dissertation committee. Professor Alleyne's insights into the practical application of control theory and performance constraints, the training I received from Professor Liberzon in adaptive control and switching systems, and Professor Namachchivaya's expertise in dynamical systems and bifurcation theory were valuable in the development of this dissertation.

For this work, I thankfully acknowledge financial support from

- A Vietnam Education Foundation fellowship,
- National Aeronautics and Space Administration through an SBIR Phase I contract, order no. NNX12CE97P, awarded to CU Aerospace, L.L.C.,
- National Robotics Initiative Competitive Grant no. 2014-67021-22109 from the USDA National Institute of Food and Agriculture,
- Teaching assistantships from the Department of Mechanical Science and Engineering, UIUC.

I thank my fellow labmates in the Applied Dynamics Laboratory, my classmates and teachers at UIUC. They not only enriched my understanding of dynamical systems and control theory, but also made my graduate school experience more enjoyable.

Finally, I am profoundly grateful to my parents, my wife and my brother, for their unbounded love and support, and for caring so much. My wife, Trinh, has been my best friend and a great companion during this incredible journey. I dedicate this dissertation to them.

TABLE OF CONTENTS

LIST OF TABLES

LIST OF FIGURES

LIST OF ABBREVIATIONS

DDE	Delay Differential Equation
DOF	Degree Of Freedom
LTI	Linear, Time-Invariant
MIMO	Multi-Input-Multi-Output
MRAC	Model Reference Adaptive Controller
ODE	Ordinary Differential Equation
RMSD	Root-Mean-Square Deviation Percentage
SISO	Single-Input-Single-Output

CHAPTER 1

INTRODUCTION AND MOTIVATION

1.1 Context

Robotic technology has revolutionized every corner of industry. While robots are widely used in well structured and static workspaces, for example in assembly and manufacturing tasks, they have also recently been employed in more challenging environments such as space, underwater, offshore and agriculture applications. In space missions, manipulators are mounted on a base that is floating freely in space (therefore the term free-floating manipulators). They serve to perform repair operations, inspection, construction of structures and scientific experiments. They are also used to orient telescope and communication devices or to collect debris [35]. Ground-based mobile manipulators have a growing range of applications that include planetary exploration such as the Mars rovers, rescue missions, deactivation of explosive devices, and removal of hazardous materials [81, 145]. Offshore and underwater platforms have become new application territories for robotic technology, especially in rapidly-changing and challenging environments. Example tasks include moving loads, performing maintenance, assisting with construction, as well as other unmanned tasks on ships, seaborne platforms, and underwater vehicles [41, 85, 88, 118].

On of the motivating contexts of this dissertation is the application of robotics to agriculture. This field has only recently attracted attention as an opportunity for robotic, autonomous mechanization aiming to improve productivity or to perform unmanned tasks in challenging environments [14]. Extensive reviews of systems for guidance of autonomous

[1]Certain parts in this chapter is taken from [101] and [102] with the permission from the publisher.

agricultural vehicles can be found in the recent literature [17, 21, 144]. Robotic manipulation systems for harvesting various types of fruits and vegetables have been described in [11, 33, 37, 50, 51],[53]–[58],[65, 123, 125, 149]. Similar principles have been applied for deleafing [56], for automating general orchard work [95], and for milking [92, 115]. Autonomous mobile robots have also been used for agricultural inspection. Robotic inspection systems are usually composed of cameras or sensors handled by a manipulator operating on a vehicle. For example, mobile robots carrying vision systems that are capable of accurately discriminating weeds from crops are reviewed in [129]. Other robots use imaging systems or sensors for detecting plant water stress [66] and calcium deficiency in lettuce [133], as well as for monitoring water [46] and measuring moisture [52]. Robotic sprayers are usually used to take actions following the results of inspection. For instance, robots have been designed to direct nozzles to spray detected weeds [13, 70, 73].

Unlike traditional application territories of robotic technology, such as manufacturing, production, assembly, and transportation, there are significant technical challenges that prevent robotics from being more pervasive in such an essential industry as agriculture. Among these, irregularly shaped fields with random obstacles; variable row spacing, orientation, and size between fields and between crops; and uneven terrain with varying soil conditions pose barriers to the deployment of robotic technologies. Such operating conditions are a significant challenge for robotic manipulation, since most current control architectures assume mounting on stationary platforms, or highly accurate model representations of the robotic system, including the platform dynamics in the case of mounting on moving vehicles. The next section reviews the state of the art in control of moving-base manipulators as well as the outstanding challenges in this area of research.

1.2 Control of Robots Operating on a Dynamic Platform

Robot manipulators have long been considered as testbeds for research in nonlinear control theory. Early work on adaptive control of fixed-base manipulators was mostly based on model-reference adaptive-control architectures [32, 60, 105], the linear-in-parameter property of dynamic structure [28, 112, 130] and the passivity of rigid robot dynamics [15, 107, 113]. Under relevant assumptions on the robots' dynamic properties, these control strategies were demonstrated to estimate certain types of unknown model parameters successfully and achieve desired performance.

The extension of these classical control schemes to the context of a manipulator installed on a dynamic platform, however, is challenging and still an ongoing research area. When the actuators driving certain degrees of freedom of the robotic systems in the aforementioned scenarios are turned off, the robotic systems become underactuated. In addition, the dynamics of the manipulator and the platform are mutually coupled due to conservation of momentum. This adds tremendous challenges as compared with fixed-based manipulators [120]. Firstly, the equations of motion for the unactuated degrees of freedom now act as constraints on the control design. As these are intrinsically nonholonomic, it is not possible to solve for the underactuated states in terms of the controlled states. Consequently, model-reduction methods fail to reduce the system's dimension [111]. Moreover, according to Brockett's theorem [19], it is impossible to asymptotically stabilize a nonholonomic system to an equilibrium point by a continuous and time-invariant state-feedback control law, despite its controllability. Secondly, with complicated platform structures, or unknown terrain geometries in the case of mobile manipulators, or in challenging environments, including manipulators operating on ships and offshore platforms in high sea states, the platform dynamics are usually unmodeled and add large inertial terms and disturbances to the description of the manipulator dynamics. Example control designs include switching schemes based on support-vector-machine regression [77], a combination of fuzzy and backstepping control [150], adaptive control based on estimation of a bounded parameterization of the

unknown dynamics [78, 146], and adaptive variable structure control [89].

The most popular methods for controlling underactuated moving-base manipulators involve adopting the adaptive-control frameworks for fixed-base manipulators. Recent examples of control schemes in this category for free-floating space manipulators include [114] which constructs a dynamically equivalent model for parameterization and control of the original system dynamics, [137] which assumes passivity and other structure properties to eliminate the need for measuring the platform acceleration, [3] which proposes an adaptive controller based on the reaction dynamics between the active and passive parts in the system, and [138] which combines a recursive formulation of control torque and the platform's reference velocity and acceleration to achieve desirable tracking performance. For mobile manipulators, work in [23] designs an interaction control scheme, which is composed of an adaptation algorithm and an input-output linearizing controller. A trajectory and force tracking control problem is addressed in [30], which presents an adaptive controller based on a suitably reduced dynamic model to control a model with some unknown inertia parameters.

Work in [91] employs a Frenét-like description to transform the kinematics of nonholonomic mobile platforms to generic driftless dynamics, which are then stabilized by two control schemes for the kinematics and dynamics, respectively. In the presence of disturbances, [18] combines a regressor-based adaptive scheme with an estimator for the disturbance to improve tracking performance of mobile manipulators. Work in [4] develops an image-based visual controller for mobile manipulators to track objects in three-dimensional space. The adaptive laws are designed based on the assumption that the robot dynamics can be parameterized linearly in terms of the unknown parameters in the model. In the context of marine robotics, an adaptive controller that assumes passivity in the robot structure and an adaptive-sliding control scheme are presented in [38] to compensate for model uncertainties. The analysis in [7, 8] decomposes the system dynamics into control elements of individual bodies to derive a modular controller for manipulators mounted to an underwater vehicle. The control scheme in [62] allows underwater vehicle-manipulator systems to track both a prescribed sub-region

as well as uncertain tasks.

The existing adaptive-control algorithms reviewed here rely on the *linear-in-parameter property* of Lagrangian systems. Specifically, they exploit the dynamic structure and the passivity of rigid robot dynamics to factor the model description in terms of a regression matrix and a vector of unknown parameters, and proceed to implement adaptive laws to estimate these parameters. While the linear-in-parameter property is an acceptable model parameterization for many fixed-based manipulators, it is not applicable to others, such as robots with complicated link and/or joint geometries, unknown lengths, or with nonlinear mass distribution, stiffness, or damping. Furthermore, these controllers require construction of a well-defined and complicated model regression matrix, which involves correct selection of the coefficient matrix of the joint velocity from among several options [36]. The use of the model regression matrix, which must contain no uncertainty, also implies high dependence of the control algorithms on system modeling.

In moving-base manipulators, the reliance on the linear-in-parameter property may further undermine system performance. Firstly, accurate modeling of the platform dynamics is much more challenging than modeling the manipulator. Platforms are often complex structures with many uncalibrated parameters and uncertainties. In addition, moving-platform robots often operate in challenging environments such as outer space, underwater, offshore, across uneven terrains, or on ships operating in high seas [41]–[44], [67, 85]. Even when the ship stands still, modeling of the ship's structure is a very difficult task. Capturing the inputs to the ship's equation of motion due to the influence of waves, ocean currents, and wind is even more challenging, if not impossible. The treatment in [41] avoids these problems by assuming that the oscillations of the ship are known *a priori* for all time. This assumption is eliminated in [42, 44] by two intriguing methods for predicting the ship's motion, including an auto-regressive predictor and a predictor that superposes a series of sinusoidal waves. However, these methods require re-calibration of the parameters in the algorithms for different sea locations. In addition, the prediction accuracy can only be achieved with advanced sensors,

such as wave cameras and sensors that measure interaction forces on the ship from waves and wind [44]. Similarly, in the case of mobile manipulators, most adaptive controllers are formulated with the assumption that the robots are moving across perfectly even terrain.

The aforementioned challenges motivate the first main contribution of this dissertation. ***We design an adaptive controller which is independent of system modeling and can achieve desired tracking for manipulators that operate on an underactuated dynamic platform.*** The control scheme proposed here is inspired by the work in [61], which proposed the use of a filter in the control input of a reference model adaptive controller to improve the robustness of a linear single input system. The architecture decouples the estimation loop from the control loop to facilitate a significant increase in the rate of estimation and adaptation, without a corresponding loss of robustness.

This work develops a control scheme for an underactuated system consisting of a manipulator mounted on a moving platform with unmodeled dynamics. The proposed controller employs a fast adaptation scheme while maintaining bounded deviation from a nonadaptive reference system. In particular, the control design is tolerant of time delays in the control loop, and maintains clean control channels even in the presence of measurement noise due to the use of a low-pass filter structure in the control input. Tuning of the filter also allows for shaping the nominal response and enhancing the delay robustness.

1.3 Delay robustness in robot control systems

Time delay is ubiquitous in many robotic systems, such as mobile robots [26, 128], unmanned and aerial vehicles [9, 75, 124], networked robots [87, 94, 109], robots in manufacturing [132, 47], and teleoperated robots [5, 74, 82]. Interestingly, as discussed in [39, 45, 63], any unmodeled dynamics can be equivalently represented by a delay in the plant input. In addition, small delays are sometimes injected voluntarily in the control laws to stabilize the plants, as well as to alleviate the effects of uncertain dynamics [64, 121, 147]. However, in

most systems, time delay in the control loop induces instability, and is resistant to many classical controllers [106].

In the presence of time delay, the closed-loop dynamical system is given by a delay differential equation (DDE), whose functional state evolves in a infinite dimensional function space, in contrast to the finite dimensional state of an ordinary differential equation (ODE). It is not a trivial exercise, and sometimes even impossible, to extend results from the analysis of ODEs to that of DDEs. In addition, it is well known that the behavior of solutions to a delay system can be much more complicated than the behavior of solutions to the same system with zero delay [48]. For example, the solution to a DDE around an equilibrium can be analyzed by its spectrum of its linearization, which includes an infinite number of eigenvalues, as compared to a finite number of eigenvalues for an ODE [40].

In linear, time-invariant (LTI) systems, the time-delay margin, a direct indicator of system robustness [59], can be computed from the linear frequency response. In nonlinear control systems, however, there is no general method for computing the time-delay margin, and robustness may be estimated, at best, on a case-by-case basis. In the case of the model-reference adaptive controller (MRAC) and its modifications, such analysis relies on the use of Lyapunov-Krasovskii functionals and Padé approximants. For example, in [31, 90, 104], it is shown that the time-delay margin of an MRAC system decays to zero as the adaptive gain goes to infinity. In contrast, a guaranteed positive time-delay margin for arbitrary large adaptive gain for adaptive control scheme proposed in [61] applied to an LTI plant was established in [20] via appropriately constructed LTI systems. The alternative approach in [98] proves the guaranteed robustness of a similarly designed control scheme. However, these studies are both restricted to linear plants.

The focus on delay robustness motivates the second main contribution of this dissertation. ***We establish a positive lower bound for the time-delay margin, which is independent of the adaptive gain, for an adaptive control scheme designed for systems with unknown nonlinearities and constant input-gain matrices.***

Furthermore, the analysis is extended to adaptive control systems with time-varying and nonlinear input-gain matrices.

1.4 Controlled Cooperation of networked robots

Cooperative control of networked manipulators has attracted much recent attention. The purpose of controlled synchronization is to achieve certain cooperation among a large group of robots. As an example, early work in [122] proposed a scheme to synchronize identical robots to track a shared desired trajectory using a nonlinear observer. This controller requires all-to-all interconnection of the robots. In addition, the nonlinear observer for estimating accelerations is formulated using a complete and accurate model of the robots.

An adaptive approach was proposed in [24, 25] for synchronizing Lagrangian systems using nonlinear estimators based on convergence results in contraction theories, see also [84, 117, 136]. When the common desired trajectory is unavailable, stability of the controlled system is achieved only if all systems are identical. In contrast with the previous cases which produce satisfactory performance with constant time delay, the control scheme in [1, 2] is able to synchronize a group of manipulators in the presence of time-varying communication delay. Robot synchronization is also addressed in [83] in the presence of interaction forces on the mechanical systems from a human operator. Such cooperative control scenarios were extended to task space in [80] using passivity-based approaches discussed in [22, 131, 148]. Work in [139, 140] studied the synchronization problem with uncertainties in both system dynamics and the Jacobian matrix. The controller was extended to drive the robots' angular velocities to their average value in [141], and was designed to account for the case of communication delay in [142].

The adaptive control algorithms in the cited literature again rely on the linear-in-parameter property of Lagrangian systems. As stated previously, they parameterize a robot's dynamic structure as a product of a well-defined regression matrix and a vector of unknown pa-

rameters. For fixed-base manipulators, since these assumptions often apply, the unknown parameters can be estimated by appropriate adaptive laws.

In contrast, when manipulators are mounted on a dynamic platform, the geometry and mass distribution of the overall robot-and-platform system may be too complicated to accurately construct the regression matrices. In addition, uncertain large variations in the platform's inertial properties disturb the control system and are not modulated by the adaptive controllers. Examples include significant platform motions driven by unknown environmental factors, such as high sea states and wind and current conditions for manipulators operating on a ship or an offshore platform.

The absence in the literature of the development of adaptive controllers for networked moving-base manipulators motivates the third main contribution of this dissertation. ***We develop adaptive controllers for synchronization and consensus of a network of manipulators mounted on a dynamic platform in the presence of communication delays.*** The control scheme is independent of any detailed system modeling of the platform and the manipulators. The proposed controller is shown to have bounded estimation error and to make the networked system track a nonadaptive reference system closely. The synchronization objective is achieved despite the presence of communication delay, as well as unmodeled dynamics of the platform. When there is no common desired trajectory, the joint angles of all robots are driven to a consensus configuration. Moreover, the consensus values can be controlled via a leader-follower algorithm.

1.5 Timeline of development

A preliminary formulation of an adaptive controller for a robotic manipulator designed by following the $\mathcal{L}_1$ control architecture in [61] was first presented in [99] in August, 2013. Notably, in this first paper, the control law included explicit dependence on the mass matrix and, therefore, knowledge about the plant. In later work, this assumption was removed.

In particular, in a preliminary technical report [100], posted online in January 2014, we developed a control scheme, which does not depend explicitly on the plant. Notably, the theoretical proof of transient performance bounds still assumes known inertia matrix. A corrected proof was subsequently documented in a journal publication [102], which appeared online in November 2014. This paper extended the analysis to an arbitrary underactuated Lagrangian system. In this dissertation, we continue the analysis of an arbitrary underactuated Lagrangian system by establishing rigorously the delay robustness of the control formulation, independently of the adaptive gain, for bounded desired trajectories.

The control formalism was later applied to networks of robots in a conference paper [101], presented in September, 2014, showing again that stability and transient performance can be guaranteed with sufficiently large adaptive gain. In this dissertation, we establish the stability of the closed-loop system in the presence of communication delays, independently of the delay.

The paper in [12] by a different group of authors, to be presented at ICRA in May, 2015, has implemented the control scheme in [100] for a parallel kinematic manipulator. The controller is shown to outperform a proportional-derivative scheme.

1.6 Outline of the dissertation

Chapter 2 develops an adaptive controller for underactuated robotic systems with unmodeled dynamics. The control scheme is motivated by the applications of manipulators operating on dynamic platforms. The proposed formulation is tested in different trajectory-tracking scenarios: (i) a manipulator installed on a ship operating in a high-sea state with uncertain environmental disturbances and (ii) a mobile manipulator moving across a rough terrain of unknown geometry. The simulation results illustrate the tracking performance of the proposed control algorithm, its ability to deal with unmodeled dynamics, and its robustness to measurement noise and time delay, while maintaining smooth control signals. Other

than the introduction and conclusion, the content of this chapter is reproduced from the paper "Adaptive Control of Underactuated Robots with Unmodeled Dynamics," published in *Robotics and Autonomous Systems [102]*, and included here with permission from the publisher.

The ability of the control scheme to tolerate time delay in the control loop, which is an indicator of robustness, is demonstrated extensively in Chapter 3. An LTI system is established in order to derive a conservative lower bound on the critical time delay associated with a static reference input and in the limit of large estimation gains. In addition, a numerical method is proposed for quantifying the robustness against time delay of the system's response to a given static reference input based on techniques of parameter continuation. The content of this chapter is reproduced from the paper "Marginal stability in $\mathcal{L}_1$-adaptive control of manipulators" [99], published in the *Proceedings of the* 9^{th} *International Conference on Multibody Systems, Nonlinear Dynamics, and Control*, 2013, and included with permission from the publisher.

Chapter 4 studies the delay robustness of the adaptive control framework designed for a class of nonlinear systems with constant input-gain matrices. The analysis shows that this controller has a positive lower bound for the time-delay margin. In particular, if the input delay is below this lower bound, then the state and control input of the adaptive control system follow those of a nonadaptive, robust reference system closely. The analysis also suggests a way to compute this lower bound for the delay robustness using a Padé approximant. The material in this chapter is based on a journal manuscript submitted for review [103]. The analysis is generalized for a nonlinear system with time-varying and state-dependent input-gain matrix in Chapter 5. In comparison with Chapter 4, where the analysis mainly relies on the use of Laplace transforms, the analysis in Chapter 5 is based on input-output maps and deals with time-varying DDEs.

In Chapters 6 and 7, the control framework is extended to the context of cooperative control of networked manipulators operating on an underactuated dynamic platform in the

presence of communication delays. Analogously to the single manipulator case, the theoretical analysis based on input-output maps of functional differential equations shows that the adaptive control system's behavior matches closely that of a nonadaptive reference system. The tracking-synchronization objective is achieved despite the effects of communication delays and unknown dynamics of the platform. When there is no common desired trajectory, the modified controller drives all robots to a consensus configuration. In addition, a leader-follower scheme is proposed that allows for the control of the constant and time-varying consensus values. A special case, where there is no communication delay, of the work in Chapters 6 and 7 appeared in "Synchronization and Consensus of a Robot Network on an Underactuated Dynamic Platform" published in the *Proceedings of 2014 IEEE/RSJ Conference of Intelligent Robots and Systems (IROS 2014)* [101].

CHAPTER 2

ADAPTIVE CONTROL OF UNDERACTUATED ROBOTS WITH UNMODELED DYNAMICS

In this chapter[1], we develop a controller for an underactuated system consisting of a manipulator mounted on a moving platform with unmodeled dynamics. The control scheme, which is independent of system modeling, promotes the use of a filter in the control input of a reference model adaptive controller to maintain the control system's robustness. The proposed controller employs a fast adaptation scheme while maintaining bounded deviation from a nonadaptive reference system. In particular, the control design is tolerant of time delays in the control loop, and maintains clean control channels even in the presence of measurement noise due to the use of a low-pass filter structure in the control input. Tuning of the filter also allows for shaping the nominal response and enhancing the delay robustness.

The proposed controller is implemented for two example underactuated robotic systems in two trajectory-tracking contexts: 1) a manipulator mounted on a ship operating in a high-sea state under uncertain environmental disturbances on the ship dynamics from wind, waves, and ocean currents; and 2) a mobile manipulator moving across a rough terrain of unknown geometry. The first task is used to assess the tracking performance when the platform motions contribute large inertia and nonlinearity to the manipulator dynamics. The second task demonstrates the proposed controller's effectiveness when the manipulator dynamics are mutually coupled with the platform dynamics, whose high-frequency motions are induced by both the manipulator motions and traversal across a rough terrain via a suspension system. The control objectives in these two tasks are achieved under both velocity-measurement

[1]The material in this chapter is taken from [102] with the permission from the publisher. The introduction and the conclusion are modified to agree with the flow of the dissertation. In addition, here, the models are put in the simulation sections instead of the appendix as in [102].

noise and time delay in the control signal.

The remainder of this chapter is organized as follows. A template dynamic model of an underactuated robotic system is described in Sect. 2.1. The text presents a broad-strokes description of a popular approach for adaptive control of such systems, including its potential shortcomings. Section 2.2 presents preliminary results that are used in the analysis in the following sections. The proposed adaptive control design is introduced and analyzed in Sect. 2.3. The main results on the transient performance bounds are discussed in Sect. 2.4. Section 2.5 illustrates the trajectory-tracking performance of the control design in the context of a robot arm mounted on a ship with uncertain dynamics, including in the presence of actuator delay and measurement noise. Sect. 2.6 considers the implementation of the proposed controller in a mobile manipulator whose platform motions are disturbed by motion across an uneven and unknown terrain, with the addition of a nonholonomic constraint on the platform kinematics. A concluding discussion in Sect. 2.7 reviews the advantages of the proposed design and points to open problems in its characterization.

2.1 Dynamic Model of Underactuated Robotic Systems

Let a superscribed dot denote differentiation with respect to time t. In the absence of nonholonomic constraints on the system kinematics, the dynamics of a robotic manipulator mounted on a platform, and with several unactuated degrees of freedom, are governed by equations of motion of the form [120]

$$\begin{bmatrix} M_{aa}(q) & M_{au}(q) \\ M_{au}^T(q) & M_{uu}(q) \end{bmatrix} \ddot{q} + \begin{bmatrix} C_a(q,\dot{q}) \\ C_u(q,\dot{q}) \end{bmatrix} \dot{q} + \begin{bmatrix} G_a(q) \\ G_u(q) \end{bmatrix} = \begin{bmatrix} u \\ 0 \end{bmatrix} + \begin{bmatrix} D_{aa}(t) \\ D_{uu}(t) \end{bmatrix}, \qquad (2.1)$$

where $q^T = \left[q_a^T, q_u^T\right]$, the n generalized coordinates contained in the column vector q_a describe the actuated degrees of freedom, and the m generalized coordinates contained in the column vector q_u describe the unactuated degrees of freedom of the robotic system. The column

vectors u, D_{aa} and D_{uu} contain the time-dependent control-input torques and bounded time-dependent unknown disturbances to the actuated and unactuated degrees of freedom, respectively. The inertia matrices M_{aa}, M_{uu} and M are all positive-definite, symmetric, and bounded. The remaining terms include Coriolis and centripetal effects, gravity and other conservative forces, as well as dissipative and velocity-dependent mechanisms.

A popular adaptive approach (e.g., [137, 3, 18]) for controlling the system described above is based on the so-called *linear-in-parameter* property of Lagrangian systems, which here takes the form

$$\begin{bmatrix} M_{aa}(q) & M_{au}(q) \\ M_{au}^T(q) & M_{uu}(q) \end{bmatrix} \ddot{q}_r + \begin{bmatrix} C_a(q,\dot{q}) \\ C_u(q,\dot{q}) \end{bmatrix} \dot{q}_r + \begin{bmatrix} G_a(q) \\ G_u(q) \end{bmatrix} = \begin{bmatrix} Y_a(q,\dot{q},\dot{q}_r,\ddot{q}_r) \\ Y_u(q,\dot{q},\dot{q}_r,\ddot{q}_r) \end{bmatrix} a \qquad (2.2)$$

for some vector a of model parameters, and for arbitrary reference trajectories $q_r^T = [q_{ar}^T, q_{ur}^T]$ of the actuated and unactuated generalized coordinates of the system. In practice, the model parameters contained in a are assumed to be unknown and, therefore, to be estimated in real-time by an estimator $\hat{a}$. In this case, the *regression matrices* $Y_a(q,\dot{q},\dot{q}_r,\ddot{q}_r)$ and $Y_u(q,\dot{q},\dot{q}_r,\ddot{q}_r)$ are assumed to be known functions of the actual and reference dynamics for all time. Given a defining relationship for the reference trajectory in terms of the actual and desired dynamics, the control signal is then designed to have the following general form:

$$u = \text{P.D.} + Y_a(q,\dot{q},\dot{q}_r,\ddot{q}_r)\hat{a}, \qquad (2.3)$$

where P.D. represents proportional-derivative, negative-feedback control terms that are responsible for repressing disturbances, and designed for specific control tasks and performance tuning. The time history of the parameter estimate $\hat{a}$ is governed by adaptive laws, designed with the tracking error as feedback in order to compensate for the nonlinearity in the model. For example, [137] considers the task of controlling a free-floating space manipulator in its task space. Here, the reference trajectory is the output of a reference system whose input

includes a sliding-variable formulation of the end-effector tracking error. Similarly, the P.D. term in Eq. (2.3) is taken to be proportional to this sliding variable. Furthermore, the adaptive law is designed as follows:

$$\dot{\hat{a}} = -\Gamma \begin{bmatrix} Y_a(q, \dot{q}, \dot{q}_r, \ddot{q}_r) \\ Y_u(q, \dot{q}, \dot{q}_r, \ddot{q}_r) \end{bmatrix}^T (\dot{q} - \dot{q}_r) \tag{2.4}$$

with Γ being an adaptive gain. A similar formulation is employed for estimation of the Jacobian matrix that relates the system joint space to the corresponding task space.

Two fundamental assumptions are used in the formulation of the adaptive control strategy described above, namely i) the existence of a factorization of the left-hand side of Eqn. (2.2) in terms of a product of a matrix and a vector of model parameters and ii) that the matrix is known and the vector can be estimated. For fixed-base manipulators, these assumptions often apply, i.e., the unknown model parameters may be collected in a vector and the dynamics appropriately factored.

When the unknown parameters appear as nonlinear terms, factorization is no longer possible. Even in cases where factorization is possible in principle, the complexity of the geometry and mass distribution of the overall manipulator-and-platform system may make it prohibitively difficult to construct the regression matrices Y_a and Y_u, especially when the number of degrees of freedom is large. This is particularly common for moving-base manipulators, mounted on platforms whose structure may change in time and involve many uncalibrated parameters. In this case, the design of the controller for the manipulator requires detailed information about the geometry and mass distribution of the platform, which may not be available or even predictable, as changes to the latter are imposed by other control loops.

In the absence of certain knowledge of the regression matrices Y_a and Y_u, uncertainty associated with large variations in the inertial and geometric properties of the platform enters the control problem as disturbances that are not accommodated within the adaptive control

design. Examples include significant platform motions driven by unknown environmental factors, such as uneven terrain for ground vehicles, or high sea states and uncertain wind and current conditions for manipulators based on ships or off-shore platforms, all of which may vary with location and time. In these cases, disturbance rejection must be handled by the design of the P.D. terms, typically by using very large numerical values for the proportional and derivative gains, with likely loss of system robustness.

To address these observations, the control design in this dissertation avoids the linear-in-parameter factorization entirely. Here, all modeling terms in Eq. (2.1), including M_{aa}, M_{au}, M_{uu}, C_a, C_u, G_a, G_u, D_{aa}, and D_{uu}, are considered unknown functions of time. Before deriving the control scheme, the equations of motion in Eq. (2.1) are converted to a reduced form to demonstrate the reasoning behind the controller design that follows. Specifically, by solving for $\ddot{q}_u$ in the bottom component of Eq. (2.1), we get

$$\ddot{q}_u = M_{uu}^{-1}(q)\left(-M_{au}^T(q)\ddot{q}_a - C_u(q,\dot{q})\dot{q} - G_u(q) + D_{uu}(t)\right). \tag{2.5}$$

Substitution in the top component of Eq. (2.1) then yields

$$M_a(q)\ddot{q}_a + N_a(q,\dot{q}) = u + D_a(q,t), \tag{2.6}$$

where

$$M_a(q) = M_{aa}(q) - M_{au}(q)M_{uu}^{-1}(q)M_{au}^T(q). \tag{2.7}$$

$$N_a(q,\dot{q}) = C_a(q,\dot{q})\dot{q} + G_a(q) - M_{au}(q)M_{uu}^{-1}(q)\left(C_u(q,\dot{q})\dot{q} + G_u(q)\right), \tag{2.8}$$

$$D_a(q,t) = D_{aa}(t) - M_{au}(q)M_{uu}^{-1}(q)D_{uu}(t). \tag{2.9}$$

Since

$$\begin{vmatrix} M_{aa}(q) & M_{au}(q) \\ M_{au}^T(q) & M_{uu}(q) \end{vmatrix} = |M_a(q)| \cdot |M_{uu}(q)| \tag{2.10}$$

(see, e.g., [127]), it follows that M_a must be invertible. Moreover, it is trivial to show that M_a^{-1} is a symmetric positive definite matrix. In addition, there exist bounding constants m_l and m_h such that

$$0 < m_l \mathbb{I} \leq M_a^{-1}(q) \leq m_h \mathbb{I}, \quad \text{for all} \quad q \in \mathbb{R}^{m+n} \tag{2.11}$$

As seen in Eq. (2.6), the coefficients governing the dynamics in the actuated degrees of freedom depend on the time-histories of the unactuated degrees of freedom (and vice versa). In the analysis below, we assume that $q_u(t)$ and $\dot{q}_u(t)$ can be bounded a priori for all time. We revisit this assumption in the concluding section. In the next sections, we design an adaptive controller that is independent of any detailed knowledge of the system model, and proceed to demonstrate successful estimation of the unknown model coefficients, as well as close tracking of the actuated degrees of freedom along the corresponding desired trajectories.

2.2 Preliminaries

2.2.1 An input-output map

For each smooth function $v : \mathbb{R} \to \mathbb{R}^{n+m}$, let $\Phi_v : \mathbb{R} \times \mathbb{R} \to \mathbb{R}^{n \times n}$ be the unique solution to the initial-value problem

$$\frac{\partial}{\partial t}\Phi_v(t, t') = -kM_a^{-1}\big(v(t)\big)\Phi_v(t, t'), \quad \Phi_v(t', t') = \mathbb{I}, \tag{2.12}$$

where the symmetric matrix M_a is a smooth function of its argument, and

$$0 < m_l \mathbb{I} \leq M_a^{-1}(q) \leq m_h \mathbb{I}, \quad \text{for all} \quad q \in \mathbb{R}^{n+m}. \tag{2.13}$$

Using the Gronwall lemma, it follows that

$$\operatorname{tr}\big(\Phi_v^T(t,t')\Phi_v(t,t')\big) \leq ne^{-2km_l(t-t')} \tag{2.14}$$

and, consequently, that $\Phi_{v,ij}(t,t') \leq \sqrt{n}e^{-km_l(t-t')}$ for $i,j = 1,\ldots,n$, independently of v. The $\mathcal{L}_1$ norm of the linear input-output map

$$\mathcal{F}_v : \eta \mapsto -k\int_0^t \Phi_v(t,t')\eta(t')\,\mathrm{d}t' \tag{2.15}$$

is then given by

$$\|\mathcal{F}_v\|_{\mathcal{L}_1} \triangleq \max_{1\leq i\leq n}\left(\sum_{j=1}^{n}\sup_{t\geq t^*,t^*\in\mathbb{R}^+}\int_{t^*}^{t} k\left|\Phi_{v,ij}(t,t')\right|\,\mathrm{d}t'\right) \leq \frac{n\sqrt{n}}{m_l}, \tag{2.16}$$

independently of v.

Let $\mathcal{M}_v[\eta] \triangleq M_a^{-1}(v)\eta$. Since the matrix M_a^{-1} is bounded, it follows that the compositions $\mathcal{M}_v \circ \mathcal{F}_v$ and $\mathcal{F}_v \circ \mathcal{M}_v$ also have bounded norm, independently of v. Moreover, since $\partial\Phi_v(t,t')/\partial t' = \Phi_v(t,t')kM_a^{-1}(v(t'))$, it follows by integration by parts that

$$\mathcal{F}_v[\dot{\eta}] = -k\left(\mathcal{F}_v \circ \mathcal{M}_v + \mathcal{I}\right)[\eta], \tag{2.17}$$

provided that $\eta(0) = 0$.

2.2.2 Parameterizations and bounds

Let $\tau > 0$ be given, and consider a differentiable function $\eta(t,\zeta) : \mathbb{R}\times\mathbb{R}^p \to \mathbb{R}^n$, such that

$$\|\eta(t,0)\|_\infty \leq Z < \infty \tag{2.18}$$

and

$$\|\zeta\|_\infty \leq \xi \Rightarrow \left\|\frac{\partial \eta(t,\zeta)}{\partial t}\right\|_\infty \leq d_{\eta_t}(\xi) < \infty, \quad \left\|\frac{\partial \eta(t,\zeta)}{\partial \zeta}\right\|_\infty \leq d_{\eta_\zeta}(\xi) < \infty \tag{2.19}$$

for arbitrary ξ and $t \in [0,\tau]$. Let $\|f_t\|_{\mathcal{L}_\infty}$ denote the restriction of the $\mathcal{L}_\infty$ norm to the interval $[0,t]$, and suppose that the differentiable functions $r(t)$ and $\chi(t)$ satisfy the inequality

$$\|\chi_t\|_{\mathcal{L}_\infty} \leq Q_1\|r_t\|_{\mathcal{L}_\infty} + Q_2,\ t \in [0,\tau] \tag{2.20}$$

for some positive constants Q_1 and Q_2. Let

$$\bar{\rho}(\rho) \triangleq \max\{\rho+1, Q_1(\rho+1)+Q_2\}, \tag{2.21}$$

and define

$$L_\rho \triangleq \frac{\bar{\rho}(\rho)}{\rho} d_{\eta_\zeta}\big(\bar{\rho}(\rho)\big) \tag{2.22}$$

and $\zeta(t) \triangleq \big(r(t), \chi(t)\big)$. Together with (2.20), the bound $\|r_\tau\|_{\mathcal{L}_\infty} \leq \rho < \infty$ implies that

$$\|\zeta_t\|_{\mathcal{L}_\infty} \leq \max\{\|r_t\|_{\mathcal{L}_\infty}, \|\chi_t\|_{\mathcal{L}_\infty}\} < \bar{\rho}(\rho) \tag{2.23}$$

and, using the bounds in (2.18) and (2.19),

$$\|\eta_t\|_\infty \leq \|\big(\eta(t,\zeta(t)) - \eta(t,0)\big)\|_\infty + \|\eta(t,0)\|_\infty < \rho L_\rho + Z \tag{2.24}$$

for $t \in [0,\tau]$. If, in addition, $\|\dot{r}_\tau\|_{\mathcal{L}_\infty} \leq d_r < \infty$, then:

Lemma 2.1. *There exist continuous, piecewise-differentiable functions $\theta(t) \in \mathbb{R}^n$ and $\sigma(t) \in \mathbb{R}^n$ such that*

$$\eta\big(t,\zeta(t)\big) = \theta(t)\|r_t\|_{\mathcal{L}_\infty} + \sigma(t),\ t \in [0,\tau]. \tag{2.25}$$

On this interval, $\|\theta(t)\|_\infty < L_\rho$ *and* $\|\sigma(t)\|_\infty < L_\rho Q_2 + Z + \alpha$ *for some arbitrary* $\alpha > 0$*, and, within any subinterval of differentiability,* $\|\dot{\theta}(t)\|_\infty < d_\theta < \infty$ *and* $\|\dot{\sigma}(t)\|_\infty < d_\sigma < \infty$*.*

Proof. See proof of Lemma A.9.2 in [61]. □

The conclusions of Lemma 2.1 hold in the special case that $\chi(t) \triangleq \big(q_a(t), q_u(t), \dot{q}_u(t)\big)$, where the functions $q_u(t)$ and $\dot{q}_u(t)$ are bounded for all t, and

$$\dot{q}_a - \dot{q}_{\rm ad} + \lambda(q_a - q_{\rm ad}) = r \tag{2.26}$$

for $\lambda > 0$ and some bounded function $q_{\rm ad}(t)$ with all bounded derivatives. Indeed, in this case

$$\|\chi_t\|_{\mathcal{L}_\infty} \leq \|q_{a,t}\|_{\mathcal{L}_\infty} + \max\{\|q_{u,t}\|_{\mathcal{L}_\infty}, \|\dot{q}_{u,t}\|_{\mathcal{L}_\infty}\} \leq Q_1\|r_t\|_{\mathcal{L}_\infty} + Q_2, \tag{2.27}$$

where $Q_1 = \|(s+\lambda)^{-1}\|_{\mathcal{L}_1} = \lambda^{-1}$ and

$$Q_2 = \|(s+\lambda)^{-1}(q_a(0) - q_{\rm ad}(0))\|_{\mathcal{L}_\infty} + \|q_{ad,t}\|_{\mathcal{L}_\infty} + \max\{\|q_{u,t}\|_{\mathcal{L}_\infty}, \|\dot{q}_{u,t}\|_{\mathcal{L}_\infty}\}. \tag{2.28}$$

As a byproduct, it follows that $\|q_{a,\tau}\|_{\mathcal{L}_\infty}$ and $\|\dot{q}_{a,\tau}\|_{\mathcal{L}_\infty}$ are both finite.

Suppose, instead, that $\eta(t,\zeta)$ satisfies (2.18) and (2.19), $r(t)$ and $\chi(t)$ satisfy (2.20), and

$$r(t) = \mathcal{A}[\eta(t, \zeta(t))] + \mathcal{B}[r(0)\delta(t)], \tag{2.29}$$

where $\zeta(t) \triangleq \big(r(t), \chi(t)\big)$, and $\mathcal{A}$ and $\mathcal{B}$ are linear integral operators such that $\|\mathcal{A}\|_{\mathcal{L}_1} = A < \infty$, and $\|\mathcal{B}[r(0)\delta(t)]\|_{\mathcal{L}_\infty} = B < \infty$. Then,

Lemma 2.2. *The inequalities* $\|r(0)\|_\infty < \rho$ *and* $A(\rho L_\rho + Z) + B < \rho$ *imply that* $\|r_\tau\|_{\mathcal{L}_\infty} < \rho$*.*

Proof. Suppose that $\|r_\tau\|_{\mathcal{L}_\infty} \geq \rho$. Then $\|r(0)\|_\infty < \rho$ implies that there exists a $\hat{\tau} \in [0, \tau]$, such that

$$\|r(t)\|_\infty < \rho, \quad \forall t \in [0, \hat{\tau}), \quad \text{and} \quad \|r_{\hat{\tau}}\|_{\mathcal{L}_\infty} = \|r(\hat{\tau})\|_\infty = \rho. \tag{2.30}$$

Using (2.29) and (2.24) we obtain

$$\|r_{\hat{\tau}}\|_{\mathcal{L}_\infty} \leq A\|\eta_{\hat{\tau}}\|_{\mathcal{L}_\infty} + B < \rho, \tag{2.31}$$

contradicting the original inequality. □

2.2.3 Estimation bounds

Given positive scalars x_b and ε, let $f : \mathbb{R}^n \to \mathbb{R}$ be given by

$$f : x \to \frac{\|x\|^2 - (x_b - \varepsilon)^2}{2\varepsilon x_b - \varepsilon^2} \tag{2.32}$$

such that $f|_{\|x\|=x_b-\varepsilon} = 0$ and $f|_{\|x\|=x_b} = 1$, and define the *projection operator* [71]:

$$\mathbf{Proj} : (x, y; x_b, \varepsilon) \to \begin{cases} y - f(x)\left(y^T \frac{\nabla f(x)}{\|\nabla f(x)\|}\right)\frac{\nabla f(x)}{\|\nabla f(x)\|} & \text{if } f(x) > 0 \text{ and } y^T\nabla f(x) > 0 \\ y & \text{otherwise} \end{cases} \tag{2.33}$$

for $x, y \in \mathbb{R}^n$. Then, following [71], for $\Gamma > 0$,

$$\dot{x} = \Gamma\,\mathbf{Proj}(x, y; x_b, \varepsilon) \text{ and } \|x(0)\| \leq x_b \Rightarrow \|x(t)\| \leq x_b,\ \forall t. \tag{2.34}$$

Moreover, provided that $\|x^*\| \leq x_b - \varepsilon$,

$$\left(x - x^*\right)^T\left(\mathbf{Proj}(x, y; x_b, \varepsilon) - y\right) \leq 0. \tag{2.35}$$

Now let $\tau > 0$ and $\varepsilon > 0$ be given, and suppose that $\theta(t)$ and $\sigma(t)$ are continuous, piecewise-differentiable functions that satisfy $\|\theta(t)\|_\infty < \theta_b - \varepsilon < \infty$ and $\|\sigma(t)\|_\infty < \sigma_b - \varepsilon < \infty$ for all $t \in [0, \tau]$, and, within any subinterval of differentiability, $\|\dot{\theta}(t)\|_\infty < d_\theta < \infty$ and $\|\dot{\sigma}(t)\|_\infty < d_\sigma < \infty$. Let the symmetric, positive-definite matrix P satisfy the Lyapunov equation $A_{\text{sp}}^\top P + PA_{\text{sp}} = -Q$, for some arbitrary symmetric, positive-definite matrix Q and

Hurwitz matrix A_{sp}. Finally, for some function $\mu(t)$, consider the initial-value problems

$$\dot{r} = A_m r + \mu + \theta \|r_t\|_{\mathcal{L}_\infty} + \sigma, \quad r(0) = r_0 \tag{2.36}$$

and

$$\dot{\hat{r}} = A_m r + \mu + \hat{\theta} \|r_t\|_{\mathcal{L}_\infty} + \hat{\sigma} + A_{\text{sp}} \tilde{r}, \quad \hat{r}(0) = r_0, \tag{2.37}$$

$$\dot{\hat{\theta}} = \Gamma \, \mathbf{Proj}\big(\hat{\theta}, -P\tilde{r} \|r_t\|_{\mathcal{L}_\infty}; \theta_b, \varepsilon\big), \quad \hat{\theta}(0) = \hat{\theta}_0, \tag{2.38}$$

$$\dot{\hat{\sigma}} = \Gamma \, \mathbf{Proj}\big(\hat{\sigma}, -P\tilde{r}; \sigma_b, \varepsilon\big), \quad \hat{\sigma}(0) = \hat{\sigma}_0, \tag{2.39}$$

where $\tilde{r} \triangleq \hat{r} - r$, $\|\hat{\theta}_0\| \leq \theta_b$, and $\|\hat{\sigma}_0\| \leq \sigma_b$.

Lemma 2.3. *Let $\lambda_{\min}(S)$ and $\lambda_{\max}(S)$ denote the smallest and largest eigenvalue, respectively, of a positive-definite symmetric matrix S. Then,*

$$\|\tilde{r}_\tau\|_{\mathcal{L}_\infty} \leq \sqrt{\frac{\nu_m}{\lambda_{\min}(P)\Gamma}}, \tag{2.40}$$

where

$$\nu_m \triangleq 4(\theta_b^2 + \sigma_b^2) + 4\frac{\lambda_{\max}(P)}{\lambda_{\min}(Q)}\big(\theta_b d_\theta + \sigma_b d_\sigma\big). \tag{2.41}$$

Proof. Let $\tilde{\theta} \triangleq \hat{\theta} - \theta$ and $\tilde{\sigma} \triangleq \hat{\sigma} - \sigma$ and define the Lyapunov function

$$V \triangleq \tilde{r}^T P \tilde{r} + \frac{1}{\Gamma}(\tilde{\theta}^T \tilde{\theta} + \tilde{\sigma}^T \tilde{\sigma}). \tag{2.42}$$

It follows that

$$V(0) \leq \frac{4}{\Gamma}\left(\theta_b^2 + \sigma_b^2\right) < \frac{\nu_m}{\Gamma}. \tag{2.43}$$

We show by contradiction that

$$V(t) \leq \frac{\nu_m}{\Gamma}, \quad \forall t \in [0, \tau]. \tag{2.44}$$

To this end, choose $\hat{\tau} \in (0, \tau]$ such that $\dot{\theta}$ and $\dot{\sigma}$ are continuous on $[0, \hat{\tau})$. Suppose that $V(\bar{\tau}) > \nu_m/\Gamma$ and $\dot{V}(\bar{\tau}) \geq 0$ for some $\bar{\tau} < \hat{\tau}$. It follows from (2.42) that

$$\|\tilde{r}(\bar{\tau})\|_\infty^2 > \frac{4}{\Gamma \lambda_{\min}(Q)} \big(\theta_b d_\theta + \sigma_b d_\sigma\big). \tag{2.45}$$

Moreover, by the properties of the projection operators,

$$\dot{V} \leq -\tilde{r}^T Q \tilde{r} + \frac{2}{\Gamma} \big|\tilde{\theta}^T \dot{\theta} + \tilde{\sigma}^T \dot{\sigma}\big| \leq -\|\tilde{r}\|_\infty^2 \, \lambda_{\min}(Q) + \frac{4}{\Gamma} \big(\theta_b d_\theta + \sigma_b d_\sigma\big) \tag{2.46}$$

for all $t \in [0, \hat{\tau}]$, and we arrive at a contradiction by evaluation at $t = \bar{\tau}$. By continuity, $V(t) \leq \nu_m/\Gamma$ for all $t \in [0, \hat{\tau}]$. Equation (2.42) then implies that

$$\|\tilde{r}_{\hat{\tau}}\|_{\mathcal{L}_\infty} \leq \sqrt{\frac{\nu_m}{\lambda_{\min}(P)\Gamma}}\,. \tag{2.47}$$

By repeating this analysis for each subsequent interval of continuity of $\dot{\theta}$ and $\dot{\sigma}$, we conclude that (2.47) holds with $\hat{\tau}$ replaced by τ. □

Suppose that the function $\eta(t, \zeta)$ satisfies (2.18) and (2.19). Let $\zeta(t) := \big(r(t), \chi(t)\big)$, where

$$\dot{r}(t) = A_m r(t) + \mu(t) + \eta(t, \zeta(t)), \quad r(0) = r_0 \tag{2.48}$$

for some function $\mu(t)$. Suppose that $r(t)$ and $\chi(t)$ satisfy (2.20), $\|r_\tau\|_{\mathcal{L}_\infty} < \rho < \infty$, and $\|\mu_\tau\|_{\mathcal{L}_\infty} < \infty$. In this case, Eq. (2.24) implies $\|\eta_\tau\|_{\mathcal{L}_\infty} < \infty$. Equation (2.36) and the bounds on θ, σ, $\dot{\theta}$ and $\dot{\sigma}$ then follow from Lemma 2.1 and the conclusions of Lemma 2.3 again apply.

Suppose, in addition, that $\mu = \mathcal{M}[u]$, where $\|\mathcal{M}\|_{\mathcal{L}_1} < \infty$ and $\|u_\tau\|_{\mathcal{L}_\infty} = u_b < \infty$. Then, the conclusions of Lemma 2.3 follow also by replacing μ by u in Eqs. (2.36) and (2.37), σ by $\sigma + (\mathcal{M} - \mathcal{I})\, u$ in Eq. (2.36), and σ_b by $\sigma_b + (\|\mathcal{M}\|_{\mathcal{L}_1} + 1)\, u_b$ in Eq. (2.39).

2.3 Adaptive controller for underactuated robots

Let the desired time histories for the robot's actuated degrees of freedom be described by the vector-valued function $q_{\rm ad}(t)$ and suppose that this is bounded with bounded derivatives. In the definition of the auxiliary kinematic variable (cf. the sliding control formulation in [130])

$$r \triangleq \dot{q}_a - \dot{q}_{\rm ad} + \lambda \left(q_a - q_{\rm ad} \right), \tag{2.49}$$

the choice $\lambda > 0$ ensures that Eq. (2.49) is an exponentially stable system for q_a. Indeed, as long as the controller drives r to a neighborhood of 0, the joint trajectory q_a converges to a neighborhood of $q_{\rm ad}$ exponentially fast.

Let A_m be a Hurwitz matrix and set $\mu \triangleq M_a^{-1}(q)u$. It follows by substitution of Eqs. (2.6) and (2.49) into the time derivative of Eq. (2.49) that

$$\dot{r}(t) = A_m r(t) + \mu(t) + \eta(t, \zeta(t)), \tag{2.50}$$

where $\zeta \triangleq (r, q_a, q_u, \dot{q}_u)$ and the *nonlinearity* $\eta(t, \zeta(t))$ is obtained from

$$\eta(t, \zeta) \triangleq M_a^{-1}(q)\big(D_a(q,t) - N_a(q, \dot{q}_a, \dot{q}_u)\big) - \ddot{q}_{\rm ad}(t) + \lambda(\dot{q}_a - \dot{q}_{\rm ad}(t)) - A_m r \tag{2.51}$$

with $\dot{q}_a = r + \dot{q}_{\rm ad}(t) - \lambda \left(q_a - q_{\rm ad}(t) \right)$. Here,

$$\eta(t, 0) = M_a^{-1}(0)\big(D_a(0,t) - N_a(0, \dot{q}_{\rm ad}(t) + \lambda q_{\rm ad}(t), 0)\big) - \ddot{q}_{\rm ad}(t) + \lambda^2 q_{\rm ad}(t) \tag{2.52}$$

whose norm is bounded for all t by some constant Z provided that similar expectations are placed on the disturbances $D_a(0,t)$. We similarly restrict attention to disturbances that guarantee that

$$\|\zeta\|_\infty \leq \xi \Rightarrow \left\| \frac{\partial \eta(t,\zeta)}{\partial t} \right\|_\infty \leq d_{\eta_t}(\xi) < \infty, \quad \left\| \frac{\partial \eta(t,\zeta)}{\partial \zeta} \right\|_\infty \leq d_{\eta_\zeta}(\xi) < \infty \tag{2.53}$$

for arbitrary ξ and all t. The objective of the following sections is to establish an adaptive control formulation for u that ensures predictable performance bounds for the system response and the control input.

2.3.1 Nonadaptive reference system

Let $k > 0$ denote the *bandwidth* of the first-order low-pass filter $k/(s+k)$. For an arbitrary smooth function $v : \mathbb{R} \to \mathbb{R}^{m+n}$, consider the system $\mathcal{R}_v$ obtained by appending

$$\mu(t) = M_a^{-1}\big(v(t)\big)u(t) \tag{2.54}$$

and

$$\dot{u}(t) = -k\mu(t) - k\eta\big(t, \zeta(t)\big), \quad u(0) = 0 \tag{2.55}$$

to Eqs. (2.49) and (2.50). Let Φ_v be the unique solution to the initial-value problem

$$\frac{\partial}{\partial t}\Phi_v(t,t') = -kM_a^{-1}\big(v(t)\big)\Phi_v(t,t'), \quad \Phi_v(t',t') = \mathbb{I}, \tag{2.56}$$

It follows that

$$u(t) = \mathcal{F}_v[\eta(t,\zeta(t))] \triangleq -k\int_0^t \Phi_v(t,t')\eta(t',\zeta(t'))\,\mathrm{d}t' \tag{2.57}$$

and

$$\mu(t) = \mathcal{D}_v[\eta(t,\zeta(t))] \triangleq M_a^{-1}\big(v(t)\big)\mathcal{F}_v[\eta(t,\zeta(t))] \tag{2.58}$$

in terms of the linear input-output maps $\mathcal{F}_v$ and $\mathcal{D}_v$. As shown in 2.2.1,

$$b_{\mathcal{F}} \triangleq \sup_v \|\mathcal{F}_v\|_{\mathcal{L}_1} < \infty. \tag{2.59}$$

Now, let $\mathcal{I}$ be the identity map and $\mathcal{H}$ be the linear input-output map corresponding to

the transfer function $(s\mathbb{I} - A_m)^{-1}$. It follows that

$$r(t) = \big(\mathcal{H} \circ (\mathcal{I} + \mathcal{D}_v)\,\big)[\eta(t, \zeta(t))] + \mathcal{H}[r(0)\delta(t)], \tag{2.60}$$

where $b_1 \triangleq \sup_v \|\mathcal{H} \circ (\mathcal{I} + \mathcal{D}_v)\|_{\mathcal{L}_1} < \infty$ and $\|\mathcal{H}[r(0)\delta(t)]\|_{\mathcal{L}_\infty} < \infty$. In the special case that $r(0) = 0$, rearranging the terms in Eqs. (2.50) and (2.55) yields

$$r(s) = (s\mathbb{I} - A_m)^{-1}\,(u(s) + \eta_u(s))\,, \tag{2.61}$$

where

$$u(s) = -\frac{k}{s+k}\eta_u(s) \tag{2.62}$$

and $\eta_u(t) \triangleq \big(M_a^{-1}\big(v(t)\big) - \mathbb{I}\big)u(t) + \eta\big(t, \zeta(t)\big)$. In this case, it follows that

$$\|r\|_{\mathcal{L}_\infty} \leq \big\|s(s\mathbb{I} - A_m)^{-1}\big\|_{\mathcal{L}_1} \left\|\frac{1}{s+k}\right\|_{\mathcal{L}_1} \|\eta_u\|_{\mathcal{L}_\infty} \leq \frac{2}{k}\big((m_h+1)b_{\mathcal{F}} + 1\big)\,\|\eta\|_{\mathcal{L}_\infty}\,, \tag{2.63}$$

i.e., that

$$b_1 \leq \frac{2}{k}\big((m_h+1)b_{\mathcal{F}} + 1\big). \tag{2.64}$$

Let Z and $L_{\rho_{\text{ref}}}$ be defined as in Eqs. (2.18) and (2.22) in 2.2.2, respectively. Since $b_1 \to 0$ uniformly in v as $k \to \infty$, it follows that there exists a K, such that the *stability condition*

$$b_1 < \frac{\rho_{\text{ref}} - \|\mathcal{H}[r(0)\delta(t)]\|_{\mathcal{L}_\infty}}{L_{\rho_{\text{ref}}}\rho_{\text{ref}} + Z} \tag{2.65}$$

is satisfied for some $\rho_{\text{ref}} > \|\mathcal{H}[r(0)\delta(t)]\|_{\mathcal{L}_\infty}$ provided that $k > K$. Then, from the remarks following Lemma 2.1 and the result of Lemma 2.2 in 2.2.2, we conclude that if $\|r(0)\|_\infty < \rho_{\text{ref}}$, then the bounds $\|r\|_{\mathcal{L}_\infty} < \rho_{\text{ref}}$ and $\|u\|_{\mathcal{L}_\infty} < b_{\mathcal{F}}(L_{\rho_{\text{ref}}}\rho_{\text{ref}} + Z)$ must hold for $\mathcal{R}_v$, independently of v. In particular, this conclusion must hold for the nonadaptive reference system obtained

by substituting the actual time histories $q(t)$ for $v(t)$, and we arrive at

Theorem 2.1. *Consider the nonadaptive reference system*

$$\dot{r}_{\text{ref}}(t) = A_m r_{\text{ref}}(t) + M_a^{-1}(q(t))u_{\text{ref}}(t) + \eta(t, \zeta_{\text{ref}}(t)), \quad r_{\text{ref}}(0) = r_0 \tag{2.66}$$

$$\dot{u}_{\text{ref}}(t) = -k\left(M_a^{-1}(q(t))u_{\text{ref}}(t) + \eta\big(t, \zeta_{\text{ref}}(t)\big)\right), \quad u_{\text{ref}}(0) = 0 \tag{2.67}$$

where $q = (q_a, q_u)$, $\zeta_{\text{ref}} = (r_{\text{ref}}, q_{\text{a,ref}}, q_u, \dot{q}_u)$, $\dot{q}_{\text{a,ref}} = r_{\text{ref}} + \dot{q}_{\text{ad}}(t) - \lambda\left(q_{\text{a,ref}} - q_{\text{ad}}(t)\right)$, *and* $q_{\text{a,ref}}(0) = q_a(0)$. *For sufficiently large* k, *there exists a positive scalar* ρ_{ref}, *such that* $\|r_{\text{ref}}(0)\|_\infty < \rho_{\text{ref}}$ *implies that* $\|r_{\text{ref}}\|_{\mathcal{L}_\infty} < \rho_{\text{ref}}$ *and* $\|u_{\text{ref}}\|_{\mathcal{L}_\infty} < b_{\mathcal{F}}(L_{\rho_{\text{ref}}}\rho_{\text{ref}} + Z)$.

From Eq. (2.60) and (2.64), it follows that

$$\|r(t) - \mathcal{H}[r(0)\delta(t)]\|_{\mathcal{L}_\infty} = \mathcal{O}\left(k^{-1}\right) \tag{2.68}$$

for $k \to \infty$. We obtain

Lemma 2.4. *The response of* $\mathcal{R}_v$ *converges to* $e^{A_m t}r_0$ *when* $k \to \infty$.

Lemma 2.4 implies that the response of the nonadaptive reference system will converge to a neighborhood of 0 exponentially fast. The size of the neighborhood is inversely proportional to the filter bandwidth k.

2.3.2 Design of the adaptation laws and the state predictor

By Theorem 2.1 and the remarks following Lemma 2.1 in 2.2.2, it follows that, in the nonadaptive reference system, and provided that $\|r_{\text{ref}}(0)\|_\infty < \rho_{\text{ref}}$, the parameterization $\eta(t, \zeta_{\text{ref}}(t)) = \theta_{\text{ref}}(t)\|r_{ref,t}\|_{\mathcal{L}_\infty} + \sigma_{\text{ref}}(t)$ holds for all t, in terms of a pair of continuous, piecewise-differentiable and uniformly bounded functions θ_{ref} and σ_{ref}. Equivalently,

$$\dot{r}_{\text{ref}} = A_m r_{\text{ref}} + u_{\text{ref}} + \theta_{\text{ref}}\|r_{ref,t}\|_{\mathcal{L}_\infty} + \bar{\sigma}_{\text{ref}} \tag{2.69}$$

and

$$\dot{u}_{\text{ref}} = -k\left(u_{\text{ref}} + \theta_{\text{ref}}\|r_{ref,t}\|_{\mathcal{L}_\infty} + \bar{\sigma}_{\text{ref}}\right), \tag{2.70}$$

where

$$\bar{\sigma}_{\text{ref}} \triangleq \sigma_{\text{ref}} + (M_a^{-1}(q) - \mathbb{I})u_{\text{ref}} \tag{2.71}$$

is similarly bounded.

We proceed to consider an adaptive control design for the original dynamics in Eqs. (2.49) and (2.50) in lieu of Eq. (2.55). Analogous to Eqs. (2.69) and (2.70), consider the state predictor

$$\dot{\hat{r}} = A_m r + u + \hat{\theta}\|r_t\|_{\mathcal{L}_\infty} + \hat{\sigma} + A_{\text{sp}}\tilde{r}, \quad \hat{r}(0) = r_0, \tag{2.72}$$

and control design

$$\dot{u} = -k\big(u + \hat{\theta}\|r_t\|_{\mathcal{L}_\infty} + \hat{\sigma}\big), \quad u(0) = 0, \tag{2.73}$$

where $\tilde{r} \triangleq \hat{r} - r$ is the prediction error and A_{sp} is a Hurwitz matrix of loop-shaping parameters that may be tuned to reject oscillations caused by high-frequency disturbances or noise, as well as to make $\tilde{r}$ converge to 0 faster. Here, $\hat{\theta}$ and $\hat{\sigma}$ model adaptive estimates for θ and $\bar{\sigma}$, governed by the projection-based laws

$$\dot{\hat{\theta}} = \Gamma\,\mathbf{Proj}\big(\hat{\theta}, -P\tilde{r}\|r_t\|_{\mathcal{L}_\infty}; \theta_b, \varepsilon\big), \quad \hat{\theta}(0) = \hat{\theta}_0, \tag{2.74}$$

$$\dot{\hat{\sigma}} = \Gamma\,\mathbf{Proj}\big(\hat{\sigma}, -P\tilde{r}; \sigma_b, \varepsilon\big), \quad \hat{\sigma}(0) = \hat{\sigma}_0, \tag{2.75}$$

in terms of the *adaptive gain* $\Gamma \in \mathbb{R}^+$, and the positive-definite, symmetric matrix P, obtained as the solution to the Lyapunov equation $A_{\text{sp}}^\top P + P A_{\text{sp}} = -\mathbb{I}$. As defined in 2.2.3, the *projection operator* $\mathbf{Proj}(\cdot,\cdot\,;\cdot,\cdot)$, ensures that $\|\hat{\theta}(t)\|_\infty \leq \theta_b$ and $\|\hat{\sigma}(t)\|_\infty \leq \sigma_b$ provided

that $\hat{\theta}_0$ and $\hat{\sigma}_0$ satisfy these same bounds.

2.4 Performance bounds

In this section, we prove that the state and control input of the proposed adaptive control system governed by Eqs. (2.49)-(2.50) and (2.72)-(2.75) follow those of the nonadaptive reference system $\mathcal{R}_q$ closely, provided that the bandwidth k, the adaptive gain Γ, the scalar λ, and the bounds θ_b and σ_b are chosen appropriately. In particular, we prove the following theorem:

Theorem 2.2. *Suppose that $\rho_{\rm ref} > \|r(0)\|_\infty$ and that $\rho_{\rm ref}$ and k satisfy the condition* (2.65)*, and choose $\lambda \geq 1$. Then, for $\nu \ll 1$, there exist θ_b, σ_b, and $C > 0$, such that*

$$\|\hat{r} - r\|_{\mathcal{L}_\infty} \leq \nu, \quad \|r_{\rm ref} - r\|_{\mathcal{L}_\infty} = \mathcal{O}(\nu), \quad \|u_{\rm ref} - u\|_{\mathcal{L}_\infty} = \mathcal{O}(\nu), \tag{2.76}$$

provided that $\Gamma\nu^2 \geq C$.

Proof. Suppose that $\nu > 0$ is given. Since $\|r_{\rm ref}(0) - r(0)\|_\infty = 0 < 1$ and $\|u_{\rm ref}(0) - u(0)\|_\infty = 0$, it follows by continuity that there exists a $\tau > 0$, $\tau > 0$, such that $\|(r_{\rm ref} - r)_\tau\|_{\mathcal{L}_\infty} < 1$ and $\|(u_{\rm ref} - u)_\tau\|_{\mathcal{L}_\infty} < \infty$. Theorem 2.1 implies that

$$\|r_\tau\|_{\mathcal{L}_\infty} < \rho_{\rm ref} + 1, \quad \|u_\tau\|_{\mathcal{L}_\infty} < \infty. \tag{2.77}$$

By the remarks following Lemma 2.3 in 2.2.3, there exist θ_b, σ_b, and $C > 0$ (independent of τ), such that

$$\|\tilde{r}_\tau\|_{\mathcal{L}_\infty} \leq \sqrt{C/\Gamma}, \tag{2.78}$$

which does not exceed ν provided that $\Gamma\nu^2 \geq C$. It further follows from (2.49) and the

definition of $q_{\mathrm{a,ref}}$ in Theorem 2.1 that

$$\|(q_{\mathrm{a,ref}} - q)_\tau\|_{\mathcal{L}_\infty} \leq Q_1 \|(r_{\mathrm{ref}} - r)_\tau\|_{\mathcal{L}_\infty}, \tag{2.79}$$

where $Q_1 = \|(s+\lambda)^{-1}\|_{\mathcal{L}_1} = 1/\lambda \leq 1$. It follows that

$$\|(\zeta_{\mathrm{ref}} - \zeta)_\tau\|_{\mathcal{L}_\infty} \leq \|(r_{\mathrm{ref}} - r)_\tau\|_{\mathcal{L}_\infty} \tag{2.80}$$

and, consequently,

$$\|(\eta_{\mathrm{ref}} - \eta)_\tau\|_{\mathcal{L}_\infty} \leq d_{\eta_\zeta}\big(\bar{\rho}_{\mathrm{ref}}(\rho_{\mathrm{ref}})\big) \|(\zeta_{\mathrm{ref}} - \zeta)_\tau\|_{\mathcal{L}_\infty} \leq L_{\rho_{\mathrm{ref}}} \|(r_{\mathrm{ref}} - r)_\tau\|_{\mathcal{L}_\infty}. \tag{2.81}$$

Equations (2.50), (2.66), (2.67), (2.72) and (2.73) imply that

$$r_{\mathrm{ref}} - r = \mathcal{H}\big[\mathcal{M}_q\left[u_{\mathrm{ref}} - u\right] + \eta_{\mathrm{ref}} - \eta\big], \tag{2.82}$$

where

$$u_{\mathrm{ref}} - u = \mathcal{F}_q\left[\eta_{\mathrm{ref}} - \eta + A_{\mathrm{sp}}\tilde{r} - \dot{\tilde{r}}\right] = \mathcal{F}_q[\eta_{\mathrm{ref}} - \eta] + \mathcal{F}_q[A_{\mathrm{sp}}\tilde{r}] + k\left(\mathcal{F}_q \circ \mathcal{M}_q + \mathcal{I}\right)[\tilde{r}]. \tag{2.83}$$

These result in the bounds

$$\|(r_{\mathrm{ref}} - r)_\tau\|_{\mathcal{L}_\infty} \leq b_1 L_{\rho_{\mathrm{ref}}} \|(r_{\mathrm{ref}} - r)_\tau\|_{\mathcal{L}_\infty} + b_2 \|\tilde{r}_\tau\|_{\mathcal{L}_\infty} \tag{2.84}$$

and

$$\|(u_{\mathrm{ref}} - u)_\tau\|_{\mathcal{L}_\infty} \leq b_{\mathcal{F}} L_{\rho_{\mathrm{ref}}} \|(r_{\mathrm{ref}} - r)_\tau\|_{\mathcal{L}_\infty} + b_3 \|\tilde{r}_\tau\|_{\mathcal{L}_\infty}, \tag{2.85}$$

where

$$b_2 \triangleq \sup_{v \in \mathbb{R}^{m+n}} \|\mathcal{H} \circ \mathcal{M}_v \circ \big(\mathcal{F}_v \circ \mathcal{A}_{\text{sp}} + k(\mathcal{F}_v \circ \mathcal{M}_v + \mathcal{I})\big)\|_{\mathcal{L}_1} \tag{2.86}$$

and

$$b_3 \triangleq \sup_{v \in \mathbb{R}^{m+n}} \|\mathcal{F}_v \circ \mathcal{A}_{\text{sp}} + k(\mathcal{F}_v \circ \mathcal{M}_v + \mathcal{I})\|_{\mathcal{L}_1} \tag{2.87}$$

are both finite. The stability condition in (2.65) implies that $1 - b_1 L_{\rho_{\text{ref}}} > 0$. We conclude that

$$\|(r_{\text{ref}} - r)_\tau\|_{\mathcal{L}_\infty} \leq \frac{b_2}{1 - b_1 L_{\rho_{\text{ref}}}} \|\tilde{r}_\tau\|_{\mathcal{L}_\infty} \tag{2.88}$$

and

$$\|(u_{\text{ref}} - u)_\tau\|_{\mathcal{L}_\infty} \leq \left(\frac{b_2 b_{\mathcal{F}} L_{\rho_{\text{ref}}}}{1 - b_1 L_{\rho_{\text{ref}}}} + b_3 \right) \|\tilde{r}_\tau\|_{\mathcal{L}_\infty}. \tag{2.89}$$

The claim follows by choosing Γ such that the product in (2.88) is strictly less than 1. □

2.4.1 Properties of the proposed control formulation

We note that the components of the proposed control scheme in Eqs. (2.49) and (2.72)-(2.75) do not require any modeling knowledge of the system in Eq. (2.1). The uncertain nonlinearity η in Eq. (2.51) of the robotic system is estimated via the fast adaptation laws (2.74) and (2.75). The controller then drives the sliding variable r defined in Eq. (2.49) close to zero so that the actuated degrees of freedom converge toward their desired values. The presence of the low-pass filters in the adaptive control signal in Eq. (2.73) implies that the proposed controller aims for only partial compensation of the unknown nonlinearity, in order to maintain clean control channels with only low-frequency content. This contradicts traditional adaptive-control algorithms that are always designed toward perfect compensation of the

robot nonlinearity.

In traditional adaptive controllers for manipulators, the degree of adaptation, the robustness against time delays and unmodeled dynamics, and the tracking performance are coupled. The adaptation rate can be significantly boosted by raising the adaptive gain, which in turn improves the response performance. However, high adaptive gain will induce high-frequency signals in the control channels. As a result, the adaptive control system becomes very sensitive to uncertainties and time delay, i.e., loses robustness. In contrast, in the proposed control architecture depicted in Fig. 2.1, the control signal makes use of the estimate for the unknown nonlinearity to partially compensate for this nonlinearity. A low-pass filter is integrated in the control signal to block any high-frequency signal off the control channels and keep them clean and smooth. This filter structure decouples the estimation loop from the control loop and allows for arbitrarily large values of the adaptive gain (limited only by available hardware). In fact, as suggested by the rigorous analysis in [61] for a linear, constant-coefficient, single-input system with an architecture related to that proposed here, the time-delay margin of the adaptive control system is likely bounded away from 0, ensuring guaranteed robustness.

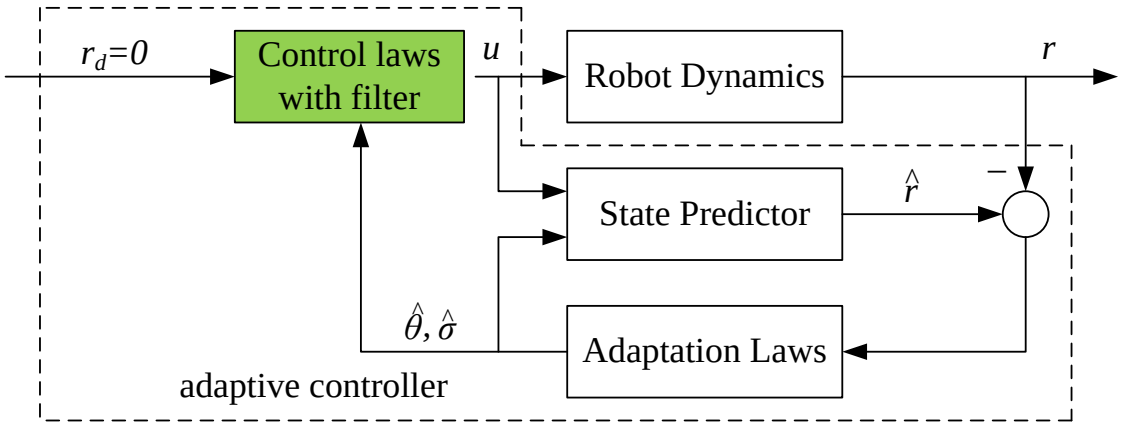

Figure 2.1: Block diagram of the proposed control design.

The characteristics of the proposed adaptive controller are represented by two independent indicators:

1. The adaptive gain Γ, which determines the rate of adaptation, as well as the deviation between the adaptive control system and a nonadaptive reference system governing the ideal response;

2. The filter bandwidth k, which determines the deviation of the ideal response from an exponential decay to 0, as well as the system's ability to tolerate input delay (cf. Sect. 2.5.5).

The objectives of a practical implementation based on the described control design are to choose the parameter values λ, A_m, A_{sp}, Γ, and k in order to achieve desirable performance bounds on the prediction error $\tilde{r}$, as well as to drive r sufficiently close to zero so that q_a approaches the desired value q_{ad} within some desired bound. The adaptive gain Γ and the loop-shaping gain A_{sp} decide the rate of adaptation. The matrix A_m characterizes proportional-derivative feedback terms for fine-tuning the performance.

2.5 Manipulators operating on ships

2.5.1 Simulation model

We restrict attention in this section to a typical pick-and-place manipulator operating on a ship in a high sea state, a scenario also investigated in [41, 42, 43, 44]. The system is sketched in Fig. 2.2, in which $w := (\mathbf{w}_1, \mathbf{w}_2, \mathbf{w}_3)$ is an inertial reference triad (with gravity along the negative $\mathbf{w}_3$-axis) and $b := (\mathbf{b}_1, \mathbf{b}_2, \mathbf{b}_3)$ is a triad rigidly attached to the ship. We restrict attention to motions of the ship described by $(\phi_b,\ x_b,\ z_b)$, where ϕ_b represents the rolling angle of the ship (i.e., the rotation of w about $\mathbf{w}_3$ that yields b), and x_b and z_b represent the displacement of the ship's center of mass C_{ship} relative to the inertial reference frame along $\mathbf{w}_1$ and $\mathbf{w}_3$, respectively. These motions are caused by the unknown influence of surface winds, waves, and ocean currents. Joint A connecting link 1 to the ship has two degrees of freedom represented by two triads: $a := (\mathbf{a}_1, \mathbf{a}_2, \mathbf{a}_3)$ is obtained by rotating b an angle q_3

about $\mathbf{b}_3$ and $l^{(1)} = \left(\mathbf{l}_1^{(1)}, \mathbf{l}_2^{(1)}, \mathbf{l}_3^{(1)}\right)$, attached to link 1, is obtained by rotating a an angle q_1 about $\mathbf{a}_1$. The position of the joint A of the manipulator is represented by the position vector $\mathbf{r}^{C_{\text{ship}}A} := d_A \mathbf{b}_1$. The triad $l^{(2)} = \left(\mathbf{l}_1^{(2)}, \mathbf{l}_2^{(2)}, \mathbf{l}_3^{(2)}\right)$, attached to link 2, is obtained by rotating $l^{(1)}$ an angle q_2 about $\mathbf{l}_1^{(1)}$. The relative joint angles q_1, q_2, and q_3 describe the configuration of the manipulator links relative to the platform. Points B, C_1, C_2, and E represent the joint connecting links 1 and 2, the centers of mass of links 1 and 2, and the location of the payload at the end-effector, respectively, such that $\mathbf{r}^{AB} := L_1 \mathbf{l}_3^{(1)}$, $\mathbf{r}^{BE} := L_2 \mathbf{l}_3^{(2)}$.

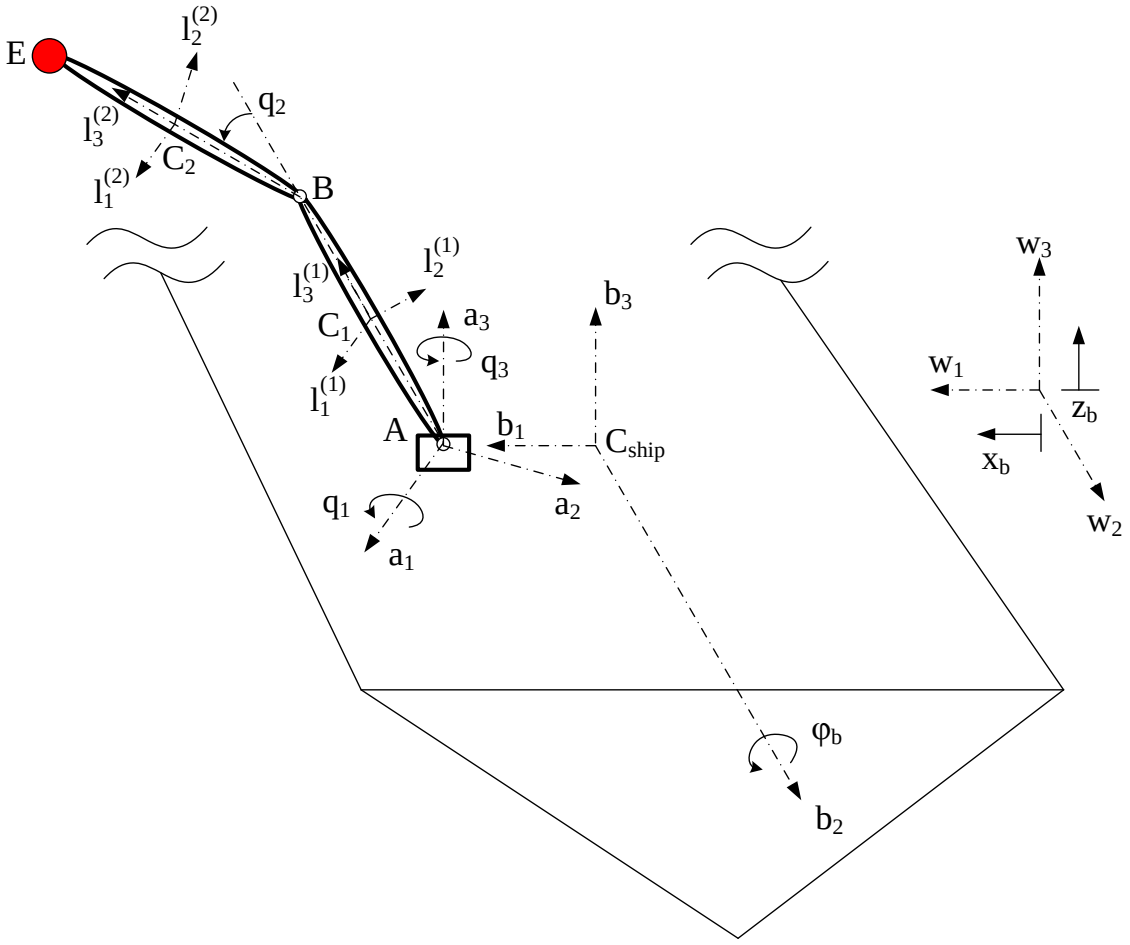

Figure 2.2: A pick-and-place manipulator mounted on a ship with uncertain dynamics.

We model the platform as a body with mass m_{ship} and moment of inertia about the $\mathbf{w}_2$ axis equal to J_{ship}. A linear spring-mass-damper model is used to describe partially the dynamic interaction between the sea and the ship with effective stiffness and damping coefficient given

by K_ϕ and C_ϕ for the ship rolling angle ϕ_b, by K_x and C_x for the displacement x_b, and by K_z and C_z for the displacement z_b. In each case, the reference value equals 0. The masses of links 1 and 2 and the payload at the end-effector are m_1, m_2 and m_e, respectively. The links are assumed to be homogeneous cylinders with radius equal to one fifth of the corresponding length.

With this system set-up, the total kinetic energy is

$$
\begin{aligned}
T = \; & 0.5(J_1 + J_2 + L_1^2\hat{m}_4 + L_2^2\hat{m}_5 + 2L_1L_2\hat{m}_2c_2)\dot{q}_1^2 + 0.5(J_2 + L_2^2\hat{m}_5)\dot{q}_2^2 + 0.25\big(J_1 + J_{1p} + J_2 \\
& + J_{2p} + L_1^2\hat{m}_4 + L_2^2\hat{m}_5 - (J_1 - J_{1p} + L_1^2\hat{m}_4)c_{1_2}^2 + 2L_1L_2\hat{m}_2c_2 - (J_2 + J_{2p} - L_2^2\hat{m}_5)c_{1_2 2_2} \\
& - 2L_1L_2\hat{m}_2c_{1_2 2}^2\big)\dot{q}_3^2 + \Big(0.5J_{\text{ship}} + L_1L_2\hat{m}_2c_1c_{12} + 0.25c_1^2(J_1 + 2L_1^2\hat{m}_4 + J_1c_{3_2}) + 0.25c_{12}^2 \\
& (J_2 + L_2^2\hat{m}_2 + J_2c_{3_2}) + 0.5d_A^2\hat{m}_3c_b^2 + 0.5c_3^2(J_{1p}s_1^2 + J_{2p}s_{12}^2) + d_AL_1c_b^2s_1s_3\hat{m}_1 + d_AL_2c_b^2 \\
& s_{12}s_3\hat{m}_2 + 0.5s_3^2(J_1 + J_2 + L_1^2c_b^2s_1^2\hat{m}_4) + 0.5c_b^2s_1s_{12}s_3^2(2L_1L_2\hat{m}_2 + L_2^2\hat{m}_5) + s_b^2\big(0.5d_A^2\hat{m}_3 \\
& + d_AL_1s_1s_3\hat{m}_1 + d_AL_2s_{12}s_3\hat{m}_2 + s_3^2(0.5L_1^2s_1^2\hat{m}_4 + L_1L_2s_1s_{12}\hat{m}_2 + 0.5L_2^2s_{12}^2\hat{m}_5)\big)\Big)\dot{\phi}_b^2 + \\
& 0.5\hat{m}_3(\dot{x}_b^2 + \dot{z}_b^2) + \big(L_1\hat{m}_1c_1c_b + L_2\hat{m}_2c_{12}c_b - (d_A\hat{m}_3 + L_1\hat{m}_1s_1s_3 + L_2\hat{m}_2s_{12}s_3)s_b\big)\dot{x}_b\dot{\phi}_b \\
& - \big(c_b(d_A\hat{m}_3 + L_1\hat{m}_1s_1s_3 + L_2\hat{m}_2s_{12}s_3) + (L_1c_1\hat{m}_1 + L_2\hat{m}_2c_{12})s_b\big)\dot{z}_b\dot{\phi}_b + c_3\dot{q}_3\big(c_b(L_1\hat{m}_1s_1 \\
& + L_2\hat{m}_2s_{12})\dot{x}_b - (L_1\hat{m}_1s_1 + L_2\hat{m}_2s_{12})s_b\dot{z}_b + \big(0.5(J_1 - J_{1p} + L_1^2\hat{m}_4)s_{1_2} + 0.5(J_2 - J_{2p} \\
& + L_2^2\hat{m}_5)s_{1_2 2_2} + L_1L_2\hat{m}_2s_{1_2 2}\big)\dot{\phi}_b\big) + \dot{q}_1\Big(\big(J_2 + L_2^2\hat{m}_5 + L_1L_2\hat{m}_2c_2)\dot{q}_2 + \big(s_1(-L_2\hat{m}_2c_bs_2s_3 \\
& - (L_1\hat{m}_1 + L_2\hat{m}_2c_2)s_b) + c_1((L_1\hat{m}_1 + L_2\hat{m}_2c_2)c_bs_3 - L_2\hat{m}_2s_2s_b)\big)\dot{x}_b - (-L_1\hat{m}_1c_bs_1 \\
& - L_2\hat{m}_2(c_2c_bs_1 + c_1c_bs_2 + c_1c_2s_3s_b - s_1s_2s_3s_b) - L_1\hat{m}_1c_1s_3s_b)\dot{z}_b + \big(d_AL_1\hat{m}_1s_1 + \\
& d_AL_2\hat{m}_2s_{12} + (J_1 + J_2 + L_1^2\hat{m}_4 + L_2^2\hat{m}_5)s_3 + 2L_1L_2\hat{m}_2c_2s_3\big)\dot{\phi}_b\Big) + \dot{q}_2\Big(L_2\big(-\hat{m}_2s_1 \\
& (c_bs_2s_3 + c_2s_b) + c_1(\hat{m}_2c_2c_bs_3 - \hat{m}_2s_2s_b)\big)\dot{x}_b + L_2\big(-\hat{m}_2c_2(c_bs_1 + c_1s_3s_b) + s_2(-\hat{m}_2c_1c_b \\
& + \hat{m}_2s_1s_3s_b)\big)\dot{z}_b + (d_AL_2\hat{m}_2c_1s_2 + (J_2 + L_2^2\hat{m}_5)s_3 + L_2\hat{m}_2c_2(d_As_1 + L_1s_3))\dot{\phi}_b\Big). \quad (2.90)
\end{aligned}
$$

The total potential energy is

$$U = g(L_1\hat{m}_1 c_1 c_b + L_2\hat{m}_2 c_{12} c_b - d_A(m_1 + m_2 + m_e)s_b + \hat{m}_3 z_b) + 0.5(K_\phi \phi_b^2 + K_x x_b^2 + K_z z_b^2). \tag{2.91}$$

The corresponding nonconservative generalized forces are

$$F_q = [u_1 + D_{aa,1},\ u_2 + D_{aa,2},\ u_3 + D_{aa,3}, -C_\phi \dot{\phi}_b + D_{uu,1}, -C_x \dot{x}_b + D_{uu,2}, -C_z \dot{z}_b + D_{uu,3}]. \tag{2.92}$$

Here, $\hat{m}_1 = 0.5m_1 + m_2 + m_e$, $\hat{m}_2 = 0.5m_2 + m_e$, $\hat{m}_3 = m_1 + m_2 + m_e + m_{\text{ship}}$, $\hat{m}_4 = 0.25m_1 + m_2 + m_e$, $\hat{m}_5 = 0.25m_2 + m_e$, $c_b = \cos\phi_b$, $c_i = \cos q_i$, $c_{i_k j} = \cos(kq_i + q_j)$, and so on.

The equations of motion are obtained from Lagrange's equations. The equations of motion are of the exact form in Eq. (2.1) with the actuated degrees of freedom $q_a = [q_1, q_2, q_3]$ and the unactuated degrees of freedom $q_u = [\phi_b, x_b, z_b]$. In these equations, the ship's mass and moment of inertia matrix, as well as the effective stiffnesses and damping coefficients along the ship's degrees of freedom, only appear in the M_{uu}, C_u and G_u components. In this particular case study, on the one hand, since the mass and size of the ship are significantly larger than those of the manipulator, the dominance of these terms in the bottom part of Eq. (2.1) implies that the motions of the manipulator have very little effect on the ship's dynamics. On the other hand, the ship's motions enter the top part of Eq. (2.1) not only via the components of the mass matrices M_{aa} and M_{au}, but also through nonlinearity contributions to the acceleration-dependent terms with the same magnitude of influence as the manipulator's dynamics.

In the numerical results reported below, and in a set of consistent units (the SI system is used throughout the dissertation), the link lengths, the masses of the two links, the payload at the end-effector, and the acceleration of gravity are given by $L_1 = 0.25$; $L_2 =$

0.2; $m_1 = 6$; $m_2 = 4$; $m_e = 5$; $g = 9.81$. The distance between C_{ship} and A is $d_A = 3$. The ship's effective mass and moment of inertia about the $\mathbf{w}_2$-axis equal $m_{\text{ship}} = 10^5$ and $J_{\text{ship}} = 1.25 \times 10^5$. The effective stiffnesses and damping coefficients parameterizing the dynamic interaction between the sea and the ship are given by $K_\phi = 10^7$, $K_x = 3\times10^5$, $K_z = 3 \times 10^5$, $C_\phi = 10^8$, $C_x = 2 \times 10^5$, and $C_z = 2 \times 10^5$. The disturbances from the environment are assumed to be given by

$$D_{uu}(t) = \begin{bmatrix} 3 \times 10^7 \sin(0.5t) \\ 3 \times 10^5 \sin(0.5t) \\ -3 \times 10^5 \cos(0.5t) \end{bmatrix} \tag{2.93}$$

and $D_{aa}(t) = 0$. A typical ship motion that results from numerical simulation is shown in Fig. 2.3. The peak-to-peak amplitudes of the ship's displacement are approximately 2 m in both the horizontal and vertical directions, and 76 degrees in the rolling angle ϕ_b. These motions contribute large unknown time-varying inertias and nonlinearity terms to the description of the manipulator dynamics.

2.5.2 Control objectives

We begin by illustrating the performance of the control design when the manipulator's joint angles are tasked to track desired trajectories given by

- step inputs with $q_{1,d}(t) = q_{2,d}(t) = q_{3,d}(t) \equiv \alpha$, for values of $\alpha \in [1, 2]$, with initial conditions $q_0 = \dot{q}_0 = (0, 0, 0)^T$; and
- sinusoidal inputs with $q_{1,d}(t) = q_{2,d}(t) = \sin 0.4t$ and $q_{3,d}(t) = \cos 0.4t$ with initial conditions $q_0 = (0.5, 0.5, 0.5)^T$ and $\dot{q}_0 = (0, 0, 0)^T$.

In the simulations in this chapter, the control parameters and the filters are tuned to the following control objectives:

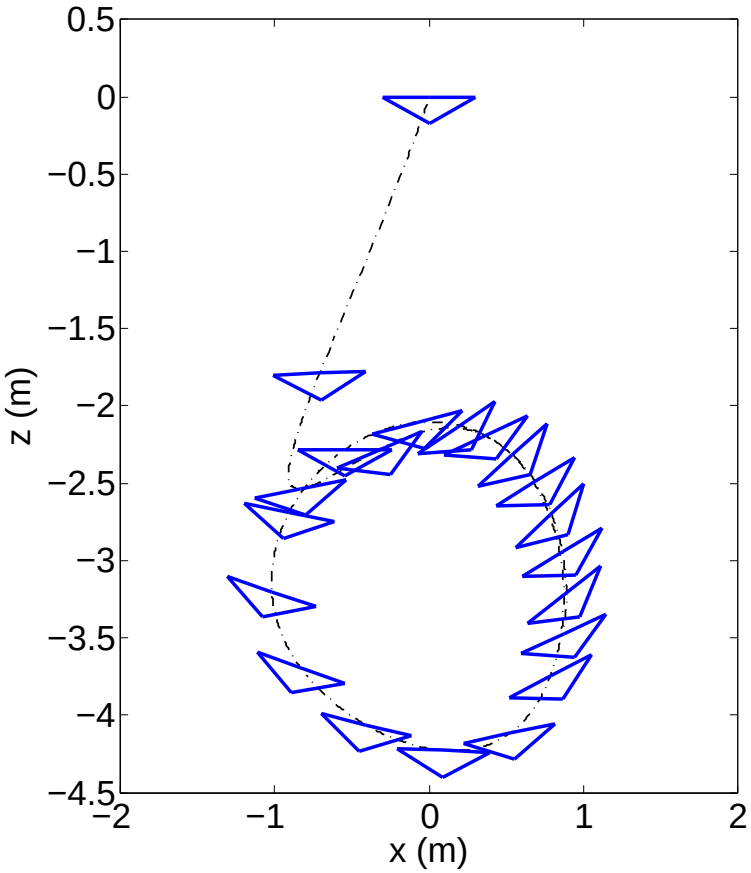

Figure 2.3: Typical oscillations of the ship under prescribed environmental disturbances.

- In the case of the step inputs, achieve a response settling time (the time required for the response to reach and stay within 2% of the final value) of less than 3 s, with maximum overshoot less than 5% of the desired values.

- In the case of the sinusoidal inputs, achieve a root-mean-square deviation percentage (denoted below by RMSD%) of less than 5% under various disturbances, including time delay and measurement noise. Here, RMSD% is defined as the percentage of a response's root-mean-square deviation from its desirable trajectory over the time history relative to the peak-to-peak amplitude of the desired trajectory.

To achieve these objectives, the parameter λ in Eq. (2.49) is here set to 2, the adaptive gain Γ is set to 10^6, and the tracking response characteristics are governed by the design matrix $A_m = -\text{diag}(30, 20, 15)$. The filter bandwidth k in (2.73) is set to 10 (Hz). The matrix of

loop-shaping parameters A_{sp} in Eq. (2.72) is set to $0.1\sqrt{\Gamma\mathbb{I}}$. In the projection based adaptive laws in Eqs. (2.74)-(2.75), we set $\theta_b = \sigma_b = 100$, $\epsilon = 0.1$, and $\hat{\theta}_0 = \hat{\sigma}_0 = 0$.

The numerical results below were obtained from a Simulink-based implementation of the system's equations of motion and the proposed control scheme. Default Simulink tolerances and settings were used throughout.

2.5.3 Performance in ideal working conditions

Figs. 2.4 and 2.5 show the manipulator's response to the proposed control actuation for step inputs with different values of α and for the sinusoidal input, respectively. As seen in the bottom panels, for both types of desired trajectories, the control signals are smooth and clean, in spite of the use of high-rate adaptive estimation to accommodate nonlinearity and model uncertainty while retaining small prediction errors. For the step input, the maximum overshoot is 4.1%, and the maximum settling time is 2.76 s. As seen in Fig. 2.4, the system response scales approximately with the size of the step. This implies predictable responses of the proposed adaptive control system when the desired values are varied. For the sinusoidal input in Fig. 2.5, the maximum tracking RMSD% is 3.64%. The system responses quickly converge to the desired time histories despite the large inertia and nonlinearity added due to the unmodeled dynamics of the ship. Consistent with the theory discussed in the previous sections, an increase in the filter bandwidth results in improved tracking performance, i.e., reduced tracking RMSD%. However, better tracking is achieved with the trade-off of the system robustness, i.e., the adaptive control system is less tolerant of time delays in the control signal.

2.5.4 Control performance with time delay and measurement noise

Next, we consider the performance of the adaptive control system in the presence of velocity measurement noise, with a time delay of 50 ms in the control signal. To this end, unfiltered,

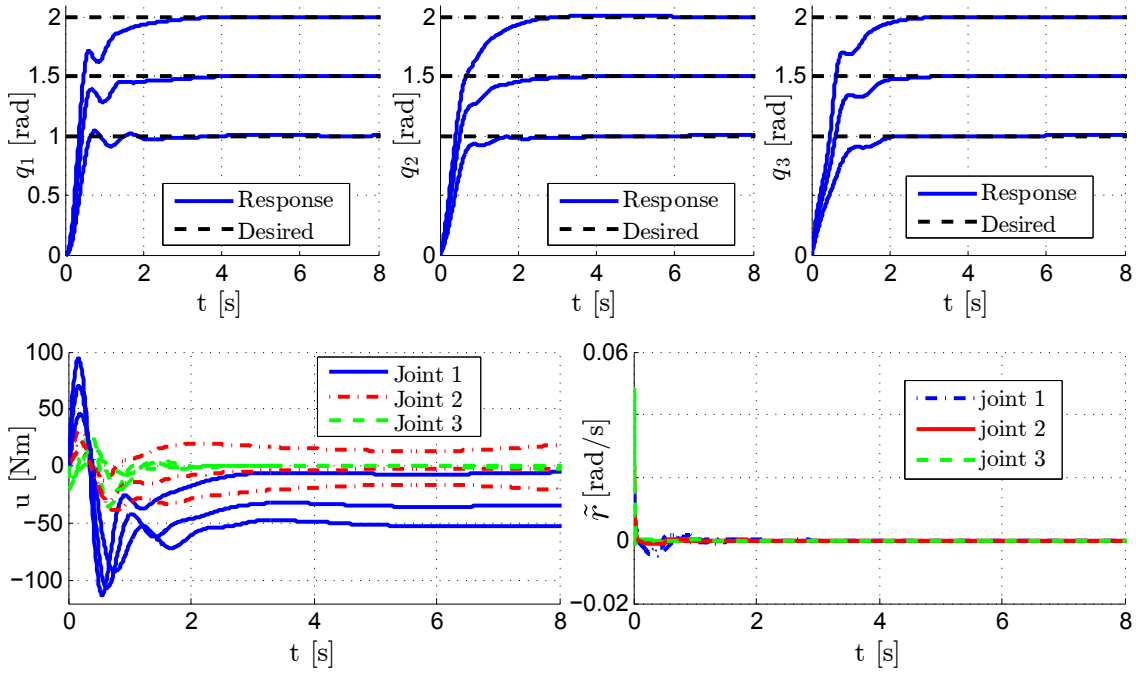

Figure 2.4: Performance of the proposed controller under ideal working conditions for various step inputs.

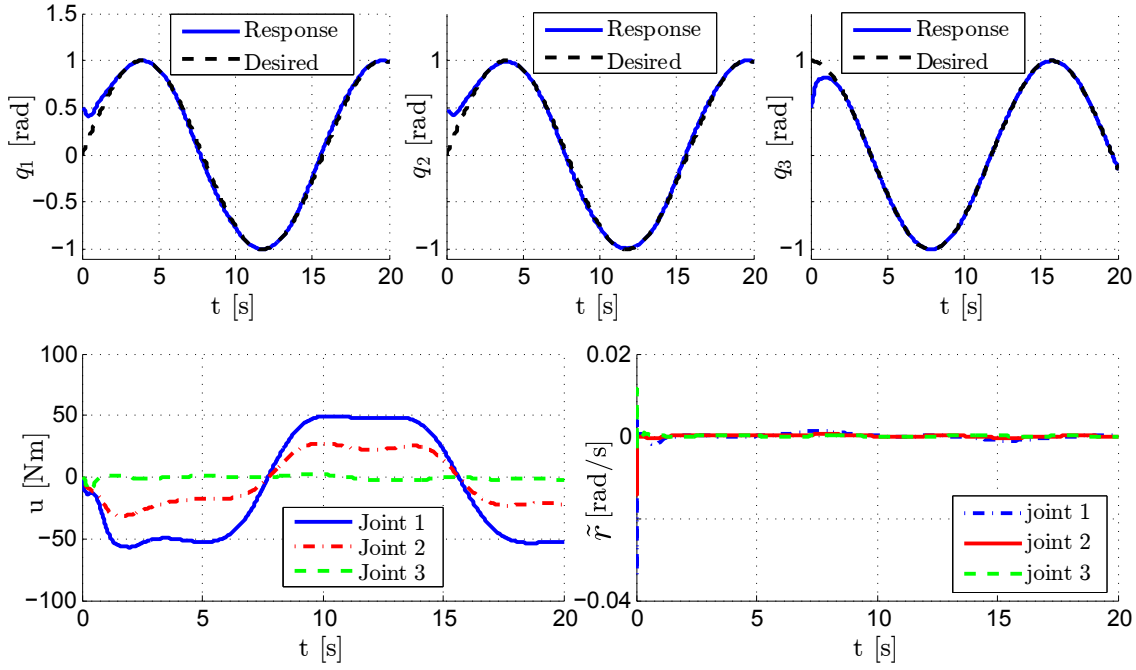

Figure 2.5: Performance of the proposed controller under ideal working conditions for sinusoidal inputs.

uniformly distributed noise in the range $[-0.15, 0.15]$ rad/s and with sample time of 10 ms was added to the angular velocity measurements. This measurement noise is reflected in

the right bottom panel in Fig. 2.6, since the velocity measurements appear explicitly in the definition of r. As seen in this figure, without any further tuning, the proposed adaptive controller successfully rejects the noise. The control scheme still maintains desirable tracking performance with the maximum tracking RMSD% of 4.21%, which is very close the previous case with the time delay in the control signals. This demonstrates the robustness of the proposed controller to noisy measurements. In addition, the control signals are clean and implementable because all the high-frequency and noisy contributions are completely filtered out of the control channel.

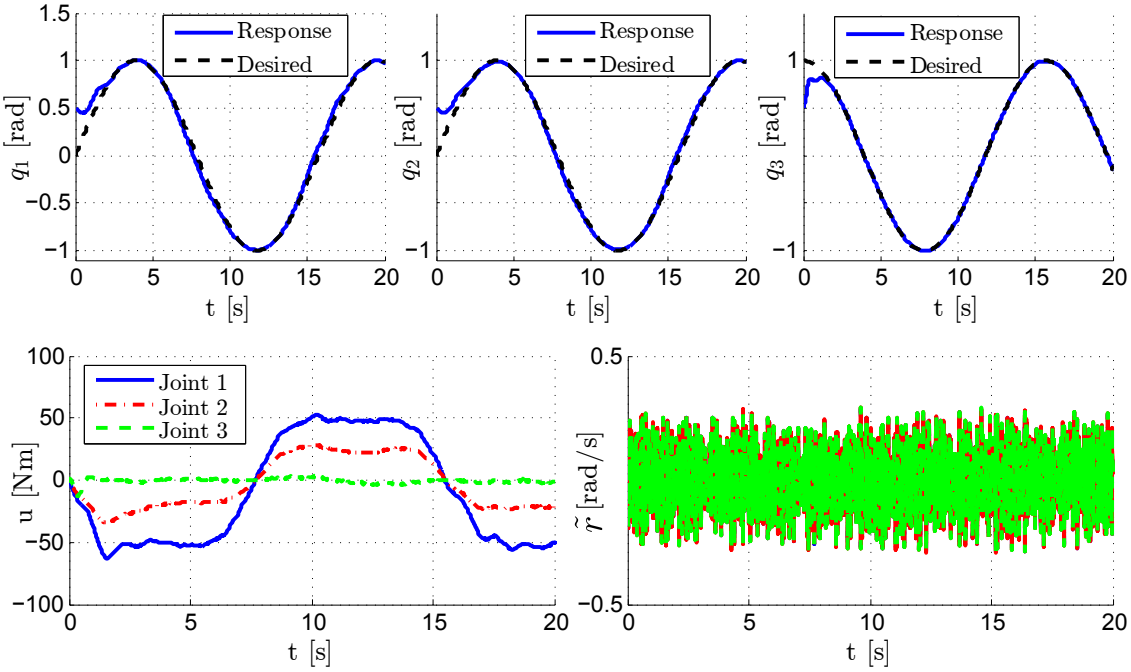

Figure 2.6: Performance of the proposed controller in the presence of 50 ms actuator time delay and velocity measurement noise in the range $[-0.15,\ 0.15]$ rad/s and with sample time of 0.01 s.

2.5.5 Robustness

We proceed to analyze the robustness of the adaptive controller by investigating its performance in the presence of time delays in the control input. It is a well-known property of control systems that the presence of time delay in the control loop may destabilize the

systems (see, for example, [106]). Furthermore, as discussed in [45, 63], any unmodeled dynamics can be equivalently represented by a delay in the plant input. In LTI systems, the phase margin or, alternatively, the time-delay margin are reliable indicators of the system robustness [59]. In nonlinear control systems, since the phase margin is not computable, we need an alternative method for checking the system's robustness, i.e., its ability to tolerate input delay [45, 121]. In this chapter, we define the *critical time delay* as the maximum input delay for which the controller is able to maintain bounded performance over a given time interval, for each choice of system parameters and desired trajectory $q_d(t)$. Consistent with the literature, we use the critical time delay for some representative trajectory as an indicator of the system robustness.

In order to numerically estimate the critical time delay, we replace $u(t)$ in Eq. (2.1), and in the definition of μ preceding Eq. (2.50), by $u(t-d)$, and let $q_d(t)$ be given by the constant trajectory $(1, 1, 1)$. For each choice of parameter values, define the critical time delay d_{crit} as the largest value of d for which $\|q_a(t)\|_\infty < 10$ for $t \in [0, 20]$. Groups of discrete estimates of d_{crit} are shown in Fig. 2.7 for $k = 10$, 20, 30, and 40 Hz. For purposes of comparison, the figure includes estimated values of d_{crit} in the case that Eq. (2.73) is replaced by the unfiltered form $u(t) = -\hat{\theta}(t)\|r_t\|_{\mathcal{L}_\infty} - \hat{\sigma}(t)$, in which case the control structure is that of an indirect model-reference controller, popular in adaptive control of nonlinear systems. The results show that increasing the filter bandwidth deteriorates the system robustness to delay. For finite bandwidth, the critical time delay remains well above zero across the entire range of adaptive gains and shows no sign of deteriorating as $\Gamma \to \infty$. In contrast, for the case of the traditional model-reference controller, the critical time delay is close to zero ($\sim 10^{-3}$) for the entire range of the adaptive gain. This is consistent with the fact that model-reference controllers have zero robustness margin in the sense of the gap metric [45, 39], and are therefore expected to exhibit limited robustness to input delay for any given desired trajectory.

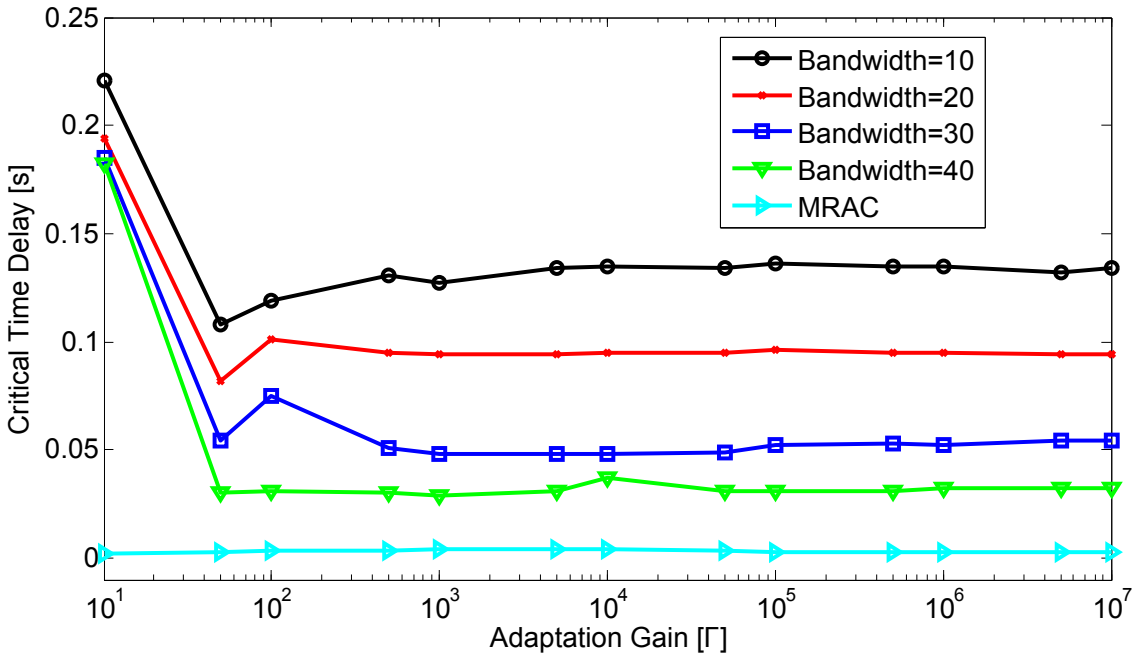

Figure 2.7: The dependence of the critical time delay on the adaptation rate for different values of filter bandwidth. The values of d_{crit} for case of finite bandwidth are obtained with a roundoff error of $\pm 5 \times 10^{-4}$. In the case of the model-reference controller (corresponding to infinite filter bandwidth), the roundoff error is $\pm 5 \times 10^{-5}$.

2.6 Mobile manipulators with suspension systems moving on rough terrains

The case study in the previous section considers a practical situation of a manipulator mounted on a ship operating in a high-sea state under uncertain environmental disturbances. The unactuated dynamics of the ship and the actuated dynamics of the manipulator are coupled in such a way that the unmodeled ship motions add very large time-varying inertia and nonlinearity to the description of the manipulator dynamics. However, since the mass of the manipulator is significantly smaller than that of the ship, its motions have little effect on those of the ship.

In this section, we consider the context of a mobile manipulator for which the unactuated and actuated dynamics are *strongly* coupled. In addition, the platform oscillates with much higher frequency than in the case of the ship, as the disturbances from a rough terrain are transmitted to the platform via a suspension. In the control design, we again consider

the system dynamics as being completely unmodeled. A slight twist is the inclusion of a nonholonomic constraint on the platform kinematics.

2.6.1 Dynamics of a mobile manipulator

The model of a mobile manipulator of interest is sketched in Fig. 2.8, in which $w := (\mathbf{w}_1, \mathbf{w}_2, \mathbf{w}_3)$ is an inertial reference triad and the triad $b := (\mathbf{b}_1, \mathbf{b}_2, \mathbf{b}_3)$ is obtained by rotating w an angle ϕ_h about the vertical axis $\mathbf{w}_3$. The position of the platform's center of mass B relative to the inertial reference frame is represented by the displacements x_v and y_v along $\mathbf{w}_1$ and $\mathbf{w}_2$, respectively. The triad $a := (\mathbf{a}_1, \mathbf{a}_2, \mathbf{a}_3)$, attached to the platform, is obtained by rotating b an angle ϕ_p about $\mathbf{b}_2$. The point A represents the joint connecting link 1 of the manipulator to the platform, such that $\mathbf{r}^{BA} := L_{BA}\mathbf{a}_1$. The triad $l^{(1)} := \left(\mathbf{l}_1^{(1)}, \mathbf{l}_2^{(1)}, \mathbf{l}_3^{(1)}\right)$, attached to link 1, is obtained by rotating a an angle q_1 about $\mathbf{a}_2$. The triad $l^{(2)} := \left(\mathbf{l}_1^{(2)}, \mathbf{l}_2^{(2)}, \mathbf{l}_3^{(2)}\right)$, attached to link 2, is obtained by rotating $l^{(1)}$ an angle q_2 about $\mathbf{l}_2^{(1)}$. Points D, C_1, C_2, and E represent the joint connecting links 1 and 2, the centers of mass of links 1 and 2, and the location of the payload at the end-effector, respectively, such that $\mathbf{r}^{AD} := L_1\mathbf{l}_3^{(1)}$, $\mathbf{r}^{DE} := L_2\mathbf{l}_3^{(2)}$.

From this set-up, relative to the platform, the manipulator has two degrees of freedom, represented by the relative joint angles q_1 and q_2. The configuration of the platform relative to the inertial reference frame is described by the position coordinates x_v and y_v, the heading angle ϕ_h, and the pitching angle ϕ_p. The platform is attached to the chassis of a rover via a suspension system to smooth oscillations of the platform that might be induced by an uneven terrain. The chassis' configuration relative to the inertial frame is assumed to be identical to that of the platform other than in its pitching angle, which is here assumed to be an explicit function of time that is unknown to the control design. Finally, the motion of the chassis is constrained in such a way that the velocity of the platform's center of mass is perpendicular to the axis of the driving wheels, i.e., parallel to $\mathbf{b}_1$.

We assume generalized forces associated with the q_1 and q_2 degrees of freedom, given by the

control torques u_1 and u_2 applied at the joints A and D, respectively. Under the assumption that the pitching motion of the platform is unactuated, the generalized force corresponding to ϕ_p equals 0. The generalized forces corresponding to the remaining degrees of freedom, x_v, y_v, and ϕ_h, are assumed to be obtained from a matrix product $B(q_v)u_v$. Here, the control input u_v may be parameterized by two independent control signals representing, for example, the torques applied to the left and right driving wheels, respectively. The resultant expression for the kinetic potential energy is

$$\begin{aligned} T = \; & 0.5(J_1 + J_2 + L_2^2\hat{m}_5 + L_1^2\hat{m}_4 + 2L_1L_2\hat{m}_2c_2)\dot{q}_1^2 + 0.5(J_2 + L_2^2\hat{m}_5)\dot{q}_2^2 + 0.25\big(J_1 + J_{1p} + J_2 \\ & + J_{2p} + J_h + L_{BA}^2\hat{m}_6 + L_2^2\hat{m}_5 + L_1^2\hat{m}_4 + (J_h + L_{BA}^2\hat{m}_6)c_{p_2} - (J_1 - J_{1p} + L_1^2\hat{m}_4)c_{1_2p_2} + \\ & 2L_1L_2\hat{m}_2c_2 - (J_2 - J_{2p} + 0.25L_2^2m_2)c_{1_2{2_2}p_2} - (L_2^2m_e + 2L_1L_2\hat{m}_2)c_{1_2{2_2}p_2} + 2L_1L_{BA}\hat{m}_7(s_1 \\ & + s_{1p_2}) + L_2L_{BA}m_2(s_{12} + s_{12p_2})\big)\dot{\phi}_h^2 + 0.5\big(J_1 + J_2 + J_p + L_{BA}^2\hat{m}_6 + L_2^2\hat{m}_5 + L_1^2\hat{m}_4 + \\ & 2L_1L_2\hat{m}_2c_2 + 2L_{BA}(L_1\hat{m}_7s_1 + L_2m_2s_{12})\big)\dot{\phi}_p^2 + 0.5\hat{m}_8(\dot{x}_b^2 + \dot{y}_b^2) + (J_2 + L_2^2\hat{m}_5 + L_1L_2\hat{m}_2 \\ & c_2)\dot{q}_1\dot{q}_2 + \dot{\phi}_p\Big(\big(J_1 + J_2 + L_2^2\hat{m}_5 + L_1^2\hat{m}_4 + 2L_1L_2\hat{m}_2c_2 + L_{BA}(L_1\hat{m}_7s_1 + 0.5L_2m_2s_{12})\big)\dot{q}_1 \\ & + (J_2 + L_2^2\hat{m}_5 + L_1L_2\hat{m}_2c_2 + 0.5L_2L_{BA}m_2s_{12})\dot{q}_2\Big) + c_h\Big(\big((L_1\hat{m}_1c_{1p} + L_2\hat{m}_2c_{12p} - L_{BA} \\ & \hat{m}_6s_p)\dot{\phi}_p + (L_1\hat{m}_1c_{1p} + L_2\hat{m}_2c_{12p})\dot{q}_1 + L_2\hat{m}_2c_{12p}\dot{q}_2\big)\dot{x}_b + (L_{BA}\hat{m}_6c_p + L_1\hat{m}_1s_{1p} + L_2\hat{m}_2 \\ & s_{12p})\dot{\phi}_h\dot{y}_b\Big) + s_h\big((-L_{BA}\hat{m}_6c_p - L_1\hat{m}_1s_{1p} + L_2\hat{m}_2s_{12p})\dot{\phi}_h\dot{x}_b + ((L_1\hat{m}_1c_{1p} + L_2\hat{m}_2c_{12p} - \\ & L_{BA}\hat{m}_6s_p)\dot{\phi}_p + (L_1\hat{m}_1c_{1p} + L_2\hat{m}_2c_{12p})\dot{q}_1 + L_2\hat{m}_2c_{12p}\dot{q}_2)\dot{y}_b\big). \end{aligned} \tag{2.94}$$

The total potential energy is

$$U = 0.5K_p\phi_p^2 + g(c_p(L_1\hat{m}_1c_1 + L_2\hat{m}_2c_{12}) - 3L_{BA}m_es_p). \tag{2.95}$$

The corresponding nonconservative generalized forces are

$$F_q = [u_1 + D_{rr,1},\ u_2 + D_{rr,2},\ \ -C_p\dot{\phi}_p + D_{rr,3},\ \frac{b}{2r_w}(u_r - u_l) + D_{pp,1},$$
$$\frac{\cos\phi_h}{r_w}(u_r + u_l) - \sin\phi_h\ell + D_{pp,2},\ \frac{\sin\phi_h}{r_w}(u_r + u_l) + \cos\phi_h\ell + D_{pp,3}]. \tag{2.96}$$

Here, $\hat{m}_1$ through $\hat{m}_5$ are defined in the same way as before, and $\hat{m}_6 = m_1 + m_2$, $\hat{m}_7 = 0.5m_1 + m_2$, $\hat{m}_8 = m_1 + m_2 + m_e + m_b$. The quantity ℓ is the Lagrange multiplier associated with the nonholonomic constraint, u_r and u_l are the input torques to the right and left wheels, respectively, $r_w = 0.1$ is the driving wheel's radius, and $b = 0.5$ is the width of the platform.

The equations of motion are obtained from Lagrange's and take the form

$$\begin{bmatrix} M_{rr}(q) & M_{rv}(q) \\ M_{rv}^T(q) & M_{vv}(q) \end{bmatrix} \begin{bmatrix} \ddot{q}_r \\ \ddot{q}_v \end{bmatrix} + \begin{bmatrix} N_{rr}(q,\dot{q}) \\ N_{vv}(q,\dot{q}) \end{bmatrix} = \begin{bmatrix} u_r \\ B(q_v)u_v \end{bmatrix} + \begin{bmatrix} 0 \\ A^T(\phi_h)l \end{bmatrix} + \begin{bmatrix} D_{rr} \\ D_{pp} \end{bmatrix}, \tag{2.97}$$

where $u_r = [u_1, u_2, 0]^T$, $A(\phi_h)$ is the coefficient matrix of $\dot{q}_v$ in the velocity constraint, and l is the corresponding Lagrange multiplier. It follows that the system has six geometric degrees of freedom and five dynamic degrees of freedom. In the control design below, the unactuated pitching angle ϕ_p is assumed to be a bounded function of time.

A popular reduction method is employed to convert the lower part of Eq. (2.97) for the rover's locomotion to equations in independent coordinates (see, e.g., [18]). Let s denote the speed of the rover in the direction of motion and consider the vector $v \triangleq [s, \dot{\phi}_h]^T$. The allowable motions of the rover may then be described by the relationship

$$\dot{q}_v = S(\phi_h)v, \tag{2.98}$$

where $S(\phi_h)$ is a full-rank matrix, whose columns are a smooth basis for the null space of

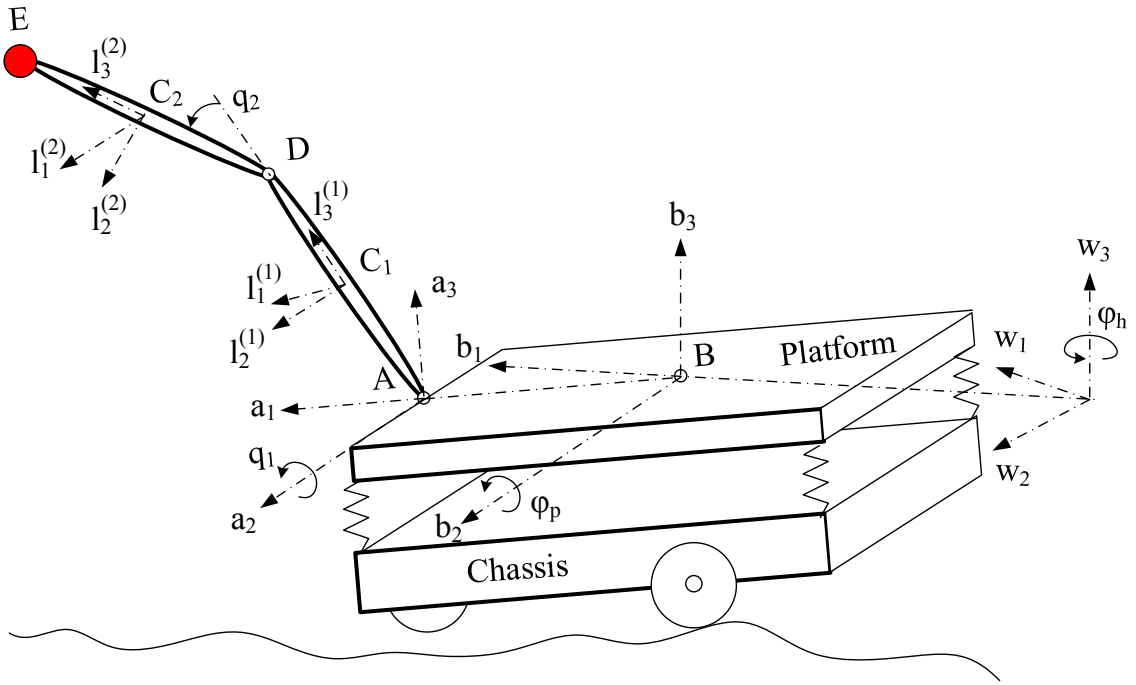

Figure 2.8: A mobile manipulator mounted on a platform suspended from a chassis moving across an uneven terrain.

$A(\phi_h)$. Since $S^T(\phi_h)S(\phi_h)$ is invertible by construction, it follows that

$$v = \Big(S^T(\phi_h)S(\phi_h)\Big)^{-1} S^T(\phi_h)\dot{q}_v. \tag{2.99}$$

Substitution into the equations of motion and multiplication of the bottom part with $S^T(\phi_h)$ then yields

$$\begin{bmatrix} M_{rr}(q) & M_{rv}(q)S(\phi_h) \\ S^T(\phi_h)M_{rv}^T(q) & S^T(\phi_h)M_{vv}(q)S(\phi_h) \end{bmatrix} \begin{bmatrix} \ddot{q}_r \\ \dot{v} \end{bmatrix} + \begin{bmatrix} N_{rr}(q,\dot{q}) \\ S^T(\phi_h)N_{vv}(q,\dot{q}) \end{bmatrix} = \begin{bmatrix} u_r \\ \bar{u}_v \end{bmatrix} + \begin{bmatrix} D_{rr} \\ S^T(\phi_h)D_{pp} \end{bmatrix} \tag{2.100}$$

where the components of $\bar{u}_v \triangleq S^T(\phi_h)B(q_a)u_v$ correspond to independent control inputs for the speed and rate of change of heading of the rover.

From a state-space representation point of view, the description of the kinematics in

terms of 12 states (six position coordinates and six velocity coordinates) in Eq. (2.97) with one nonholonomic velocity constraint $A(\phi_h)\dot{q}_v = 0$ has been reduced to a system of three second-order differential equations and five first-order equations in eleven states (six position coordinates and five velocity coordinates). To accommodate a control design analogous to that in Sect. 3, we first rearrange Eq. (2.100) to yield (cf. [30])

$$\begin{bmatrix} M_{aa}(q) & M_{as}(q) & M_{au}(q) \\ M_{as}^T(q) & M_{ss}(q) & M_{su}(q) \\ M_{au}^T(q) & M_{su}^T(q) & M_{uu}(q) \end{bmatrix} \begin{bmatrix} \ddot{q}_a \\ \dot{s} \\ \ddot{q}_u \end{bmatrix} + \begin{bmatrix} N_a(q,\dot{q}) \\ N_s(q,\dot{q}) \\ N_u(q,\dot{q}) \end{bmatrix} = \begin{bmatrix} u_a \\ u_s \\ 0 \end{bmatrix} + \begin{bmatrix} D_{aa} \\ D_{ss} \\ D_{uu} \end{bmatrix}, \quad (2.101)$$

where $q_a \triangleq [q_1, q_2, \phi_h]$ and $q_u = \phi_p$. Now let

$$r \triangleq \begin{bmatrix} r_a \\ r_s \end{bmatrix} = \begin{bmatrix} \dot{q}_a - \dot{q}_{\mathrm{ad}} + \lambda(q_a - q_{\mathrm{ad}}) \\ s - s_d \end{bmatrix}. \quad (2.102)$$

Elimination of $\ddot{q}_u$ using the bottom part of Eq. (2.101), and noting the absence of explicit dependence of the equations of motion on x_v and y_v, then again yields

$$\dot{r} = A_m r + M_a^{-1} u + \eta, \quad r(0) = r_0, \quad (2.103)$$

for some functions M_a and $\eta(t,\zeta)$, where $\zeta^T \triangleq [r^T, \chi^T]$ and $\chi \triangleq \left[q_a^T, q_u^T, \dot{q}_u^T\right]$. Here, it follows that

$$\|\chi_t\|_{\mathcal{L}_\infty} \leq \max\{\|q_{a,t}\|_{\mathcal{L}_\infty}, \|q_{u,t}\|_{\mathcal{L}_\infty}, \|\dot{q}_{u,t}\|_{\mathcal{L}_\infty}\}. \quad (2.104)$$

The definition of r in Eq. (2.102) implies

$$\|q_{a,t}\|_{\mathcal{L}_\infty} \leq \left\|(s\mathbb{I} + \lambda)^{-1}\right\|_{\mathcal{L}_1} \|r_{a,t}\|_{\mathcal{L}_\infty} + \left\|q_{\mathrm{ad}}(s) + (s\mathbb{I} + \lambda)^{-1}\big(q_a(0) - q_{\mathrm{ad}}(0)\big)\right\|_{\mathcal{L}_\infty}. \quad (2.105)$$

Now, from Eqs. (2.104) and (2.105) together with the observations that $\|r_{a,t}\|_{\mathcal{L}_\infty} \leq \|r_t\|_{\mathcal{L}_\infty}$ and the assumption that the unactuated degree of freedom is bounded, it follows that there

exist positive numbers Q_1 and Q_2 such that

$$\|\chi_t\|_{\mathcal{L}_\infty} \leq Q_1\|r_t\|_{\mathcal{L}_\infty} + Q_2, \tag{2.106}$$

which is the same inequality as in Eq. (2.20) in 2.2.2.

The remainder of the control design now proceeds as in Sect. 3, bearing in mind the implications of the modified sliding formulation in Eq. (2.102). In particular, the adaptive controller estimates and compensates for the nonlinearity η to drive r to a neighborhood of zero, such that q_a and s converge to the vicinities of the corresponding desired trajectories $q_{\rm ad}$ and s_d. The latter does not, however, guarantee convergence in the position of the rover, since this is not part of the feedback control design.

2.6.2 Numerical results

In the numerical results reported below, the link lengths and the masses of the two manipulator links and the payload are $L_1 = 0.25$, $L_2 = 0.2$, $m_1 = 6$, $m_2 = 5$, and $m_e = 5$, respectively. The mass m_p of the platform equals 20 and the moments of inertia about $\mathbf{a}_1$, $\mathbf{a}_2$ and $\mathbf{a}_3$ are 0.75, 1.75 and 2.5, respectively. The distance between B and A is $L_{BA} = 0.1$. The effective stiffness and damping of the suspension system is $K_p = 50$ and $C_p = 1$, respectively. In addition, $D_{aa}(t) = 0$ and $D_{ss}(t) = 0$, and the disturbance to the platform, due to disturbances to the pitch of the chassis from traversal across rough terrain and transmitted via the suspension system, is assumed to be given by $D_{uu}(t) = 3\sin(5t) + 3\sin(3t)$. As a result, the pitching angle of the platform will have the typical motion given in Fig. 2.9.

The proposed control scheme is implemented for the system dynamics in Eqs. (2.99)-(2.100), without assuming any detailed knowledge of the system model, in order to track a desired trajectory given by the time histories $q_{1d}(t) = \sin(0.4t)$, $q_{2d}(t) = \cos(0.4t)$, $\phi_{hd}(t) = \sin(0.5t) + \cos(0.3t)$, $s_d = 0.5t$, in the presence of velocity measurement noise in the range $[-0.15, 0.15]$ and a time delay of 50 ms in the control signal. The control architecture is

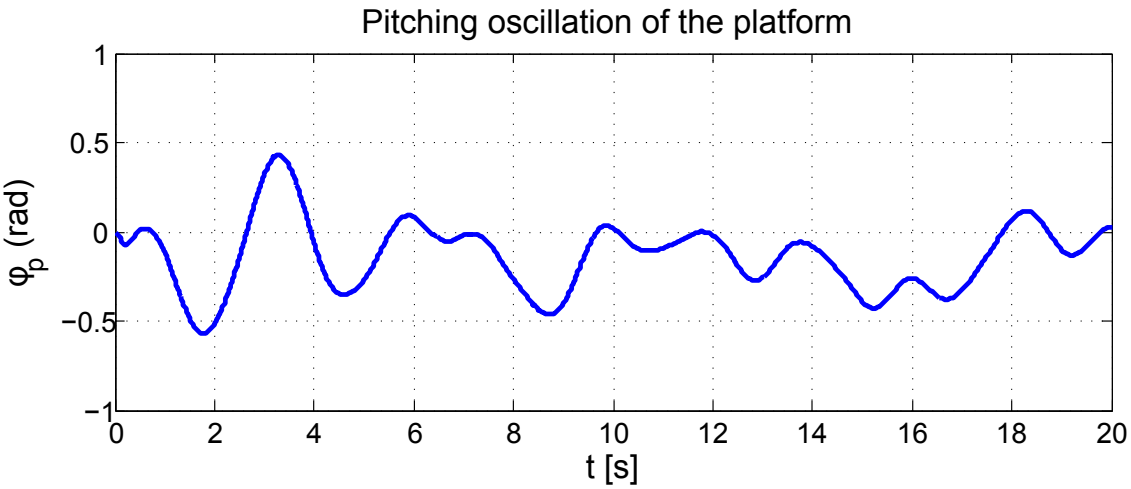

Figure 2.9: Typical pitch angle of the platform during operation.

parameterized by $A_m = \text{diag}(20, 10, 15, 5)$ and the same values of λ, Γ, and k as before. The 4×4 matrix A_{sp} is set to $0.1\sqrt{\Gamma}\mathbb{I}$. With this choice the tracking RMSD% is less than 5% for all relevant degrees of freedom.

The results are shown in Fig. 2.10. The level of measurement noise is reflected by the right bottom panel for the prediction error, which is computed directly using the noisy measured velocity. Despite the time delay and measurement noise, the adaptive control signals remain smooth because high-frequency signals are blocked by the low-pass filter. Here, the high-frequency oscillations in the platform pitching angle, induced by the rough terrain, are evident in the control channels. However, the control objective is still met with the RMSD% for the manipulator's two joints, as well as for the steering angle and the speed of the rover being 4.47%, 4.87%, 3.02% and 2.08%, respectively. It is remarked that this performance is achieved not only in the presence of measurement noise, but also with a delay of 50 ms in the control signal.

2.7 Conclusion

Traditional control architectures employ the linear-in-parameter property of Lagrangian systems to obtain the factorization in Eq. (2.2) in terms of a model regression matrix and a

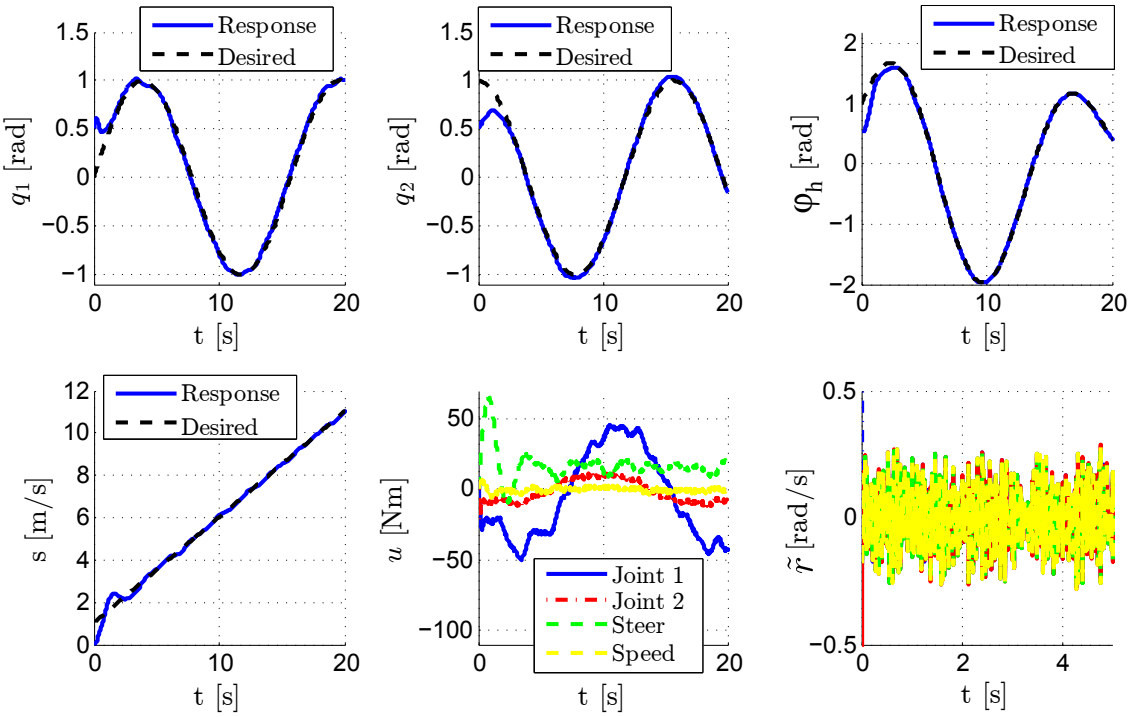

Figure 2.10: Performance of the proposed controller in the presence of 50 ms actuator time delay and velocity measurement noise in the range $[-0.15,\ 0.15]$ rad/s and with sample time of 0.01 s.

vector of unknown parameters, which is to be estimated by relevant adaptive laws, of which Eq. (2.4) is an example. The construction of the regression matrices in Eq. (2.2) requires information about the structure/geometry of the platform such as the position of the platform's center of mass, the platform's moment of inertia, the location of the manipulator relative to the platform center of mass, and so on. If the other dynamic factors, for example the movements of humans or equipment in the platform, is integrated in the equations of motion, then the modeling process to construct such regression matrices may not be feasible.

In contrast, this chapter has described a robust adaptive controller, inspired by the framework proposed in [61] with a low-pass filter in the control input, for an underactuated system of a robot installed on a (moving) platform. The controller does not require the construction of regression matrices, while the dynamics of the entire system are unmodeled. As evidenced by fundamental theoretical results on the existence of computable performance bounds, this framework successfully separates the adaptation loop from the control loop, thereby allowing

for arbitrary increases in the adaptation rate (bounded only by hardware constraints) without sacrificing the system's robustness, and allows for a predictable transient response with smooth and implementable control signals. With the introduction of a variable transformation, inspired by earlier work in [130], and an innovative control design, the formulation is able to compensate for the nonlinearity and uncertainties in the dynamic model without assuming any knowledge of the system modeling.

A limitation of the theoretical analysis in this chapter is that it is restricted to systems where the unactuated degrees of freedom are assumed to be bounded a priori despite being influenced by the actuated degrees of freedom of the system. Examples include mobile manipulators where their platforms are significantly more massive than the manipulators, although satisfactory performance may also result in systems where the two are more strongly coupled as seen in the rover's simulation.

Numerical simulations were used to illustrate the control paradigm in trajectory tracking tasks imposed on two scenarios: (1) a robot arm mounted on a ship operating in a high-sea state, and (2) a mobile manipulator moving across a rough terrain. In the first context, the ship has three unactuated degrees of freedom, which are disturbed by unknown environmental factors, e.g., wind, waves, and ocean currents. In the context of the mobile manipulator operating on a rough terrain, the disturbances from the unmodeled geometry of the terrain are transmitted to the platform via the suspension system of the rover. In contrast to traditional adaptive controllers, for which the lack of knowledge about the ship dynamics and rover motion violates basic assumptions of the control design, the proposed controller is independent of the system modeling, and therefore especially useful for systems with unmodeled dynamics. The results demonstrate desirable tracking performance and clean and smooth control signals with different types of disturbances, including measurement noise and unknown time delay.

The successful design of the proposed control architecture relies upon a key parameterization of the nonlinear contribution to the robot equations of motion in terms of two time-

varying parameters with the $\mathcal{L}_\infty$ norm of the sliding state as a regressor. The controller further employs projection operators in the adaptive laws to impose bounds on the parameter estimates, and uses a low-pass filter in the control signal to keep the control-signal frequencies below the available control-system bandwidth. In this case, Theorem 2.2 implies close agreement between the system response and the control signal, on the one hand, and the corresponding time histories for a suitably formulated nonadaptive reference system, on the other hand, provided that the adaptive gain is chosen sufficiently large. Any deviation between the system response and the desired trajectory observed in the numerical results may be traced to the need to maintain a finite filter bandwidth, in order to guarantee robustness. This is the design trade-off between performance and robustness of the proposed control architecture.

The control scheme proposed in this chapter for underactuated robotic systems is relatively simple with the state predictor in Eq. (2.72), the adaptive control signal in Eq. (2.73), and the adaptation laws in Eqs. (2.74) and (2.75). In addition, the control formulation is independent of system modeling. Hence, the same control structure can be used for any Lagrangian system, including serial manipulators or parallel robots, while current adaptive controllers for manipulators require reconstruction of the regression matrix for each application, or accurate estimation of the system model. Furthermore, though the control scheme is demonstrated for a robot mounted on a ship and a mobile manipulator, it can be directly implemented for free-floating space manipulators whose dynamics have the exact form in Eq. (2.1), as well as any fixed-base manipulators whose equations of motion are simpler than those considered here.

We finally comment on the observations made regarding the critical time delay during the two trajectory-tracking tasks considered above. The simulation results show that increasing the filter bandwidth deteriorates the system robustness to delay. For finite bandwidth, the critical time delay remains well above zero across the entire range of adaptive gains and shows no sign of deteriorating as the adaptive gain is increased to a large value. This agrees

with the analysis in [61] for the case of a linear, constant-coefficient, single-input system, in which the basic control architecture supports the formulation of theoretical lower bounds on the time delay margin, through the use of a suitably formulated equivalent LTI system. The issue of delay robustness in the proposed control framework is further studied in Chapters 3, 4 and 5.

CHAPTER 3

MARGINAL STABILITY IN AN ADAPTIVE CONTROL SCHEME FOR MANIPULATORS

In Chapter 2, an adaptive controller for general Lagrangian systems that enables fast adaptation without compromising robustness was designed. The proposed adaptive control system decoupled the estimation loop from the control loop through the introduction of a low-pass filter in the control input. Design of the filter structure also allowed for shaping the nominal response and, as further explored in this chapter, enhancing the time-delay margin.

This chapter[1] provides further analysis of the robustness of the $\mathcal{L}_1$ control framework presented in Chapter 2 for a simplified system model via the study of the critical time delay at which stability is lost for a given static reference input. The effects of time delay in the $\mathcal{L}_1$ control system with static reference inputs are next demonstrated using direct numerical simulations. This analysis provides an opportunity to illustrate approaches to suppress delay-induced instability that are uniquely supported by the control architecture designed in Chapter 2, for example, by redesigning the filter structure to remove high-frequency oscillations and introducing time delay in the state predictor. In addition, inspired by the results in [20], a MIMO LTI system is constructed to derive a conservative lower bound of the critical time delay of the controller of interest with a static reference input. Finally, we propose a method for computing the critical time delay of nonlinear control systems by monitoring the roots of the characteristic equation associated with a linearization of the delay system about a given equilibrium. This formulation lends itself to the application of methods of numerical continuation [34] in order to compute the dependence of the critical time delay on control parameters, such as the adaptive gain or filter bandwidth.

[1]The material in this chapter is taken from [99] with the permission from the publisher. The introduction and the conclusion are modified to agree with the flow of the dissertation.

3.1 Delay-induced instability

The objective of this section is to demonstrate the $\mathcal{L}_1$ control system's responses to different values of the time delay in the control input u. The dynamics of an fixed-base n-link robotic manipulator, described by a matrix q of joint angles, are governed by equations of motion of the form

$$M\big(q\big)\ddot{q} + V_m\big(q,\dot{q}\big)\dot{q} + G\big(q\big) + F\big(\dot{q}\big) + D = u_T \tag{3.1}$$

where u_T and D denote time-dependent input torques and bounded unknown disturbances, respectively. With the variable transformation

$$r = \dot{q} + \Lambda q \tag{3.2}$$

and the decomposition of the input torque

$$u_T = M(q)(A_m r + u) \tag{3.3}$$

(the dependence on $M(q)$ may be removed without loss of generality), Eqn. (3.1) may be transformed to the following form

$$\dot{r}(t) = A_m r(t) + u(t) - f\big(t,\zeta(t)\big), \quad r(0) = r_0 \tag{3.4}$$

where $\zeta^T = \big[r^T, q^T\big]$, $f\big(t,\zeta(t)\big)$ lumps all nonlinearities and unknown disturbances, and A_m denotes a Hurwitz matrix introduced to shape the system's transient response. The $\mathcal{L}_1$ control scheme for this system, which is designed in Chapter 2, consists of the state estimator in (2.72), the control input in (2.73), and the adaptation laws in (2.74) and (2.75). Next, we define different terminologies for the system ability to tolerate time delay in the control input.

Let the time-delay margin of a nonlinear control system be defined as an upper bound on the actuator time delay, beyond which there exists at least one reference input that yields unbounded growth in the linearization about the corresponding desired trajectory. An objective of this study is to generalize techniques from the analysis of the time-delay margin for SISO $\mathcal{L}_1$ control systems [61] to that of MIMO systems applicable to typical robotic devices.

A more restrictive notion of robustness is the study of the critical time delay associated with unbounded growth for a given reference input, or class of reference inputs. As an example, results demonstrating the robustness of an $\mathcal{L}_1$ controller for manipulators operating on a dynamic platform to actuator time delay for specific oscillatory reference inputs were provided in Chapter 2. As the discussion in the present chapter is restricted to the study of the critical time delay associated with a static reference input, we include in this section results from a numerical study of the corresponding system dynamics.

Consider the controlled motion of a typical pick-and-place manipulator two degrees of freedom at the shoulder and a single-degree-of-freedom revolute joint at the elbow for a given static reference input. The manipulator is operating on a static platform. Suppose that the link lengths, the masses of the three links, the payload at the end-effector, and the acceleration of gravity are given by $L_1 = 1$, $L_2 = 0.8$, $L_3 = 0.2$, $m_1 = 10$, $m_2 = 10$, $m_3 = 5$, $m_e = 5$, and $g = 9.81$ in a consistent set of units. With $q_d = \begin{pmatrix} 1 & 1 & 1 \end{pmatrix}^T$, $\Lambda = \mathrm{diag}(3, 3, 1)$, $\Gamma = 10^6$, $A_m = \mathrm{diag}(-3, -4, -3)$, $K_{\mathrm{sp}} = \mathrm{diag}(100, 100, 100)$, and $C(s)$ consisting of identical first-order filters with bandwidth of 20, numerical experiments reveal unbounded local growth and sustained finite-amplitude oscillations about the reference configuration for an actuator time delay of approximately 0.07.

Below this critical time delay, the system performance is found to exhibit initial transient oscillations with a decaying envelope, with amplitude and decay time scale growing with the actuator time delay. As an example, numerical results demonstrate sustained satisfactory performance for an actuator time delay of 0.05 relative to the nominal case of no time delay.

For an actuator time delay of 0.06, the tracking performance of the $\mathcal{L}_1$ control remains desirable as illustrated in Fig. 3.1, with some initial transient oscillations in the prediction error and the control input. As the time delay is increased to 0.068, the decay rate of oscillations induced by the initial conditions on the state response and control inputs is significantly slower than for lower time delays, as shown in Fig. 3.2. The effects of time delay are particularly pronounced in the control channels and in the prediction error, which exhibit significantly larger amplitudes of oscillation than in Fig. 3.1. Here, larger prediction errors cause larger oscillations in the adaptive estimates obtained from Eqns. (2.74) and (2.75) and, consequently, a larger amplitude of the control input $u(t)$ according to Eqn. (2.73).

This observation suggests a way to suppress the instability induced by time delay by incorporating knowledge of the delay in the predictor or filter design, so as to eliminate significant deviations between the predicted and actual response. As an example, Fig. 3.3 shows the system behavior in the presence of a time delay in the control term in the equation governing the state predictor (2.72), identical in value to that imposed at the plant input. The oscillations caused by the time delay in Fig. 3.2 are largely removed. Using this methodology, it is possible to boost the critical time delay from 0.07 in the absence of state-predictor delay to a maximum of 0.43.

Similar performance improvements below the critical time delay may be obtained by suitable tuning of the filters $C(s)$. The oscillations in Fig. 3.2 can be largely eliminated by tuning the bandwidth ω of the first-order filter $C(s)$, or by selecting a higher-order filter. To illustrate this, we keep the delay of 0.068 in the plant control input (the delay in the state predictor is set to zero) and decrease the filters' bandwidth to 10. The result obtained is virtually identical to Fig. 3.3. The critical time delay with this filter bandwidth is 0.119. Alternatively, we may replace the first order filter by the second-order filter $(13s+2)/(s^2+13s+2)$, which has a lower bandwidth compared to the initial filter, to obtain essentially the same result as in Fig. 3.3. The critical time delay with this second-order filter is 0.098. In both cases, the lower bandwidth eliminates most of the high-frequency components of the control input and

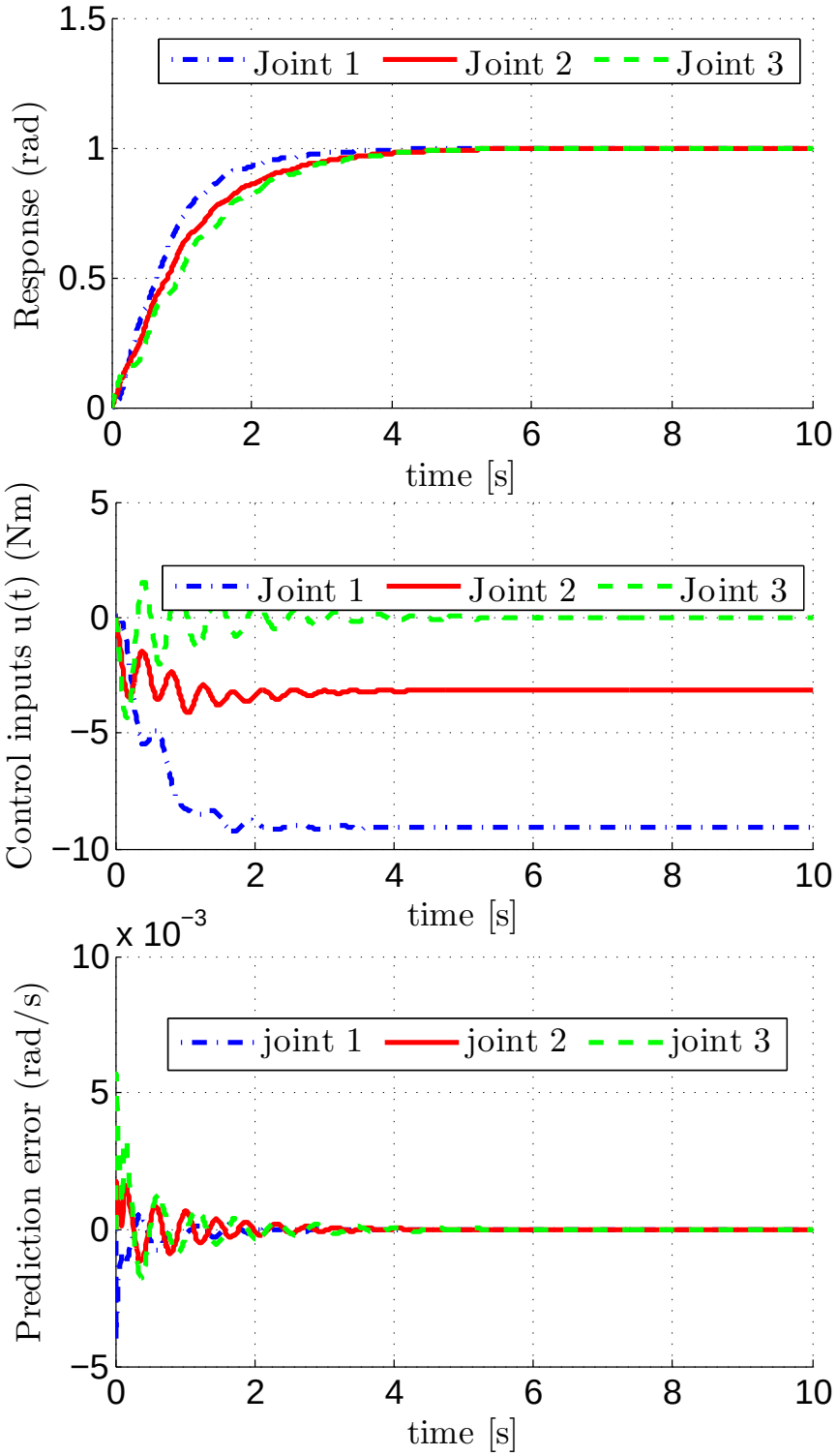

Figure 3.1: Performance of the $\mathcal{L}_1$ controller with actuator time delay of 60 ms.

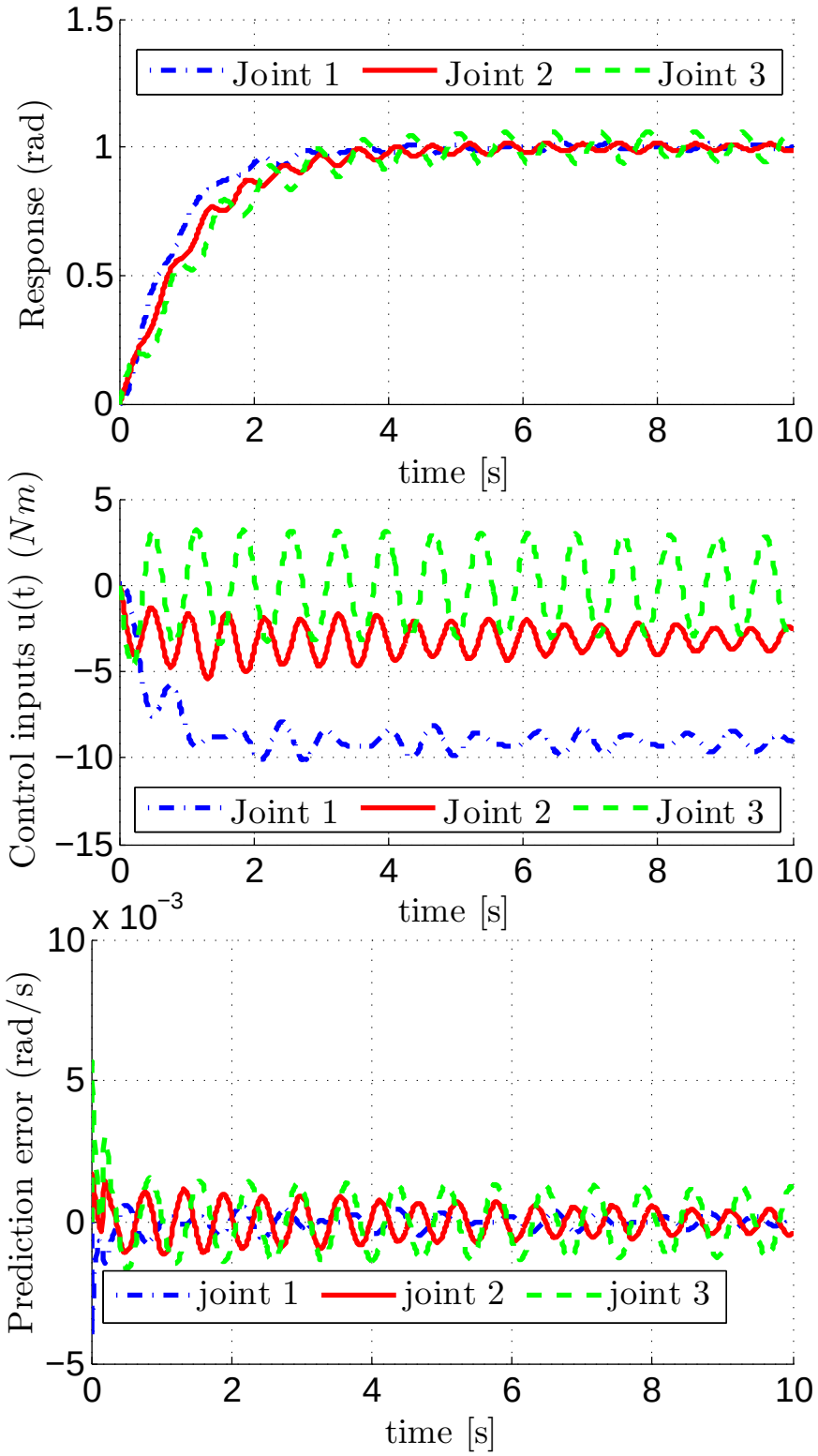

Figure 3.2: Performance of the $\mathcal{L}_1$ controller with actuator time delay of 68 ms.

nearly recovers the system performance under the ideal conditions of no time delay.

3.2 Estimating a lower bound for the critical time delay via LTIs

In this section, we derive a lower bound on the critical time delay that the $\mathcal{L}_1$ control system can accommodate with a static reference input r_d. Under the assumption that the robot function f is not explicitly dependent on time, we first linearize the manipulator dynamics in (3.4) about the corresponding steady state configuration to obtain

$$\dot{r} = A_m r + u - (L_1 r + L_2 q + L_3), \quad r(0) = r_0 \tag{3.5}$$

where r and q are related by (3.2), and the Jacobian matrices:

$$L_1 = \frac{\partial f}{\partial r}(\zeta_d), \quad L_2 = \frac{\partial f}{\partial q}(\zeta_d), \quad L_3 = f(\zeta_d) \tag{3.6}$$

Inspired by the analysis in [20], we next consider the multi-input-multi-output, linear time-invariant system given by

$$\dot{q}_l = r_l - \Lambda q_l, \quad q_l(0) = q_0 \tag{3.7}$$

and

$$\dot{r}_l = A_m r_l + u_{ld} - \eta, \quad r_l(0) = r_0 \tag{3.8}$$

where $\eta(t) \triangleq L_1 r_l(t) + L_2 q_l(t) + L_3$, $u_{ld} \triangleq u_l(t-\tau)$, $\tilde{u}_l(s) \triangleq u_{ld}(s) - u_l(s)$, and

$$u_l(s) = C(s)\big(\eta(s) - A_m r_d - \tilde{u}_l(s) - \chi_l(s)\big) \tag{3.9}$$

Here, the control input u_l is the output of a linear equation, while the control input of the original $\mathcal{L}_1$ system is the output of a nonlinear equation. Moreover, the exogenous signal $\chi_l(t)$ is a vector instead of a scalar signal as in [20].

For the corresponding formulation of an LTI system for a SISO system, it was proved in

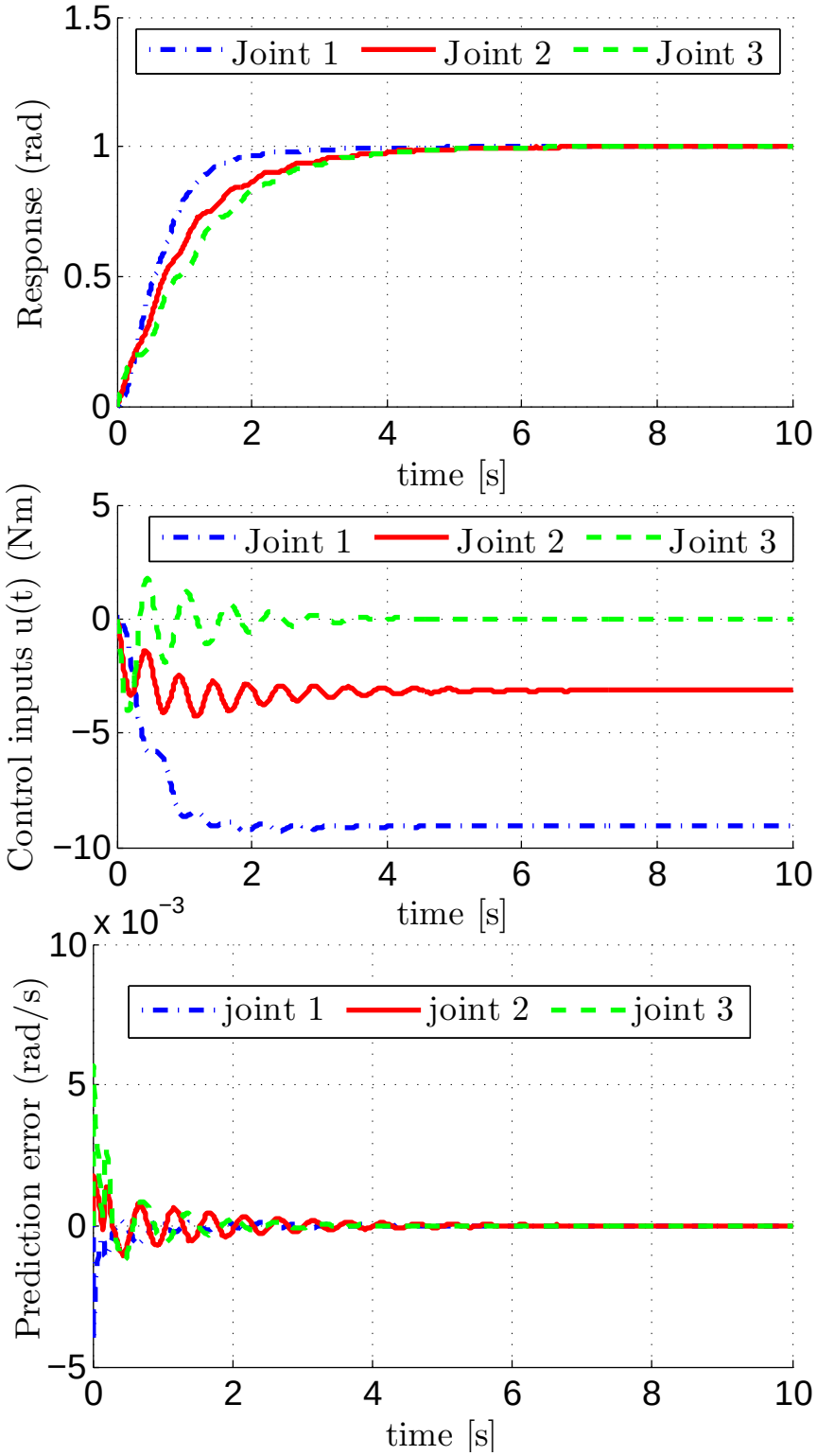

Figure 3.3: Performance of the $\mathcal{L}_1$ controller with actuator time delay of 68 ms together with the introduction of a delay of 68 ms in the state predictor.

[20] that

- For large enough adaptive gain and for $\tau < \tau_m$ there exists a bounded exogenous signal $\chi_l(t)$ such that $r_l(t) = r(t)$ and $u_l(t) = u(t)$;

- For arbitrary bounded $\chi_l(t)$, if $\tau < \tau_m$ then the $r_l(t)$, $u_l(t)$ and $\tilde{u}_l$ are bounded, and hence so are $r(t)$ and $u(t)$.

These observations imply that the time-delay margin of the LTI system provides a strict lower bound for the time-delay margin of the $\mathcal{L}_1$ control system. In the absence of a proof for the MIMO case, we proceed to analyze the latter with the conjecture that a similar correspondence may be established there.

Without loss of generality, we consider the case of zero initial conditions. From (3.7) and (3.8), we have

$$r_l(s) = \bar{H}(s)\big(u_{ld}(s) - L_3 s^{-1}\big) \tag{3.10}$$

where

$$\bar{H}(s) \triangleq \big(s\mathbb{I} - A_m + \bar{L}(s)\big)^{-1} \tag{3.11}$$

and

$$\bar{L}(s) \triangleq L_1 + L_2(s\mathbb{I} + \Lambda)^{-1} \tag{3.12}$$

Substituting (3.10) and the definition of $\tilde{u}_l$ in (3.9) now yields

$$u_l(s) = \big(\mathbb{I} - C(s)\big)^{-1}\big(\chi_r(s) - \chi_f(s)\big) \tag{3.13}$$

where

$$\chi_r(s) \triangleq C(s)\big(k_g r_d(s) - \chi_l(s)\big) \tag{3.14}$$

$$\chi_f(s) \triangleq C(s)\big(1 - \bar{L}(s)\bar{H}(s)\big)(u_{ld} - L_3) \tag{3.15}$$

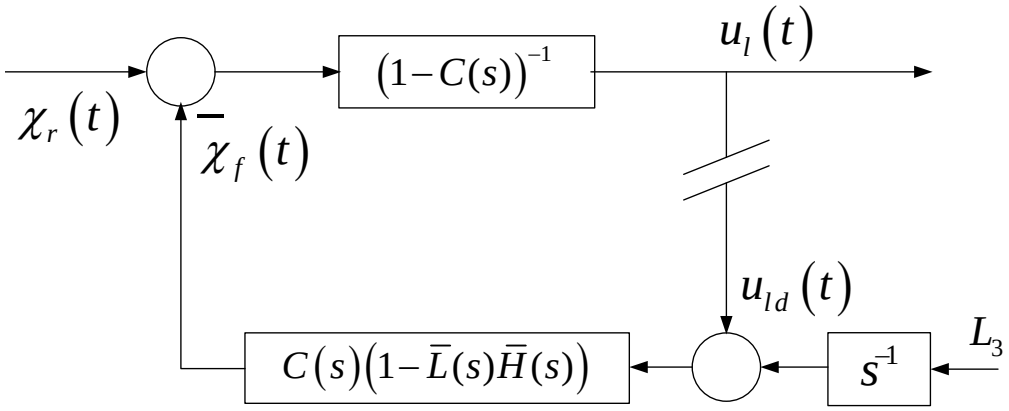

Figure 3.4: Block diagram of the LTI system used to derive a lower bound on the critical time-delay for the $\mathcal{L}_1$ control system for a static reference input.

whose block diagram is illustrated in Fig. 3.4. This system has the following matrix of loop transfer functions:

$$L_o = \big(\mathbb{I} - C(s)\big)^{-1} C(s)\big(1 - \bar{L}(s)\bar{H}(s)\big) \tag{3.16}$$

Since, in the analysis in [20] of a SISO system, the loop transfer function corresponding to L_o is scalar, the phase margin may be obtained by traditional means, including Nyquist or Bode plots. For the case of a matrix-valued loop transfer function, we rely on the method described in Chapter 5 of [72] to estimate the phase margin ϕ_m and the gain crossover frequency ω_{gc}. Here, the estimate of the phase margin is obtained from

$$\phi_m = 2\sin^{-1}\left(\frac{\beta_\sigma}{2}\right) \tag{3.17}$$

where $\beta_\sigma = \min_\omega \sigma_{\min}\left(\mathbb{I} + L_o^{-1}(j\omega)\right)$ and $\sigma_{\min}(A)$ denotes the smallest singular value of the matrix A. Similarly, the gain-crossover frequency ω_{gc} is the frequency at which $\sigma_{\max}\big(L_o(j\omega)\big)$ crosses 0 dB, where $\sigma_{\max}(A)$ denotes the largest singular value of the matrix A. The estimated

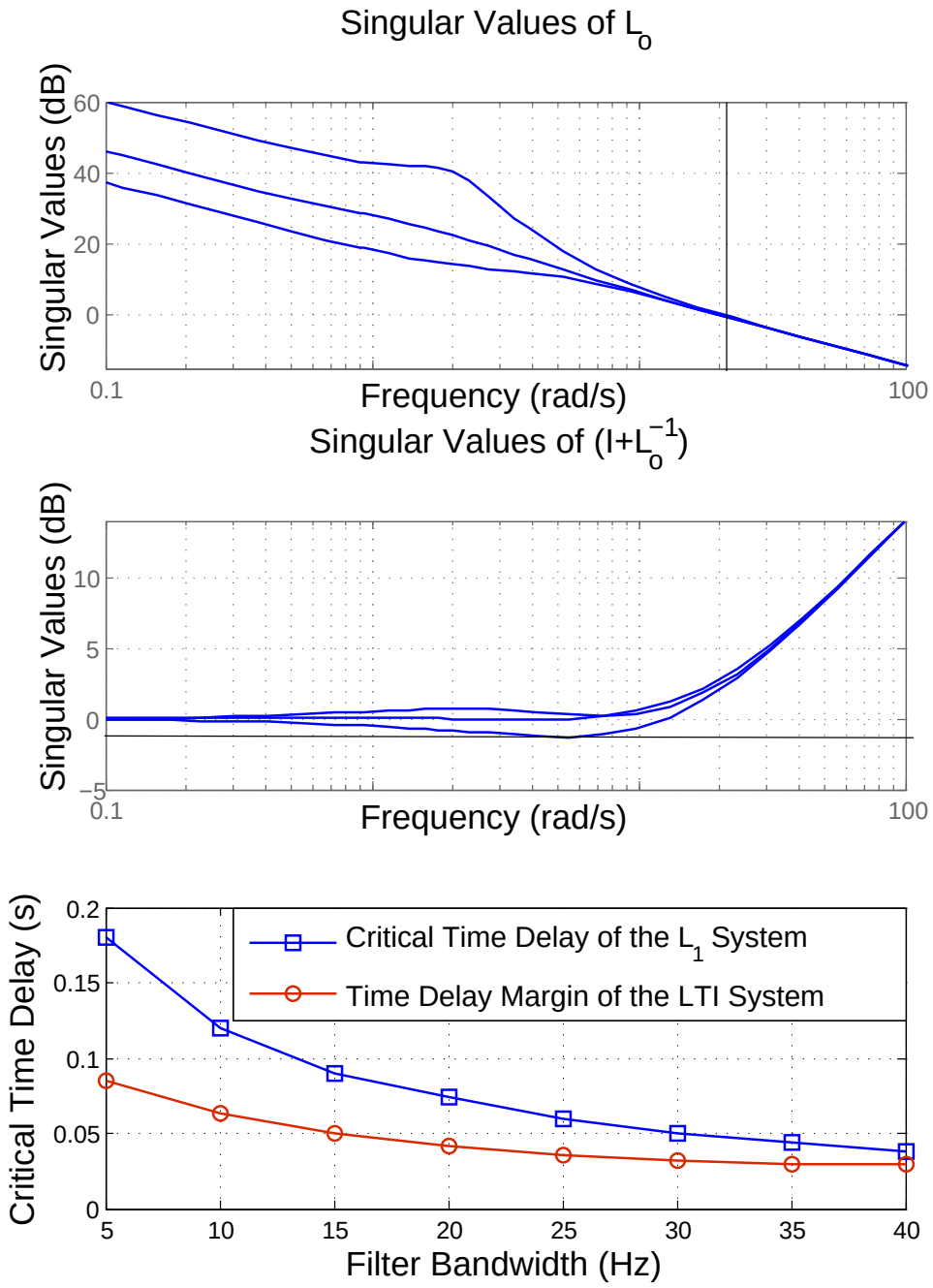

Figure 3.5: Analysis of time-delay margin of LTI system and comparison against critical time delays of the adaptive control system. (upper panel) Singular values of $L_o(j\omega)$ with gain-crossover frequency ω_{gc} indicated by solid vertical line. (middle panel) singular values of $(\mathbb{I} + L_o^{-1}(j\omega))$ with phase margin ϕ_m obtained from minimum singular value indicated by solid horizontal line. (lower panel) critical time delay versus the filter bandwidth of $\mathcal{L}_1$ system (square markers) and the predicted time-delay margin for the LTI system (round markers), respectively.

time-delay margin of the LTI system is now given by

$$\tau_m = \frac{\phi_m}{\omega_{gc}} \tag{3.18}$$

As discussed in [72], the estimate of the time-delay margin computed by this method is very conservative. As long as the time delay in the control input is less than τ_m, the linear, time-invariant system is guaranteed to be stable. As suggested previously, we conjecture that τ_m also provides a lower bound for the critical time delay of the original $\mathcal{L}_1$ system.

To illustrate this analysis, consider again the three-degree-of-freedom manipulator and the corresponding $\mathcal{L}_1$ control system considered in the previous section with $q_d = \begin{pmatrix} 1 & 1 & 1 \end{pmatrix}^T$ and $r_d = \begin{pmatrix} 3 & 3 & 1 \end{pmatrix}^T$. From the graphs of the singular values of $L_o(j\omega)$ in the top panel of Fig. 3.5, we obtain the gain-crossover frequency of 22 rad/s. Similarly, the graphs of the singular values of $\mathbb{I} + L_o^{-1}(j\omega)$ in the middle panel of Fig. 3.5 gives $\beta_\sigma = -1.28$ dB and, consequently, $\phi_m = 0.892$ rad. Equation (3.18) then yields an estimate of the time-delay margin $\tau_m = 0.041$ s, which we assume to provide a conservative lower bound of the critical time delay of the $\mathcal{L}_1$ control system. The results of repeating this procedure with different values of the filter bandwidth are shown in the bottom panel of Fig. 3.5 together with the critical time delay of the adaptive control system estimated by numerical simulation. As seen in the figure, the critical time delay of the adaptive system is always above that of the LTI system, consistent with the conjecture.

3.3 Parameter Continuation

As suggested in previous sections, the critical time delay of a nonlinear control system is defined as that value of the actuator time delay beyond which unbounded growth is expected for some reference input in the linearization around the reference trajectory. In the analysis of the $\mathcal{L}_1$ system that lead to the numerical results shown in the bottom panel of Fig. 3.5,

the critical time delay was found by increasing the actuator time delay until the response exhibits sustained, finite-amplitude oscillations.

In this section, we consider an alternative way of finding the critical time delay for static reference inputs by monitoring the roots of the corresponding characteristic equation obtained by linearization around the desired state. In this case, the appearance of sustained, finite-amplitude oscillations is associated with a supercritical Hopf bifurcation, in which the two complex conjugate roots with largest real part cross the imaginary axis, rendering the equilibrium state linearly unstable.

To demonstrate the concept, we first consider the following scalar system, in which a time delay τ is introduced in the control signal before its application to the plant:

$$\dot{x}(t) = ax(t) + b\big(u(t-\tau) + \theta x(t)\big) \tag{3.19}$$

The control objective is now to make $x(t)$ to follow the desired trajectory $x_d(t)$. We proceed by constructing an $\mathcal{L}_1$ controller, of similar structure to those considered in the previous sections of this chapter. Specifically, let

$$u(t) = -k_m x(t) + u_{\rm ad}(t) \tag{3.20}$$

so as to yield

$$\dot{x}(t) = ax(t) - k_m x(t-\tau) + b\big(u_{\rm ad}(t-\tau) + \theta x(t)\big) \tag{3.21}$$

With $a - bk_m = a_m$ the following state predictor is now used to estimate the system state

$$\dot{\hat{x}}(t) = a_m \hat{x}(t) + b\big(\hat{\theta}(t)x(t) + u_{\rm ad}(t)\big) \tag{3.22}$$

Here, the adaptive estimate $\hat{\theta}$ of the unknown parameter θ is governed by

$$\dot{\hat{\theta}}(t) = -\Gamma x(t) b\big(\hat{x}(t) - x(t)\big) \tag{3.23}$$

Finally, let

$$u_{\rm ad}(s) = C(s)\big(-\hat{\eta}(s) + k_g x_d(s)\big) \tag{3.24}$$

where $\hat{\eta}(s)$ is the Laplace transform of $\hat{\eta}(t) \triangleq \hat{\theta}(t)x(t)$ and $C(s)$ is a first-order filter with bandwidth is ω. In the time domain, Eqns. (3.19)-(3.24) can be written in the following short form

$$\dot{z} = h\big(t, z(t), z(t-\tau)\big). \tag{3.25}$$

where $z \triangleq \begin{pmatrix} x & \hat{x} & \hat{\theta} & u_{\rm ad} \end{pmatrix}^T$.

Suppose, for example, that $a = 1$, $b = 1$, $a_m = -1$, $b_m = 1$, $\theta = 0.1$, $p = 1$, $k_g = 1$, and $x_d(t) = 1$. Then, the linearization of the governing differential equations about the steady state $z_{ss} = \begin{pmatrix} 1 & 1 & 0.1 & 0.9 \end{pmatrix}^T$ yields the delay-differential equation

$$\dot{z}(t) = Az(t) + A_\tau z(t-\tau) \tag{3.26}$$

where

$$A = \begin{pmatrix} 1.1 & 0 & 0 & 0 \\ 0.1 & -1 & 1 & 1 \\ \Gamma & -\Gamma & 0 & 0 \\ -0.1\omega & 0 & -\omega & -\omega \end{pmatrix}, \quad \text{and} \quad A_\tau = \begin{pmatrix} -2 & 0 & 0 & 1 \\ 0 & 0 & 0 & 0 \\ 0 & 0 & 0 & 0 \\ 0 & 0 & 0 & 0 \end{pmatrix} \tag{3.27}$$

The corresponding characteristic equation in the unknown roots λ is then given by

$$\det\left[L(z_{ss}, \Gamma, \tau, \omega, \lambda)\right] = 0 \tag{3.28}$$

where $L(z_{ss}, \Gamma, \tau, \omega, \lambda) = \lambda \mathbb{I} - A - A_\tau e^{-\lambda\tau}$.

For $\tau \neq 0$, although Eqn. (3.28) has an infinite number of complex roots, the number of roots in any right half plane can be shown to be finite. A subset of the system's spectrum in the complex plane for $(\Gamma, \tau, \omega) = (800, 0.4, 10)$ is illustrated by Fig. 3.6. A pair of roots at $1.7 \pm i3.8$ establishes the possibility of unbounded growth in the linearized equations. As τ is decreased, this pair of roots shifts to the left and is found to cross the imaginary axis for $\tau \approx 0.08$ corresponding to a Hopf bifurcation.

Using the MATLAB-based continuation toolbox DDE-BIFTOOL, we may use the Hopf bifurcation point for $\Gamma = 800$ and $\omega = 10$ as an initial guess for computing the implicitly defined solution manifold of the system of equations

$$\begin{cases} h(z_{ss}, z_{ss}) = 0 \\ \det\left[L(z_{ss}, \Gamma, \omega, \tau, j\Omega)\right] = 0. \end{cases} \tag{3.29}$$

corresponding to the existence of an equilibrium state z_{ss} with a root of the corresponding characteristic equation at $j\Omega$. By separating the characteristic equation into real and imaginary parts, this corresponds to 6 equations in 8 unknowns $(z_{ss}, \Gamma, \omega, \tau, \Omega)$. It follows that the solution manifold is two-dimensional and may be locally parameterized by some combination of two of these unknowns. Sample one-dimensional submanifolds of the solution manifold for different fixed values of the filter bandwidth ω obtained using DDE-BIFTOOL are represented by the graphs in Fig. 3.7. In each case, the linear stability of the equilibrium state at z_{ss} switches between stable and unstable as the corresponding solution curve is crossed, with z_{ss} being stable for sufficiently small time delays τ.

For large values of the adaptive gain Γ, the critical time delay appears to plateau at a fixed value providing a guaranteed stability margin for static reference inputs at high adaptation rates (this is expected from the general theory for SISO systems for arbitrary reference inputs). For small values of Γ, the solution manifolds fall off sharply initially. For $\omega = 10$ and 15, two folds are found along the solution manifold providing for an interval of time

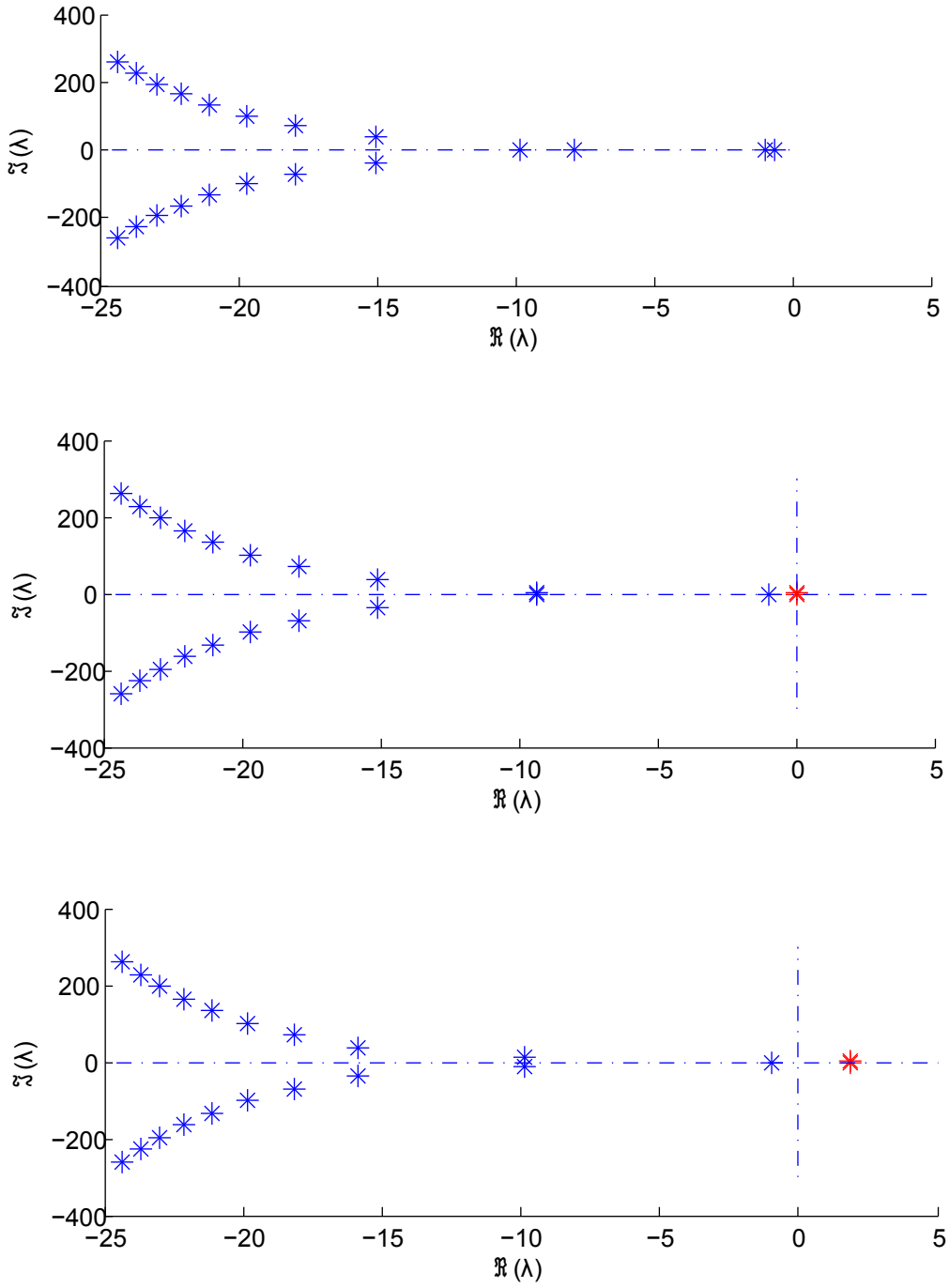

Figure 3.6: Roots of (3.28) in the complex plane obtained using the Matlab-based toolbox DDE-BIFTOOL [34]: Top panel: $(\Gamma, \tau, \omega) = (800, 0.05, 10)$, when the system is stable with all eigenvalues on the left-half complex plane; Middle panel: $(\Gamma, \tau, \omega) = (800, 0.08, 10)$, when Hopf bifurcation occurs, and two rightmost eigenvalues cross the imaginary axis; Bottom panel: $(\Gamma, \tau, \omega) = (800, 0.4, 10)$, when the rightmost eigenvalues lie on the right-half complex plane, and the system is unstable.

delays for which stable behavior is observed above the first critical time delay.

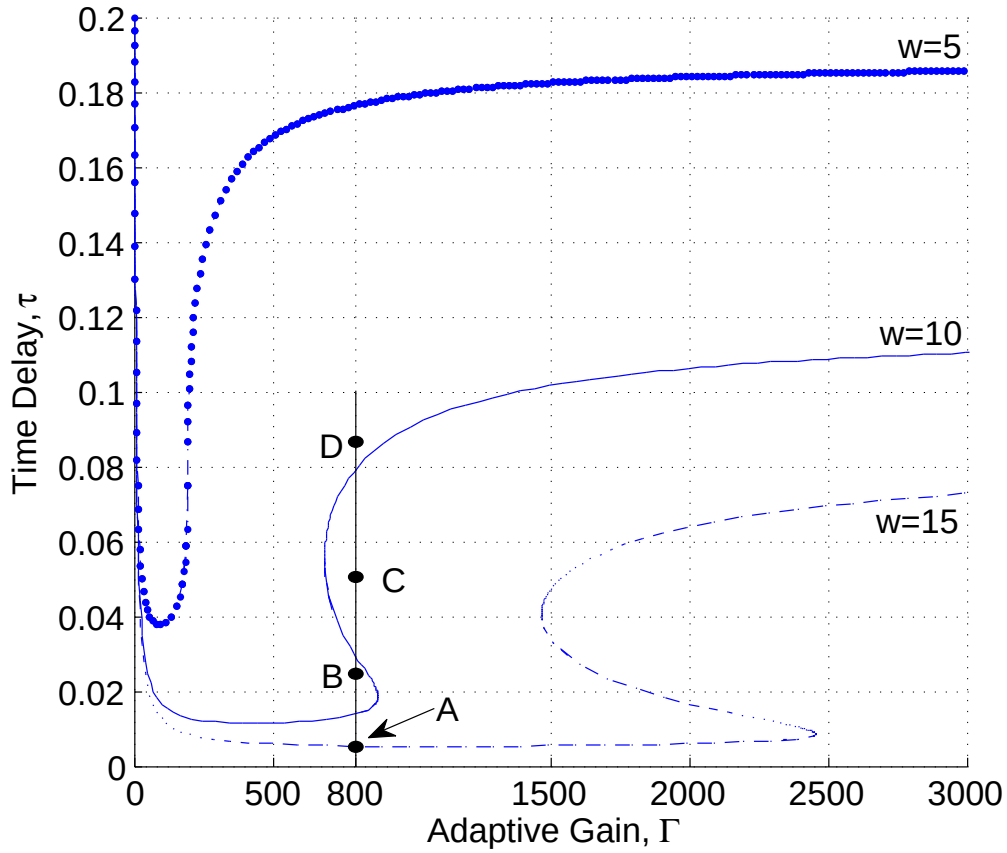

Figure 3.7: The curve of critical time delay versus adaptive gain for $\omega = 5$, 10, and 15. The points A through D along the vertical line segment at $\Gamma = 800$ are further explored in Fig. 3.8.

Consider, in particular, the sequence of time histories of the system response obtained through numerical simulation and shown in Fig. 3.8. Here, the delay τ is increased from zero along the vertical line $\Gamma = 800$ in the parameter plane in Fig. 3.7 for $\omega = 10$. In each case, the initial condition is chosen close to the desired steady-state value of 1. At point A, below the curve of critical time delays, the system's response appears stable. In contrast, at point B, the parameters have crossed the curve of critical time delays and the response exhibits oscillations that grow in amplitude away from the desired response. At point C, the parameters have again crossed the curve of critical time delays and the initial transient oscillations decay quickly. Finally, at point D, sustained, finite-amplitude oscillations are

again observed in the system response.

We finally comment on the applicability of this method to a simplified version of the $\mathcal{L}_1$ controller considered in the beginning of this chapter. Specifically, consider the nonlinear control system given by

$$\begin{aligned}
\dot{q}(t) &= r(t) - \Lambda q(t), \quad q(0) = q_0 && (3.30)\\
\dot{r}(t) &= A_m r(t) + u(t-\tau) - \eta(t), \quad r(0) = r_0 && (3.31)\\
\dot{\hat{r}}(t) &= A_m \hat{r}(t) + u(t) - \hat{\eta}(t), \quad \hat{r}(0) = r_0 && (3.32)\\
u(s) &= C(s)\left(\hat{\eta}(s) - A_m r_d(s)\right) && (3.33)
\end{aligned}$$

where

$$\begin{aligned}
\eta(t) &= L_1 r(t) - L_2 q(t) + L_3 && (3.34)\\
\hat{\eta}(t) &= \hat{L}_1 r(t) + \hat{L}_2 q(t) + \hat{L}_3 && (3.35)
\end{aligned}$$

and

$$\begin{aligned}
\dot{\hat{L}}_1(t) &= \Gamma r(t)\tilde{r}^T(t)P, \quad \hat{L}_1(0) = L_{10} && (3.36)\\
\dot{\hat{L}}_2(t) &= \Gamma q(t)\tilde{r}^T(t)P, \quad \hat{L}_2(0) = L_{20} && (3.37)\\
\dot{\hat{L}}_3(t) &= \Gamma P\tilde{r}(t), \quad \hat{L}_3(0) = L_{30} && (3.38)
\end{aligned}$$

For a static reference input r_d, there exists a hyperplane of equilibrium states of the system of differential equations given by (3.30)-(3.33) and (3.36)-(3.38). It follows that the corresponding characteristic equation has one or several roots at 0 thus yielding a singular continuation problem for the computation of the curve of critical time delays. This singularity must be removed before the parameter continuation approach may be applied to the robot manipulator, for example, by modifying the adaptive laws in (3.36), (3.37) and (3.38)

to select desired target values for a subset of the adaptive estimates.

3.4 Conclusion

This chapter presents a numerical study of the robustness to actuator time delay of the $\mathcal{L}_1$ adaptive control architecture for robot manipulators presented in Chapter 2. As supported by the numerical analysis, the $\mathcal{L}_1$ control formulation provides for lower bounds on the critical time delay for given static reference inputs with instability associated with a flutter (Hopf) bifurcation in the control system response.

Several remarks are in order to put the preliminary contribution of this chapter into perspective. Although tuning of the filter structure and the introduction of time delays in the equation governing the state predictor were both shown to suppress the instability associated with actuator time delays, such modifications may degrade other performance characteristics, e.g., bounds on the $r(t) - r_d(t)$. Furthermore, neither simulation nor parameter continuation may be used to arrive at rigorous estimates of the *time-delay margin*, since these techniques are at best restricted to particular classes of reference inputs. Such observations, notwithstanding, critical time delays computed, for example, using numerical continuation may provide useful design criteria in practical control applications.

The analysis in this chapter shows initial steps toward a complete theory for the delay robustness of the adaptive control framework studied in this dissertation. In the next chapter, we take one step further and present theoretical analysis that rigorously proves that there exists a lower bound for the time delay margin of a class of nonlinear systems.

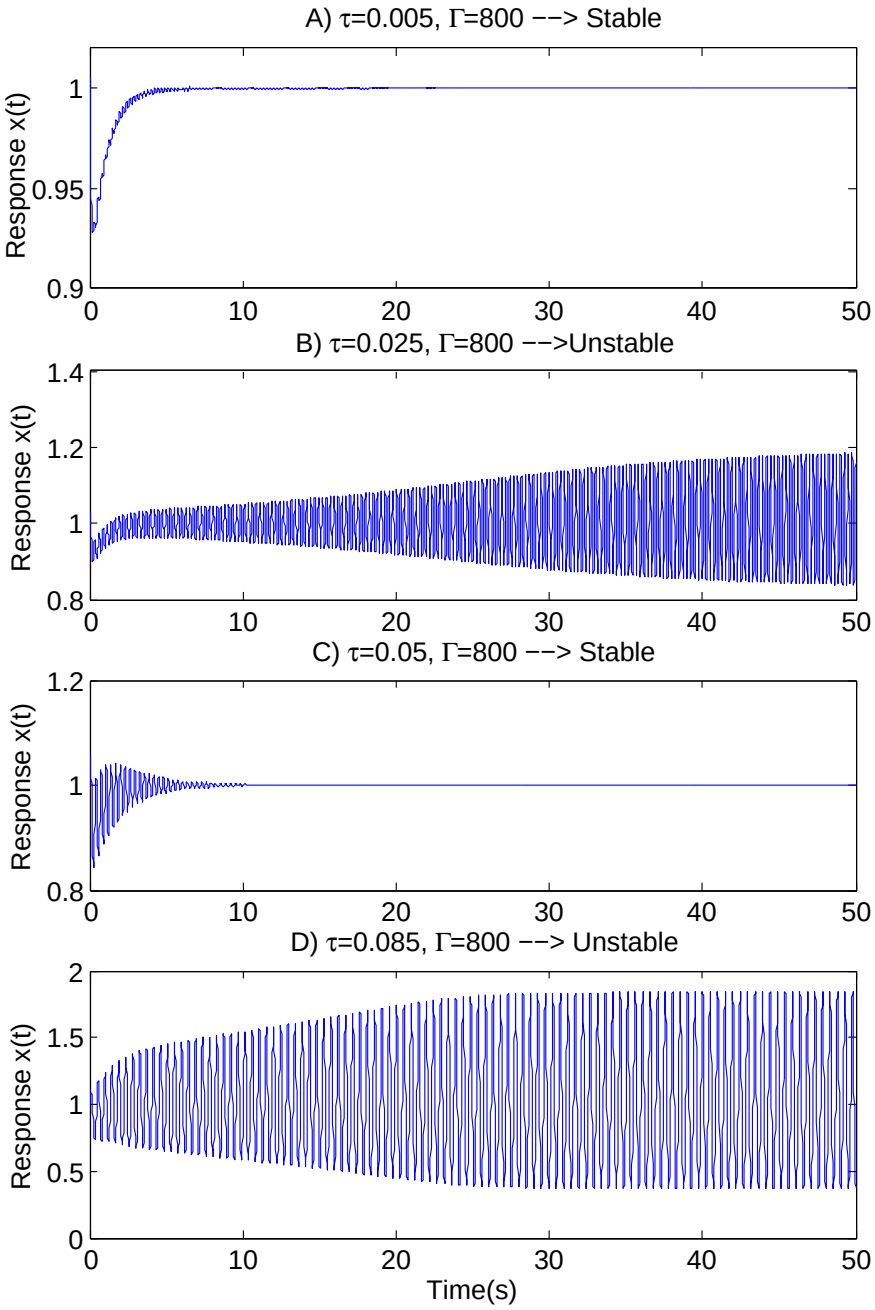

Figure 3.8: System responses for the points A, B, C, and D in the parameter plane $\Gamma - \tau$ in Fig. 3.7.

CHAPTER 4

DELAY ROBUSTNESS OF ADAPTIVE CONTROLLERS: CONSTANT INPUT-GAIN MATRICES

Time delay is an integral part of most robotic systems. In many systems, time delay in the control loop induces instability, and is resistant to many classical controllers [106]. In the presence of time delay, the closed-loop dynamical system is given by a delay differential equation (DDE), whose functional state evolves in a infinite dimensional function space. Many results from ODE theory do not apply to DDEs. In addition, it is well known that the behavior of solutions to a delay system can be much more complicated than the behavior of solutions to the same system with zero delay [48]. In nonlinear delay systems, there is no general method for computing the time-delay margin. In this chapter, we establish a positive lower bound for the time-delay margin, which is independent of the adaptive gain, for an adaptive control algorithm formulated for systems with unknown nonlinearities and constant input-gain matrices.

This chapter is organized as follows. Section 4.1 describes the system of interest and discusses how different types of systems can be converted to the presented form. Assumptions regarding the system are also stated here. In Section 4.2, we construct a nonadaptive reference system, and investigate its continuous dependence on the input delay. In addition, using continuity arguments, we establish a delay-dependent stability condition, which is associated with the existence of a positive lower bound for its time-delay margin of the reference system. Section 4.3 discusses the design of the adaptive controller and establishes transient performance bounds when the input delay is below the lower bound. The effect of the input delay on the system response is demonstrated in Section 4.4 through simulation. In Section 4.5, we estimate the lower bound for the time-delay margin using the method of

Padé approximants. Section 4.6 gives concluding remarks.

4.1 The open-loop plant

Let the state and output of a dynamical system be represented by the vectors $r(t) \in \mathbb{R}^n$ and $y(t) \in \mathbb{R}^m$, respectively, where $n \geq m$, and assume that the system dynamics may be described in state-space form by the equations

$$\dot{r}(t) = A(t)r(t) + B\Big(\omega u(t-\epsilon) + \eta_0\big(t, r(t)\big)\Big), \tag{4.1}$$

$$y(t) = Dr(t), \tag{4.2}$$

and $r(0) = r_0$, where $\epsilon \geq 0$ denotes a time delay in the control input $u(t) \in \mathbb{R}^m$. Suppose that $A : \mathbb{R} \mapsto \mathbb{R}^{n\times n}$ is an unknown, bounded, and smooth matrix function of time, $B \in \mathbb{R}^{n\times m}$ and $D \in \mathbb{R}^{m\times n}$ are known constant matrices, $\omega \in \mathbb{R}^{m\times m}$ is an unknown constant input-gain matrix, and $\eta_0(t, r)$ is a *nonlinearity* that includes time-varying disturbances. The objective of the control design is to construct a closed-loop system that drives $y(t)$ to a desired trajectory $y_d(t)$, with suitable performance characteristics. To this end, consider the following definition.

Definition 4.1. *Given $b_d > 0$ and $b_{\text{ic}} > 0$, the closed-loop system is said to* admit a transient performance bound *if there exists a ρ, such that*

$$\|y_d\|_{\mathcal{L}_\infty} \leq b_d \text{ and } \|r_0\|_\infty \leq b_{\text{ic}} \Rightarrow \|r\|_{\mathcal{L}_\infty} \leq \rho. \tag{4.3}$$

If the closed-loop system admits a transient performance bound when $\epsilon = 0$, then its time-delay margin *is the maximum input delay that the system can tolerate without violating* (4.3).

The analysis in this chapter establishes the existence of a positive lower bound on the

time-delay margin of the closed-loop system obtained from a suitably constructed adaptive control scheme, as long as the adaptive gain is sufficiently large.

Equations of the form (4.1)-(4.2) arise in the study of aerial vehicles [49], manipulators linearized about a quasi-static trajectory with nonlinear disturbances [93], cable-driven manipulators [108], and mobile agents [134]. A version of these equations with time and state-dependent coefficient matrix ω is obtained for Lagrangian systems, e.g., using a sliding variable formulation as in [102], or by expressing the equations of motion in first-order form (see [97] and [76]). In all of these cases, ω is positive-definite.

We make the following assumptions:

Assumption 4.1. *The matrix B has full rank, i.e., the contribution of the control input to $\dot{r}$ equals zero only if $u = 0$. It follows that $B^\top B$ is nonsingular.*

Assumption 4.2. *The input-gain matrix ω is positive definite.*

Assumption 4.3. *The matrices $A(t)$, B, and the Hurwitz matrix A_m are matched, i.e., the columns of the difference $A(t) - A_m$ are in the column span of B.*

When Assumption 4.3 is satisfied, it may be possible to achieve certain given control objectives by tuning A_m through the addition of linear combinations of the columns of B. Taking this assumption into account, equation (4.1) can be transformed to

$$\dot{r}(t) = A_m r(t) + B\Big(\omega u(t-\epsilon) + \eta\big(t, r(t)\big)\Big) \tag{4.4}$$

for some $\eta\big(t, r(t)\big)$.

Assumption 4.4. *For each $\delta > 0$, the partial derivatives of $\eta(t, r)$ are piecewise continuous and uniformly bounded on the cylinder $\{t \geq 0, \|r\|_\infty \leq \delta\}$. In particular, let $d_{\eta_r}(\delta)$ denote the bound on $\partial\eta(t, r)/\partial r$. In addition, assume that $\|\eta(t, 0)\| \leq Z$, where Z is some positive constant.*

4.2 Nonadaptive reference system

In this section, we analyze a nonadaptive reference system that represents the ideal behavior for the adaptive control system. The analysis establishes a stability condition for the reference system, and shows the existence of a positive lower bound for its time-delay margin, which quantifies the delay robustness.

Specifically, let $k > 0$ be a given scalar, and consider the closed-loop *nonadaptive, delay-differential, reference system* obtained by appending

$$\dot{u}(t) = -k\omega u(t-\epsilon) - k\eta\big(t, r(t)\big) - kK_d y_d(t), \tag{4.5}$$

with $K_d \triangleq (DA_m^{-1}B)^{-1}$ and $u(t) = 0,\ \forall t \in [-\epsilon, 0]$, to (4.2) and (4.4). We proceed to investigate the continuity of solutions of (4.5) with respect to t and ϵ.

4.2.1 Continuous dependence on input delay

Consider the following linear DDE

$$\dot{F}(t;\epsilon) = -k\omega F(t-\epsilon;\epsilon) - k\mathbb{I}\delta(t), \tag{4.6}$$

with $F(t,\epsilon) = 0,\ \forall t \in [-\epsilon, 0]$, obtained from (4.5) by substituting the Dirac impulse $\delta(t)$ in lieu of the input excitation $\eta\big(t, r(t)\big) + K_d y_d(t)$.

Lemma 4.1. *The DDE in* (4.6) *has no finite escape time.*

Proof. Assume that (4.6) has a finite escape time. In particular, suppose that

$$\big\|F(t;\epsilon)\big\| < \infty,\ \forall t \in [0, t_e) \tag{4.7}$$

and

$$\lim_{t \to t_e} \|F(t;\epsilon)\| = \infty. \tag{4.8}$$

It follows from (4.6) that

$$\big\|F(t_e;\epsilon)\big\| \leq \left\| -k\omega \int_0^{t_e} F(\lambda - \epsilon;\epsilon)\mathrm{d}\lambda \right\| + k \leq k\|\omega\| \int_0^{t_e-\epsilon} \big\|F(\lambda;\epsilon)\big\|\mathrm{d}\lambda + k < \infty, \tag{4.9}$$

since (4.7) implies that $\big\|F(t;\epsilon)\big\|$ is bounded for $t \in [0, t_e - \epsilon]$. Since $F(t;\epsilon)$ is a continuous function in t (see Section 2.2 of [48], p. 37), we have arrived at a contradiction. □

Lemma 4.2. *For every $T > 0$, $F(t;\epsilon)$ is a continuous function of $\epsilon \geq 0$, uniformly in $t \in [0, T]$.*

Proof. Consider an arbitrary convergent sequence ϵ_m, such that

$$\lim_{m \to \infty} \epsilon_m = \bar{\epsilon}, \tag{4.10}$$

for some given $\bar{\epsilon} > 0$. For nonzero $\epsilon \approx \bar{\epsilon}$, let $\tilde{F}(\tau, \epsilon) := F(\epsilon\tau;\epsilon)$ be defined for $\tau \in [0, \tilde{T}]$, for some $\tilde{T} > T/\bar{\epsilon}$. It follows that

$$\dot{\tilde{F}}(\tau;\epsilon) = -\epsilon k\omega \tilde{F}(\tau - 1;\epsilon) - \epsilon k\delta(\epsilon\tau), \tag{4.11}$$

with $\tilde{F}(\tau;\epsilon) = 0,\ \forall \tau \in [-1, 0]$. Integrating both sides of (4.11) leads to

$$\tilde{F}(\tau;\epsilon) = -\epsilon k\omega \int_0^{\tau} \tilde{F}(\lambda - 1;\epsilon)\mathrm{d}\lambda - k\mathbb{I}. \tag{4.12}$$

It follows from (4.12) that $\|\tilde{F}(\tau;\epsilon_m) - \tilde{F}(\tau;\bar{\epsilon})\|$ is bounded by

$$
\begin{aligned}
&k\|\omega\| \int_0^\tau \left\| \epsilon_m \tilde{F}(\lambda - 1; \epsilon_m) - \bar{\epsilon}\tilde{F}(\lambda - 1; \bar{\epsilon}) \right\| \mathrm{d}\lambda \\
&\leq k\|\omega\|\epsilon_m \int_0^\tau \|\tilde{F}(\lambda - 1; \epsilon_m) - \tilde{F}(\lambda - 1; \bar{\epsilon})\| \mathrm{d}\lambda + k\|\omega\| \int_0^\tau \left\| (\epsilon_m - \bar{\epsilon})\tilde{F}(\lambda - 1; \bar{\epsilon}) \right\| \mathrm{d}\lambda. \quad (4.13)
\end{aligned}
$$

By a change of variables, and use of the initial condition, it follows that $\|\tilde{F}(\tau;\epsilon_m) - \tilde{F}(\tau;\bar{\epsilon})\|$ is bounded by

$$
k\|\omega\|\epsilon_m \int_0^\tau \|\tilde{F}(\lambda;\epsilon_m) - \tilde{F}(\lambda;\bar{\epsilon})\| \mathrm{d}\lambda + R(\epsilon_m, \bar{\epsilon}), \quad (4.14)
$$

where

$$
R(\epsilon_m, \bar{\epsilon}) \triangleq |\epsilon_m - \bar{\epsilon}|k\|\omega\| \int_0^{\tilde{T}} \left\| \tilde{F}(\lambda - 1; \bar{\epsilon}) \right\| \mathrm{d}\lambda. \quad (4.15)
$$

Since $\tilde{F}(\tau;\bar{\epsilon})$ is bounded by Lemma 4.1,

$$
\lim_{m\to\infty} R(\epsilon_m, \bar{\epsilon}) = 0. \quad (4.16)
$$

By the Gronwall lemma,

$$
\begin{aligned}
&\sup_{\tau\in[0,\tilde{T}]} \|\tilde{F}(\tau;\epsilon_m) - \tilde{F}(\tau;\bar{\epsilon})\| \leq R(\epsilon_m, \bar{\epsilon})\mathrm{e}^{k\epsilon_m\|\omega\|\tilde{T}} \\
&\quad \Rightarrow \lim_{m\to\infty} \sup_{\tau\in[0,\tilde{T}]} \|\tilde{F}(\tau;\epsilon_m) - \tilde{F}(\tau;\bar{\epsilon})\| = 0 \quad (4.17)
\end{aligned}
$$

Finally,

$$
\|F(t;\epsilon_m) - F(t;\bar{\epsilon})\| \leq \left\| \tilde{F}\left(\frac{t}{\epsilon_m};\epsilon_m\right) - \tilde{F}\left(\frac{t}{\epsilon_m};\bar{\epsilon}\right) \right\| + \left\| F\left(t\frac{\bar{\epsilon}}{\epsilon_m};\bar{\epsilon}\right) - F(t;\bar{\epsilon}) \right\|. \quad (4.18)
$$

By the uniform continuity, for fixed ϵ, of $F(t;\epsilon)$ in t on the compact interval $[0, T]$, it follows

that

$$\lim_{m\to\infty}\sup_{t\in[0,T]}\|F(t;\epsilon_m)-F(t;\bar{\epsilon})\|=0, \tag{4.19}$$

i.e., that $F(t;\epsilon)$ is continuous in ϵ for $\epsilon>0$, uniformly in t on $[0,T]$.

Suppose, instead, that $\bar{\epsilon}=0$.

Then,

$$\begin{aligned}\|F(t;\epsilon_m)-F(t;0)\| \le k\|\omega\|\int_0^t \|F(\lambda;\epsilon_m)-F(\lambda;0)\|\mathrm{d}\lambda \\ + k\|\omega\|\int_0^t \|F(\lambda-\epsilon_m;\epsilon_m)-F(\lambda;\epsilon_m)\|\mathrm{d}\lambda.\end{aligned} \tag{4.20}$$

Again, applying the Gronwall lemma gives

$$\|F(t;\epsilon_m)-F(t;0)\| \le k\|\omega\|\mathrm{e}^{k\|\omega\|t}\int_0^t \|F(\lambda-\epsilon_m;\epsilon_m)-F(\lambda;\epsilon_m)\|\mathrm{d}\lambda. \tag{4.21}$$

It follows from (4.6) that

$$\begin{aligned}F(t-\epsilon;\epsilon) &= -k\omega\int_0^{t-\epsilon}F(\lambda-\epsilon;\epsilon)\mathrm{d}\lambda - k\mathbb{I} = -k\omega\int_{-\epsilon}^{t-2\epsilon}F(\lambda;\epsilon)\mathrm{d}\lambda - k\mathbb{I} \\ &= -k\omega\int_0^t F(\lambda;\epsilon)\mathrm{d}\lambda + k\omega\int_{t-2\epsilon}^t F(\lambda;\epsilon)\mathrm{d}\lambda - k\mathbb{I}.\end{aligned} \tag{4.22}$$

It follows from [48] (p. 16) that there exist positive constants β_1 and β_2, independent of ϵ, such that

$$\|F(t;\epsilon)\| \le \beta_1\mathrm{e}^{\beta_2 t} \le \beta_1\mathrm{e}^{\beta_2 T} \tag{4.23}$$

as $t\in[-\epsilon,T]$. Hence,

$$k\omega\int_{t-2\epsilon}^t F(\lambda;\epsilon)\mathrm{d}\lambda \le k\|\omega\|\beta_1\mathrm{e}^{\beta_2 T}2\epsilon \triangleq R_1(\epsilon). \tag{4.24}$$

Note here that $\lim_{m\to\infty} R_1(\epsilon_m) = 0$. From (4.6) and (4.22) we obtain

$$\|F(t-\epsilon_m;\epsilon_m) - F(t;\epsilon_m)\| \le R_1(\epsilon_m) + k\|\omega\| \int_0^t \|F(\lambda;\epsilon_m) - F(\lambda-\epsilon_m;\epsilon_m)\|\,\mathrm{d}\lambda. \tag{4.25}$$

It follows from the Gronwall lemma that

$$\lim_{m\to\infty} \sup_{t\in[-\epsilon,T]} \|F(t-\epsilon_m;\epsilon_m) - F(t;\epsilon_m)\| \le \mathrm{e}^{k\|\omega\|T} \lim_{m\to\infty} R_1(\epsilon_m) = 0. \tag{4.26}$$

Thus from (4.21) and (4.26), we arrive at the continuity of $F(t;\epsilon)$ in ϵ at $\epsilon = 0$, uniformly in t on $[0,T]$. □

Lemma 4.3. *$F(t;\epsilon)$ is a continuous function of ϵ, for ϵ sufficiently small, uniformly in $t \in [0,\infty)$.*

Proof. It follows from (4.6) that, when the delay $\epsilon = 0$, the equation is exponentially stable as $k\omega$ is positive definite. Therefore, there is an interval $[0,\epsilon_{\mathrm{us}})$ for the delay, on which (4.6) is exponentially stable. In fact, following [48] (p. 182), there exist positive scalars C and $\alpha(\epsilon_s)$, independent of the delay ϵ, such that

$$\|F(t;\epsilon)\| \le c\mathrm{e}^{-\alpha(\epsilon_s)t},\ \forall\epsilon\in[0,\epsilon_s],\ \text{and}\ \ t\in[0,\infty) \tag{4.27}$$

for any $\epsilon_s < \epsilon_{\mathrm{us}}$.

For such an ϵ_s, consider a convergent sequence ϵ_m with $\lim_{m\to\infty}\epsilon_m = \bar\epsilon$, where $\bar\epsilon \in [0,\epsilon_s)$. Then, for $0 < \delta \ll 2c$, and with $T_l \triangleq \frac{1}{\alpha(\epsilon_s)}\ln(\frac{2c}{\delta})$, we have

$$\sup_{t\in[T_l,\infty)} \|F(t;\epsilon_m) - F(t;\bar\epsilon)\| \le 2c\mathrm{e}^{-\alpha(\epsilon_s)T_l} = \delta \tag{4.28}$$

for sufficiently large m. Further, by the previous lemma,

$$\sup_{t\in[0,T_l]} \|F(t;\epsilon_m) - F(t;\bar\epsilon)\| \le \delta \tag{4.29}$$

for sufficiently large m. It follows from (4.28) and (4.29) that there exists an integer M, such that $m \geq M$ implies

$$\sup_{t\in[0,\infty)} \|F(t;\epsilon_m) - F(t;\bar{\epsilon})\| \leq \delta. \tag{4.30}$$

Thus, $F(t;\epsilon)$ is continuous in ϵ on $[0,\epsilon_{\rm us})$, uniformly in t on $[0,\infty)$. □

Lemma 4.4. *Let $\Phi(t;\epsilon)$ denote the solution to*

$$\dot{\Phi}(t,\epsilon) = A_m\Phi(t,\epsilon) + B\omega F(t-\epsilon,\epsilon) + B\delta(t) \tag{4.31}$$

with $\Phi(0,\epsilon) = 0$, and $F(t-\epsilon,\epsilon)$ is the solution to (4.6). Then, $\Phi(t;\epsilon)$ is continuous in ϵ on $[0,\epsilon_{\rm us})$, uniformly in t on $[0,\infty)$.

Proof. Given $\epsilon_s < \epsilon_{\rm us}$, consider a convergent sequence ϵ_m with $\lim_{m\to\infty} \epsilon_m = \bar{\epsilon}$, where $\bar{\epsilon} \in [0,\epsilon_s)$. Consider an arbitrary $\delta \in [0,1)$. By applying the variation-of-constants formula to (4.31), it follows that $\|\Phi(t;\epsilon_m) - \Phi(t;\bar{\epsilon})\|$ is bounded by

$$\|B\|\|\omega\| \int_0^t \|F(\lambda-\epsilon_m,\epsilon_m) - F(\lambda-\bar{\epsilon},\bar{\epsilon})\|\mathrm{d}\lambda, \tag{4.32}$$

since $\|\mathrm{e}^{A_m(t-\lambda)}\| \leq 1$ for $\lambda \in [0,t]$ and $t \in [0,\infty)$ and A_m Hurwitz. Let $T_h \triangleq -\frac{1}{\alpha(\epsilon_s)}\ln\delta$. For sufficiently large m, it follows by continuity and from the previous lemmas that $\|\Phi(t;\epsilon_m) - \Phi(t;\bar{\epsilon})\|$ is bounded, for all $t \in [0,\infty)$, by

$$\|B\|\|\omega\| \left(\int_0^{T_h} \frac{\delta}{T_h}\mathrm{d}\lambda + \int_{T_h}^{\infty} 2c\mathrm{e}^{-\alpha(\epsilon_s)\lambda}\mathrm{d}\lambda \right) = \|B\|\|\omega\| \left(1 + \frac{2c}{\alpha(\epsilon_s)}\right)\delta. \tag{4.33}$$

Since the right-hand side of this inequality is proportional to δ, we conclude that $\Phi(t;\epsilon)$ is continuous in ϵ on $[0,\epsilon_{\rm us})$, uniformly in t on $[0,\infty)$.

□

With minimal modifications to the proof, we arrive at the following lemma.

Lemma 4.5. *Let $\Psi(t;\epsilon)$ be the solution to*

$$\dot{\Psi}(t,\epsilon) = A_m\Psi(t,\epsilon) + B\omega F(t-\epsilon,\epsilon)K_d \tag{4.34}$$

with $\Psi(0,\epsilon) = 0$, and $F(t-\epsilon,\epsilon)$ is the solution to (4.6), and some constant matrix K_d. The function $\Psi(t;\epsilon)$ is continuous in ϵ on $[0,\epsilon_{\text{us}})$, uniformly in t on $[0,\infty)$.

4.2.2 A stability condition

Since ω is constant, (4.5) implies that

$$u(s) = F(s;\epsilon)\big(\eta(s) + K_d y_d(s)\big), \tag{4.35}$$

where

$$F(s;\epsilon) \triangleq -k\big(s\mathbb{I} + k\omega \mathrm{e}^{-\epsilon s}\big)^{-1} \tag{4.36}$$

is the Laplace transform of the solution $F(t;\epsilon)$ to (4.6), and $\eta(s)$ and $y_d(s)$ are the Laplace transforms of $\eta(t,r(t))$ and $y_d(t)$, respectively.

Let

$$\|P(s)\|_{\mathcal{L}_1} \triangleq \max_{i=1,\ldots,n} \sum_{j=1}^{n} \int_0^\infty |P_{ij}(t)|\mathrm{d}t, \tag{4.37}$$

denote the $\mathcal{L}_1$-norm of the transfer function $P(s)$, in terms of the components $P_{ij}(t)$ of the corresponding impulse response matrix. It follows from Lemma 4.3 that

$$g(\epsilon) \triangleq \|F(s;\epsilon)\|_{\mathcal{L}_1} \tag{4.38}$$

is continuous in $\epsilon \in [0,\epsilon_{\text{us}})$. Since $k\omega$ is positive definite, $g(0)$ is finite. By continuity, g is

bounded on $[0, \epsilon_{\text{us}})$. On this interval,

$$\|u\|_{\mathcal{L}_\infty} \leq g(\epsilon)\big(\|\eta\|_{\mathcal{L}_\infty} + K_d\|y_d\|_{\mathcal{L}_\infty}\big). \tag{4.39}$$

Similarly, it follows from (4.4) and (4.35) that

$$r(s) = \Phi(s;\epsilon)\eta(s) + \Psi(s;\epsilon)y_d(s) + (s\mathbb{I} - A_m)^{-1}r_0, \tag{4.40}$$

where $H(s) \triangleq (s\mathbb{I} - A_m)^{-1}B$, and

$$\Phi(s;\epsilon) \triangleq H(s)\big(\mathbb{I} + \omega \mathrm{e}^{-\epsilon s}F(s;\epsilon)\big), \tag{4.41}$$

$$\Psi(s;\epsilon) \triangleq H(s)\omega \mathrm{e}^{-\epsilon s}F(s;\epsilon)K_d, \tag{4.42}$$

are the Laplace transforms of the solutions $\Phi(t;\epsilon)$ and $\Psi(t;\epsilon)$ to (4.31) and (4.34), respectively. It follows from Lemma 4.4 that

$$f(\epsilon) \triangleq \|\Phi(s;\epsilon)\|_{\mathcal{L}_1} \tag{4.43}$$

is continuous on $[0, \epsilon_{\text{us}})$.

We proceed to show that $f(0) < \infty$. To this end, consider the special case that $\epsilon = 0$, $r_0 = 0$ and $y_d(t) = 0$. Let $\eta_u \triangleq \omega u - u + \eta$, such that

$$\|\eta_u\|_{\mathcal{L}_\infty} \leq \big((\|\omega\| + 1)g(0) + 1\big)\|\eta\|_{\mathcal{L}_\infty}. \tag{4.44}$$

Rearranging the terms in (4.4) yields

$$r(s) = H(s)\big(u(s) + \eta_u(s)\big), \tag{4.45}$$

where, by (4.5),

$$u(s) = -\frac{k}{s+k}\eta_u(s). \tag{4.46}$$

It follows that

$$\begin{aligned}\|r\|_{\mathcal{L}_\infty} &\leq \left\|s(s\mathbb{I} - A_m)^{-1}\right\|_{\mathcal{L}_1} \|B\| \left\|\frac{1}{s+k}\right\|_{\mathcal{L}_1} \|\eta_u\|_{\mathcal{L}_\infty} \\ &\leq \frac{2}{k}\|B\|\big((\|\omega\|+1)g(0)+1\big)\,\|\eta\|_{\mathcal{L}_\infty}\,. \end{aligned} \tag{4.47}$$

From (4.40) it follows that

$$f(0) \leq \frac{2}{k}\|B\|\big((\|\omega\|+1)g(0)+1\big). \tag{4.48}$$

Consider next the delay-dependent norms

$$\rho_d(\epsilon) \triangleq \|\Psi(s;\epsilon)\|_{\mathcal{L}_1} \tag{4.49}$$

and

$$\rho_{\text{ic}} \triangleq \|(s\mathbb{I} - A_m)^{-1}\|_{\mathcal{L}_1}, \tag{4.50}$$

which represent the effects of the desired trajectory y_d and the initial condition r_0 on the solution to (4.40). Here, $\rho_d(0)$ and ρ_{ic} are both finite, since $\Phi(s;0) = H(s)F(s;0)$ is a stable transfer function and A_m is Hurwitz. Moreover, by Lemma 4.5, $\rho_d(\epsilon)$ is continuous on $[0, \epsilon_{\text{us}})$.

Lemma 4.6. *Given $b_d > 0$ and $b_{\text{ic}} > 0$, there exists a k, a ρ_{ref}, and an ϵ_l, such that*

$$f(\epsilon) \leq \frac{\rho_{\text{ref}} - \rho_d(\epsilon)b_d - \rho_{\text{ic}}b_{\text{ic}}}{L_{\rho_{\text{ref}}}\rho_{\text{ref}} + Z}, \quad \forall \epsilon \in [0, \epsilon_l], \tag{4.51}$$

where

$$L_{\rho_{\text{ref}}} \triangleq \frac{\rho_{\text{ref}}+1}{\rho_{\text{ref}}} d_{\eta_r}(\rho_{\text{ref}}+1). \tag{4.52}$$

Proof. Choose $\rho_{\text{ref}} > \rho_{\text{ic}}b_{\text{ic}} + \rho_d(0)b_d$. Then, since $f(0) \to 0$ as $k \to \infty$, it follows that there

exists a K, such that $k > K$ implies that

$$f(0) < \frac{\rho_{\text{ref}} - \rho_d(0)b_d - \rho_{\text{ic}}b_{\text{ic}}}{L_{\rho_{\text{ref}}}\rho_{\text{ref}} + Z}. \tag{4.53}$$

For such a k, the claim now follows by the continuity of $f(\epsilon)$ and $\rho_d(\epsilon)$, where ϵ_l equals the smallest value of ϵ that results in equality in (4.51). □

In Section 4.2.4 below, we show that if, in addition, $\rho_{\text{ref}} > b_{\text{ic}}$, then the closed-loop reference system admits a transient performance bound for any $\epsilon < \epsilon_l$. Furthermore, in Section 4.3.2, we show that, for sufficiently large adaptive gains, the state and control input of the closed-loop adaptive control system follow those of the reference system closely. This implies that ϵ_l is a lower bound for the time-delay margin of the closed-loop adaptive control system.

4.2.3 The upper bound of ϵ_l

The quantity ϵ_{us} was defined earlier as the smallest positive value of ϵ for which $F(s;\epsilon)$ has a pole on the imaginary axis. It follows from the definition of $f(\epsilon)$ in (4.43) that

$$f(\epsilon) = \left\| s(s\mathbb{I} - A_m)^{-1}BF(t;\epsilon)/k \right\|_{\mathcal{L}_1}, \tag{4.54}$$

where $s(s\mathbb{I} - A_m)^{-1}B$ is a stable transfer function for A_m Hurwitz. It follows that $f(\epsilon_{\text{us}})$ is infinite, i.e., that $\epsilon_l < \epsilon_{\text{us}}$.

We now seek the delay value at which the rightmost eigenvalues of $F(s;\epsilon)$ cross the imaginary axis. When $\omega \in \mathbb{R}$, Let $s = j\alpha$, where j is the imaginary unit. Applying Euler's formula to the denominator of $F(s;\epsilon)$ yields

$$s + k\omega e^{-\epsilon s} = k\omega\cos(\epsilon\alpha) + j(\alpha - k\omega\sin(\epsilon\alpha)). \tag{4.55}$$

By setting the real part of (4.55) to zero we get $\alpha^* = \frac{n\pi + \frac{\pi}{2}}{\epsilon^*}$, where $n \in \mathbb{Z}$. Taking this into

account, we set the imaginary part of (4.55) to zero to arrive at

$$\epsilon^* = \frac{n\pi + \frac{\pi}{2}}{k\omega \sin(n\pi + \frac{\pi}{2})} \tag{4.56}$$

When $\omega \in \mathbb{R}^{m\times m}$, since ω is positive definite, it can be diagonalized as follows:

$$\omega = U\Lambda U^{-1}$$

where $U \in \mathbb{R}^{m\times m}$ is an orthogonal matrix, with $U^{-1} = U^\top$, and $\Lambda \in \mathbb{R}^{m\times m}$ is a diagonal matrix, given in the following form

$$\Lambda = \text{diag}[\lambda_{ii}],\ i = 1, ..., m$$

where λ_{11}, λ_{22}, ...λ_{mm} are the eigenvalues of matrix ω, and they are all positive. Then,

$$s\mathbb{I} + ke^{-\epsilon s}\omega = U(s\mathbb{I} + ke^{-\epsilon s}\Lambda)U^{-1} \tag{4.57}$$

$F(s;\epsilon)$ is then given by the inverse of (4.57),

$$F(s;\epsilon) = -kU\text{diag}\Big[\frac{1}{s + ke^{-\epsilon s}\lambda_{ii}}\Big]U^{-1},\ i = 1, ..., m \tag{4.58}$$

The analysis in this case again follows the scalar case to obtain (4.56), in which ω is now replaced by λ_{ii}.

Consider the above two cases for ω, and from (4.56), we can get the following expression

$$\epsilon_{\text{us}} = \frac{\pi}{2k\lambda_m}, \tag{4.59}$$

where λ_m is the maximum eigenvalue of ω.

From the above analysis, ϵ_{us} is always inversely proportional to the filter bandwidth k.

Since ϵ_{us} is the upper bound for ϵ_l, ϵ_l must lie in the envelope formed by ϵ_{us}, which decreases as k increases.

4.2.4 Transient performance of the reference system

In this section, we show that the closed-loop reference system may be designed to admit a transient performance bound even for nonzero input delay.

Theorem 4.1. *Denote the solution to the nonadaptive reference system formed by* (4.2), (4.4) *and* (4.5) *by* $\big(r_{\text{ref}}(t), u_{\text{ref}}(t), y_{\text{ref}}(t)\big)$. *Then, given* $b_d > 0$ *and* $b_{\text{ic}} > 0$, *there exists a* k, *such that*

$$\|y_d\|_{\mathcal{L}_\infty} \leq b_d \text{ and } \|r_0\|_\infty \leq b_{\text{ic}} \Rightarrow \|r_{\text{ref}}\|_{\mathcal{L}_\infty} \leq \rho_{\text{ref}} \tag{4.60}$$

for some ρ_{ref} *and for all* ϵ *smaller than the corresponding* ϵ_l. *In addition,* $\|u_{\text{ref}}\|_{\mathcal{L}_\infty} < \infty$.

Proof. Choose $\rho_{\text{ref}} > \max\left(b_{\text{ic}}, \rho_{\text{ic}} b_{\text{ic}} + \rho_d(0) b_d\right)$. Suppose there exists a $T > 0$, such that the truncated norm $\|r_{\text{ref},T}\|_{\mathcal{L}_\infty}$ on the interval $[0, T]$ is greater than or equal to ρ_{ref}. Since $r_{\text{ref}}(0) = r_0$, there exists a $\hat{T} \in [0, T]$, such that

$$\|r_{\text{ref}}(t)\|_\infty < \rho_{\text{ref}}, \ \forall t \in [0, \hat{T}), \tag{4.61}$$

and

$$\|r_{\text{ref}}(\hat{T})\|_\infty = \rho_{\text{ref}}. \tag{4.62}$$

Let $\eta_{\text{ref}}(t) \triangleq \eta\big(t, r_{\text{ref}}(t)\big)$. It follows from Appendix B of [102] and Assumption 4.4 that

$$\|\eta_{\text{ref},\hat{T}}\|_{\mathcal{L}_\infty} < \rho_{\text{ref}} L_{\rho_{\text{ref}}} + Z. \tag{4.63}$$

Together with (4.4), (4.5) and (4.51), this leads to

$$\|r_{\text{ref},\hat{T}}\|_{\mathcal{L}_\infty} < \rho_{\text{ref}}, \tag{4.64}$$

and we have arrived at a contradiction. The boundedness of u_{ref} follows, as in [102], immediately from (4.39) and the bound on η_{ref} in (4.63), which holds for all time. □

Remark 4.1. *Suppose that $y_d(t)$ is constant. Then, since*

$$\lim_{s\to 0} Ds\Psi(s;\epsilon)y_d(s) = DA_m^{-1}BK_d y_d = y_d \tag{4.65}$$

and

$$\lim_{s\to 0} s(s\mathbb{I} - A_m)^{-1}r_0 = 0, \tag{4.66}$$

it follows that, for large t

$$\|y(t) - y_d\|_\infty \leq Df(\epsilon)\|\eta\|_{\mathcal{L}_\infty} < Df(\epsilon)(\rho_{\text{ref}}L_{\rho_{\text{ref}}} + Z). \tag{4.67}$$

Since $f(0) = \mathcal{O}(k^{-1})$, it follows that

$$\|y(t) - y_d\|_\infty = \mathcal{O}(k^{-1}) \tag{4.68}$$

when $\epsilon = 0$. No such conclusion follows for $\epsilon \neq 0$.

4.3 An adaptive control scheme and its transient performance

In this section, we first design the adaptive controller for the system of interest, along the line of the general framework of adaptive control proposed in [61]. We then prove guaranteed bounds on the estimation error and on the deviations between the state and control input of the proposed adaptive control system and those of the nonadaptive reference system.

4.3.1 Control design

Let the control input $u(t)$ be the solution to the differential equation

$$\dot{u}(t) = -k\big(u(t) + \hat{\theta}(t)\|r_t\|_{\mathcal{L}_\infty} + \hat{\sigma}(t) + K_d y_d(t)\big), \tag{4.69}$$

where $u(0) = 0$, and the functions $\hat{\theta}$ and $\hat{\sigma}$ are governed by the projection-based adaptive laws (cf. [71])

$$\dot{\hat{\theta}}(t) = \Gamma\, \mathbf{Proj}\big(\hat{\theta}(t), -B^\top P\tilde{r}(t)\|r_t\|_{\mathcal{L}_\infty}; \theta_b, \nu\big), \tag{4.70}$$

$$\dot{\hat{\sigma}}(t) = \Gamma\, \mathbf{Proj}\big(\hat{\sigma}(t), -B^\top P\tilde{r}(t); \sigma_b, \nu\big), \tag{4.71}$$

with $\hat{\theta}(0) = \hat{\theta}_0$ and $\hat{\sigma}(0) = \hat{\sigma}_0$, in terms of the estimation error $\tilde{r} \triangleq \hat{r} - r$, where

$$\dot{\hat{r}}(t) = A_m r(t) + A_{\mathrm{sp}}\tilde{r}(t) + B\big(u(t) + \hat{\theta}(t)\|r_t\|_{\mathcal{L}_\infty} + \hat{\sigma}(t)\big) \tag{4.72}$$

and $\hat{r}(0) = r_0$. Here, the positive scalar k corresponds to the bandwidth of the first-order low-pass filter $k/(s+k)$. Moreover, A_{sp} is a Hurwitz matrix, which may be tuned to reduce any noise in the state predictor $\hat{r}$. The *projection operators* $\mathbf{Proj}(\cdot,\cdot;\cdot,\cdot)$ are here implemented in terms of the bounds θ_b and σ_b, the tolerance ν, and the positive-definite matrix P, obtained as the solution to the Lyapunov equation $A_{\mathrm{sp}}^\top P + PA_{\mathrm{sp}} = -\mathbb{I}$. The implementation ensures that $\|\hat{\theta}(t)\|_\infty \leq \theta_b$ and $\|\hat{\sigma}(t)\|_\infty \leq \sigma_b$ provided that $\hat{\theta}_0$ and $\hat{\sigma}_0$ satisfy these same bounds. Finally, $\Gamma > 0$ is the adaptive gain.

4.3.2 Transient performance of the adaptive system

In this section, we analyze the transient performance of the proposed adaptive closed-loop control system. The theorem below states that if $\epsilon < \epsilon_l$, and the bandwidth k, the adaptive gain Γ, and the bounds θ_b and σ_b are chosen appropriately, then the state and control input

of the adaptive closed-loop control system governed by (4.4) and (4.69)-(4.72) follow those of the reference system closely. In particular,

Theorem 4.2. *Suppose b_d and b_{ic} are given, and ρ_{ref} and k are chosen as in Section 4.2.2 and assume that ϵ is less than the corresponding ϵ_l. Then, there exists a $C > 0$, such that, for $\psi \ll 1$, $\|\tilde{r}\|_{\mathcal{L}_\infty} \leq \psi$ and*

$$\|r_{\text{ref}} - r\|_{\mathcal{L}_\infty}, \ \|u_{\text{ref}} - u\|_{\mathcal{L}_\infty} \tag{4.73}$$

are bounded from above by $b_r\psi$ and $b_u\psi$ for some positive constants b_r and b_u, provided that $\Gamma\psi^2 \geq C$.

Since ϵ_l is a positive, lower bound for the time-delay margin of the nonadaptive reference system, it is also a positive, lower bound for the time-delay margin of the adaptive closed-loop control system, which guarantees that $\|r\|_{\mathcal{L}_\infty} \leq \rho_{\text{ref}} + b_r\psi$.

Before proving this theorem, we show that the state predictor tracks the system state with the estimation error inversely proportional to the square root of the adaptive gain.

Lemma 4.7. *Suppose that*

$$\|r_\tau\|_{\mathcal{L}_\infty} < \rho_{\text{ref}} + 1, \quad \|u_\tau\|_{\mathcal{L}_\infty} < \rho_{\text{u}} < \infty \tag{4.74}$$

for some τ. Then, there exists a $C > 0$, which is independent of τ, such that the truncated norm

$$\|\tilde{r}_\tau\|_{\mathcal{L}_\infty} \leq \sqrt{C/\Gamma}. \tag{4.75}$$

Proof. Because of the bound in (4.74), the parameterization

$$\eta(t, r(t)) = \theta(t)\|r_t\|_{\mathcal{L}_\infty} + \sigma(t) \tag{4.76}$$

holds for all $t \in [0, \tau]$, in terms of a pair of continuous, piecewise-differentiable and uniformly

bounded functions θ and σ that satisfy $\|\theta(t)\| < \theta_b$, $\|\dot{\theta}(t)\| < d_\theta$, $\|\sigma(t)\| < \sigma_b$, and $\|\dot{\sigma}(t)\| < d_\sigma$ (see Lemma A.9.2 in [61]), with bounds that are independent of τ. Hence, from (4.4) and (4.72), we get

$$\dot{\tilde{r}}(t) = A_{\rm sp}\tilde{r}(t) + B\big(\tilde{\theta}(t)\|r_t\|_{\mathcal{L}_\infty} + \tilde{\sigma}(t)\big), \tag{4.77}$$

and $\tilde{r}(0) = 0$, where $\tilde{\theta} \triangleq \hat{\theta} - \theta$, $\tilde{\sigma} \triangleq \hat{\sigma} - \bar{\sigma}$, and

$$\bar{\sigma}(t) = \sigma(t) + \omega u(t - \epsilon) - u(t). \tag{4.78}$$

By the assumption on u and the bound on σ, $\|\bar{\sigma}(t)\| \leq \bar{\sigma}_b$, with $\bar{\sigma}_b$ independent of τ. Moreover,

$$\dot{\bar{\sigma}}(t) = \dot{\sigma}(t) + \omega \dot{u}(t - \epsilon) - \dot{u}(t). \tag{4.79}$$

By the assumptions on $r(t)$ and $u(t)$, (4.4) and (4.69)-(4.71), imply that $\dot{r}$ and $\dot{u}$ are bounded by constants independent of τ. Hence, $\|\dot{\bar{\sigma}}(t)\|_\infty \leq d_{\bar{\sigma}}$, with $d_{\bar{\sigma}}$ independent of τ.

Consider the Lyapunov function candidate

$$V(t) = \tilde{r}^\top(t)P\tilde{r}(t) + \frac{1}{\Gamma}(\tilde{\theta}^\top(t)\tilde{\theta}(t) + \tilde{\sigma}^\top(t)\tilde{\sigma}(t)). \tag{4.80}$$

By the properties of the projection operators,

$$\dot{V}(t) \leq -\tilde{r}^\top(t)\tilde{r}(t) + \frac{2}{\Gamma}\big|\tilde{\theta}^\top(t)\dot{\theta}(t) + \tilde{\sigma}^\top(t)\dot{\tilde{\sigma}}(t)\big| \leq -\|\tilde{r}\|_2^2 + \frac{4}{\Gamma}\big(\theta_b d_\theta + \sigma_b d_{\bar{\sigma}}\big). \tag{4.81}$$

We have

$$V(0) \leq \frac{4}{\Gamma}\left(\theta_b^2 + \sigma_b^2\right) < \frac{\nu_m}{\Gamma}, \tag{4.82}$$

where $\nu_m \triangleq 4(\theta_b^2 + \sigma_b^2) + 4\lambda_{\max}(P)\big(\theta_b d_\theta + \sigma_b d_{\bar{\sigma}}\big)$. We now show by contradiction that

$$V(t) \leq \frac{\nu_m}{\Gamma}, \quad \forall t \in [0, \tau]. \tag{4.83}$$

To this end, choose $\hat{\tau} \in (0, \tau]$ such that $\dot{\theta}$ and $\dot{\sigma}$ are continuous on $[0, \hat{\tau})$. Suppose that $V(\bar{\tau}) > \nu_m/\Gamma$ and $\dot{V}(\bar{\tau}) \geq 0$ for some $\bar{\tau} < \hat{\tau}$. It follows that

$$\frac{\nu_m}{\Gamma} < V(\bar{\tau}) \leq \|\tilde{r}(\bar{\tau})\|_2^2 \lambda_{\max}(P) + \frac{4}{\Gamma}\big(\theta_b^2 + \bar{\sigma}_b^2\big).$$

Hence,

$$\|\tilde{r}(\bar{\tau})\|_2^2 > \frac{4}{\Gamma}\big(\theta_b d_\theta + \sigma_b d_{\bar{\sigma}}\big). \tag{4.84}$$

By substituting (4.84) in (4.81) we have $\dot{V}(\bar{\tau}) < 0$, which contradicts the assumption that $\dot{V}(\bar{\tau}) \geq 0$. Thus, $V(t) \leq \frac{\nu_m}{\Gamma}$ for all $t \in [0, \hat{\tau})$. Since $V(t)$ is a continuous function, $V(t) \leq \frac{\nu_m}{\Gamma}$ for all $t \in [0, \hat{\tau}]$. Consequently,

$$\|\tilde{r}_{\hat{\tau}}\|_{\mathcal{L}_\infty} \leq \sqrt{\frac{\nu_m}{\lambda_{\min}(P)\Gamma}}\,. \tag{4.85}$$

By repeating this analysis for each subsequent interval of continuity of $\dot{\theta}$ and $\dot{\sigma}$, we conclude that (4.85) holds with $\hat{\tau}$ replaced by τ, and the claim follows. □

Lemma 4.8. *Let $\tilde{\eta}(t) \triangleq \tilde{\theta}(t)\|r_t\|_{\mathcal{L}_\infty} + \tilde{\sigma}(t)$. When $\epsilon \leq \epsilon_l$, there exists a constant b_0 such that*

$$\|F(s;\epsilon)\tilde{\eta}(s)\|_{\mathcal{L}_\infty} \leq b_0 \|\tilde{r}\|_{\mathcal{L}_\infty}. \tag{4.86}$$

Proof. From (4.77) we have

$$B^\top \dot{\tilde{r}} = B^\top A_{\rm sp} \tilde{r} + B^\top B \tilde{\eta} \tag{4.87}$$

and, consequently,

$$\tilde{\eta}(s) = B^*(s\mathbb{I} - A_{\rm sp})\tilde{r}(s) \tag{4.88}$$

where the pseudoinverse $B^* = (B^\top B)^{-1}B^\top$, since $B^\top B$ is nonsingular by Assumption 4.1. Moreover, from (4.6), it follows that

$$sF(s;\epsilon) = -k\big(\mathbb{I} + \omega \mathrm{e}^{-\epsilon s}F(s;\epsilon)\big) \tag{4.89}$$

Since $\|F(s;\epsilon)\|_{\mathcal{L}_1}$ is bounded for $\epsilon \leq \epsilon_l$, it follows that the norm $\|sF(s;\epsilon)\|_{\mathcal{L}_1}$ is bounded. Thus,

$$\|F(s;\epsilon)\tilde{\eta}(s)\|_{\mathcal{L}_\infty} \leq \|sF(s;\epsilon)B^*\tilde{r}(s)\|_{\mathcal{L}_\infty} + \|F(s;\epsilon)B^*A_{\rm sp}\tilde{r}(s)\|_{\mathcal{L}_\infty} \tag{4.90}$$

and the claim follows. □

We proceed to prove Theorem 4.2.

Proof. Since

$$\|r_{\rm ref}(0) - r(0)\|_\infty = 0 < 1, \quad \|u_{\rm ref}(0) - u(0)\|_\infty = 0, \tag{4.91}$$

it follows by continuity that there exists a $\tau > 0$, such that $\|(r_{\rm ref} - r)_\tau\|_{\mathcal{L}_\infty} < 1$ and $\|(u_{\rm ref} - u)_\tau\|_{\mathcal{L}_\infty} < \infty$. Theorem 4.1 then leads to (4.74). It follows that

$$\|\tilde{r}_\tau\|_{\mathcal{L}_\infty} \leq \sqrt{C/\Gamma}. \tag{4.92}$$

for some $C > 0$, which is independent of τ.

Next, it follows from (4.69) and (4.76) that

$$\dot{u}(t) = -k\Big(\omega u(t-\epsilon) + \eta(t, r(t)) + \tilde{\eta}(t) + K_d y_d(t)\Big) \tag{4.93}$$

and, consequently,

$$u(s) = F(s;\epsilon)\big(\eta(s) + \tilde{\eta}(s) + K_d y_d(s)\big). \tag{4.94}$$

It follows from (4.36) and (4.94) that

$$u_{\text{ref}}(s) - u(s) = F(s;\epsilon)\big(\eta_{\text{ref}}(s) - \eta(s) - \tilde{\eta}(s)\big). \tag{4.95}$$

It further follows from Assumption 4.4 and (4.52) that

$$\|(\eta_{\text{ref}} - \eta)_\tau\|_{\mathcal{L}_\infty} \leq L_{\rho_{\text{ref}}} \|(r_{\text{ref}} - r)_\tau\|_{\mathcal{L}_\infty} \tag{4.96}$$

and, using Lemma 4.8,

$$\|(u_{\text{ref}} - u)_\tau\|_{\mathcal{L}_\infty} \leq g(\epsilon) L_{\rho_{\text{ref}}} \|(r_{\text{ref}} - r)_\tau\|_{\mathcal{L}_\infty} + b_0 \|\tilde{r}_\tau\|_{\mathcal{L}_\infty}. \tag{4.97}$$

From (4.4) we now obtain

$$r_{\text{ref}}(s) - r(s) = H(s)\big(\omega \mathrm{e}^{-\epsilon s}(u_{\text{ref}}(s) - u(s)) + \eta_{\text{ref}}(s) - \eta(s)\big). \tag{4.98}$$

Together with (4.95)-(4.96) and Lemma 4.8, this results in the bound

$$\|(r_{\text{ref}} - r)_\tau\|_{\mathcal{L}_\infty} \leq f(\epsilon) L_{\rho_{\text{ref}}} \|(r_{\text{ref}} - r)_\tau\|_{\mathcal{L}_\infty} + b_2 \|\tilde{r}_\tau\|_{\mathcal{L}_\infty}, \tag{4.99}$$

where $b_2 \triangleq b_0 \|H(s)\omega \mathrm{e}^{-\epsilon s}\|_{\mathcal{L}_1}$, which is finite for $\epsilon \in [0, \epsilon_l)$.

When $\epsilon \in [0, \epsilon_l)$, the stability condition in (4.51) holds and implies that $1 - f(\epsilon) L_{\rho_{\text{ref}}} > 0$. Thus, from (4.97) and (4.99), we conclude that

$$\|(r_{\text{ref}} - r)_\tau\|_{\mathcal{L}_\infty} \leq \frac{b_2}{1 - f(\epsilon) L_{\rho_{\text{ref}}}} \|\tilde{r}_\tau\|_{\mathcal{L}_\infty} \tag{4.100}$$

and

$$\|(u_{\text{ref}} - u)_\tau\|_{\mathcal{L}_\infty} \leq \left(\frac{g(\epsilon) b_2 L_{\rho_{\text{ref}}}}{1 - f(\epsilon) L_{\rho_{\text{ref}}}} + b_0 \right) \|\tilde{r}_\tau\|_{\mathcal{L}_\infty}. \tag{4.101}$$

The claim then follows by choosing ψ and Γ such that the right-hand side of (4.100) is strictly less than 1 and $\sqrt{C/\Gamma} < \psi$. □

In the next two sections, we will demonstrate the destabilizing effect of input delay. In addition, we use Padé approximants to estimate the lower bound ϵ_l for the time delay margin by monitoring the stability condition in (4.51) when the delay is being gradually increased.

4.4 Numerical analysis

To illustrate the effect of the input delay, as well as the delay robustness of the closed-loop system, we consider the system in (4.4) with

$$\begin{aligned} A(t) &= \begin{pmatrix} \sin(t) & 0 & 0 \\ 0 & \cos(t) & 0 \\ 0 & 0 & \cos(2t) \end{pmatrix}, \; B = \mathbb{I}, \omega = \begin{pmatrix} 1.8 & 0.3 & 0.5 \\ 0.3 & 0.6 & 0.2 \\ 0.5 & 0.2 & 1.2 \end{pmatrix}, \\ r_0 &= \begin{pmatrix} 0 \\ 0 \\ 0 \end{pmatrix}, \; D = \mathbb{I}, \eta(t, r) = \begin{pmatrix} r^\top r + \sin(r_1) r_1 r_2 + r_3 \\ r_3^2 + r_1 r_2 + 1 - \mathrm{e}^{-3t} \\ r_2^3 + 0.1 r_3 \cos(2t) \end{pmatrix} \end{aligned} \tag{4.102}$$

The control parameters are set to: $\theta_b = \sigma_b = 100$, $\nu = 0.1$, $\Gamma = 10^5$, $A_{\text{sp}} = -0.1\sqrt{\Gamma}$, $A_m = -2\mathbb{I}$, and the desired trajectory is $y_d = (1\ 1\ 1)^\top$. A low-pass filter with a bandwidth of 10 is used in the control input. When increasing the input delay from zero, numerical experiments reveal that the tracking objective is achieved with smooth control input, even though high adaptation rate is used. Fig. 4.1 shows a typical satisfactory performance when the input delay $\epsilon \in [0, 0.04]$. When the delay is slightly greater than 0.04, the system response and input start exhibiting initial transient oscillations with a decaying envelope,

with amplitude and decay time scale growing with the input time delay. Local growth to a sustained finite-amplitude oscillation about the desired trajectory is observed for an input delay of approximately 0.065, as depicted in Fig. 4.2. For input delay greater than approximately 0.07, the response appears to escape to infinity in finite time.

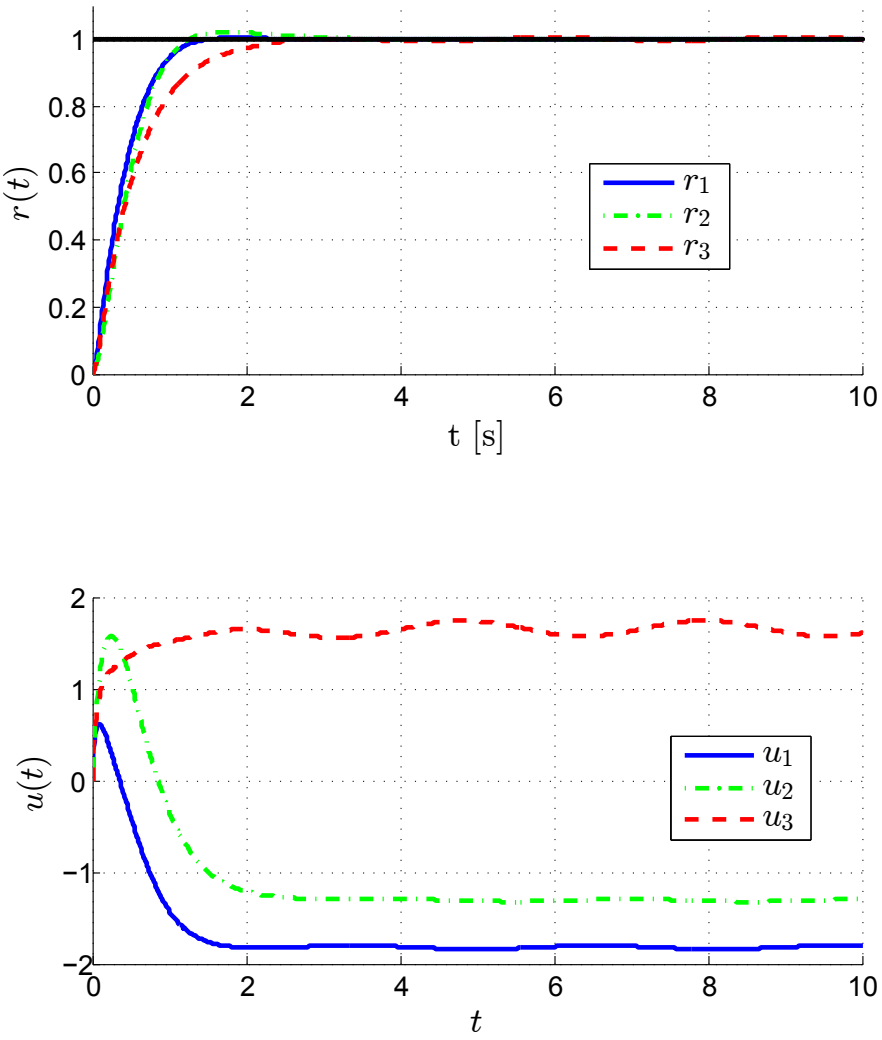

Figure 4.1: Desirable tracking performance of the designed adaptive control system for the input delay $\epsilon = 0.04$ with smooth control input despite the fast adaptation.

4.5 Quantifying the lower bound for the time-delay margin

For a given $b_d > 0$ and $b_{\text{ic}} > 0$, the theoretical analysis shows the existence of a bandwidth k, such that the adaptive closed-loop control system admits a transient performance bound

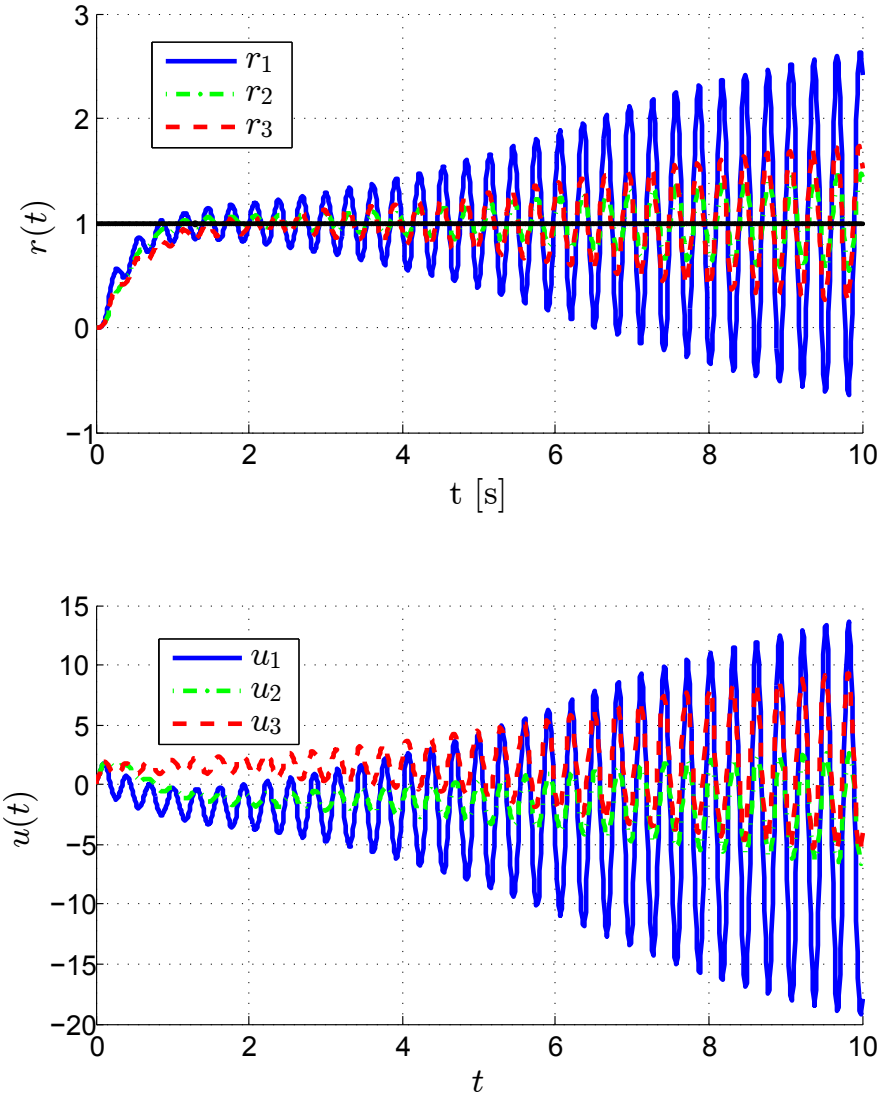

Figure 4.2: Typical unstable response and control input when the input delay is 0.065 and above.

for some ρ_{ref} when ϵ is less than the corresponding ϵ_l, which is positive for some range of values of ρ_{ref}. This implies that the supremum of ϵ_l over this range of values is a guaranteed lower bound for the time delay margin of the adaptive closed-loop control system.

This section proposes a method for estimating ϵ_l, using the delay-dependent stability condition (4.51) and Padé approximants. For convenience, we gather the delay-dependent terms in (4.51) and let $h(\epsilon, \rho_{\text{ref}}) \triangleq f(\epsilon) + \frac{\rho_d(\epsilon) b_d}{L_{\rho_{\text{ref}}} \rho_{\text{ref}} + Z}$. Then the delay-dependent stability

condition (4.51) becomes

$$h(\epsilon, \rho_{\text{ref}}) \leq \frac{\rho_{\text{ref}} - \rho_{\text{ic}} b_{\text{ic}}}{L_{\rho_{\text{ref}}} \rho_{\text{ref}} + Z} \triangleq h_l(\rho_{\text{ref}}), \ \forall \epsilon \in [0, \epsilon_l], \tag{4.103}$$

where $h_l(\rho_{\text{ref}})$ is a function of ρ_{ref} and is independent of the delay ϵ. Furthermore, we approximate the transfer function $e^{-\epsilon s}$ in the definition of $f(\epsilon)$ and $\rho_d(\epsilon)$ by its (n, n) Padé approximant [135], so that the $\mathcal{L}_1$ norms and, consequently, $h(\epsilon, \rho_{\text{ref}})$ may be evaluated in terms of the poles of rational transfer functions.

In the following subsections, we consider separately examples of the cases where the range of applicable values of ρ_{ref} is unbounded and finite, respectively.

4.5.1 Unbounded range

Consider the system (4.4) with

$$A(t) = \begin{pmatrix} 0 & 1 \\ \sin(t) & \cos(t) \end{pmatrix}, A_m = \begin{pmatrix} 0 & 1 \\ -1 & -1.4 \end{pmatrix},$$
$$B = \begin{pmatrix} 0 \\ 1 \end{pmatrix}, \ \omega = 1.2, \ D = \begin{pmatrix} 1 & 0 \end{pmatrix}, \tag{4.104}$$

and

$$\eta(t, r) = (0.5 - 0.8\mathrm{e}^{-0.3t}) \cos(2r_1) + \cos(\pi t) \sin(r_1 + r_2). \tag{4.105}$$

In this case, Assumption 4.4 is satisfied with $d_{\eta_r}(\delta) = 2$, for all δ. It follows that $L_{\rho_{\text{ref}}} = 2(\rho_{\text{ref}} + 1)/\rho_{\text{ref}}$ and, consequently, that $h(\epsilon, \rho_{\text{ref}})$ and $h_l(\rho_{\text{ref}})$ decrease and increase, respectively, for increasing values of ρ_{ref}, and converge on $f(\epsilon)$ and 0.5 when $\rho_{\text{ref}} \to \infty$. Thus, the supremum of ϵ_l should be evaluated over an unbounded range of values of ρ_{ref}.

In the absence of a method for locating such a supremum, we rely on the following heuristic:

since the gap between the $h(\epsilon, \rho_{\text{ref}})$ and $h_l(\rho_{\text{ref}})$ increases to a maximum of $f(\epsilon) - 0.5$ with increasing values of ρ_{ref}, let the supremum be approximated by the value of ϵ_l for some large ρ_{ref}. For example, let $b_d = 10$ and $b_{\text{ic}} = 5$ and choose $\rho_{\text{ref}} = 1000$, for which the stability condition is satisfied at $\epsilon = 0$ for k greater than approximately 2.25. in Fig. 4.3, the horizontal line corresponds to the value of $h_l(\rho_{\text{ref}})$ and each of the curves represent $h(\epsilon, \rho_{\text{ref}})$ for different integer values of k in the range $5, \ldots, 110$. As seen from the numerical results, the higher the filter bandwidth, the faster the variation of the $h(\epsilon, \rho_{\text{ref}})$ curve.

The blue curve in Fig. 4.4 is an interpolation of the estimated values of ϵ_l as a function of bandwidth k, extracted from the data in Fig. 4.3. The green curve is the upper bound for ϵ_l given in (4.59). The time-delay margin of the system of interest is also estimated by forward simulation, in which $r_0 = \begin{pmatrix} 0.5 & -1 \end{pmatrix}^\top$ and the same control parameters as in the previous section are used. For each value of the filter bandwidth, the input delay is increased from zero until the system response blows up beyond $\rho_{\text{ref}} = 1000$. In Fig. 4.4, the delay value when this happens is represented by a red square for a unit-step desired trajectory, and by a blue circle for a sinusoidal desired trajectory with unit amplitude, for each value of the bandwidth. As seen in the figure, these estimates are virtually identical. Moreover, the lower bound given by the estimated supremum of ϵ_l, as well as its upper bound ϵ_{us}, are tight estimates of the actual time delay margin. Finally, we note that higher filter bandwidth deteriorates the system's ability to tolerate input delay. This is consistent with the observation that, when $k \to \infty$, the proposed adaptive closed-loop control scheme becomes an MRAC, for which it is well-known that the time-delay margin decreases to zero at high adaptation rate.

4.5.2 Finite range

Consider, next, the following nonlinearity

$$\eta(t, r) = 0.3 r_1 \sin(0.1 r_1) + 0.5 r_2 \cos(2t). \tag{4.106}$$

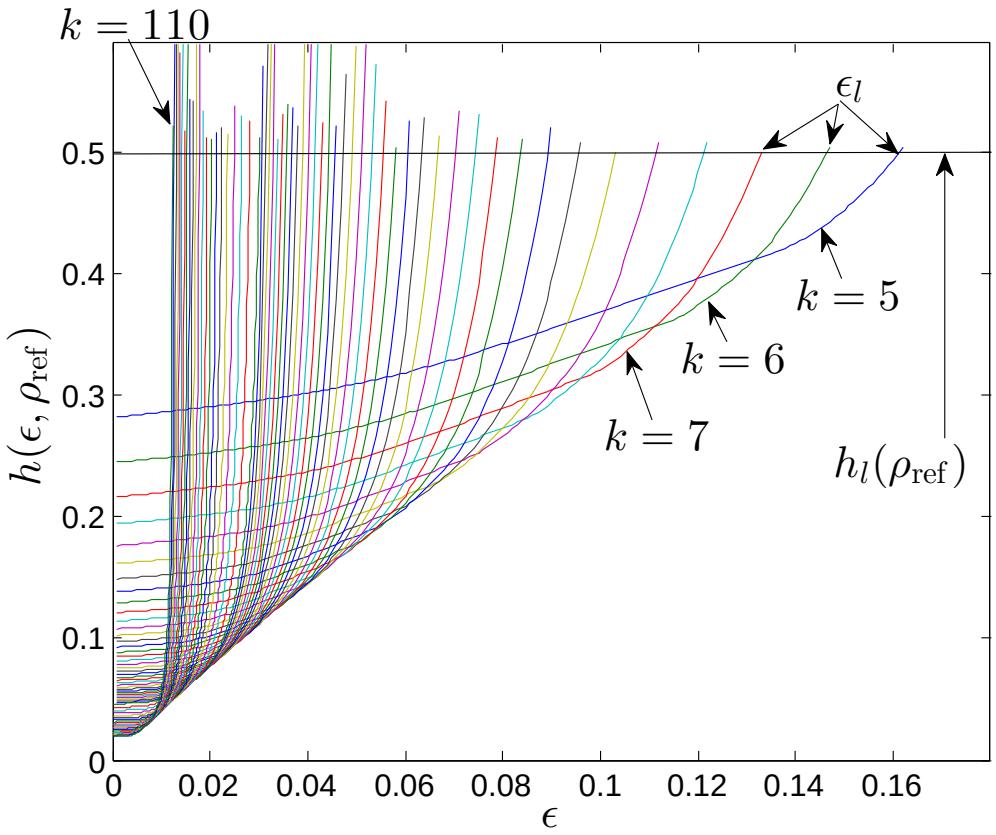

Figure 4.3: The intersection of $h(\epsilon, \rho_{\text{ref}})$ with respect to ϵ and the horizontal dashed line indicates the value of the lower bound ϵ_l for the time-delay margin.

In this case, the function $d_{\eta_r}(\delta)$ is bounded from below by $0.03\delta + 0.5$. This implies that $h_l(\rho_{\text{ref}})$ converges to 0 as $\rho_{\text{ref}} \to \infty$ and, therefore, that the supremum of ϵ_l should be evaluated over a finite range of values of ρ_{ref}.

We again rely on a heuristic for estimating this supremum. Specifically, let ρ_{ref} equal the maximizer for the difference $h_l(\rho_{\text{ref}}) - h(0, \rho_{\text{ref}})$. For example, with $b_d = 5$ and $b_{\text{ic}} = 2$, we find $\rho_{\text{ref}} \approx 22$. The estimated corresponding ϵ_l is shown over a range of bandwidths k in Fig. 4.5. The figure also includes a graph of the upper bound ϵ_{us}, obtained from (4.59), as well as the time delay margin estimated by forward simulation with the initial condition $r_0 = \begin{pmatrix} -2 & 2 \end{pmatrix}^\top$ and different desired trajectories $r_d(t)$ of identical norm. The figure confirms that $\rho_{\text{ref}} = 22$ gives a bound on the time delay margin that is tighter than that obtained using other values in some range.

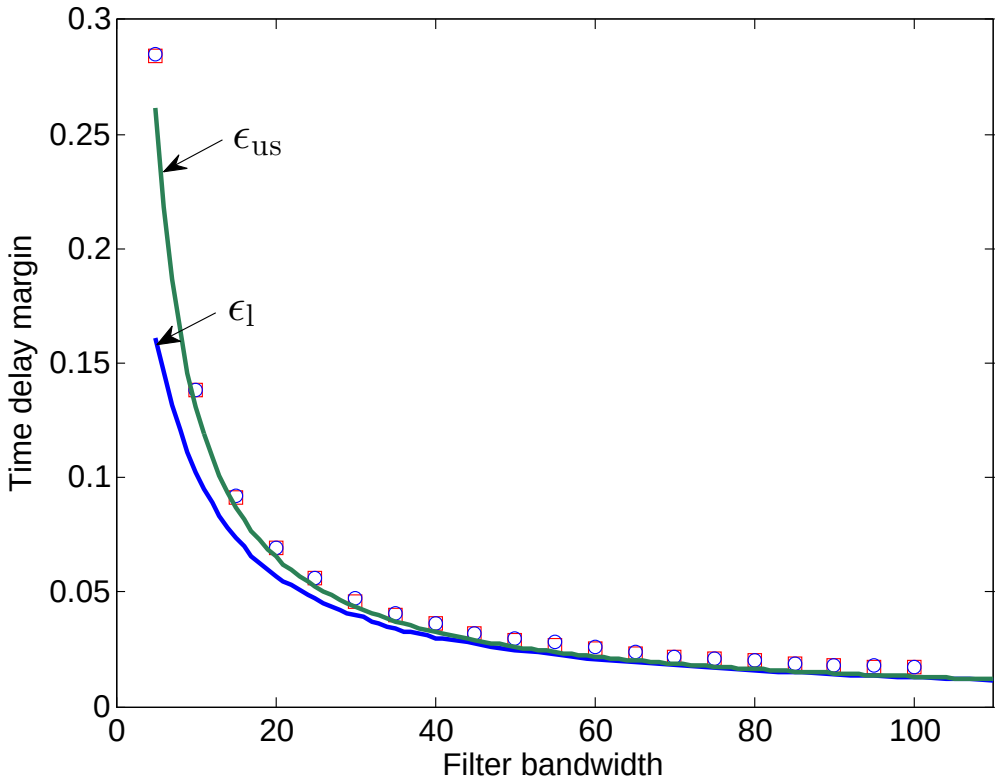

Figure 4.4: Comparison between the time-delay margins computed by the proposed analysis and the margins estimated by forward simulation of the DDE for two different desired trajectories $r_d(t)$ with identical norm. The squares and circles represent the time delay margin for unit step and sinusoidal desired trajectories, respectively obtained from forward simulations.

4.6 Conclusions

This chapter proves the existence of a positive lower bound for the delay robustness of a proposed adaptive controller for a class of systems with unknown nonlinearities. The analysis uses continuity arguments, and the existence of transient performance bounds in the case of zero delay, to prove the delay robustness of a nonadaptive reference system. It proceeds to show that adaptation with sufficiently large gain can ensure close tracking of the ideal response of the reference system by the response of the adaptive closed-loop system, without negatively affecting the delay robustness. Finally, the analysis suggests a way to numerically estimate the lower bound for the time-delay margin using Padé approximants.

In this chapter, we assumed that the input gain matrix ω was constant. It is of interest to

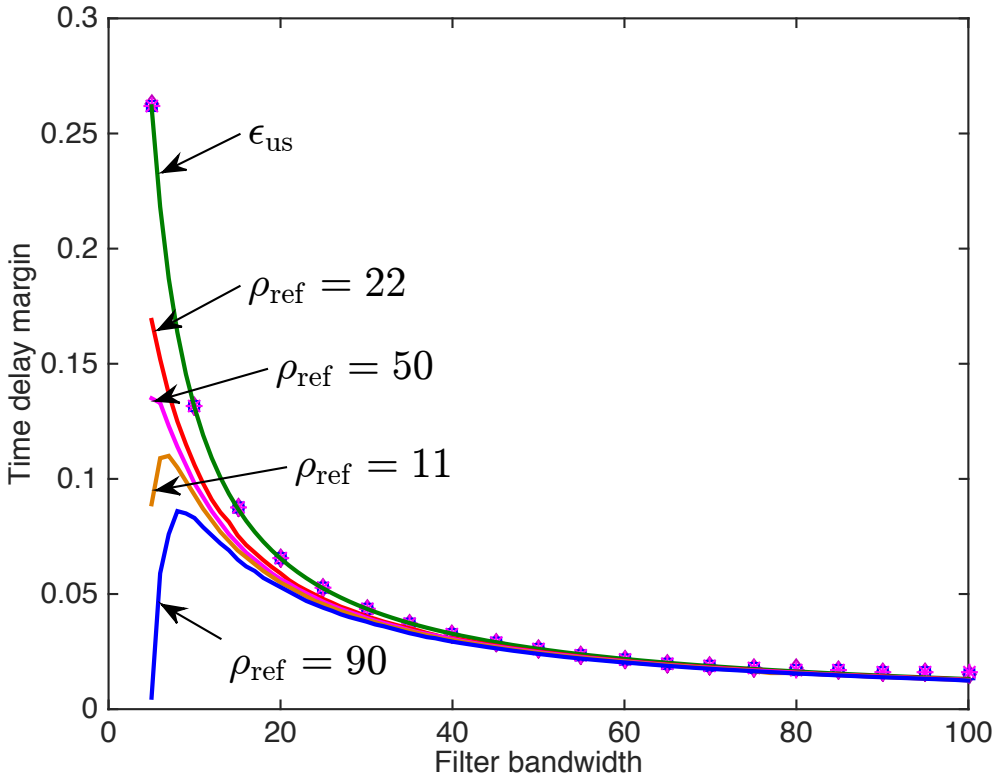

Figure 4.5: Comparison between the time-delay margins computed by the proposed analysis and the margins estimated by forward simulation of the DDE for system nonlinearity $\eta_1(t, r)$, with the identical initial condition and different desired trajectories $r_d(t)$ of the identical norm. The diamonds, the squares and the asterisks represent the time delay margin for $y_d = 5$, $y_d = 5\sin(t)$ and $y_d = 5(1 - \mathrm{e}^{-0.2t})\sin(2t)$, respectively

generalize the analysis to the context with time and state dependent input gain, as appears in most models of Lagrangian systems. Chapter 5 will resolve this more general problem.

Time delays come in different flavors. Here, we studied the input delay robustness, i.e. the system's ability to tolerate delay in the control input. In the case of a network of manipulators (cf. [101]), it is also interesting to consider transient performance bounds in the presence of communication delays. In Chapters 6 and 7, we will develop a delay-independent stability condition applicable to a control design for networked manipulators operating on a dynamic platform by following the framework presented in dissertation.

CHAPTER 5

DELAY ROBUSTNESS OF ADAPTIVE CONTROLLERS: TIME-VARYING, NONLINEAR INPUT-GAIN MATRICES

The last chapter established the existence of a lower bound for the time delay margin of a nonlinear system in which the input-gain matrix was constant. In this chapter, we study the delay robustness of a more general class of nonlinear control systems with time-varying and state-dependent input-gain matrices. The control structure belongs to the general framework presented in Chapter 2, which is composed of a state predictor for estimating the system dynamics, and a projection-based adaptation scheme that enables the control input to compensate for the nonlinearities. As before, a low-pass filter is used to allow for fast adaptation while maintaining a smooth control input. The analysis establishes a positive lower bound for the time-delay margin of this controller. In particular, if the input delay is below the lower bound then the state and control input of the adaptive control system follow those of a nonadaptive, robust reference system closely.

The chapter is organized as follows. Section 5.1 presents the nonlinear system of interest, which has a time-varying and state-dependent input-gain matrix. This model represents a wide range of Lagrangian systems. In Section 5.2, we investigate the continuous dependence of the fundamental solution matrix of the DDE of interest with respect to the delay. Chapter 5.3 establishes the reference system and defines input-output maps of DDEs as well as their norms. This section also shows the uniform stability of the closed-loop reference system when the input delay is below certain value. In Section 5.4, we review the adaptive control scheme presented in Chapter 2 that uses a low-pass filter in the control input to maintain the system robustness. Moreover, this section shows that the transient performance of the adaptive control system is guaranteed as long as the delay is less than the lower bound.

Section 5.5 presents concluding remarks of the chapter.

5.1 Nonlinear system

Consider the following nonlinear system:

$$\dot{x}(t) = A_m x(t) + B_m\Big(\Omega\big(t, x(t)\big)u(t-\epsilon) + \eta\big(t, x(t)\big)\Big), \tag{5.1}$$

$$h(t) = Dx(t), \tag{5.2}$$

where $x(t) \in \mathbb{R}^n$ is the system state, $u(t) \in \mathbb{R}^m$ is the control input, ϵ is the input delay, $h(t) \in \mathbb{R}^m$ is the output, $\Omega\big(t, x(t)\big) \in \mathbb{R}^{m\times m}$ is a time-varying and state-dependent input-gain matrix, $\eta(t, x(t)) \in \mathbb{R}^m$ is an unknown nonlinearity, $A_m \in \mathbb{R}^{n\times n}$ is a Hurwitz matrix, $B_m \in \mathbb{R}^{n\times m}$ and $D \in \mathbb{R}^{m\times n}$ are known constant matrices. The control objective is to design $u(t)$ such that the output $h(t)$ tracks a desired trajectory $h_d(t)$ when the input delay ϵ is less than certain time delay margin despite the unknown nonlinearity $\eta\big(t, x(t)\big)$ and the unknown input gain $\Omega\big(t, x(t)\big)$.

We make the following assumptions:

Assumption 5.1. *The matrix B_m has full rank, i.e., the contribution of the control input to $\dot{r}$ equals zero only if $u = 0$. It follows that $B_m^\top B_m$ is nonsingular.*

Assumption 5.2. *The input-gain matrix $\Omega\big(t, x\big)$ is positive definite and bounded uniformly in t and x, i.e. $0 < \omega_l \mathbb{I} \leq \Omega\big(t, x\big)$ and $\|\Omega\big(t, x\big)\| \leq \omega_h$, where ω_l and ω_h are finite positive numbers, for all t and x. In addition the partial derivatives of $\Omega\big(t, x\big)$ are bounded in t and x.*

Assumption 5.3. *There exists a constant $Z > 0$ such that $\|\eta(t, 0)\|_\infty \leq Z$ for all $t \geq 0$. In addition,*

$$\|x\|_\infty \leq \xi \Rightarrow \left\|\frac{\partial \eta(t, x)}{\partial x}\right\|_\infty \leq d_{\eta_x}(\xi) < \infty \tag{5.3}$$

and the partial derivative of η with respect to t is similarly bounded by a function of ξ for all $t \geq 0$.

5.2 Some properties of a DDE

Consider a DDE of the form

$$\dot{z}(t) = A(t)z(t) + B(t)z(t-\epsilon) + y(t), \quad z(t) = z_0 \ \ \forall t \in [-\epsilon, 0], \tag{5.4}$$

where ϵ is a time delay, the matrices $A(t)$ and $B(t)$ are continuous in time and bounded, i.e. there exist a and b such that $\sup_{t\in[0,\infty)} \|A(t)\|_\infty = a$ and $\sup_{t\in[0,\infty)} \|B(t)\|_\infty = b$. Denote by Φ the fundamental solution matrix of the above DDE that satisfies

$$\begin{aligned} \frac{\partial}{\partial t}\Phi(t, t_0; \epsilon) &= A(t)\Phi(t, t_0; \epsilon) + B(t)\Phi(t-\epsilon, t_0; \epsilon), \quad \forall (t, t_0) \in [t_0, \infty) \times [0, \infty) \\ \Phi(t, t; \epsilon) &= \mathbb{I}, \quad \forall t \in [0, \infty), \\ \Phi(t, t_0; \epsilon) &= 0, \quad \forall (t, t_0) \in [t_0 - \epsilon, t_0] \times [0, \infty). \end{aligned} \tag{5.5}$$

The purpose of this section to explore the continuity of the fundamental solution matrix $\Phi(t, t_0; \epsilon)$ in the delay ϵ. First, we show that $\Phi(t, t_0; \epsilon)$ has no finite escape time by the following lemma.

Lemma 5.1. *The solution to* (5.5) *has no finite escape time.*

Proof. Assume that this statement is not true. Let $t_e > t_0$ be the smallest finite escape time of $\Phi(t, t_0; \epsilon)$, i.e.

$$\|\Phi(t, t_0; \epsilon)\| < \infty \ \ \forall t \in [t_0, t_e), \quad \text{and} \quad \lim_{t \to t_e} \|\Phi(t, t_0; \epsilon)\| = \infty. \tag{5.6}$$

Integrating both sides of (5.5) with $t \in [t_0, t_e)$ leads to

$$\Phi(t, t_0; \epsilon) = \mathbb{I} + \int_{t_0}^{t} \big(A(s)\Phi(s, t_0; \epsilon) + B(s)\Phi(s-\epsilon, t_0; \epsilon)\big)\mathrm{d}s. \tag{5.7}$$

It follows that

$$\big\|\Phi(t, t_0; \epsilon)\big\| \leq 1 + a\int_{t_0}^{t} \|\Phi(s, t_0; \epsilon)\|\,\mathrm{d}s + b\int_{t_0}^{t} \|\Phi(s-\epsilon, t_0; \epsilon)\|\,\mathrm{d}s. \tag{5.8}$$

Applying the Gronwall lemma yields

$$\big\|\Phi(t, t_0; \epsilon)\big\| \leq \mathrm{e}^{a(t-t_0)}\Big(1 + b\int_{t_0}^{t} \big\|\Phi(s-\epsilon, t_0; \epsilon)\big\|\mathrm{d}s\Big) = \mathrm{e}^{a(t-t_0)}\Big(1 + b\int_{t_0}^{t-\epsilon} \big\|\Phi(s, t_0; \epsilon)\big\|\mathrm{d}s\Big), \tag{5.9}$$

where the last equality is obtained using a suitable change of variable and the fact that $\Phi(s, t_0; \epsilon) = 0\ \forall s \in [t_0 - \epsilon, t_0]$. Hence, $\lim\limits_{t \to t_e} \big\|\Phi(t, t_0; \epsilon)\big\| < \infty$ due to the fact that $\big\|\Phi(s, t_0; \epsilon)\big\|$ is bounded for $s \in [t_0, t_e - \epsilon]$ according to the inequality in (5.6). This contradicts the equality in (5.6). The claim then follows. □

Lemma 5.2. *The solution to* (5.5) *has the following exponential estimate*

$$\|\Phi(t, t_0; \epsilon)\| \leq e^{(a+b)(t-t_0)}. \tag{5.10}$$

Proof. Since the solution to (5.5) does not escape to infinity in finite time, from (5.8) we get

$$\|\Phi(t, t_0; \epsilon)\| \leq 1 + (a+b)\int_{t_0}^{t} \|\Phi(s, t_0; \epsilon)\|\,\mathrm{d}s,\ \ \forall t \in [t_0, \infty). \tag{5.11}$$

Applying the Gronwall lemma to this leads to (5.10). □

Lemma 5.3. *Suppose there exists a positive definite matrix P such that all eigenvalues of $A^\top(t)P + B^\top(t)P + PA(t) + PB(t)$ lie in the left-half complex plane for all t. Then* (5.5) *is exponentially stable, and the exponential estimate is independent of the delay ϵ, when ϵ is*

small enough. In particular, there exist $c_1 > 0$ *and* $c_2 < 0$ *such that*

$$\|\Phi(t, t_0; \epsilon)\| \leq c_1 e^{c_2 t}.$$

Proof. Inspired by the analysis in [48], pp. 126–136, we will employ the Razumikhin theorem to show the claim. In general, Lyapunov-Razumikhin functions often result in delay-independent stability conditions. Our intention here is to obtain a delay-dependent condition to establish a critical delay, below which (5.5) is uniformly asymptotically stable. Therefore, we consider the following transformation of the homogeneous equation of (5.4). The Leibniz-Newton formula provides

$$\begin{aligned}
z(t) - z(t-\epsilon) &= \int_{t-\epsilon}^{t} \dot{z}(s)\mathrm{d}s \\
\Rightarrow z(t-\epsilon) &= z(t) - \int_{t-\epsilon}^{t} \dot{z}(s)\mathrm{d}s = z(t) - \int_{t-\epsilon}^{t} \big(A(s)z(s) + B(s)z(s-\epsilon)\big)\mathrm{d}s \\
\Rightarrow \dot{z}(t) &= A(t)z(t) + B(t)z(t) - B(t)\int_{t-\epsilon}^{t} \big(A(s)z(s) + B(s)z(s-\epsilon)\big)\mathrm{d}s. \qquad (5.12)
\end{aligned}$$

Consider the Lyapunov-Razumikhin function candidate $V(z) = z^\top P z$. We have

$$\begin{aligned}
\dot{V}(z(t)) &= \dot{z}^\top(t)Pz(t) + z^\top(t)P\dot{z}(t) \\
&= \Big(z^\top(t)A^\top(t) + z^\top(t)B^\top(t) - \int_{t-\epsilon}^{t} \big(z^\top(s)A^\top(s) + z^\top(s-\epsilon)B^\top(s)\big)\mathrm{d}s B^\top(t)\Big)Pz(t) \\
&\quad + z^\top(t)P\Big(A(t)z(t) + B(t)z(t) - B(t)\int_{t-\epsilon}^{t} \big(A(s)z(s) + B(s)z(s-\epsilon)\big)\mathrm{d}s\Big) \\
&\leq z^\top(t)\Big(A^\top(t)P + B^\top(t)P + PA(t) + PB(t)\Big)z(t) \\
&\quad + 2b\|P\|_\infty\|z(t)\| \int_{t-\epsilon}^{t} \big(a\|z(s)\| + b\|z(s-\epsilon)\|\big)\mathrm{d}s \\
&\leq \lambda_{\sup}\|z(t)\|^2 + 2b\|P\|_\infty\|z(t)\| \int_{t-\epsilon}^{t} \big(a\|z(s)\| + b\|z(s-\epsilon)\|\big)\mathrm{d}s, \qquad (5.13)
\end{aligned}$$

where $\lambda_{\sup} = \sup_{t\in[0,\infty)} \lambda_{\max}\big(A^\top(t)P + B^\top(t)P + PA(t) + PB(t)\big)$, with $\lambda_{\max}(\cdot)$ being the maximum eigenvalue of a matrix.

Now, if $V(z(t-t')) < pV(z(t))$ for all $t' \in [0,\epsilon]$, where $p>1$ is a constant, then

$$\|z(t-t')\| \leq \|z(t)\| \sqrt{p \frac{\lambda_{\min}(P)}{\lambda_{\max}(P)}}, \tag{5.14}$$

for all $t' \in [0,\epsilon]$. Replacing t by $t-\epsilon$ leads to

$$\|z(t-t'-\epsilon)\| \leq \|z(t-\epsilon)\| \sqrt{p \frac{\lambda_{\min}(P)}{\lambda_{\max}(P)}}, \tag{5.15}$$

which implies

$$\|z(s-\epsilon)\| \leq \|z(t-\epsilon)\| \sqrt{p \frac{\lambda_{\min}(P)}{\lambda_{\max}(P)}} \leq \|z(t)\| p \frac{\lambda_{\min}(P)}{\lambda_{\max}(P)}, \ \forall s \in [t-\epsilon, t]. \tag{5.16}$$

This and (5.13) lead to

$$\begin{aligned} \dot{V}(z(t)) &\leq \lambda_{\sup}\|z(t)\|^2 + 2b\|P\|_\infty \left(a\sqrt{p \frac{\lambda_{\min}(P)}{\lambda_{\max}(P)}} + bp \frac{\lambda_{\min}(P)}{\lambda_{\max}(P)} \right) \|z(t)\|^2 \int_{t-\epsilon}^{t} \mathrm{d}s \\ &= \underbrace{\left(\lambda_{\sup} + 2\epsilon b\|P\|_\infty \left(a\sqrt{p \frac{\lambda_{\min}(P)}{\lambda_{\max}(P)}} + bp \frac{\lambda_{\min}(P)}{\lambda_{\max}(P)} \right) \right)}_{-\lambda_\Delta(\epsilon)} \|z(t)\|^2. \end{aligned} \tag{5.17}$$

Since all eigenvalues of $A^\top(t)P + B^\top(t)P + PA(t) + PB(t)$ lie on the left-half plane, $\lambda_{\sup}$ is negative. Therefore, with

$$\epsilon_{us} \triangleq \frac{-\lambda_{\sup}}{2b\|P\|_\infty \left(a\sqrt{p \frac{\lambda_{\min}(P)}{\lambda_{\max}(P)}} + bp \frac{\lambda_{\min}(P)}{\lambda_{\max}(P)} \right)} > 0,$$

if $\epsilon \leq \epsilon_{\mathrm{as}}$ for an arbitrary $\epsilon_{\mathrm{as}} < \epsilon_{\mathrm{us}}$, then the unforced equation of (5.4) is uniformly asymptotically stable according to the Razumikhin theorem (see [48], p. 127). This means for

every bounding constant z_b, there exists a t_b such that

$$\|z(t-\epsilon)\| \leq z_b, \ \forall t \geq t_0 + t_b. \tag{5.18}$$

Notably, from the proof of the Razumikhin theorem in [48], pp. 127-129, t_b depends on the delay via the relationship

$$t_b = c_0/\lambda_\Delta, \tag{5.19}$$

for some delay-independent constant c_0. According to (5.17), $\lambda_\Delta(\epsilon) \geq \lambda_\Delta(\epsilon_{\text{as}})$. Therefore, we obtain

$$t_b \leq c_0/\lambda_\Delta^{-1}(\epsilon_{\text{as}}) \triangleq \bar{t}_b, \tag{5.20}$$

for all $\epsilon \leq \epsilon_{\text{as}}$. This also implies that (5.18) is true for all $t \geq t_0 + \bar{t}_b$, and hence

$$\|z(t)\| \leq z_b, \ \forall t \geq t_0 + \bar{t}_b. \tag{5.21}$$

From the definition of the Lyapunov-Razumikhin function, since P is a symmetric matrix, we have

$$\|z(t)\|^2 \lambda_{\min}(P) \leq V\big(z(t)\big) \leq \|z(t)\|^2 \lambda_{\max}(P). \tag{5.22}$$

It then follows from this, (5.13), (5.18) and (5.21) that

$$\begin{aligned}
\dot{V}\big(z(t)\big) &\leq \frac{\lambda_{\sup}}{\lambda_{\max}(P)} V\big(z(t)\big) + 2b\|P\|_\infty \|z(t)\| \int_{t-\epsilon}^{t} \big(a\|z(s)\| + b\|z(s-\epsilon)\|\big) \mathrm{d}s \\
&\leq \frac{\lambda_{\sup}}{\lambda_{\max}(P)} V\big(z(t)\big) + 2b\|P\|_\infty z_b^2 \big(a+b\big) \int_{t-\epsilon}^{t} \mathrm{d}s \\
&\leq \frac{\lambda_{\sup}}{\lambda_{\max}(P)} V\big(z(t)\big) + 2b\|P\|_\infty z_b^2 \big(a+b\big)\epsilon_{\text{as}}, \ \forall t \geq t_0 + \bar{t}_b.
\end{aligned} \tag{5.23}$$

Applying Gronwall lemma to (5.23) leads to

$$\|z(t)\|^2\lambda_{\min}(P) \leq V\big(z(t)\big) \leq \mathrm{e}^{\frac{\lambda_{\sup}}{\lambda_{\max}(P)}(t-t_0-\bar{t}_b)}2b\|P\|_\infty z_b^2\big(a+b\big)\epsilon_{\mathrm{as}},\ \forall t \geq t_0+\bar{t}_b, \tag{5.24}$$

where all the constants are independent of ϵ. The claim then follows since the solution to (5.5) is constructed with columns being the linearly independent solutions to the homogeneous equation of (5.4). □

Lemma 5.4. *For every $T > 0$, $\Phi(t, t_0; \epsilon)$ is a continuous function of $\epsilon \geq 0$, uniformly in $t \in [t_0, T]$, with $t_0 \leq T$.*

Proof. Consider an arbitrary convergent sequence ϵ_m, such that

$$\lim_{m\to\infty} \epsilon_m = \bar{\epsilon}, \tag{5.25}$$

for some given $\bar{\epsilon} > 0$. For nonzero $\epsilon \approx \bar{\epsilon}$, let $\tilde{\Phi}(\tau, \tau_0; \epsilon) \triangleq \Phi(\epsilon\tau, \epsilon\tau_0; \epsilon)$ be defined for $\tau \in [t_0, \bar{\tau}]$, for some $\bar{\tau} > T/\bar{\epsilon}$. It follows that

$$\begin{aligned}
&\frac{\partial}{\partial\tau}\tilde{\Phi}(\tau, \tau_0; \epsilon) = \epsilon A(\epsilon\tau)\tilde{\Phi}(\tau, \tau_0; \epsilon) + \epsilon B(\epsilon\tau)\tilde{\Phi}(\tau-1, \tau_0; \epsilon), \quad \forall(\tau, \tau_0) \in [\tau_0, \infty) \times [0, \infty) \\
&\quad \tilde{\Phi}(\tau, \tau; \epsilon) = \mathbb{I}, \quad \forall\tau \in [0, \infty), \\
&\quad \tilde{\Phi}(\tau, \tau_0; \epsilon) = 0, \quad \forall(\tau, \tau_0) \in [\tau_0 - 1, \tau_0] \times [0, \infty).
\end{aligned} \tag{5.26}$$

Integrating both sides of (5.26) leads to

$$\tilde{\Phi}(\tau, \tau_0; \epsilon) = \mathbb{I} + \int_{\tau_0}^{\tau} \epsilon A(\epsilon\tau)\tilde{\Phi}(s, \tau_0; \epsilon)\mathrm{d}s + \int_{\tau_0}^{\tau} \epsilon B(\epsilon\tau)\tilde{\Phi}(s-1, \tau_0; \epsilon)\mathrm{d}s. \tag{5.27}$$

Since $\|\tilde{\Phi}(s, \tau_0; \epsilon_m) - \tilde{\Phi}(s, \tau_0; \bar{\epsilon})\| = 0, \quad \forall s \in [\tau_0 - 1, \tau_0]$, we have

$$\int_{\tau_0}^{\tau} \|\tilde{\Phi}(s-1, \tau_0; \epsilon_m) - \tilde{\Phi}(s-1, \tau_0; \bar{\epsilon})\|\mathrm{d}s \leq \int_{\tau_0}^{\tau} \|\tilde{\Phi}(s, \tau_0; \epsilon_m) - \tilde{\Phi}(s, \tau_0; \bar{\epsilon})\|\mathrm{d}s. \tag{5.28}$$

Taking this into account, it follows from (5.27) that

$$
\begin{aligned}
&\|\tilde{\Phi}(\tau,\tau_0;\epsilon_m)-\tilde{\Phi}(\tau,\tau_0;\bar{\epsilon})\| \le \int_{\tau_0}^{\tau} \left\|\epsilon_m A(\epsilon_m\tau)\tilde{\Phi}(s,\tau_0;\epsilon_m)-\bar{\epsilon}A(\bar{\epsilon}\tau)\tilde{\Phi}(s,\tau_0;\bar{\epsilon})\right\|\mathrm{d}s\\
&+\int_{\tau_0}^{\tau}\left\|\epsilon_m B(\epsilon_m s)\tilde{\Phi}(s-1,\tau_0;\epsilon_m)-\bar{\epsilon}B(\bar{\epsilon}s)\tilde{\Phi}(s-1,\tau_0;\bar{\epsilon})\right\|\mathrm{d}s\\
&\le \int_{\tau_0}^{\tau}\|\epsilon_m A(\epsilon_m s)\|\,\|\tilde{\Phi}(s,\tau_0;\epsilon_m)-\tilde{\Phi}(s,\tau_0;\bar{\epsilon})\|\mathrm{d}s+\int_{\tau_0}^{\tau}\|\epsilon_m A(\epsilon_m s)-\bar{\epsilon}A(\bar{\epsilon}s)\|\left\|\tilde{\Phi}(s,\tau_0;\bar{\epsilon})\right\|\mathrm{d}s\\
&+\int_{\tau_0}^{\tau}\|\epsilon_m B(\epsilon_m s)\|\,\|\tilde{\Phi}(s-1,\tau_0;\epsilon_m)-\tilde{\Phi}(s-1,\tau_0;\bar{\epsilon})\|\mathrm{d}s\\
&+\int_{\tau_0}^{\tau}\|\epsilon_m B(\epsilon_m s)-\bar{\epsilon}B(\bar{\epsilon}s)\|\left\|\tilde{\Phi}(s-1,\tau_0;\bar{\epsilon})\right\|\mathrm{d}s\\
&\le \epsilon_m(a+b)\int_{\tau_0}^{\tau}\|\tilde{\Phi}(s,\tau_0;\epsilon_m)-\tilde{\Phi}(s,\tau_0;\bar{\epsilon})\|\mathrm{d}s+R(\tau,\tau_0;\epsilon_m,\bar{\epsilon}),
\end{aligned}
\tag{5.29}
$$

where

$$
\begin{aligned}
&R(\tau,\tau_0;\epsilon_m,\bar{\epsilon}) \triangleq\\
&\int_{\tau_0}^{\tau}\|\epsilon_m A(\epsilon_m s)-\bar{\epsilon}A(\bar{\epsilon}s)\|\left\|\tilde{\Phi}(s,\tau_0;\bar{\epsilon})\right\|\mathrm{d}s+\int_{\tau_0}^{\tau}\|\epsilon_m B(\epsilon_m s)-\bar{\epsilon}B(\bar{\epsilon}s)\|\left\|\tilde{\Phi}(s-1,\tau_0;\bar{\epsilon})\right\|\mathrm{d}s
\end{aligned}
\tag{5.30}
$$

$$
\le \mathrm{e}^{(a+b)(\bar{\tau}-\tau_0)}\int_{\tau_0}^{\tau}\left(\|\epsilon_m A(\epsilon_m s)-\bar{\epsilon}A(\bar{\epsilon}s)\|+\mathrm{e}^{-(a+b)}\|\epsilon_m B(\epsilon_m s)-\bar{\epsilon}B(\bar{\epsilon}s)\|\right)\mathrm{d}s, \tag{5.31}
$$

where the inequality is obtained using (5.10). The continuity of $A(t)$ and $B(t)$ in t in a finite interval implies that for every δ_1, there exists M such that if $m > M$ then

$$
\|\epsilon_m A(\epsilon_m s)-\bar{\epsilon}A(\bar{\epsilon}s)\|+\mathrm{e}^{-(a+b)}\|\epsilon_m B(\epsilon_m s)-\bar{\epsilon}B(\bar{\epsilon}s)\| \le \delta_1. \tag{5.32}
$$

Substitution of (5.32) into (5.31) yields

$$
\sup_{\tau\in[\tau_0,\bar{\tau}]} R(\tau,\tau_0;\epsilon_m,\bar{\epsilon}) \le \mathrm{e}^{(a+b)(\bar{\tau}-\tau_0)}\int_{\tau_0}^{\bar{\tau}}\delta_1\mathrm{d}s = \mathrm{e}^{(a+b)(\bar{\tau}-\tau_0)}\,(\bar{\tau}-\tau_0)\,\delta_1. \tag{5.33}
$$

Applying the Gronwall lemma to (5.29) leads to

$$\sup_{\tau\in[\tau_0,\bar{\tau}]} \|\tilde{\Phi}(\tau,\tau_0;\epsilon_m)-\tilde{\Phi}(\tau,\tau_0;\bar{\epsilon})\| \le \sup_{t\in[\tau_0,\bar{\tau}]} R(\tau,\tau_0;\epsilon_m,\bar{\epsilon})\mathrm{e}^{\epsilon_m(a+b)(\tau-\tau_0)}$$
$$\le \mathrm{e}^{(a+b)(\bar{\tau}-\tau_0)}\,(\bar{\tau}-\tau_0)\,\delta_1\mathrm{e}^{\epsilon_m(a+b)(\bar{\tau}-\tau_0)} \triangleq \delta_2. \tag{5.34}$$

In summary, we have shown that for every δ_2 there exists M such that $m > M$ implies (5.34).

Finally,

$$\|\Phi(t,t_0;\epsilon_m)-\Phi(t,t_0;\bar{\epsilon})\| \le \left\|\tilde{\Phi}\left(\frac{t}{\epsilon_m},\frac{t_0}{\epsilon_m};\epsilon_m\right)-\tilde{\Phi}\left(\frac{t}{\epsilon_m},\frac{t_0}{\epsilon_m};\bar{\epsilon}\right)\right\|$$
$$+\left\|\Phi\left(t\frac{\bar{\epsilon}}{\epsilon_m},t_0\frac{\bar{\epsilon}}{\epsilon_m};\bar{\epsilon}\right)-\Phi(t,t_0;\bar{\epsilon})\right\|. \tag{5.35}$$

By the uniform continuity, for fixed ϵ, of $\Phi(t,t_0;\epsilon)$ in t and t_0 on the compact interval $[t_0,T]$, it follows that

$$\lim_{m\to\infty}\sup_{t\in[0,T]}\|\Phi(t,t_o;\epsilon_m)-\Phi(t,t_0;\bar{\epsilon})\|=0, \tag{5.36}$$

i.e., that $\Phi(t,t_0;\epsilon)$ is continuous in ϵ for $\epsilon>0$, uniformly in t on $[t_0,T]$.

Suppose, instead, that $\bar{\epsilon}=0$.

Then from (5.7), we have

$$\begin{aligned}
&\|\Phi(t,t_0;\epsilon_m)-\Phi(t,t_0;0)\| \\
&\quad\le \int_{t_0}^{t}\big\|A(s)\big(\Phi(s,t_0;\epsilon_m)-\Phi(s,t_0;0)\big)\big\|\,\mathrm{d}s+\int_{t_0}^{t}\big\|B(s)\big(\Phi(s-\epsilon_m,t_0;\epsilon_m)-\Phi(s,t_0;0)\big)\big\|\,\mathrm{d}s \\
&\quad\le \int_{t_0}^{t} a\,\|\Phi(s,t_0;\epsilon_m)-\Phi(s,t_0;0)\|\,\mathrm{d}s \\
&\quad+\int_{t_0}^{t} b\big(\,\|\Phi(s-\epsilon_m,t_0;\epsilon_m)-\Phi(s,t_0;\epsilon_m)\|+\|\Phi(s,t_0;\epsilon_m)-\Phi(s,t_0;0)\|\,\big)\mathrm{d}s \\
&\quad\le \int_{t_0}^{t}\Big(b\|\Phi(s-\epsilon_m,t_0;\epsilon_m)-\Phi(s,t_0;\epsilon_m)\|+(a+b)\|\Phi(s,t_0;\epsilon_m)-\Phi(s,t_0;0)\|\Big)\mathrm{d}s.
\end{aligned} \tag{5.37}$$

Again, applying the Gronwall lemma gives

$$\|\Phi(t,t_0;\epsilon_m)-\Phi(t,t_0;0)\| \le b\mathrm{e}^{(a+b)(t-t_0)}\int_{t_0}^{t}\|\Phi(s-\epsilon_m,t_0;\epsilon_m)-\Phi(s,t_0;\epsilon_m)\|\mathrm{d}s. \tag{5.38}$$

We now show that the norm on the right-hand side of (5.38) converges to zero as m goes to infinity.

It follows from (5.7) that

$$\begin{aligned}
\Phi(t-\epsilon,t_0;\epsilon) &= \mathbb{I}+\int_{t_0}^{t-\epsilon}\big(A(s)\Phi(s,t_0;\epsilon)+B(s)\Phi(s-\epsilon,t_0;\epsilon)\big)\mathrm{d}s\\
&= \mathbb{I}+\int_{t_0}^{t-\epsilon}A(s)\Phi(s,t_0;\epsilon)\mathrm{d}s+\int_{t_0-\epsilon}^{t-2\epsilon}B(s+\epsilon)\Phi(s,t_0;\epsilon)\big)\mathrm{d}s\\
&= \mathbb{I}+\int_{t_0}^{t-\epsilon}A(s)\Phi(s,t_0;\epsilon)\mathrm{d}s+\int_{t_0}^{t}B(s+\epsilon)\Phi(s,t_0;\epsilon)\mathrm{d}s\\
&\quad -\int_{t-2\epsilon}^{t}B(s+\epsilon)\Phi(s,t_0;\epsilon)\mathrm{d}s.
\end{aligned} \tag{5.39}$$

Consequently,

$$\begin{aligned}
\Phi(t,t_0;\epsilon_m)-\Phi(t-\epsilon_m,t_0;\epsilon_m) &= \int_{t_0}^{t}\big(A(s)\Phi(s,t_0;\epsilon_m)+B(s)\Phi(s-\epsilon_m,t_0;\epsilon_m)\big)\mathrm{d}s\\
&\quad -\int_{t_0}^{t-\epsilon_m}A(s)\Phi(s,t_0;\epsilon_m)\mathrm{d}s-\int_{t_0}^{t}B(s+\epsilon_m)\Phi(s,t_0;\epsilon_m)\mathrm{d}s\\
&\quad +\int_{t-2\epsilon_m}^{t}B(s+\epsilon_m)\Phi(s,t_0;\epsilon_m)\mathrm{d}s\\
&= \int_{t_0}^{t}\big(B(s)\Phi(s-\epsilon_m,t_0;\epsilon_m)-B(s+\epsilon_m)\Phi(s,t_0;\epsilon_m)\big)\mathrm{d}s\\
&\quad +\int_{t-\epsilon_m}^{t}A(s)\Phi(s,t_0;\epsilon_m)\mathrm{d}s+\int_{t-2\epsilon_m}^{t}B(s+\epsilon_m)\Phi(s,t_0;\epsilon_m)\mathrm{d}s\\
&= \int_{t_0}^{t}\big(B(s)\Phi(s-\epsilon_m,t_0;\epsilon_m)-B(s+\epsilon_m)\Phi(s-\epsilon_m,t_0;\epsilon_m)\big)\mathrm{d}s\\
&\quad +\int_{t_0}^{t}\big(B(s+\epsilon_m)\Phi(s-\epsilon_m,t_0;\epsilon_m)-B(s+\epsilon_m)\Phi(s,t_0;\epsilon_m)\big)\mathrm{d}s\\
&\quad +\int_{t-\epsilon_m}^{t}A(s)\Phi(s,t_0;\epsilon_m)\mathrm{d}s+\int_{t-2\epsilon_m}^{t}B(s+\epsilon_m)\Phi(s,t_0;\epsilon_m)\mathrm{d}s.
\end{aligned} \tag{5.40}$$

By applying the norm triangle inequality, we get

$$\begin{aligned}\|\Phi(s-\epsilon_m,t_0;\epsilon_m)-\Phi(s,t_0;\epsilon_m)\| &= \int_{t_0}^{t}\big\|B(s+\epsilon_m)\big\|\big\|\Phi(s-\epsilon_m,t_0;\epsilon_m)-\Phi(s,t_0;\epsilon_m)\big\|\mathrm{d}s \\ &+ \underbrace{\int_{t_0}^{t}\big\|B(s)-B(s+\epsilon_m)\big\|\big\|\Phi(s-\epsilon_m,t_0;\epsilon_m)\big\|\mathrm{d}s}_{R_1(t,t_0;\epsilon_m)} \\ &+ \underbrace{\int_{t-\epsilon_m}^{t}\|A(s)\Phi(s,t_0;\epsilon_m)\|\mathrm{d}s+\int_{t-2\epsilon_m}^{t}\|B(s+\epsilon_m)\Phi(s,t_0;\epsilon_m)\|\mathrm{d}s}_{R_2(t,t_0;\epsilon_m)}. \quad (5.41)\end{aligned}$$

Notice the similarity between R_1 and R in (5.30). By applying the same analysis for obtaining (5.33), we have

$$\lim_{m\to\infty}\sup_{t\in[t_0,T]}R_1(t,t_0;\epsilon_m)=0. \quad (5.42)$$

As for $R_2(t,t_0;\epsilon_m)$, using (5.10) we have

$$\begin{aligned}R_2(t,t_0;\epsilon_m) &\le a\int_{t-\epsilon_m}^{t}\mathrm{e}^{(a+b)(s-t_0)}\mathrm{d}s+b\int_{t-2\epsilon_m}^{t}\mathrm{e}^{(a+b)(s-t_0)}\mathrm{d}s \\ &\le \mathrm{e}^{(a+b)(T-t_0)}\Big(a\int_{t-\epsilon_m}^{t}\mathrm{d}s+b\int_{t-2\epsilon_m}^{t}\mathrm{d}s\Big)=\mathrm{e}^{(a+b)(T-t_0)}(a+2b)\epsilon_m\triangleq\bar{R}_2(\epsilon_m),\end{aligned} \quad (5.43)$$

where the inequalities are obtained using (5.10) and the fact the $t\in[t_0,T]$. Note here that $\lim_{m\to\infty}\bar{R}_2(\epsilon_m)=0$.

Taking (5.42) into account, we use the Gronwall lemma on (5.41) to arrive at

$$\begin{aligned}&\lim_{m\to\infty}\sup_{t\in[t_0,T]}\|\Phi(s-\epsilon_m,t_0;\epsilon_m)-\Phi(s,t_0;\epsilon_m)\| \\ &\qquad\le \mathrm{e}^{b(T-t_0)}\Big(\lim_{m\to\infty}\bar{R}_2(\epsilon_m)+\lim_{m\to\infty}\sup_{t\in[t_0,T]}R_1(t,t_0;\epsilon_m)\Big)=0.\end{aligned} \quad (5.44)$$

It follows from (5.44) that for every δ there exists M such that $m>M$ implies $\sup_{t\in[t_0,T]}\|\Phi(s-$

$\epsilon_m, t_0; \epsilon_m) - \Phi(s, t_0; \epsilon_m)\| \leq \delta$. Substitution of this into supremum of (5.38) yields

$$\sup_{t\in[t_0,T]} \|\Phi(t, t_0; \epsilon_m) - \Phi(t, t_0; 0)\| \leq b\mathrm{e}^{(a+b)(T-t_0)} \int_{t_0}^{T} \delta \mathrm{d}s = b\mathrm{e}^{(a+b)(T-t_0)}(T - t_0)\delta, \tag{5.45}$$

which can be made arbitrarily small with small enough δ. Thus, $\Phi(t, t_0; \epsilon)$ is continuous at $\epsilon = 0$, independently of $t \in [t_0, T]$. □

Lemma 5.5. *Suppose there exists a positive definite matrix P such that all eigenvalues of $A^\top(t)P + B^\top(t)P + PA(t) + PB(t)$ lie in the left-half complex plane for all t. When ϵ is small enough, the solution $\Phi(t, t_0; \epsilon)$ to (5.5) is continuous in ϵ, uniformly in $t \in [t_0, \infty)$.*

Proof. It follows from Lemma 5.3 that there is an interval $[0, \epsilon_{\mathrm{as}}]$ for the delay ϵ, on which there exist $c_1 > 0$ and $c_2 < 0$ such that the solution to (5.5)

$$\|\Phi(t, t_0; \epsilon)\| \leq c_1\mathrm{e}^{c_2 t}. \tag{5.46}$$

Consequently, there is a class $\mathcal{KL}$ function β such that (see Lemma 4.5 in [68], pp. 150)

Consider a convergent sequence $\epsilon_m \leq \epsilon_{\mathrm{as}}$ with $\lim_{m\to\infty} \epsilon_m = \bar{\epsilon}$, where $\bar{\epsilon} \leq \epsilon_s$. It follows from (5.46) that with $T_l = \frac{\ln(\delta/2c_1)}{c_2} > 0$, where $\delta << 2c_1$, we have the bound

$$\sup_{t\in[T_l,\infty)} \|\Phi(t, t_0; \epsilon_m) - \Phi(t, t_0; \bar{\epsilon})\| \leq \delta. \tag{5.47}$$

Further, the analysis on a finite interval implies

$$\sup_{t\in[0,T_l]} \|\Phi(t, t_0; \epsilon_m) - \Phi(t, t_0; \bar{\epsilon})\| \leq \delta \tag{5.48}$$

for sufficiently large m. It follows from (5.47) and (5.48) that for every $\delta > 0$, there exists an integer M, such that $m \geq M$ implies

$$\sup_{t\in[0,\infty)} \|\Phi(t, t_0; \epsilon_m) - \Phi(t, t_0; \bar{\epsilon})\| \leq \delta. \tag{5.49}$$

Thus, $\Phi(t, t_0; \epsilon)$ is continuous in ϵ on $[0, \epsilon_{\text{as}}]$, uniformly in t on $[0, \infty)$. □

5.3 A reference system, input-output maps and their properties

5.3.1 Definition of input-output maps

We first consider the following nonadaptive reference system

$$\dot{x}_r(t) = A_m x_r(t) + B_m\Big(\Omega\big(t, x(t)\big)u_r(t-\epsilon) + \eta_r(t)\Big), \quad x_r(t) = x_0 \ \ \forall t \in [-\epsilon, 0], \tag{5.50}$$

$$\dot{u}_r(t) = -k\Omega\big(t, x(t)\big)u_r(t-\epsilon) - k\eta_r(t) - kK_d h_d(t), \quad u_r(t) = 0 \ \ \forall t \in [-\epsilon, 0], \tag{5.51}$$

$$h_r(t) = Dx_r(t), \tag{5.52}$$

where, $x_r \in \mathbb{R}^n$ and $u_r(t) \in \mathbb{R}^m$ are the state and the control input, $\eta_r(t) \triangleq \eta(t, x_r(t))$, k is a control parameter, and $K_d \triangleq \left(DA_m^{-1}B_m\right)^{-1}$. The nonadaptive reference system represents the ideal dynamics for the system of interest in (5.1) and (5.2) when the nonlinearity and the input delay value are known to its controller, as seen in (5.51). So implementation of this system in reality is not practical. Nonetheless, we will design an adaptive control system that behaves almost identically to this ideal system for sufficiently small delay.

Remark 5.1. *Note that $x(t)$, which appears in $\Omega\big(t, x(t)\big)$, is the state of the actual system in* (5.1)*, but an exogenous signal in the reference system.*

Next, we write this reference system in the form of (5.4)

$$\begin{bmatrix} \dot{x}_r(t) \\ \dot{u}_r(t) \end{bmatrix} = \underbrace{\begin{bmatrix} A_m & 0 \\ 0 & 0 \end{bmatrix}}_{A(t)} \begin{bmatrix} x_r(t) \\ u_r(t) \end{bmatrix} + \underbrace{\begin{bmatrix} 0 & B_m\Omega\big(t, x(t)\big) \\ 0 & -k\Omega\big(t, x(t)\big) \end{bmatrix}}_{B(t)} \begin{bmatrix} x_r(t-\epsilon) \\ u_r(t-\epsilon) \end{bmatrix} + \begin{bmatrix} \eta_r(t) \\ -k\eta_r(t) - kK_d h_d(t) \end{bmatrix}. \tag{5.53}$$

Denote by $\Phi : [-\epsilon, \infty) \times [0, \infty) \to \mathbb{R}^{(m+n)\times(m+n)}$ the fundamental solution matrix of the above DDE. Let $\Phi(t, t_0; \epsilon) = \begin{bmatrix} \Phi_{11}(t, t_0; \epsilon) \in \mathbb{R}^{n\times n} & \Phi_{12}(t, t_0; \epsilon) \in \mathbb{R}^{n\times m} \\ \Phi_{21}(t, t_0; \epsilon) \in \mathbb{R}^{m\times n} & \Phi_{22}(t, t_0; \epsilon) \in \mathbb{R}^{m\times m} \end{bmatrix}$, which is governed by (5.5), in particular:

$$\frac{\partial}{\partial t}\Phi_{11}(t, t_0; \epsilon) = A_m\Phi_{11}(t, t_0; \epsilon) + B_m\Omega\big(t, x(t)\big)\Phi_{21}(t - \epsilon, t_0; \epsilon), \quad \forall (t, t_0) \in [t_0, \infty) \times [0, \infty) \tag{5.54}$$

$$\frac{\partial}{\partial t}\Phi_{12}(t, t_0; \epsilon) = A_m\Phi_{12}(t, t_0; \epsilon) + B_m\Omega\big(t, x(t)\big)\Phi_{22}(t - \epsilon, t_0; \epsilon), \quad \forall (t, t_0) \in [t_0, \infty) \times [0, \infty) \tag{5.55}$$

$$\frac{\partial}{\partial t}\Phi_{21}(t, t_0; \epsilon) = -k\Omega\big(t, x(t)\big)\Phi_{21}(t - \epsilon, t_0; \epsilon), \quad \forall (t, t_0) \in [t_0, \infty) \times [0, \infty) \tag{5.56}$$

$$\frac{\partial}{\partial t}\Phi_{22}(t, t_0; \epsilon) = -k\Omega\big(t, x(t)\big)\Phi_{22}(t - \epsilon, t_0; \epsilon), \quad \forall (t, t_0) \in [t_0, \infty) \times [0, \infty) \tag{5.57}$$

$$\Phi(t, t; \epsilon) = \mathbb{I}, \quad \forall t \in [0, \infty),$$

$$\Phi(t, t_0; \epsilon) = 0, \quad \forall (t, t_0) \in [t_0 - \epsilon, t_0] \times [0, \infty).$$

Notice that since $\Phi_{21}(t, t_0; \epsilon) = 0 \; \forall t \le t_0$, it follows from (5.56) that $\Phi_{21}(t, t_0; \epsilon) = 0 \; \forall (t, t_0) \in [t_0 - \epsilon, \infty) \times [0, \infty)$.

Lemma 5.6. *It is possible to design A_m and k independently such that all eigenvalues of $A^\top(t)P + B^\top(t)P + PA(t) + PB(t)$ lie in the left-half complex plane, for some positive definite matrix P.*

Proof. Let the Hurwitz matrix $A_m = aA_0$, where $a > 0$ is a scaling factor and A_0 is a Hurwitz matrix. Consider

$$P = \begin{bmatrix} P_0 & 0 \\ 0 & \mathbb{I}_m \end{bmatrix}, \tag{5.58}$$

where P_0 is the unique solution of the Lyapunov equation $A_0^\top P + PA_0 = -\mathbb{I}_n$. In addition,

since $\Omega\big(t, x(t)\big)$ is a symmetric matrix, there exists a orthogonal matrix $U(t)$ such that

$$U^\top(t)\Omega\big(t, x(t)\big)U(t) = D_\Omega(t)$$

where $D_\Omega(t)$ is a diagonal matrix. We have

$$\begin{aligned}
&\begin{bmatrix} \mathbb{I} & 0 \\ 0 & U^\top(t) \end{bmatrix} \Big(A^\top(t)P + B^\top(t)P + PA(t) + PB(t)\Big) \begin{bmatrix} \mathbb{I} & 0 \\ 0 & U(t) \end{bmatrix} \\
&= \begin{bmatrix} \mathbb{I} & 0 \\ 0 & U^\top(t) \end{bmatrix} \begin{bmatrix} A_m^\top P_0 + P_0 A_m & P_0 B_m \Omega\big(t, x(t)\big) \\ \Omega\big(t, x(t)\big) B_m^\top P_0 & -2k\Omega\big(t, x(t)\big) \end{bmatrix} \begin{bmatrix} \mathbb{I} & 0 \\ 0 & U(t) \end{bmatrix} \\
&= \begin{bmatrix} -a\mathbb{I}_n & P_0 B_m \Omega\big(t, x(t)\big)U(t) \\ U^\top(t)\Omega\big(t, x(t)\big) B_m^\top P_0 & -2kU^\top(t)\Omega\big(t, x(t)\big)U(t) \end{bmatrix} \\
&= \begin{bmatrix} -a\mathbb{I}_n & P_0 B_m \Omega\big(t, x(t)\big)U(t) \\ U^\top(t)\Omega\big(t, x(t)\big) B_m^\top P_0 & -2kD_\Omega(t) \end{bmatrix}.
\end{aligned} \tag{5.59}$$

Note here that though P_0 depends on A_0, it is independent of a. Hence, the off-diagonal terms in (5.59) are independent of a and k. As stated in [16], the Gershgorin circle theorem implies that every eigenvalue of a matrix lies within at least one of the Gershgorin discs. A Gershgorin disc is defined as a closed disc centered at a diagonal element of the matrix with the radius as the sum of the absolute values of the other elements in the corresponding row. Therefore, in (5.59), when a and k are increased, the Gershgorin discs of this matrix move to the left in the complex plane. Thus by independently designing a and k large enough, the eigenvalues of $A^\top(t)P + B^\top(t)P + PA(t) + PB(t)$ can be made strictly negative. □

Taking the result in Lemma 5.6 into account, according to Lemma 5.5, it is possible to chose k and A_m such that there exists a positive upper bound ϵ_{as} for the delay such that Φ and its components are continuous in $\epsilon \in [0, \epsilon_{\text{as}})$, uniformly in $t \in [0, \infty)$.

In terms of the fundamental solution matrix, the solution to (5.53) can be written in the

following variation-of-constant form (cf. [143, 151, 6])

$$\begin{bmatrix} x_r(t) \\ u_r(t) \end{bmatrix} = \begin{bmatrix} x_{\rm ic}(t) \\ u_{\rm ic}(t) \end{bmatrix} + \int_{t_0}^{t} \begin{bmatrix} \Phi_{11}(t,t';\epsilon) & \Phi_{12}(t,t';\epsilon) \\ \Phi_{21}(t,t';\epsilon) & \Phi_{22}(t,t';\epsilon) \end{bmatrix} \begin{bmatrix} \eta_r(t) \\ -k\eta_r(t) - kK_d h_d(t) \end{bmatrix} \mathrm{d}t' \tag{5.60}$$

$$\begin{bmatrix} x_{\rm ic}(t) \\ u_{\rm ic}(t) \end{bmatrix} = \Big(\Phi(t,0;\epsilon) + \int_{t_0}^{\epsilon} \Phi(t,t';\epsilon)B(t')\mathrm{d}t'\Big) \begin{bmatrix} x_0 \\ 0 \end{bmatrix} \tag{5.61}$$

Equivalently,

$$x_r(t) = x_{\rm ic}(t,x_0) + \int_0^t \Big(\Phi_{11}(t,t';\epsilon) - k\Phi_{12}(t,t';\epsilon)\Big)\eta_r(t')\mathrm{d}t' - k\int_0^t \Phi_{12}(t,t';\epsilon)K_d h_d(t')\mathrm{d}t' \tag{5.62}$$

$$u_r(t) = -k\int_0^t \Phi_{22}(t,t';\epsilon)\big(\eta_r(t') + K_d h_d(t')\big)\mathrm{d}t' \tag{5.63}$$

where $x_{\rm ic}(t) = \Phi_{11}(t,t';\epsilon)x_0$. We now define linear input-output maps for the delay system in (5.50) and (5.51) in terms of the fundamental solution matrix as follows

$$\mathcal{F}^\epsilon : y \to \int_0^t \Big(\Phi_{11}(t,t';\epsilon) - k\Phi_{12}(t,t';\epsilon)\Big)y(t')\mathrm{d}t' \tag{5.64}$$

$$\mathcal{D}^\epsilon : y \to -k\int_0^t \Phi_{12}(t,t';\epsilon)K_d y(t')\mathrm{d}t' \tag{5.65}$$

$$\mathcal{G}^\epsilon : y \to -k\int_0^t \Phi_{22}(t,t';\epsilon)y(t')\mathrm{d}t'. \tag{5.66}$$

Furthermore, define the multiplicative map $\mathcal{M} : y(t) \to \Omega\big(t,x(t)\big)y(t)$ and the delay map $\mathcal{E}^\epsilon : y(t) \to y(t-\epsilon)$. In addition, let $\mathcal{I}$ be the identity map and $\mathcal{H}$ be the linear input-output map corresponding to the transfer function $(s\mathbb{I} - A_m)^{-1}B_m$. The variation-of-constant formulas

in (5.62) and (5.63) can be written in terms of these maps:

$$x_r = x_{\text{ic}} + \mathcal{F}^\epsilon[\eta_r] + \mathcal{D}^\epsilon[h_d] \tag{5.67}$$

$$u_r = \mathcal{G}^\epsilon[\eta_r + K_d h_d]. \tag{5.68}$$

In the following series of remarks, we derive expressions that relate the defined maps.

Remark 5.2. *It follows from Eq.* (5.50) *and* (5.68) *that*

$$x_r(t) = x_{\text{ic}} + \big(\mathcal{H} \circ \mathcal{M} \circ \mathcal{E}^\epsilon \circ \mathcal{G}^\epsilon + \mathcal{H}\big)\big[\eta_r(t)\big] + \big(\mathcal{H} \circ \mathcal{M} \circ \mathcal{E}^\epsilon \circ \mathcal{G}^\epsilon\big)[K_d h_d]. \tag{5.69}$$

Hence,

$$\mathcal{F}^\epsilon[y] = \big(\mathcal{H} \circ \mathcal{M} \circ \mathcal{E}^\epsilon \circ \mathcal{G}^\epsilon + \mathcal{H}\big)[y] \tag{5.70}$$

$$\mathcal{D}^\epsilon[y] = \big(\mathcal{H} \circ \mathcal{M} \circ \mathcal{E}^\epsilon \circ \mathcal{G}^\epsilon\big)[K_d y]. \tag{5.71}$$

Remark 5.3. *We rearrange Eq.* (5.51) *as follows*

$$\dot{u}_r = -k\Omega\big(t, x(t)\big)u_r + k\Omega\big(t, x(t)\big)u_r - k\Omega\big(t, x(t)\big)u_r(t-\epsilon) - k(\eta_r + K_d h_d). \tag{5.72}$$

Applying the input-output map definition in Eqs. (5.57) *and* (5.66) *with zero delay to Eq.* (5.72) *leads to*

$$u_r = \mathcal{G}^0\big[-\mathcal{M}[u_r] + \mathcal{M} \circ \mathcal{E}^\epsilon[u_r] + \eta_r + K_d h_d\big]. \tag{5.73}$$

Solving for u_r in Eq. (5.73)*, we get*

$$u_r = \big((\mathcal{I} + \mathcal{G}^0 \circ \mathcal{M} - \mathcal{G}^0 \circ \mathcal{M} \circ \mathcal{E}^\epsilon)^{-1} \circ \mathcal{G}^0\big)[\eta_r + K_d h_d]. \tag{5.74}$$

Thus, comparing (5.68) *and* (5.74) *leads to*

$$\mathcal{G}^{\epsilon}[\cdot] \triangleq \left((\mathcal{I} + \mathcal{G}^0 \circ \mathcal{M} - \mathcal{G}^0 \circ \mathcal{M} \circ \mathcal{E}^{\epsilon})^{-1} \circ \mathcal{G}^0\right)[\cdot]. \tag{5.75}$$

Note that when $\epsilon = 0$*, the map* $\mathcal{F}^{\epsilon}$ *becomes* $\mathcal{F}^0$*.*

Remark 5.4. *Since* $\partial\Phi_{22}(t,t';0)/\partial t' = \Phi_{22}(t,t';0)k\Omega(t',x(t'))$*, it follows from* (5.57)*,* (5.66) *and integration by parts that*

$$\begin{aligned}\mathcal{G}^0[\dot{y}] &= -k\int_0^t \Phi_{22}(t,t';0)\frac{\mathrm{d}y(t')}{\mathrm{d}t'}\,\mathrm{d}t' = -k\Phi_{22}(t,t;0)y(t) + k\int_0^t \frac{\partial\Phi_{22}(t,t';0)}{\partial t'}y(t')\,\mathrm{d}t' \\ &= -ky + k\int_0^t \Phi_{22}(t,t';0)k\Omega(t',x(t'))y(t')\,\mathrm{d}t' = -k\left(\mathcal{I} + \mathcal{G}^0 \circ \mathcal{M}\right)[y],\end{aligned} \tag{5.76}$$

provided that $y(0) = 0$*.*

Remark 5.5. *With the map* $\mathcal{G}_v^0$ *being invertible, by applying the results in* (5.75) *and* (5.76) *we get*

$$\begin{aligned}\mathcal{G}^{\epsilon}[\dot{y}] &= \mathcal{G}^{\epsilon} \circ \left(\mathcal{G}^0\right)^{-1} \circ \mathcal{G}^0[\dot{y}] = -k\mathcal{G}^{\epsilon} \circ \left(\mathcal{G}^0\right)^{-1} \circ (\mathcal{I} + \mathcal{G}^0 \circ \mathcal{M})[y] \\ &= -k\mathcal{G}^{\epsilon} \circ \left(\mathcal{G}^0\right)^{-1} \circ (\mathcal{I} + \mathcal{G}^0 \circ \mathcal{M} - \mathcal{G}^0 \circ \mathcal{M} \circ \mathcal{E}^{\epsilon})[y] - k\mathcal{G}^{\epsilon} \circ \mathcal{M} \circ \mathcal{E}^{\epsilon}[y].\end{aligned}$$

Hence,

$$\mathcal{G}^{\epsilon}[\dot{y}] = -k(\mathcal{I} + \mathcal{G}^{\epsilon} \circ \mathcal{M} \circ \mathcal{E}^{\epsilon})[y]. \tag{5.77}$$

5.3.2 Norm of an input-output map

The $\mathcal{L}_1$ norm of the map $\mathcal{G}^{\epsilon}$ is then given by

$$\|\mathcal{G}^{\epsilon}\|_{\mathcal{L}_1} \triangleq \max_{1\le i\le n}\left(\sum_{j=1}^{n}\sup_{t\ge t^*, t^*\in\mathbb{R}^+}\int_{t^*}^{t} k\left|\Phi_{22}^{ij}(t,t';\epsilon)\right|\,\mathrm{d}t'\right), \tag{5.78}$$

where $\Phi_{22}^{ij}(t,t';\epsilon)$ denotes the components of $\Phi_{22}(t,t';\epsilon)$. The $\mathcal{L}_1$ norm of other input-output maps is defined in the same way.

It follows from the continuity of $\Phi(t,t';\epsilon)$ in $\epsilon \in [0,\epsilon_{\text{as}})$, uniformly in $t \in [0,\infty)$, that

$$f(\epsilon) = \|\mathcal{F}^\epsilon\|_{\mathcal{L}_1} \tag{5.79}$$

$$d(\epsilon) = \|\mathcal{D}^\epsilon\|_{\mathcal{L}_1} \tag{5.80}$$

$$g(\epsilon) = \|\mathcal{G}^\epsilon\|_{\mathcal{L}_1} \tag{5.81}$$

are continuous in ϵ. Now, by applying the Gronwall lemma to (5.57), we get that $\Phi_{22}(t,t';0)$ decays to zero exponentially fast, since $-k\Omega\big(t,x(t)\big)$ is uniformly negative definite. Consequently, the map $\mathcal{G}^0$ is exponentially stable and the value $g(0)$ is finite. Hence, by continuity, there exists an ϵ_u such that $g(\epsilon)$ is finite for all $\epsilon \in [0,\epsilon_u)$. In addition, it follows from (5.55) that when $\Phi_{22}(t,t';0)$ is decaying, $\Phi_{12}(t,t';0)$ converges to zero exponentially fast. Thus, $d(\epsilon)$ is also finite for all $\epsilon \in [0,\epsilon_u)$.

5.3.3 A delay-dependent sufficient stability condition

In the special case that the delay $\epsilon = 0$ and $r(0) = 0$, rearranging the terms in Eqs. (5.50) and (5.51) yields

$$x_r(s) = (s\mathbb{I} - A_m)^{-1} B_m \left(u_r(s) + \eta_u(s)\right), \tag{5.82}$$

where

$$u_r(s) = -\frac{k}{s+k}\eta_u(s) \tag{5.83}$$

and $\eta_u(t) \triangleq \Omega\big(t,x(t)\big)u_r(t) - u_r(t) + \eta_r(t)$, whose norm is

$$\|\eta_u\|_{\mathcal{L}_\infty} \le (\omega_h+1)\|\mathcal{G}^0\|_{\mathcal{L}_1}\|\eta_r\|_{\mathcal{L}_\infty} + \|\eta_r\|_{\mathcal{L}_\infty} \le \big((\omega_h+1)g(0)+1\big)\|\eta_r\|_{\mathcal{L}_\infty}. \tag{5.84}$$

In this case, it follows that

$$\|x_r\|_{\mathcal{L}_\infty} \leq \left\|s(s\mathbb{I} - A_m)^{-1}\right\|_{\mathcal{L}_1} \|B_m\| \left\|\frac{1}{s+k}\right\|_{\mathcal{L}_1} \|\eta_u\|_{\mathcal{L}_\infty} \leq \frac{2}{k}\|B_m\|\big((\omega_h+1)g(0)+1\big)\,\|\eta_r\|_{\mathcal{L}_\infty}. \tag{5.85}$$

This and (5.67) with zero delay, zero initial condition and zero desired trajectory lead to

$$f(0) = \|\mathcal{F}^0\|_{\mathcal{L}_1} \leq \frac{2}{k}\|B_m\|\big((\omega_h+1)g(0)+1\big). \tag{5.86}$$

Define

$$\rho_{\text{ic}} \triangleq \sup_t \|\Phi_{11}(t,t',0)\|. \tag{5.87}$$

Then,

Lemma 5.7. *Given $b_d > 0$ and $b_{\text{ic}} > 0$, there exists a k, a ρ_r, and an ϵ_l, such that*

$$f(\epsilon) \leq \frac{\rho_r - d(\epsilon)b_d - \rho_{\text{ic}}b_{\text{ic}}}{L_{\rho_r}\rho_r + Z}, \quad \forall \epsilon \in [0, \epsilon_l], \tag{5.88}$$

where

$$L_{\rho_r} \triangleq \frac{\rho_r + 1}{\rho_r} d_{\eta_x}(\rho_r + 1). \tag{5.89}$$

Proof. Choose $\rho_r > \rho_{\text{ic}}b_{\text{ic}} + d(0)b_d$. Then, since $f(0) \to 0$ as $k \to \infty$, it follows that there exists a K, such that $k > K$ implies that

$$f(0) < \frac{\rho_r - d(0)b_d - \rho_{\text{ic}}b_{\text{ic}}}{L_{\rho_r}\rho_r + Z}. \tag{5.90}$$

For such a k, the claim now follows by the continuity of $f(\epsilon)$ and $d(\epsilon)$, where ϵ_l equals the smallest value of ϵ that results in equality in (5.88). □

Theorem 5.1. *Given $b_d > 0$ and $b_{\rm ic} > 0$, there exists a bandwidth k, such that*

$$\|h_d\|_{\mathcal{L}_\infty} \leq b_d \text{ and } \|r_0\|_\infty \leq b_{\rm ic} \Rightarrow \|x_r\|_{\mathcal{L}_\infty} \leq \rho_r \tag{5.91}$$

for some ρ_r and for all ϵ smaller than the corresponding ϵ_l. In addition, $\|u_r\|_{\mathcal{L}_\infty} < \infty$.

Proof. Choose $\rho_{\rm r} > \max\left(b_{\rm ic}, \rho_{\rm ic} b_{\rm ic} + d(0) b_d\right)$. Suppose that $\|x_r\|_{\mathcal{L}_\infty} \geq \rho_r$. Then $\|r_0\|_\infty < \rho_r$ implies that there exists a τ, such that

$$\|x_r\|_\infty < \rho_r, \quad \forall t \in [0, \tau), \quad \text{and} \quad \|x_{r,\tau}\|_{\mathcal{L}_\infty} = \|x_r(\tau)\|_\infty = \rho_r. \tag{5.92}$$

It follows from Assumption 5.3 and (5.89) that

$$\begin{aligned} \|\eta_r\|_{\mathcal{L}_\infty} &\leq \|\eta(t, x_r(t)) - \eta(t, 0)\|_{\mathcal{L}_\infty} + \|\eta(t, 0)\|_{\mathcal{L}_\infty} \\ &\leq \|x_r\|_{\mathcal{L}_\infty} d_{\eta_x}(\bar{\rho}) + Z < L_{\rho_r} \rho_r + Z, \quad \forall t \in [0, \tau]. \end{aligned} \tag{5.93}$$

Using (5.67), (5.88) and (5.93) we obtain

$$\begin{aligned} \|x_{r,\tau}\|_{\mathcal{L}_\infty} &\leq \|\mathcal{F}^\epsilon\|_{\mathcal{L}_1} \|\eta_{r,\tau}\|_{\mathcal{L}_\infty} + \|\mathcal{D}^\epsilon\|_{\mathcal{L}_1} \|h_d\|_{\mathcal{L}_\infty} + \|x_{\rm ic}\|_{\mathcal{L}_\infty} \\ &\leq f(\epsilon)(L_{\rho_r} \rho_r + Z) + d(\epsilon) b_d + \rho_{\rm ic} b_{\rm ic} < \rho_r, \end{aligned} \tag{5.94}$$

contradicting the equality in (5.92). Thus $\|x_r\|_{\mathcal{L}_\infty} < \rho_r$. The claim that $\|u_r\|_{\mathcal{L}_\infty} < \infty$ immediately follows by applying this result to (5.68). □

5.4 Adaptive control system design and transient performance

In this section, we first design an adaptive controller that decouples adaptation from the control loop, allowing for fast adaptation without deteriorating the system robustness, which is indicated by the time delay margin. In addition, we show that the state and the control

input of the proposed adaptive control system follow those of this nonadaptive reference system closely given that the input delay $\epsilon \leq \epsilon_l$. This implies that ϵ_l is a lower bound for the time delay margin of the proposed adaptive control system.

5.4.1 Design of the adaptation laws and the state predictor

By Theorem 5.1, it follows that, in the nonadaptive reference system, and provided that $\|x_r(0)\|_\infty < \rho_r$, the parameterization

$$\eta(t, x_r(t)) = \theta_r(t)\|x_{r,t}\|_{\mathcal{L}_\infty} + \sigma_r(t) \tag{5.95}$$

holds for all t, in terms of a pair of continuous, piecewise-differentiable and uniformly bounded functions θ_r and σ_r (see Lemma A.9.2 in [61]). Equivalently,

$$\dot{x}_r = A_m x_r + B_m\big(u_r + \theta_r\|x_{r,t}\|_{\mathcal{L}_\infty} + \bar{\sigma}_r\big) \tag{5.96}$$

and

$$\dot{u}_r(t) = -k\big(u_r(t) + \theta_r(t)\|x_{r,t}\|_{\mathcal{L}_\infty} + \bar{\sigma}_r(t) + K_d h_d(t)\big), \tag{5.97}$$

where $\bar{\sigma}_r(t) \triangleq \sigma_r(t) + \Omega\big(x(t)\big)u_r(t-\epsilon) - u_r(t)$ is similarly bounded.

We proceed to consider an adaptive control design for the original dynamics in Eq. (5.1). Analogous to Eqs. (5.96) and (5.97), consider the state predictor

$$\dot{\hat{x}}(t) = A_m x(t) + A_{\text{sp}}\tilde{x}(t) + B_m\big(u(t) + \hat{\theta}(t)\|x_t\|_{\mathcal{L}_\infty} + \hat{\sigma}(t)\big), \quad \hat{x}(0) = r_0, \tag{5.98}$$

and control design

$$\dot{u}(t) = -k\big(u(t) + \hat{\theta}(t)\|x_t\|_{\mathcal{L}_\infty} + \hat{\sigma}(t) + K_d h_d(t)\big), \quad u(0) = 0, \tag{5.99}$$

where $\tilde{x} \triangleq \hat{x} - x$ is the prediction error, $k > 0$ is the bandwidth of the first-order low-pass

filter $k/(s+k)$, and A_{sp} is a Hurwitz matrix of loop-shaping parameters that may be tuned to reject oscillations caused by high-frequency disturbances or noise, as well as to make $\tilde{x}$ converge to 0 faster. Here, $\hat{\theta}$ and $\hat{\sigma}$ model adaptive estimates governed by the projection-based laws [71]

$$\dot{\hat{\theta}} = \Gamma\, \mathbf{Proj}\big(\hat{\theta}, -B_m^\top P\tilde{x}\|x_t\|_{\mathcal{L}_\infty}; \theta_b, \nu\big), \quad \hat{\theta}(0) = \hat{\theta}_0, \tag{5.100}$$

$$\dot{\hat{\sigma}} = \Gamma\, \mathbf{Proj}\big(\hat{\sigma}, -B_m^\top P\tilde{x}; \sigma_b, \nu\big), \quad \hat{\sigma}(0) = \hat{\sigma}_0, \tag{5.101}$$

in terms of the adaptive gain $\Gamma \in \mathbb{R}^+$, and the positive-definite, symmetric matrix P, obtained as the solution to the Lyapunov equation $A_{\text{sp}}^\top P + PA_{\text{sp}} = -Q$, for some arbitrary positive-definite, symmetric matrix Q. As defined in Chapter 2, the *projection operator* $\mathbf{Proj}(\cdot,\cdot;\cdot,\cdot)$, ensures that $\|\hat{\theta}(t)\|_\infty \leq \theta_b$ and $\|\hat{\sigma}(t)\|_\infty \leq \sigma_b$ provided that $\hat{\theta}_0$ and $\hat{\sigma}_0$ satisfy these same bounds.

5.4.2 Performance bounds

In this section we prove that the state and control input of the proposed control system governed by Eqs. (5.1) and (5.98)-(5.101) follow those of the reference system in (5.50), (5.51) and (5.52) closely, provided that the bandwidth k, the adaptive gain Γ, the scalar λ, and the bounds θ_b and σ_b are chosen appropriately. In particular, we prove the following theorem:

Theorem 5.2. *Suppose b_d and b_{ic} are given, and ρ_r and k are chosen as in Section 5.3.3 and assume that ϵ is less than the corresponding ϵ_l. Then, there exists a $C > 0$, such that, for $\psi \ll 1$,*

$$\|\hat{x} - x\|_{\mathcal{L}_\infty} \leq \psi, \quad \|x_r - x\|_{\mathcal{L}_\infty} = \mathcal{O}(\psi), \quad \|u_r - u\|_{\mathcal{L}_\infty} = \mathcal{O}(\psi), \tag{5.102}$$

provided that $\Gamma\psi^2 \geq C$, for all h_d and r_0 satisfying $\|h_d\|_{\mathcal{L}_\infty} \leq b_d$ and $\|r_0\|_\infty \leq b_{\text{ic}}$.

Remark 5.6. *This theorem implies that $\epsilon_l > 0$ is the lower bound for the time-delay margin of the proposed adaptive control system.*

Proof. Equations (5.1) and (5.50) imply that

$$x_r - x = (\mathcal{H} \circ \mathcal{M} \circ \mathcal{E}^{\epsilon})[u_r - u] + \mathcal{H}[\eta_r - \eta]. \tag{5.103}$$

It follows from Eq. (5.99) that

$$\dot{u} = -k\big(u + \hat{\eta} + K_d h_d\big) = -k\Big(\Omega\big(t, x(t)\big)u(t-\epsilon) + \underbrace{\hat{\eta} - \eta - \Omega\big(t, x(t)\big)u(t-\epsilon) + u}_{\tilde{\eta}} + \eta + K_d h_d\Big)$$

$$= -k\Big(\Omega\big(t, x(t)\big)u(t-\epsilon) + \tilde{\eta} + \eta + K_d h_d\Big), \tag{5.104}$$

where $\hat{\eta} \triangleq \hat{\theta}\|r_t\|_{\mathcal{L}_\infty} + \hat{\sigma}$. The difference between (5.1) and (5.98) implies

$$\dot{\tilde{x}} = A_{\rm sp}\tilde{x} + B_m\tilde{\eta}, \quad \hat{x}(0) = 0. \tag{5.105}$$

Since B_m has rank m, i.e $B_m^\top B_m$ is invertible, we have

$$\tilde{\eta} = B_m^\dagger(\dot{\tilde{x}} - A_{\rm sp}\tilde{x}), \quad \hat{x}(0) = 0. \tag{5.106}$$

where $B_m^\dagger = (B_m^\top B_m)^{-1}B_m^\top$ is the pseudoinverse of B_m. According to the definition of the input-output map in (5.66) and the relationship in (5.106), the relationship in Eq. (5.104) can be written as

$$u = \mathcal{G}^{\epsilon}\big[\eta + K_d h_d + B_m^\dagger\dot{\tilde{x}} - B_m^\dagger A_{\rm sp}\tilde{x}\big]. \tag{5.107}$$

Therefore, it follows from (5.68), (5.77) and (5.107) that

$$u_r - u = \mathcal{G}^\epsilon \left[\eta_r - \eta + B_m^\dagger A_{\rm sp}\tilde{r} - B_m^\dagger \dot{\tilde{x}}\right] = \mathcal{G}^\epsilon[\eta_r - \eta] + \mathcal{G}^\epsilon[B_m^\dagger A_{\rm sp}\tilde{x}] + k(\mathcal{I} + \mathcal{G}^\epsilon \circ \mathcal{M} \circ \mathcal{E}^\epsilon)[B_m^\dagger \tilde{r}]. \tag{5.108}$$

Now, suppose that $\psi > 0$ is given. Since $\|x_r(0) - x(0)\|_\infty = 0 < 1$ and $\|u_r(0) - u(0)\|_\infty = 0$, it follows by continuity that there exists a exists a $\tau > 0$, such that $\|(x_r - x)_\tau\|_{\mathcal{L}_\infty} < 1$ and $\|(u_r - u)_\tau\|_{\mathcal{L}_\infty} < \infty$. Theorem 5.1 implies that

$$\|x_\tau\|_{\mathcal{L}_\infty} < \rho_r + 1 = \bar{\rho}, \quad \|u_\tau\|_{\mathcal{L}_\infty} < \infty. \tag{5.109}$$

It follows from (5.3) and (5.109) that

$$\|(\eta_r - \eta)_\tau\|_{\mathcal{L}_\infty} \leq d_{\eta_x}(\bar{\rho})\|(x_r - x)_\tau\|_{\mathcal{L}_\infty} \leq L_{\rho_r}\|(x_r - x)_\tau\|_{\mathcal{L}_\infty}. \tag{5.110}$$

Equations (5.103), (5.108) and (5.110) result in the bounds

$$\|(x_r - x)_\tau\|_{\mathcal{L}_\infty} \leq f(\epsilon)L_{\rho_r}\|(x_r - x)_\tau\|_{\mathcal{L}_\infty} + b_2\|\tilde{x}_\tau\|_{\mathcal{L}_\infty} \tag{5.111}$$

and

$$\|(u_r - u_\tau\|_{\mathcal{L}_\infty} \leq g(\epsilon)L_{\rho_r}\|(x_r - x)_\tau\|_{\mathcal{L}_\infty} + b_3\|\tilde{x}_\tau\|_{\mathcal{L}_\infty}, \tag{5.112}$$

where

$$b_2 \triangleq \|\mathcal{H} \circ \mathcal{M} \circ \mathcal{E}^\epsilon \circ \left(\mathcal{G}^\epsilon \circ \mathcal{B}_m^\dagger \circ \mathcal{A}_{\rm sp} + k(\mathcal{I} + \mathcal{G}^\epsilon \circ \mathcal{M} \circ \mathcal{E}^\epsilon) \circ \mathcal{B}_m^\dagger\right)\|_{\mathcal{L}_1} \tag{5.113}$$

and

$$b_3 \triangleq \|\mathcal{G}^\epsilon \circ \mathcal{B}_m^\dagger \circ \mathcal{A}_{\rm sp} + k(\mathcal{I} + \mathcal{G}^\epsilon \circ \mathcal{M} \circ \mathcal{E}^\epsilon) \circ \mathcal{B}_m^\dagger\|_{\mathcal{L}_1} \tag{5.114}$$

are both finite for all $\epsilon \in [0, \epsilon_l]$. Here, $\mathcal{A}_{\rm sp}$ and $\mathcal{B}_m^\dagger$ denote the input-output maps of the

constant matrices A_{sp} and $B_m^\dagger$, respectively. In this interval of input delay, the stability condition in (5.88) holds and implies that $1 - f(\epsilon)L_{\rho_r} > 0$. Thus, from Eq. (5.111) and (5.112), we conclude that

$$\|(x_r - x)_\tau\|_{\mathcal{L}_\infty} \leq \frac{b_2}{1 - f(\epsilon)L_{\rho_r}} \|\tilde{x}_\tau\|_{\mathcal{L}_\infty} \tag{5.115}$$

and

$$\|(u_r - u)_\tau\|_{\mathcal{L}_\infty} \leq \left(\frac{b_2 g(\epsilon) L_{\rho_r}}{1 - f(\epsilon)L_{\rho_r}} + b_3 \right) \|\tilde{x}_\tau\|_{\mathcal{L}_\infty}. \tag{5.116}$$

Next, we analyze the norm of the estimation error, $\|\tilde{x}_\tau\|_{\mathcal{L}_\infty}$, using a standard Lyapunov method. Because of these bounds on x and u, we have the parameterization for η similarly to (5.95), i.e.

$$\eta(t, x(t)) = \theta(t)\|x_t\|_{\mathcal{L}_\infty} + \sigma(t), \quad \forall t \in [0, \tau], \tag{5.117}$$

where $\theta(t)$ and $\sigma(t)$ are bounded by θ_b and σ_b, respectively. Let $\tilde{\theta} \triangleq \hat{\theta} - \theta$ and $\tilde{\sigma} \triangleq \hat{\sigma} - \bar{\sigma}$. Note that $\bar{\sigma} = \sigma + \Omega\big(t, x(t)\big)u(t - \epsilon) - u$ is bounded by some constant $\bar{\sigma}_b$ because all the terms in its expression are bounded. Moreover,

$$\dot{\bar{\sigma}} = \dot{\sigma} + \dot{\Omega}\big(t, x(t)\big)u(t - \epsilon) + \Omega\big(t, x(t)\big)\dot{u}(t - \epsilon) - \dot{u}. \tag{5.118}$$

Since $x(t)$ and $u(t)$ is bounded as in (5.109), taking into account (5.1) and (5.99), we have $\dot{x}$, $\dot{\Omega}$ and hence $\dot{u}$ are bounded. Hence, $\dot{\bar{\sigma}}$ is bounded, meaning there exists a bounding constant $d_{\bar{\sigma}}$ such that $\|\dot{\bar{\sigma}}\|_\infty \leq d_{\bar{\sigma}}$.

Consider the Lyapunov function candidate $V = \tilde{x}^T P \tilde{x} + \Gamma^{-1}(\tilde{\theta}^T\tilde{\theta} + \tilde{\sigma}^T\tilde{\sigma})$. By the properties of the projection operators,

$$\dot{V} \leq -\tilde{x}^T Q \tilde{x} + \frac{2}{\Gamma}\big|\tilde{\theta}^T\dot{\theta} + \tilde{\sigma}^T\dot{\tilde{\sigma}}\big| \leq -\|\tilde{x}\|_\infty^2 \lambda_{\min}(Q) + \frac{4}{\Gamma}\big(\theta_b d_\theta + \sigma_b d_{\bar{\sigma}}\big). \tag{5.119}$$

We have

$$V(0) \leq \frac{4}{\Gamma}\left(\theta_b^2 + \sigma_b^2\right) < \frac{\nu_m}{\Gamma}, \tag{5.120}$$

where $\nu_m \triangleq 4(\theta_b^2 + \sigma_b^2) + 4\frac{\lambda_{\max}(P)}{\lambda_{\min}(Q)}\big(\theta_b d_\theta + \sigma_b d_{\bar{\sigma}}\big)$. We now show by contradiction that

$$V(t) \leq \frac{\nu_m}{\Gamma}, \quad \forall t \in [0, \tau]. \tag{5.121}$$

To this end, choose $\hat{\tau} \in (0, \tau]$ such that $\dot{\theta}$ and $\dot{\sigma}$ are continuous on $[0, \hat{\tau})$. Suppose that $V(\bar{\tau}) > \nu_m/\Gamma$ and $\dot{V}(\bar{\tau}) \geq 0$ for some $\bar{\tau} < \hat{\tau}$. It follows that

$$\frac{\nu_m}{\Gamma} < V(\bar{\tau}) \leq \|\tilde{x}(\bar{\tau})\|_\infty^2 \lambda_{\max}(P) + \frac{4}{\Gamma}\big(\theta_b^2 + \bar{\sigma}_b^2\big). \tag{5.122}$$

Hence,

$$\|\tilde{x}(\bar{\tau})\|_\infty^2 > \frac{4}{\Gamma\lambda_{\min}(Q)}\big(\theta_b d_\theta + \sigma_b d_{\bar{\sigma}}\big). \tag{5.123}$$

By substituting (5.123) in (5.119) we have $\dot{V}(\bar{\tau}) < 0$, which contradicts the statement that $\dot{V}(\bar{\tau}) \geq 0$. Thus, $V(t) \leq \frac{\nu_m}{\Gamma}$ for all $t \in [0, \hat{\tau})$. Since $V(t)$ is a continuous function, $V(t) \leq \frac{\nu_m}{\Gamma}$ for all $t \in [0, \hat{\tau}]$. Consequently,

$$\|\tilde{x}_{\hat{\tau}}\|_{\mathcal{L}_\infty} \leq \sqrt{\frac{\nu_m}{\lambda_{\min}(P)\Gamma}}\,. \tag{5.124}$$

By repeating this analysis for each subsequent interval of continuity of $\dot{\theta}$ and $\dot{\sigma}$, we conclude that (5.124) holds with $\hat{\tau}$ replaced by τ. In other words, there exists $C > 0$ (independent of τ), such that

$$\|\tilde{x}_\tau\|_{\mathcal{L}_\infty} \leq \sqrt{C/\Gamma}, \tag{5.125}$$

which does not exceed ψ provided that $\Gamma\psi^2 \geq C$. The claim of this theorem follows by choosing ψ and Γ such that the product in the right side of (5.115) is strictly less than 1. $\square$

5.5 Summary

This chapter documents theoretical analysis showing the existence of a lower bound for the time delay margin of a class of nonlinear control systems. The plant model considered in this chapter is a generalization of the model in Chapter 4, and represents a wide range of Lagrangian systems with nonlinear and time-varying input gains. The control scheme is designed by following the framework presented in Chapter 2. Various properties of linear time-varying DDEs are established in this chapter:

- They do not have finite escape time.
- Their solution is bounded within an exponential envelop which may grow in time but is independent of the delay.
- If their coefficient matrices satisfy a certain condition, the DDEs are uniformly asymptotically stable when the delay is small enough.
- Their solution is continuous in the delay, uniformly in time in a finite interval, for any delay value.
- Their solution is continuous in the delay, uniformly in time in an infinite interval, for small enough delay.

These properties lead to the existence of a lower bound for the time delay of the nonadaptive reference system via a continuity argument for the delay stability condition. The chapter then shows that is the delay is below this lower bound, then the dynamics of the adaptive control system and the reference system are almost identical if the adaptive gain is large enough. The result implies that the two systems have the same lower bound for their time delay margin.

CHAPTER 6

TRACKING SYNCHRONIZATION

This chapter presents the analysis of synchronization of networked manipulators operating on an underactuated dynamic platform in the presence of communication delays. The proposed formulation does not require detailed information about the system model. The theoretical analysis based on input-output maps of functional differential equations shows that the adaptive control system's behavior matches closely that of a nonadaptive reference system. The tracking-synchronization objective is achieved despite the effect of communication delays, and the unknown dynamics of the platform. Simulation results illustrate the performance of the proposed control algorithms.

The chapter is organized as follows. Section 6.1 discusses background on network system and properties of different associated graphs. Section 6.2 presents the model of multiple manipulators operating on a dynamic platform. In Section 6.3, we analyze a scheme for perfect cancelation when the entire model is fully known. In contrast, Section 6.4 proposes an adaptive control algorithm for each manipulator to achieve tracking synchronization despite the unmodelled dynamics, unknown platform motion, and communication delay in the network. In Sections 6.5 and 6.6, we design a collective reference system, and establish its stability via the analysis of certain input-output maps that account for the delays. Section 6.7 shows that the collective state and control input of the proposed adaptive control system follow those of the nonadaptive reference system closely to achieve tracking synchronization. Section 6.8 closes the chapter with concluding remarks.

6.1 Network systems

Consider a network of N manipulators with the same numbers of degrees of freedom, and assume that this is represented by a simple, unsigned, directed graph that describes the communication topology associated with the network. Let $\mathcal{S}_i$ denote the set of manipulators that send their measured joint angles and angular velocities to the ith manipulator ($i \notin \mathcal{S}_i$). Let D be the degree matrix of the network, which is diagonal with the in-degree of the vertices, $|\mathcal{S}_i|$ in the ith diagonal element. In addition, denote by A_d the adjacency matrix of the network such that the (i, j)-th element is 1 if $j \in \mathcal{S}_i$, and 0 otherwise. Finally, denote by $L = D - A_d$ the graph Laplacian of the manipulator network. The graph is said to be strongly connected if there is a directed path connecting any two nodes. In this case, then $\text{rank}(L) = N - 1$, i.e., the Laplacian matrix always has a zero eigenvalue. The corresponding eigenvector is a column of ones. Moreover, all nonzero eigenvalues of L have positive real part [119].

Communication delays are inherent in networked systems due to the physical distance between nodes and the properties of the transmitters and receivers. In this chapter, we assume an identical and constant communication delay T along each edge in the network. This assumption is reasonable in practice because one can always select the transmitters and set buffers to achieve this [29].

6.2 Dynamic Model of a robot network operating on a dynamic platform

Suppose the network of manipulators is operating on a common dynamic platform, such as a ship or a ground-based vehicle. Let $q_{a,i}$ contain the n actuated generalized coordinates of each manipulator, q_p contain the m generalized coordinates of the platform, and u_i contain the input torques to the ith manipulator. When the argument t is omitted, the corresponding time dependent function is evaluated at time t. The dynamics of the individual robotic

manipulators are coupled through the dynamicas of the platform and governed by equations of motion of the form

$$M_{ai}(q_i)\ddot{q}_{a,i} + M_{pi}(q_i)\ddot{q}_p + N_{ai}(q_i, \dot{q}_i) = u_i + D_{ai},\ i = 1, ..., N, \tag{6.1}$$

where $q_i^\top \triangleq [q_{a,i}^\top, q_p^\top]$, $q^\top \triangleq [q_{a,1}^\top, ..., q_{a,N}^\top, q_p^\top]$ and the column vector D_{ai} contains bounded time-dependent unknown disturbances to the ith manipulator. The inertia matrices M_{ai} and M_{pi} are all symmetric, positive-definite, and bounded. The remaining terms include Coriolis and centripetal effects, gravity and other conservative forces, as well as dissipative and velocity-dependent contributions to the dynamics of each manipulator. Similar to Chapter 2, *we here assume that $q_p(t)$, $\dot{q}_p(t)$ and $\ddot{q}_p(t)$ can be bounded a priori for all time.*

For the ith manipulator, we introduce the kinematic variable

$$r_i = (\dot{q}_{a,i} - \dot{q}_d) + (q_{a,i} - q_d), \tag{6.2}$$

where q_d is the desired trajectory for the manipulators' joint angles. It follows from (6.1) and (6.2) that we may write

$$\dot{r}_i = \omega_i(q_i)u_i + \eta_i^{(0)}, \quad r_i(0) = r_{0,i}, \tag{6.3}$$

where $\omega_i(q_i) \triangleq M_{ai}^{-1}(q_i)$ is positive-definite and bounded, i.e., there exists positive constants ω_l and ω_h such that

$$\omega_l \mathbb{I} \leq \omega(q), \text{ and } \|\omega(q)\|_\infty \leq \omega_h, \tag{6.4}$$

with $\omega(q) \triangleq \text{diag}[\omega_i(q_i)]$. The *nonlinearity* function $\eta_i^{(0)} : \mathbb{R} \times \mathbb{R}^{2n+3m} \to \mathbb{R}^n$ captures the detailed, but unknown, nonlinear model of the manipulator dynamics, as well as the uncertain contributions that result from the moving platform. Specifically, let the arguments of $\eta_i^{(0)}$

be decomposed as (t, ζ_i), where

$$\zeta_i^\top \triangleq \left[r_i^\top, \chi_i^\top\right], \text{ and } \chi_i^\top \triangleq [q_{a,i}^\top, q_p^\top, \dot{q}_p^\top, \ddot{q}_p^\top]. \tag{6.5}$$

Here, $\eta_i^{(0)}$ is bounded at zero configuration (see [102]), i.e., there exists a constant $Z_i > 0$, such that

$$\|\eta_i^{(0)}(t,0)\|_\infty \leq Z_i, \ \forall t \geq 0. \tag{6.6}$$

We define the ideal dynamics by rewriting the equation (6.3) in the form

$$\dot{r}_i = A_{m,i} r_i + \omega_i(q_i) u_i + \eta_i, \quad r_i(0) = r_{0,i}, \tag{6.7}$$

where $A_{m,i}$ is a Hurwitz matrix to be chosen appropriately, and $\eta_i = \eta_i^{(0)} - A_{m,i} r_i$. It follows that

$$\|\eta_i(t,0)\|_\infty \leq Z_i, \ \forall t \geq 0. \tag{6.8}$$

Moreover, we restrict attention to disturbances that guarantee that (cf. Appendix B of [102]):

$$\|\zeta_i\|_\infty \leq \delta_i \Rightarrow \left\| \frac{\partial \eta_i(t, \zeta_i)}{\partial \zeta_i} \right\|_\infty \leq d_i(\delta_i) \tag{6.9}$$

and such that the partial derivative of η_i with respect to t is similarly uniformly bounded. Note that the bound $d_i(\delta_i)$ depends on the choice of $A_{m,i}$.

6.3 Perfect cancellation

The control objective in this chapter is to synchronize the motion of each manipulator with that of the other manipulators in the network while tracking a desired trajectory:

$$q_i \to q_j \to q_d, \text{ for } i, j = 1, ..., N. \tag{6.10}$$

Ideally, if η_i and $\omega_i(q)$ are known, we can compensate for the nonlinearity in (6.7) using

$$u_i = \omega_i^{-1}(q_i)\big(u_i^{sync} - \eta_i\big), \tag{6.11}$$

where u_i^{sync} remains to be designed. The general equation of motion (6.7) then becomes

$$\dot{r}_i = A_{m,i} r_i + u_i^{sync}, \quad r_i(0) = r_{0,i}. \tag{6.12}$$

Consider the following synchronization control input

$$u_i^{sync}(t) = \sum_{j \in \mathcal{S}_i} \big(r_j(t - T) - r_i(t)\big), \tag{6.13}$$

where $r(t)$ receives the value of the constant vector r_0, which contains the initial conditions of the manipulators' states, for all $t \in [-T, 0]$, and T is the communication delay. The collective synchronization control input becomes

$$u^{sync}(t) = (A_d \otimes \mathbb{I}_n) r(t - T) - (D \otimes \mathbb{I}_n) r(t), \tag{6.14}$$

where $\otimes$ denotes the Kronecker product, the column vector u^{sync} collects all u_i^{sync} for $i = 1, ..., N$, and $r^\top \triangleq [r_1^\top, r_2^\top, ..., r_N^\top]$. Substituting (6.14) into (6.12) then leads to the following

collective dynamics of the robot network

$$\dot{r}(t) = (A_m - D \otimes \mathbb{I}_n)r(t) + (A_d \otimes \mathbb{I}_n)r(t-T). \tag{6.15}$$

Let $A_m = aA_0$, where a is a positive scaling factor, and A_0 is a Hurwitz matrix. It is well known that there exists a positive definite matrix P_0 such that $A_0^\top P_0 + P_0 A_0 = -\mathbb{I}$. The matrix P_0 depends on A_0, but not on a. Consider the Lyapunov function candidate $V(r) = r^\top P_0 r$. Let $b_1 = \|P_0(D \otimes \mathbb{I}_n)\|_\infty$ and $b_2 = \|P_0(A_d \otimes \mathbb{I}_n)\|_\infty$. We have

$$\begin{aligned}
\dot{V}(r(t)) &= r^\top(t)P_0\dot{r}(t) + \dot{r}^\top(t)P_0 r(t) \\
&= r^\top(t)\big(A_m^\top P_0 + P_0 A_m\big)r(t) - 2r^\top(t)P_0(D \otimes \mathbb{I}_n)r(t) + 2r^\top(t)P_0(A_d \otimes \mathbb{I}_n)r(t-T) \\
&\leq -a\|r(t)\|^2 + 2b_1\|r(t)\|^2 + 2b_2\|r(t)\|\|r(t-T)\|.
\end{aligned} \tag{6.16}$$

Now, if $V(r(t-t')) < pV(r(t))$ for all $t' \in [0, T]$, where $p > 1$ is a constant, then

$$\|r(t-T)\| \leq \|r(t)\|\sqrt{p\frac{\lambda_{\min}(P_0)}{\lambda_{\max}(P_0)}}. \tag{6.17}$$

Substitution of (6.17) in (6.16) yields

$$\dot{V}(r(t)) \leq \left(-a + 2b_1 + 2b_2\sqrt{p\frac{\lambda_{\min}(P_0)}{\lambda_{\max}(P_0)}}\right)\|r(t)\|^2. \tag{6.18}$$

Since we can design a such that $a > 2b_1 + 2b_2\sqrt{p\frac{\lambda_{\min}(P_0)}{\lambda_{\max}(P_0)}}$, i.e. $\dot{V}(r(t)) < 0$. Therefore, given A_m satisfies this delay-independent condition, (6.15) is uniformly asymptotically stable according to the Razumikhin theorem (see [48], pp. 127). In addition, because of the form of the Lyapunov function used here, $r = 0$ is a global attractor. Hence, $r_i \to r_j \to 0$, i.e. $q_i \to q_j \to q_d$. Thus, in this case, the control objective for tracking synchronization is achieved independent of the delay.

Remark 6.1. *The Razumikhin theorem says that for uniform asymptotic stability, the con-*

dition $\dot{V}(r(t)) < 0$ is not required for all time. The negativity of $\dot{V}(r(t))$ is needed only when $V(r(t-t')) < pV(r(t))$ for all $t' \in [0,T]$. In situations where $V(r(t-t')) \geq pV(r(t))$, since $p > 1$, we have $V(r(t-t')) > V(r(t))$ for all $t' \in [0,T]$. Hence, in such cases, $V(r(t))$ is already decaying to zero.

6.4 Adaptive control scheme

We proceed to consider the case when it is not possible to achieve perfect cancellation. To this end, let the control input be composed of an adaptive part, which seeks to compensate for the nonlinearity of each manipulator, and a synchronization part, such that

$$u_i = u_i^{ad} + u_i^{sync}. \tag{6.19}$$

Specifically, we design the control input u_i^{ad} based on the adaptive control framework in Chapter 2 for a single moving-base manipulator, i.e., as the output to the linear filter

$$\dot{u}_i^{ad} = -k(u_i^{ad} + \hat{\eta}_i),\ u_i^{ad}(0) = 0, \tag{6.20}$$

where $\hat{\eta}_i(s)$ is evolving dynamically and remains to be designed. The adaptive control input seeks partial compensation of the nonlinearity by allowing only low-frequency signals in the control channels so as to maintain robustness.

Let the estimate $\hat{\eta}_i$ take the form of two time-varying functions with the measurable $\|r_{i,t}\|_{\mathcal{L}_\infty}$ as a regressor:

$$\hat{\eta}_i(t) \triangleq \hat{\theta}_i(t)\|r_{i,t}\|_{\mathcal{L}_\infty} + \hat{\sigma}_i(t), \tag{6.21}$$

where the adaptive estimates $\hat{\theta}_i(t)$ and $\hat{\sigma}_i(t)$ are governed by the projection-based laws

$$\dot{\hat{\theta}}_i = \Gamma\, \mathbf{Proj}\big(\hat{\theta}_i, -P\tilde{r}_i \|r_{i,t}\|_{\mathcal{L}_\infty}; \theta_{b,i}, \varepsilon\big), \quad \hat{\theta}_i(0) = \hat{\theta}_{i,0}, \tag{6.22}$$

$$\dot{\hat{\sigma}}_i = \Gamma\, \mathbf{Proj}\big(\hat{\sigma}_i, -P_i\tilde{r}_i; \sigma_{b,i}, \varepsilon\big), \quad \hat{\sigma}_i(0) = \hat{\sigma}_{i,0}. \tag{6.23}$$

Here, ε is the projection tolerance, $\hat{\theta}_i(t)$ and $\hat{\sigma}_i(t)$ are bounded by $\theta_{b,i}$ and $\sigma_{b,i}$, which are set by the adaptive laws, and Γ is the adaptive gain, which is the same for all manipulators. The feedback in these adaptation laws is described in terms of the *prediction error* $\tilde{r}_i \triangleq \hat{r}_i - r_i$, where the state predictor $\hat{r}_i$ is governed by the system

$$\dot{\hat{r}}_i = A_{m,i} r_i + u_i + \hat{\eta}_i + A_{l,i}\tilde{r}, \quad \hat{r}_i(0) = r_{0,i} \tag{6.24}$$

and $A_{l,i}$ is a Hurwitz matrix of loop-shaping parameters that may be tuned to reject oscillations caused by high-frequency disturbances or noise, as well as to make $\tilde{r}$ converge to 0 faster. The overall control framework is illustrated by the block diagram in Fig. 6.1.

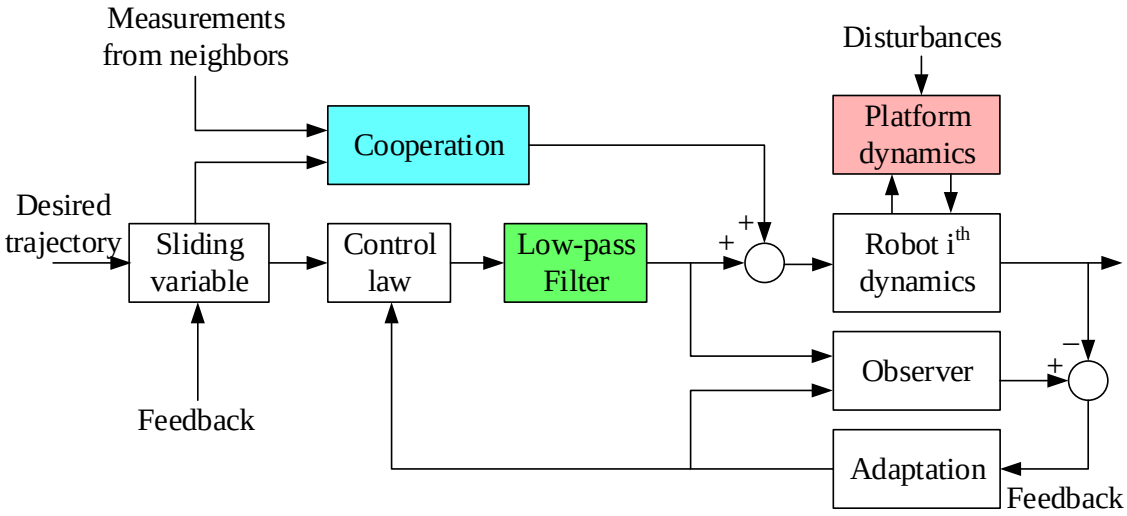

Figure 6.1: The block diagram for the cooperative control framework.

6.5 Nonadaptive reference system

Let $\mathcal{F}_q$ be the map from y to z in

$$\dot{z} = -k\big(\omega(q)z + y\big),\ z(0) = 0, \tag{6.25}$$

where $k > 0$. Here, the subscript $_q$ implies the dependence on the trajectory q. Since $\omega(q)$ is a uniform positive definite matrix, it is shown in Section 2.2 that

$$b_{\mathcal{F}} \triangleq \sup_q \|\mathcal{F}_q\|_{\mathcal{L}_1} < \infty. \tag{6.26}$$

Let $\mathcal{I}$ be the identity map, and $\mathcal{M}_q : y \to \omega(q)y$. We construct a nonadaptive, collective reference system:

$$\dot{q}_{\mathrm{a,ref}} = -q_{\mathrm{a,ref}} + r_{\mathrm{ref}} + q_d + \dot{q}_d, \quad q_{\mathrm{a,ref}}(0) = q_0 \tag{6.27}$$

$$\dot{r}_{\mathrm{ref}} = A_m r_{\mathrm{ref}} + \omega(q)u_{\mathrm{ref}} + \eta_{\mathrm{ref}}, \quad r_{\mathrm{ref}}(t) = r_0\ \forall t \in [-T, 0] \tag{6.28}$$

$$u_{\mathrm{ref}} = \mathcal{F}_q[\eta_{\mathrm{ref}}] + \big(\mathcal{F}_q \circ (\mathcal{M}_q - \mathcal{I}) + \mathcal{I}\big)[u_{\mathrm{ref}}^{sync}], \quad u_{\mathrm{ref}}(0) = 0 \tag{6.29}$$

$$u_{\mathrm{ref}}^{sync}(t) = (A_d \otimes \mathbb{I}_n)r_{\mathrm{ref}}(t - T) - (D \otimes \mathbb{I}_n)r_{\mathrm{ref}}(t), \tag{6.30}$$

where $q^\top \triangleq \big[q_{a,1}^\top, ..., q_{a,N}^\top, q_p^\top\big]$. The function η_{ref} denotes $\eta(t, \zeta_{\mathrm{ref}}(t))$, with the variables

$$\zeta^{ref\top} \triangleq \big[r^{ref\top}, \chi^{ref\top}\big], \text{ and } \chi^{ref\top} \triangleq \big[q_a^{ref\top}, q_p^\top, \dot{q}_p^\top, \ddot{q}_p^\top\big]. \tag{6.31}$$

This nonadaptive reference system represents the ideal dynamics for the robot network when the nonlinearity of each manipulator is known to its controller, as seen in (6.29), as opposed to being estimated by the adaptive scheme presented in the last section. Note here that u_{ref}^{sync} in (6.30) is analogous to u^{sync} in (6.14). Furthermore, when $k \to \infty$, we have $\mathcal{F}_q[y] = -\omega^{-1}(q)y$. In this limit, the reference system recovers the exact form of (6.15).

6.5.1 The variation-of-constants formula for DDEs

Consider the following delay differential equation

$$\dot{x}(t) = A(t)x(t) + B(t)x(t-T) + y(t), \quad x(t) = x_0, \ \forall t \in [-T, 0], \tag{6.32}$$

where $A(t)$ and $B(t)$ are continuous matrix functions, and their norms are bounded. Let Φ be the fundamental solution of the following DDE

$$\begin{aligned} \frac{\partial}{\partial t}\Phi(t,t') &= A(t)\Phi(t,t') + B(t)\Phi(t-T,t'), \quad \forall (t,t') \in [t',\infty) \times [0,\infty), \\ \Phi(t,t) &= \mathbb{I}, \quad \forall t \in [0,\infty), \\ \Phi(t,t') &= 0, \quad \forall (t,t') \in [t'-T, t') \times [0,\infty). \end{aligned} \tag{6.33}$$

Then, the solution to the DDE in (6.32) for $t \geq 0$ can be written in the following form (cf. [143, 151, 6])

$$x(t) = \bar{x}(t, x_0) + \int_0^t \Phi(t,t')y(t')\mathrm{d}t' \tag{6.34}$$

$$\bar{x}(t, x_0) = \Big(\Phi(t,0) + \int_0^T \Phi(t,t')B(t')\mathrm{d}t'\Big)x_0. \tag{6.35}$$

Consider the decomposition $x^\top = [x_1^\top \ x_2^\top]$ and $y^\top = [y_1^\top \ y_2^\top]$, where the components are column vectors with the same size, and similarly

$$\Phi = \begin{bmatrix} \Phi_{11} & \Phi_{12} \\ \Phi_{21} & \Phi_{22} \end{bmatrix}, \quad A = \begin{bmatrix} A_{11} & A_{12} \\ A_{21} & A_{22} \end{bmatrix}, \quad \text{and } B = \begin{bmatrix} B_{11} & B_{12} \\ B_{21} & B_{22} \end{bmatrix}, \tag{6.36}$$

where each block is a square matrix with the same size. In the special case that $y_2 = 0$ and

$x_2(0) = 0$,

$$x_1(t) = \bar{x}_1(t, x_0) + \int_0^t \Phi_{11}(t, t')y_1(t')\mathrm{d}t', \tag{6.37}$$

$$\bar{x}_1(t, x_0) = \Big(\Phi_{11}(t, 0) + \int_0^T \big(\Phi_{11}(t, t')B_{11}(t') + \Phi_{12}(t, t')B_{21}(t')\big)\mathrm{d}t'\Big)x_1(0). \tag{6.38}$$

6.5.2 The norm and the stability of an input-output map

Consider the following system

$$\dot{z} = A_m z + \omega(q)\big(\mathcal{F}_q \circ (\mathcal{M}_q - \mathcal{I}) + \mathcal{I}\big)[z_{sync}] + y, \tag{6.39}$$

where $z(t) = z_0,\ \forall t \in [-T, 0]$, and

$$z_{sync}(t) = (A_d \otimes \mathbb{I}_n)z(t - T) - (D \otimes \mathbb{I}_n)z(t). \tag{6.40}$$

If $v \triangleq \mathcal{F}_q \circ (\mathcal{M}_q - \mathcal{I})[z_{sync}]$, the DDE in (6.39) can be written as

$$\begin{aligned} \dot{z} &= A_m z + \omega(q)z_{sync} + \omega(q)v + y, \\ \dot{v} &= -k\Big(\omega(q)v + \big(\omega(q) - \mathbb{I}_{Nn}\big)z_{sync}\Big), \end{aligned} \tag{6.41}$$

where $v(0) = 0$. Substituting z_{sync} in (6.41) leads to

$$\begin{aligned} \begin{bmatrix} \dot{z} \\ \dot{v} \end{bmatrix} = &\underbrace{\begin{bmatrix} A_m - \omega(q)(D \otimes \mathbb{I}_n) & \omega(q) \\ k\big(\omega(q) - \mathbb{I}_{Nn}\big)(D \otimes \mathbb{I}_n) & -k\omega(q) \end{bmatrix}}_{A(t)} \underbrace{\begin{bmatrix} z \\ v \end{bmatrix}}_{x} \\ &+ \underbrace{\begin{bmatrix} \omega(q)(A_d \otimes \mathbb{I}_n) & 0 \\ -k\big(\omega(q) - \mathbb{I}_{Nn}\big)(A_d \otimes \mathbb{I}_n) & 0 \end{bmatrix}}_{B(t)} \begin{bmatrix} z(t - T) \\ v(t - T) \end{bmatrix} + \begin{bmatrix} y \\ 0 \end{bmatrix}. \end{aligned} \tag{6.42}$$

This equation has the form of (6.32). The solution z can be written in terms of the fundamental solution's components and the input y as shown in (6.37) and (6.38). Based on these, we define the linear map $\mathcal{H}_q$ from y to z in (6.39) as

$$\mathcal{H}_q : y \to \int_0^t \Phi_{11}(t, t')y(t')\mathrm{d}t'. \tag{6.43}$$

The variation-of-constant formula (6.37) is now written as

$$z(t) = \bar{z}(t, x_0) + \mathcal{H}_q[y]. \tag{6.44}$$

In addition, the $\mathcal{L}_1$ norm of $\mathcal{H}_q$ is then given by

$$\|\mathcal{H}_q\|_{\mathcal{L}_1} \triangleq \max_{1\le i\le n} \left(\sum_{j=1}^{n} \sup_{t\ge 0} \int_0^t \left|\Phi_{11}^{ij}(t, t')\right| \, \mathrm{d}t' \right), \tag{6.45}$$

where $\Phi_{11}^{ij}(t, t')$ represent the entries of the matrix $\Phi_{11}(t, t')$.

6.5.3 Exponential stability of $\mathcal{H}_q$ using a Lyapunov-Razumikhin function

By the way that $\mathcal{H}_q$ is defined as an input-output map of a time-varying delay differential equation in the previous section, it is possible that the delay T, when large enough, may destabilize $\mathcal{H}_q$. Nonetheless, in the following lemma, we show that if the control parameters A_m and k are designed to satisfy a certain delay-independent condition, the exponential stability of $\mathcal{H}_q$ is guaranteed.

Lemma 6.1. *It is possible to design A_m independently of k such that $\|\mathcal{H}_q\|_{\mathcal{L}_1}$ is finite, independently of the communication delay T.*

Proof. The map $\mathcal{H}_q$ maps y to z in (6.39). The corresponding homogeneous equation is given

by

$$\begin{aligned}\dot{z} &= A_m z(t) + \omega(q)\big(\mathcal{F}_q \circ (\mathcal{M}_q - \mathcal{I}) + \mathcal{I}\big)\Big[(A_d \otimes \mathbb{I}_n)z(t-T) - (D \otimes \mathbb{I}_n)z(t)\Big], \\ &= A_m z(t) + \mathcal{A}\big[z(t)\big] + \mathcal{B}\big[z(t-T)\big], \end{aligned} \tag{6.46}$$

where

$$\mathcal{A}\big[z(t)\big] \triangleq -\omega(q)\big(\mathcal{F}_q \circ (\mathcal{M}_q - \mathcal{I}) + \mathcal{I}\big)\big[(D \otimes \mathbb{I}_n)z(t)\big] \tag{6.47}$$

$$\mathcal{B}\big[z(t-T)\big] \triangleq \omega(q)\big(\mathcal{F}_q \circ (\mathcal{M}_q - \mathcal{I}) + \mathcal{I}\big)\big[(A_d \otimes \mathbb{I}_n)z(t-T)\big]. \tag{6.48}$$

According to (2.16), we have

$$\|\mathcal{F}_q\|_{\mathcal{L}_1} \leq \frac{Nn\sqrt{Nn}}{\omega_l}, \quad \forall q, \tag{6.49}$$

where ω_l is a positive constant such that $\omega_l \mathbb{I} \leq \omega(q)$ for all q. It follows that

$$\|\mathcal{A}\|_{\mathcal{L}_1} \leq \omega_h\Big(\frac{Nn\sqrt{Nn}}{\omega_l}(\omega_h + 1) + 1\Big)\|(D \otimes \mathbb{I}_n)\|_\infty \tag{6.50}$$

$$\|\mathcal{B}\|_{\mathcal{L}_1} \leq \omega_h\Big(\frac{Nn\sqrt{Nn}}{\omega_l}(\omega_h + 1) + 1\Big)\|(A_d \otimes \mathbb{I}_n\|_\infty. \tag{6.51}$$

As before, let $A_m = aA_0$, where a is a positive scaling factor, and A_0 is a Hurwitz matrix which achieve some control coupling among the degrees of freedom of the manipulators. There exists a positive definite matrix P_0 such that $A_0^\top P_0 + P_0 A_0 = -\mathbb{I}$. Though P_0 depends on A_0, it is independent of a. It follows from (6.50) and (6.51) that there are constants c_1 and c_2 independent of k such that $\|P_0\|_\infty \|\mathcal{A}\|_{\mathcal{L}_1} \leq c_1$ and $\|P_0\|_\infty \|\mathcal{B}\|_{\mathcal{L}_1} \leq c_2$. Consider the

Lyapunov-Razumikhin function candidate $V(z) = z^\top P_0 z$. We have

$$\begin{aligned}\dot{V}(z(t)) &= z^\top(t)P_0\dot{z}(t) + \dot{z}^\top(t)P_0 z(t) \\ &= z^\top(t)\big(A_m^\top P_0 + P_0 A_m\big)z(t) - 2z^\top(t)P_0\mathcal{A}\big[z(t)\big] + 2z^\top(t)P_0\mathcal{B}\big[z(t-T)\big] \\ &\leq -a\|z(t)\|_{\mathcal{L}_\infty}^2 + 2c_1\|z(t)\|_{\mathcal{L}_\infty}^2 + 2c_2\|z(t)\|_{\mathcal{L}_\infty}\|z(t-T)\|_{\mathcal{L}_\infty}. \end{aligned} \tag{6.52}$$

Now, if $V(z(t-t')) < pV(z(t))$ for all $t' \in [0, T]$, where $p > 1$ is a constant, then

$$\|z(t-T)\|_{\mathcal{L}_\infty} \leq \|z(t)\|_{\mathcal{L}_\infty}\sqrt{p\frac{\lambda_{\max}(P_0)}{\lambda_{\min}(P_0)}}. \tag{6.53}$$

Substitution of (6.17) in (6.52) yields

$$\dot{V}(z(t)) \leq \left(-a + 2c_1 + 2c_2\sqrt{p\frac{\lambda_{\max}(P_0)}{\lambda_{\min}(P_0)}}\right)\|z(t)\|_{\mathcal{L}_\infty}^2. \tag{6.54}$$

We can design a independent of k such that

$$a > 2c_1 + 2c_2\sqrt{p\frac{\lambda_{\max}(P_0)}{\lambda_{\min}(P_0)}}, \quad \text{i.e. } \dot{V}(z(t)) < 0. \tag{6.55}$$

Therefore, given a, and hence A_m, that satisfies this delay-independent condition, (6.46) is globally uniformly asymptotically stable according to the Razumikhin theorem (see [48], pp. 127). This means for every bounding constant z_b, there exists a t_b such that

$$\|z(t-T)\| \leq z_b, \ \forall t \geq t_b. \tag{6.56}$$

This also implies that

$$\|z(t)\| \leq z_b, \ \forall t \geq t_b. \tag{6.57}$$

From the definition of the Lyapunov-Razumikhin function, we have

$$\|z(t)\|^2\lambda_{\min}(P_0) \leq V\big(z(t)\big) \leq \|z(t)\|^2\lambda_{\max}(P_0). \tag{6.58}$$

It then follows from this and (6.52) that

$$\dot{V}\big(z(t)\big) \leq -a\frac{V\big(z(t)\big)}{\lambda_{\max}(P_0)} + 2c_1\|z(t)\|^2 + 2c_2\|z(t)\|\|z(t-T)\|. \tag{6.59}$$

Using (6.56) and (6.57), and then applying Gronwall lemma to (6.59) and lead to

$$\|z(t)\|^2\lambda_{\min}(P_0) \leq V\big(z(t)\big) \leq \mathrm{e}^{-\frac{a}{\lambda_{\max}(P_0)}(t-t_b)}2z_b^2(c_1+c_2),\ \forall t \geq t_b. \tag{6.60}$$

Hence, the homogeneous equation (6.46) is exponentially stable. Thus, the norm $\|\mathcal{H}_q\|_{\mathcal{L}_1}$ is finite. □

Lemma 6.2. *Suppose we have chosen A_m such that $\|\mathcal{H}_q\|_{\mathcal{L}_1}$ is finite. Let $\mathcal{H}_q^s : y \to \mathcal{H}_q[\dot{y}]$. Then the norm $\|\mathcal{H}_q^s\|_{\mathcal{L}_1}$ is also finite.*

Proof. Let $z = \mathcal{H}_q[\dot{y}]$. With the linear and stable maps $\mathcal{A}$ and $\mathcal{B}$ defined in (6.50) and (6.51), whose $\mathcal{L}_1$ norms are bounded, the definition of the map $\mathcal{H}_q$ together with (6.39) lead to

$$\dot{z}(t) = A_m r(t) + \mathcal{A}[z(t)] + \mathcal{B}[z(t-T)] + \dot{y}(t) \tag{6.61}$$

$$\Rightarrow \dot{z}(t) - \dot{y}(t) = A_m r(t) + \mathcal{A}[z(t)-y(t)] + \mathcal{B}\big[z(t-T)-y(t-T)\big] + \mathcal{A}[y] + \mathcal{B}[y(t-T)] \tag{6.62}$$

$$\Rightarrow z(t) = \mathcal{H}_q \circ \mathcal{A}[y(t)] + \mathcal{H}_q \circ \mathcal{B}[y(t-T)] + y = \big(\mathcal{H}_q \circ \mathcal{A} + \mathcal{H}_q \circ \mathcal{B} \circ \mathcal{E} + \mathcal{I}\big)[y], \tag{6.63}$$

where $\mathcal{E} : y \to y(t-T)$ denotes the delay map. Hence, we get $\mathcal{H}_q^s[\cdot] = \big(\mathcal{H}_q \circ \mathcal{A} + \mathcal{H}_q \circ \mathcal{B} \circ \mathcal{E} + \mathcal{I}\big)[\cdot]$, in which the norm of each term is finite. Thus, the norm $\|\mathcal{H}_q^s\|_{\mathcal{L}_1}$ is also finite. □

6.5.4 Exponential stability of the map $\mathcal{H}_q$ using a Lyapunov-Krasovskii functional

This section presents an alternative method for stability analysis of the map $\mathcal{H}_q$ using a Lyapunov-Krasovskii functional. This method leads to delay-dependent conditions for A_m and k in the form of a linear matrix inequality.

Lemma 6.3. *Given a time delay T, it is possible to design A_m and k such that the fundamental solution Φ of the DDE in (6.42) decays exponentially, and hence the map $\mathcal{H}_q$ is exponentially stable.*

Proof. Let A_m and P_0 be defined as in the previous section. Suppose P and Q are a positive definite block diagonal matrices of the form

$$P = \begin{bmatrix} P_0 & 0 \\ 0 & \mathbb{I}_{Nn} \end{bmatrix} \quad \text{and} \quad Q = \begin{bmatrix} e^{aT}k^2\mathbb{I}_{Nn} & 0 \\ 0 & \mathbb{I}_{Nn} \end{bmatrix}, \tag{6.64}$$

such that P is independent of a. The time derivative of the Lyapunov functional

$$V(x) = x^\top Px + \int_{t-T}^{t} e^{-a(t-t')}x^\top(t')Qx(t')\mathrm{d}t' \tag{6.65}$$

along the solution of the homogeneous equation of (6.42) is

$$\begin{aligned}
\dot{V} + aV &= \big(Ax + Bx(t-T)\big)^\top Px + x^\top P\big(Ax + Bx(t-T)\big) \\
&\quad + x^\top Qx - e^{-aT}x^\top(t-T)Qx(t-T) + ax^\top x \\
&= x^\top(A^\top P + PA + Q + a\mathbb{I}_{2Nn})x + x^\top(t-T)B^\top Px + x^\top PBx(t-T) \\
&\quad - e^{-aT}x^\top(t-T)Qx(t-T) \\
&= \begin{bmatrix} x^\top & x^\top(t-T) \end{bmatrix} \begin{bmatrix} A^\top P + PA + Q + a\mathbb{I}_{2Nn} & PB \\ B^\top P & -e^{-aT}Q \end{bmatrix} \begin{bmatrix} x \\ x(t-T) \end{bmatrix}.
\end{aligned} \tag{6.66}$$

From here it is obvious that

$$\dot{V} + aV < 0 \Leftarrow \begin{bmatrix} A^\top P + PA + Q + a\mathbb{I}_{2Nn} & PB \\ B^\top P & -e^{-aT}Q \end{bmatrix} < 0. \tag{6.67}$$

As $-e^{-aT}Q < 0$, it follows from Schur Complement Lemma (see Proposition 3.1 in [40]) that (6.67) is equivalent to

$$A^\top P + PA + Q + a\mathbb{I}_{2Nn} + e^{aT}BQ^{-1}B^\top < 0. \tag{6.68}$$

Again according to Schur Complement Lemma and by substituting Q given in (6.64), the condition in (6.68) is equivalent to the following two conditions

$$2A_{22} + (1+a)\mathbb{I}_{Nn} + \frac{1}{k^2}B_{21}B_{21}^\top < 0 \tag{6.69}$$

and

$$\begin{aligned} A_{11}^\top P_0 + P_0 A_{11} + (e^{aT}k^2 + a)\mathbb{I}_{Nn} + \frac{1}{k^2}B_{11}B_{11}^\top - \Big(A_{12} + A_{21}^\top + \frac{1}{k^2}B_{11}B_{21}^T\Big) \\ \times \Big(2A_{22} + (1+a)\mathbb{I}_{Nn} + \frac{1}{k^2}B_{21}B_{21}^\top\Big)^{-1}\Big(A_{21} + A_{12}^\top + \frac{1}{k^2}B_{21}B_{11}^\top\Big) < 0. \end{aligned} \tag{6.70}$$

Next, we analyze these two stability conditions:

- Since k^2 is cancelled out in $\frac{1}{k^2}B_{21}B_{21}^\top$, the condition (6.69) can be satisfied by controlling k such that A_{22} is sufficiently negative definite.

- Given such a value of k, all terms in (6.70) are independent of A_m, except for

$$A_{11}^\top P_0 + P_0 A_{11} = -a\mathbb{I}_{Nn} + (D \otimes \mathbb{I}_n)\omega(q)P_0 + P_0\omega(q)(D \otimes \mathbb{I}_n).$$

  Hence, (6.70) can be satisfied with a that is large enough.

Thus, by controlling the values of a and k, it is possible to satisfy (6.67). From the definition of the Lyapunov function in (6.65), we have $\|x\|_2^2 \leq V(x)$. Applying the Gronwall lemma to (6.67) yields

$$\|x\|_2^2 \leq V(x) < V(x(0))\mathrm{e}^{-at}. \tag{6.71}$$

This leads to the exponential stability of the unforced system of (6.42). Consequently, Φ, and hence Φ_{11}, converges to zero exponentially fast. Thus, the map $\mathcal{H}_q$ is exponentially stable and $\|\mathcal{H}_q\|_{\mathcal{L}_1}$ is finite. □

Remark 6.2. *The Lyapunov-Krasovskii functional in* (6.65) *in this section yields alternative conditions for exponential stability of the DDE of interest. However, the condition in* (6.70) *depends on the communication delay T. In addition, when k is increased, the maximum eigenvalue of A_m that satisfies* (6.70) *also increases. As will be seen in later sections, this may lead to a possible conflict with a suitably formulated stability condition. In such cases, the stability of the proposed control scheme is not guaranteed. Nonetheless, within certain restriction, it is possible to redesign the controller to remove the conflict. The modification will be discussed in Section 6.8.*

6.6 The stability condition and the bound on the collective reference system

Define a linear map $\mathcal{D}_q[\cdot] \triangleq \mathcal{M}_q \circ \mathcal{F}_q[\cdot]$. By substituting (6.29) in (6.28), we obtain

$$\dot{r}_{\mathrm{ref}} = A_m r_{\mathrm{ref}} + \omega(q)\big(\mathcal{F}_q \circ (\mathcal{M}_q - \mathcal{I}) + \mathcal{I}\big)[u_{\mathrm{ref}}^{sync}] + (\mathcal{D}_q + \mathcal{I})[\eta_{\mathrm{ref}}], \tag{6.72}$$

which has the form of (6.39). As defined in (6.43), $\mathcal{H}_q$ is the input-output map from $(\mathcal{D}_q + \mathcal{I})[\eta_{\mathrm{ref}}]$ to r_{ref} in (6.72), with u_{ref}^{sync} given in (6.30). Suppose A_m satisfy certain delay-independent stability condition (6.55), such that the map $\mathcal{H}_q$ is exponentially stable. We

can now write (6.72) in terms of the map $\mathcal{H}_q$ as follows (cf. (6.44))

$$r_{\text{ref}} = \mathcal{H}_q \circ (\mathcal{D}_q + \mathcal{I})[\eta_{\text{ref}}] + \bar{r}(t, r_0), \tag{6.73}$$

where $\bar{r}(t, r_0)$, defined in (6.38), is exponentially decaying.

Let $u^{\eta}_{\text{ref}} = \mathcal{F}_q[\eta_{\text{ref}}]$, i.e.,

$$\dot{u}^{\eta}_{\text{ref}} = -k\big(\omega(q)u^{\eta}_{\text{ref}} + \eta_{\text{ref}}\big),\ u^{\eta}_{\text{ref}}(0) = 0. \tag{6.74}$$

Define $\mathcal{H}^s_q : y \to \mathcal{H}_q[\dot{y}]$. In the special case where $r_0 = 0$, it follows from (6.73) and (6.74) that

$$\|r_{\text{ref}}\|_{\mathcal{L}_\infty} = \frac{1}{k}\left\|\mathcal{H}_q[\dot{u}^{\eta}_{\text{ref}}]\right\|_{\mathcal{L}_\infty} \leq \frac{1}{k}\|\mathcal{H}^s_q\|_{\mathcal{L}_1}\left\|u^{\eta}_{\text{ref}}\right\|_{\mathcal{L}_\infty}. \tag{6.75}$$

Since the map $\mathcal{H}_q$ is exponentially stable, it follows from Lemma 6.2 that $\mathcal{H}^s_q$ is input-to-state stable and $\|\mathcal{H}^s_q\|_{\mathcal{L}_1}$ is finite. Now let $\eta_u \triangleq \big(\omega(q) - \mathbb{I}_{Nn}\big)u^{\eta}_{\text{ref}} + \eta_{\text{ref}}$. Writing (6.74) in the Laplace domain leads to

$$\|u^{\eta}_{\text{ref}}\|_{\mathcal{L}_\infty} = \left\|\frac{k}{s+k}\eta_u(s)\right\|_{\mathcal{L}_\infty} \leq \|\eta_u\|_{\mathcal{L}_\infty}. \tag{6.76}$$

From (6.75), (6.76) and the definition of u^{η}_{ref} and η_u, we obtain

$$\|r_{\text{ref}}\|_{\mathcal{L}_\infty} \leq \frac{1}{k}\|\mathcal{H}^s_q\|_{\mathcal{L}_1}\big((\omega_h + 1)b_{\mathcal{F}} + 1\big)\left\|\eta_{\text{ref}}\right\|_{\mathcal{L}_\infty}. \tag{6.77}$$

Let

$$b_1 \triangleq \sup_q \left\|\mathcal{H}_q \circ \big(\mathcal{D}_q + \mathcal{I}\big)\right\|_{\mathcal{L}_1}. \tag{6.78}$$

It follows from (6.73) and (6.77) that

$$b_1 \leq \frac{1}{k}\|\mathcal{H}_q^s\|_{\mathcal{L}_1}\big((\omega_h+1)b_{\mathcal{F}}+1\big). \tag{6.79}$$

Since $b_1 \to 0$ as $k \to \infty$, it follows that there exists a K, such that the *stability condition*

$$b_1 < \frac{\rho_{\text{ref}} - \rho_{\text{ic}}}{\rho_{\text{ref}} L + Z} \tag{6.80}$$

is satisfied for some $\rho_{\text{ref}} > \rho_{\text{ic}}$ provided that $k > K$. Here, $\rho_{\text{ic}} \triangleq \|\bar{r}(t, r_0)\|_{\mathcal{L}_\infty}$ is bounded since $\bar{r}(t, r_0)$ is an exponentially decaying function,

$$L \triangleq \frac{\bar{\rho}}{\rho_{\text{ref}}} \max_i\{d_i(\bar{\rho})\}, \text{ and } Z \triangleq \max_i\{Z_i\}, \tag{6.81}$$

where $d_i(\cdot)$ is defined in (6.9), Z_i is the bound on $\|\eta_i(t,0)\|_\infty$, and

$$\bar{\rho} \triangleq \rho_{\text{ref}} + 1 + \bar{q}. \tag{6.82}$$

Here, $\bar{q}$ is a constant that satisfies

$$\|\zeta_{\text{ref}}\|_{\mathcal{L}_\infty} \leq \|r_{\text{ref}}\|_{\mathcal{L}_\infty} + \bar{q}, \tag{6.83}$$

which depends on the a priori bounds on q_p, $\dot{q}_p$ and $\ddot{q}_p$. Its existence is verified below.

Lemma 6.4. *Suppose that q_p, $\dot{q}_p$ and $\ddot{q}_p$ are bounded trajectories. Then there exists $\bar{q}$ such that*

$$\|\zeta\|_{\mathcal{L}_\infty} \leq \|r\|_{\mathcal{L}_\infty} + \bar{q}, \tag{6.84}$$

where $\zeta^\top = [r^\top, \chi^\top]$, $r^\top = [r_1^\top, ..., r_N^\top]$, $\chi^\top = [q_a, q_p^\top, \dot{q}_p^\top, \ddot{q}_p^\top]$, and $q_a^\top = [q_{a,1}^\top, ..., q_{a,N}^\top]$.

Proof. The collective form of (6.2) is

$$
\begin{aligned}
r &= (\dot{q}_a - \mathbf{1}_N \otimes \dot{q}_d) + (q_a - \mathbf{1}_N \otimes q_d) \\
\Rightarrow q_a(s) &= (s+1)^{-1}\Big(r(s) + \mathbf{1}_N \otimes \big(\dot{q}_d(s) + q_d(s)\big) + q_a(0)\Big) \qquad (6.85) \\
\Rightarrow \|q_a\|_{\mathcal{L}_\infty} &\leq \|r\|_{\mathcal{L}_\infty} + \underbrace{\Big\|\Big(\mathbf{1}_N \otimes \big(\dot{q}_d(s) + q_d(s)\big) + q_a(0)\Big)\Big\|_{\mathcal{L}_\infty}}_{\bar{Q}}. \qquad (6.86)
\end{aligned}
$$

It follows that

$$
\begin{aligned}
\|\chi\|_{\mathcal{L}_\infty} &\leq \|q_a\|_{\mathcal{L}_\infty} + \max\{\|q_u\|_{\mathcal{L}_\infty}, \|\dot{q}_u\|_{\mathcal{L}_\infty}, \|\ddot{q}_u\|_{\mathcal{L}_\infty}\} \\
&\leq \|r\|_{\mathcal{L}_\infty} + \underbrace{\bar{Q} + \max\{\|q_p\|_{\mathcal{L}_\infty}, \|\dot{q}_p\|_{\mathcal{L}_\infty}, \|\ddot{q}_p\|_{\mathcal{L}_\infty}\}}_{\bar{q}}. \qquad (6.87)
\end{aligned}
$$

Hence,

$$
\|\zeta\|_{\mathcal{L}_\infty} \leq \max\{\|r\|_{\mathcal{L}_\infty}, \|\chi\|_{\mathcal{L}_\infty}\} \leq \max\{\|r\|_{\mathcal{L}_\infty}, \|r\|_{\mathcal{L}_\infty} + \bar{q}\} = \|r\|_{\mathcal{L}_\infty} + \bar{q}. \qquad (6.88)
$$

Note here that the same inequality relationship in (6.84) applies to $\|\zeta\|_{\mathcal{L}_\infty}$ and $\|r_{\text{ref}}\|_{\mathcal{L}_\infty}$. □

Remark 6.3. *In the stability condition* (6.80)*, larger* $\|A_m\|_\infty$ *leads to a larger* L*, which requires a larger* k *such that* (6.80) *is satisfied. As discussed in Section 6.5.3, which presents a method that employs a Lyapunov-Razumikhin function, the delay-independent exponential stability condition in* (6.55) *for the map* $\mathcal{H}_q$ *depends only on* A_m*. Therefore, for a given* A_m*, if* k *is large enough, both conditions* (6.80) *and* (6.55) *are guaranteed to be satisfied.*

In contrast, in the stability condition (6.70) *obtained via a Lyapunov-Krasovskii functional, a larger* k *required a larger* $\|A_m\|_\infty$ *such that the linear-matrix inequality* (6.67) *is satisfied. Hence for a given* A_m*, it is possible that all values of* k *that are large enough to satisfy* (6.80) *do not satisfy* (6.70)*. In such cases, the stability of the adaptive control system is not guaranteed. Nonetheless, in a later section in this chapter, we will show that it is possible to avoid this conflict between the stability conditions by removing the dependence of* η*, and*

hence L, on A_m, albeit by restricting $A_{m,i}$ to the form $a\mathbb{I}$.

Bounds on the state, r_{ref}, and control input, u_{ref}, of the reference system are claimed by the following theorem.

Theorem 6.1. *Suppose k and A_m satisfy the stability conditions in* (6.55) *and* (6.80) *for some $\rho_{\text{ref}} > \rho_{ic}$. Then $\|r_{\text{ref}}\|_{\mathcal{L}_\infty} < \rho_{\text{ref}}$ and $\|u_{\text{ref}}\|_{\mathcal{L}_\infty} < \infty$, independently of the communication delay T.*

Proof. Suppose that $\|r_{\text{ref}}\|_{\mathcal{L}_\infty} \geq \rho_{\text{ref}}$. Then $\|r_0\|_\infty < \rho_{\text{ref}}$ implies that there exists a τ, such that

$$\|r_{\text{ref}}\|_\infty < \rho_{\text{ref}}, \quad \forall t \in [0, \tau), \quad \text{and} \quad \|r_{\text{ref},\tau}\|_{\mathcal{L}_\infty} \quad = \|r_{\text{ref}}(\tau)\|_\infty = \rho_{\text{ref}}. \tag{6.89}$$

Therefore,

$$\|\zeta_{\text{ref},\tau}\|_{\mathcal{L}_\infty} \leq \rho_{\text{ref}} + \bar{q} < \rho_{\text{ref}} + 1 + \bar{q} = \bar{\rho}. \tag{6.90}$$

Now, the property of η_i in (6.9) implies

$$\begin{aligned} &\|\eta_{ref,i}\|_{\mathcal{L}_\infty} \leq \|\big(\eta_i(t, \zeta_{ref,i}(t)) - \eta_i(t,0)\big)\|_{\mathcal{L}_\infty} + \|\eta_i(t,0)\|_{\mathcal{L}_\infty} \leq \|\zeta_{ref,i}\|_{\mathcal{L}_\infty} d_i(\bar{\rho}) + Z_i \\ \Rightarrow\ &\|\eta_{\text{ref}}\|_{\mathcal{L}_\infty} \leq \max_i \{\|\zeta_{ref,i}\|_{\mathcal{L}_\infty} d_i(\bar{\rho}) + Z_i\} \leq \|\zeta_{\text{ref}}\|_{\mathcal{L}_\infty} \max_i \{d_i(\bar{\rho})\} + Z. \end{aligned} \tag{6.91}$$

This together with (6.81) lead to

$$\|\eta_{\text{ref},\tau}\|_{\mathcal{L}_\infty} \leq \bar{\rho} \max_i \{d_i(\bar{\rho})\} + Z = \rho_{\text{ref}} L + Z. \tag{6.92}$$

Using (6.73), (6.80) and (6.92) we obtain

$$\|r_{\text{ref},\tau}\|_{\mathcal{L}_\infty} \leq \|\mathcal{H}_q \circ (\mathcal{D}_q + \mathcal{I})\|_{\mathcal{L}_1} \|\eta_\tau\|_{\mathcal{L}_\infty} + \|\bar{r}(t, r_0)\|_{\mathcal{L}_\infty} \leq b_1(\rho_{\text{ref}} L + Z) + \rho_{\text{ic}} < \rho_{\text{ref}}, \tag{6.93}$$

contradicting the equality in (6.89). Thus $\|r_{\text{ref}}\|_{\mathcal{L}_\infty} < \rho_{\text{ref}}$. The claim that $\|u_{\text{ref}}\|_{\mathcal{L}_\infty} < \infty$

immediately follows by applying this result to (6.29). □

From (6.73) and (6.79), it follows that

$$\|r_{\text{ref}}(t) - \bar{r}(t, r_0)\|_{\mathcal{L}_\infty} = \mathcal{O}\left(k^{-1}\right). \tag{6.94}$$

We obtain the following lemma

Lemma 6.5. *The response of the collective reference system, r_{ref}, converges to $\bar{r}(t, r_0)$ when $k \to \infty$.*

It follows from (6.38) that if Φ converges to zero exponentially fast then $\lim_{t\to\infty} \bar{r}(t, r_0) = 0$. Hence, Lemma 6.5 implies that the response of the nonadaptive reference system will converge to a neighborhood of 0 exponentially fast. The size of the neighborhood is inversely proportional to the filter bandwidth k.

6.7 Transient performance bounds

The following theorem shows that the collective state and control input of the proposed control system governed by (6.7), (6.13), (6.19), (6.20), (6.21), (6.22), (6.23) and (6.24) follow those of the nonadaptive reference system in (6.28)-(6.30) closely. This and Theorem 6.1 imply the stability of the proposed adaptive control system.

Theorem 6.2. *Under the assumptions on k and A_m from Theorem 6.1, for $\nu \ll 1$, there exist θ_b, σ_b and $C > 0$, such that $\|\tilde{r}\|_{\mathcal{L}_\infty} \leq \nu$, and the norms $\|r_{\text{ref}} - r\|_{\mathcal{L}_\infty}$ and $\|u_{\text{ref}} - u\|_{\mathcal{L}_\infty}$ are both $\mathcal{O}(\nu)$, independently of the communication delay T, provided that $\Gamma\nu^2 \geq C$.*

Proof. Suppose that $\nu > 0$ is given. Let $\rho_{u,ref}$ be the global bound on u_{ref} which is finite according to Theorem 6.1. Since

$$\|r_{\text{ref}}(0) - r(0)\|_\infty = 0 < 1 \text{ and } \|u_{\text{ref}}(0) - u(0)\|_\infty = 0 < 1, \tag{6.95}$$

it follows by continuity that there exists a $\tau > 0$, such that $\|(r_{\text{ref}} - r)_\tau\|_{\mathcal{L}_\infty} < 1$ and $\|(u_{\text{ref}} - u)_\tau\|_{\mathcal{L}_\infty} < 1$. Theorem 6.1 implies that

$$\|r_\tau\|_{\mathcal{L}_\infty} < \rho_{\text{ref}} + 1, \quad \|u_\tau\|_{\mathcal{L}_\infty} < \rho_{u,ref} + 1. \tag{6.96}$$

It follows from Lemma A.9.2 in [61] that there are continuous, piecewise-differentiable functions $\theta_i(t) \in \mathbb{R}^n$ and $\sigma_i(t) \in \mathbb{R}^n$ such that

$$\eta_i\big(t, \zeta_i(t)\big) = \theta_i(t)\|r_{i,t}\|_{\mathcal{L}_\infty} + \sigma_i(t),\ t \in [0, \tau]. \tag{6.97}$$

On this interval, $\|\theta_i(t)\|_\infty < \theta_{b,i}$ and $\|\sigma_i(t)\|_\infty < \sigma_{b,i}$, and, within any subinterval of differentiability, $\|\dot{\theta}_i(t)\|_\infty < d_{\theta,i} < \infty$ and $\|\dot{\sigma}_i(t)\|_\infty < d_{\sigma,i} < \infty$. From (6.7), (6.24) and (6.97) we have the estimation error

$$\dot{\tilde{r}}_i = A_{l,i}\tilde{r}_i + \tilde{\eta}_i = A_{l,i}\tilde{r}_i + \tilde{\theta}_i\|r_{i,t}\|_{\mathcal{L}_\infty} + \tilde{\sigma}_i, \tag{6.98}$$

where $\tilde{\eta}_i \triangleq \hat{\eta}_i - \eta_i - \big(\omega_i(q_i) - \mathbb{I}_n\big)u_i$ and $\tilde{\sigma}_i \triangleq \hat{\sigma}_i - \bar{\sigma}_i = \hat{\sigma}_i - \sigma_i - \big(\omega_i(q_i) - \mathbb{I}_n\big)u_i$.

Consider the following Lyapunov function candidate

$$V = \sum_{i=1}^{N}\Big[\tilde{r}_i^\top P_i \tilde{r}_i + \frac{1}{\Gamma}\big(\tilde{\theta}_i^\top\tilde{\theta}_i + \tilde{\sigma}_i^\top\tilde{\sigma}_i\big)\Big]. \tag{6.99}$$

We first find the time derivative of the above function using (6.22), (6.23) and (6.98):

$$\begin{aligned}
\dot{V} &= \sum_{i=1}^{N}\Big[\dot{\tilde{r}}_i^\top P_i\tilde{r}_i + \tilde{r}_i^\top P_i\dot{\tilde{r}}_i + \frac{2}{\Gamma}(\tilde{\theta}_i^\top\dot{\tilde{\theta}}_i + \tilde{\sigma}_i^\top\dot{\tilde{\sigma}}_i)\Big] \\
&= \sum_{i=1}^{N}\Big[(A_{l,i}\tilde{r}_i + \tilde{\theta}_i\|r_i\|_{\mathcal{L}_\infty} + \tilde{\sigma}_i)^\top P_i\tilde{r}_i + \tilde{r}_i^\top P_i(A_{l,i}\tilde{r}_i + \tilde{\theta}_i\|r_i\|_{\mathcal{L}_\infty} + \tilde{\sigma}_i) + \frac{2}{\Gamma}(\tilde{\theta}_i^\top\dot{\tilde{\theta}}_i + \tilde{\sigma}_i^\top\dot{\tilde{\sigma}}_i)\Big] \\
&= -\tilde{r}^\top Q\tilde{r} + \sum_{i=1}^{N}\Big[2\tilde{\theta}_i^\top\|r_i\|_{\mathcal{L}_\infty}P_i\tilde{r}_i + \frac{2}{\Gamma}\tilde{\theta}_i^\top\dot{\tilde{\theta}}_i + 2\tilde{\sigma}_i^\top P_i\tilde{r}_i + \frac{2}{\Gamma}\tilde{\sigma}_i^\top\dot{\tilde{\sigma}}_i\Big].
\end{aligned} \tag{6.100}$$

From the properties the projection operator, we have

$$2\tilde{\theta}_i^\top \|r_{i,\tau}\|_{\mathcal{L}_\infty} P_i \tilde{r}_i + \frac{2}{\Gamma}\tilde{\theta}_i^\top \dot{\hat{\theta}}_i = 2\tilde{\theta}_i^\top P_i \tilde{r}_i \|r_i\|_{\mathcal{L}_\infty} + \frac{2}{\Gamma}\tilde{\theta}_i^\top \Gamma \mathbf{Proj}(\hat{\theta}_i, -P_i\tilde{r}_i\|r_i\|_{\mathcal{L}_\infty}; \theta_b, \varepsilon)$$
$$= 2\tilde{\theta}_i^\top \big(P_i \tilde{r}_i \|r_i\|_{\mathcal{L}_\infty} + \mathbf{Proj}(\hat{\theta}_i, -P_i\tilde{r}_i\|r_i\|_{\mathcal{L}_\infty}; \theta_b, \varepsilon)\big) \leq 0, \quad (6.101)$$

$$2\tilde{\sigma}_i^\top P_i \tilde{r}_i + \frac{2}{\Gamma}\tilde{\sigma}_i^\top \dot{\hat{\sigma}}_i = 2\tilde{\sigma}_i^\top P_i \tilde{r}_i + \frac{2}{\Gamma}\tilde{\sigma}_i^\top \Gamma \mathbf{Proj}(\hat{\sigma}_i, -P_i\tilde{r}_i; \sigma_b, \varepsilon)$$
$$= 2\tilde{\sigma}_i^\top \big(P_i \tilde{r}_i + \mathbf{Proj}(\hat{\sigma}_i, -P_i\tilde{r}_i; \sigma_b, \varepsilon)\big) \leq 0. \quad (6.102)$$

Therefore,

$$\dot{V} \leq -\tilde{r}^\top Q \tilde{r} + \frac{2}{\Gamma}\sum_{i=1}^{N} \big|\tilde{\theta}_i^\top \dot{\theta}_i + \tilde{\sigma}_i^\top \dot{\tilde{\sigma}}_i\big|. \quad (6.103)$$

Note that $\bar{\sigma}_i = \sigma_i + \big(\omega_i(q_i) - \mathbb{I}_n\big)u_i$ is bounded by some constant $\bar{\sigma}_b$ because all the terms in its expression are bounded. Moreover,

$$\dot{\tilde{\sigma}}_i = \dot{\sigma}_i + \big(\omega_i(q_i) - \mathbb{I}_n\big)\dot{u} + \dot{\omega}(q)u. \quad (6.104)$$

Since $r(t)$ and $u(t)$ is bounded as in (6.96), taking into account (6.2), (6.7), (6.19), (6.13) and (6.20), we have $\dot{r}$, $\dot{\omega}$ and hence $\dot{u}$ are bounded. Hence, $\dot{\tilde{\sigma}}$ is bounded, meaning there exists a bounding constant $d_{\bar{\sigma}}$ such that $\|\dot{\tilde{\sigma}}\|_\infty \leq d_{\bar{\sigma}}$. Note here that $\bar{\sigma}_b$ and $d_{\bar{\sigma}}$ are dependent on ρ_{ref} and $\rho_{u,ref}$, but independent of τ.

We have

$$V(0) \leq \frac{4}{\Gamma}\sum_{i=1}^{N}(\theta_{b,i}^2 + \bar{\sigma}_{b,i}^2) < \frac{\nu_m}{\Gamma}, \quad (6.105)$$

where $\nu_m \triangleq 4\sum_{i=1}^{N}\big(\theta_{b,i}^2 + \bar{\sigma}_{b,i}^2\big) + 4\frac{\lambda_{\max}(P)}{\lambda_{\min}(Q)}\sum_{i=1}^{N}(\theta_{b,i}d_{\theta,i} + \bar{\sigma}_{b,i}d_{\bar{\sigma},i})$. We now show by contradiction

that

$$V(t) \leq \frac{\nu_m}{\Gamma}, \quad \forall t \in [0, \tau]. \tag{6.106}$$

To this end, choose $t_1 \in [0, \tau]$ such that both $\dot{\theta}(t)$ and $\dot{\sigma}(t)$ are continuous in $[0, t_1)$. It follows from (6.103) that

$$\dot{V} \leq -\|\tilde{r}\|_\infty^2 \lambda_{\min}(Q) + \frac{4}{\Gamma} \sum_{i=1}^{N} \big(\theta_{b,i} d_{\theta,i} + \bar{\sigma}_{b,i} d_{\bar{\sigma},i}\big), \tag{6.107}$$

for all $t \in [0, t_1)$. Taking (6.105) into account, if (6.106) does not hold for all $t \in [0, t_1)$, then there exists a $\bar{t} \in [0, t_1)$ such that $V(\bar{t}) > \frac{\nu_m}{\Gamma}$ and $\dot{V}$ is a non-decreasing function, i.e. $\dot{V}(\bar{t}) \geq 0$. It follows from (6.99) that

$$\frac{\nu_m}{\Gamma} < V(\bar{t}) \leq \|\tilde{r}(\bar{t})\|_\infty^2 \lambda_{\max}(P) + \frac{4}{\Gamma} \sum_{i=1}^{N} \big(\theta_{b,i}^2 + \bar{\sigma}_{b,i}^2\big).$$

This means

$$\frac{4}{\Gamma} \sum_{i=1}^{N} \big(\theta_{b,i}^2 + \bar{\sigma}_{b,i}^2\big) + \frac{4}{\Gamma} \frac{\lambda_{\max}(P)}{\lambda_{\min}(Q)} \sum_{i=1}^{N} (\theta_{b,i} d_{\theta,i} + \bar{\sigma}_{b,i} d_{\bar{\sigma},i}) < \|\tilde{r}(\bar{t})\|_\infty^2 \lambda_{\max}(P) + \frac{4}{\Gamma} \sum_{i=1}^{N} \big(\theta_{b,i}^2 + \bar{\sigma}_{b,i}^2\big). \tag{6.108}$$

Hence,

$$\|\tilde{r}(\bar{t})\|_\infty^2 > \frac{4}{\Gamma \lambda_{\min}(Q)} \sum_{i=1}^{N} \big(\theta_{b,i} d_{\theta,i} + \bar{\sigma}_{b,i} d_{\bar{\sigma},i}\big). \tag{6.109}$$

By substituting (6.109) in (6.107) we have $\dot{V}(\bar{t}) < 0$, which contradicts the statement that $\dot{V}(\bar{t}) \geq 0$. Thus, $V(t) \leq \frac{\nu_m}{\Gamma}$ for all $t \in [0, t_1)$. Since $V(t)$ is a continuous function, $V(t) \leq \frac{\nu_m}{\Gamma}$

for all $t \in [0, t_1]$. This together with (6.99) imply

$$\|\tilde{r}_\tau\|_{\mathcal{L}_\infty} \leq \sqrt{\frac{\nu_m}{\lambda_{\min}(P)\Gamma}}, \quad \forall t \in [0, t_1]. \tag{6.110}$$

By repeating this process with the next time instants at which a discontinuity of either $\dot{\theta}(t)$ or $\dot{\sigma}(t)$ occurs, we obtain the conclusion that the inequality in (6.110) holds for all $t \in [0, \tau]$. Thus, there exists a $C > 0$ (independent of τ), such that

$$\|\tilde{r}_\tau\|_{\mathcal{L}_\infty} \leq \sqrt{C/\Gamma}, \tag{6.111}$$

which does not exceed ν provided that $\Gamma\nu^2 \geq C$.

Let $\zeta^\top \triangleq \left[r^\top, \chi^\top\right]$, and $\chi^\top \triangleq \left[q_a^\top, q_p^\top, \dot{q}_p^\top\right]$. From the definition of ζ_{ref} and ζ, we have

$$\begin{aligned} \|(\zeta_{\text{ref}} - \zeta)_\tau\|_{\mathcal{L}_\infty} &\leq \max\{\|r_{\text{ref}} - r\|_{\mathcal{L}_\infty}, \|\chi_{\text{ref}} - \chi\|_{\mathcal{L}_\infty}\} \\ &\leq \max\{\|r_{\text{ref}} - r\|_{\mathcal{L}_\infty}, \|q_{\text{a,ref}} - q_a\|_{\mathcal{L}_\infty}\} \leq \|(r_{\text{ref}} - r)_\tau\|_{\mathcal{L}_\infty} \end{aligned} \tag{6.112}$$

where the last inequality comes from the fact that $q_{\text{a,ref}}(s) - q_a(s) = (s+1)^{-1}\big(r_{\text{ref}}(s) - r(s)\big)$, which follows from (6.85).

Similar to (6.91), equations (6.9), (6.81), (6.82) and (6.112) lead to

$$\begin{aligned} \|(\eta_{\text{ref}} - \eta)_\tau\|_{\mathcal{L}_\infty} &\leq \max_i \left\{d_i(\bar{\rho})\right\} \|(\zeta_{\text{ref}} - \zeta)_\tau\|_{\mathcal{L}_\infty} \leq \max_i \left\{d_i(\bar{\rho})\right\} \|(r_{\text{ref}} - r)_\tau\|_{\mathcal{L}_\infty} \\ &< L\|(r_{\text{ref}} - r)_\tau\|_{\mathcal{L}_\infty}. \end{aligned} \tag{6.113}$$

It follows from (6.20), (6.24) and (6.74) that

$$\begin{aligned}
\dot{u}^{\eta}_{\rm ref} - \dot{u}^{ad} &= -k\big(\omega(q)u^{\eta}_{\rm ref} + \eta^{ref} - u^{ad} - \hat{\eta}\big) \\
&= -k\big(\omega(q)(u^{\eta}_{\rm ref} - u^{ad}) + \omega(q)u^{ad} - u^{ad} + \eta - \hat{\eta} + \eta^{ref} - \eta\big) \\
&= -k\big(\omega(q)(u^{\eta}_{\rm ref} - u^{ad}) + \underbrace{\omega(q)u - u + \eta - \hat{\eta}}_{-\tilde{\eta}} + \eta^{ref} - \eta - \omega(q)u^{sync} + u^{sync}\big) \\
&= -k\big(\omega(q)(u^{\eta}_{\rm ref} - u^{ad}) - \tilde{\eta} + \eta^{ref} - \eta - \omega(q)u^{sync} + u^{sync}\big). \qquad (6.114)
\end{aligned}$$

Taking into account the definition of the input-output map $\mathcal{F}_q$ and the estimation error equation in (6.98), we obtain

$$\begin{aligned}
u^{\eta}_{\rm ref} - u^{ad} &= \mathcal{F}_q\big[\eta_{\rm ref} - \eta\big] - \mathcal{F}_q\big[\dot{\tilde{r}} - A_l\tilde{r}\big] - \mathcal{F}_q\big[\omega(q)u^{sync} - u^{sync}\big] \\
&= \mathcal{F}_q[\eta_{\rm ref} - \eta] + \big(\mathcal{F}_q \circ \mathcal{A}_l + k(\mathcal{F}_q \circ \mathcal{M}_q + \mathcal{I})\big)[\tilde{r}] - \mathcal{F}_q \circ (\mathcal{M}_q - \mathcal{I})[u^{sync}]. \qquad (6.115)
\end{aligned}$$

The difference between (6.19) and (6.29) gives:

$$\begin{aligned}
u_{\rm ref} - u &= (u^{\eta}_{\rm ref} - u^{ad}) + \big(\mathcal{F}_q \circ (\mathcal{M}_q - \mathcal{I}) + \mathcal{I}\big)[u^{sync}_{\rm ref}] - u^{sync} \\
&= \mathcal{F}_q[\eta_{\rm ref} - \eta] + \big(\mathcal{F}_q \circ \mathcal{A}_l + k(\mathcal{F}_q \circ \mathcal{M}_q + \mathcal{I})\big)[\tilde{r}] \\
&\quad + \big(\mathcal{F}_q \circ (\mathcal{M}_q - \mathcal{I}) + \mathcal{I}\big)[u^{sync}_{\rm ref} - u^{sync}]. \qquad (6.116)
\end{aligned}$$

Equations (6.7), (6.28) and (6.116) then imply that

$$\begin{aligned}
\dot{r}_{\rm ref} - \dot{r} &= A_m(r_{\rm ref} - r) + \omega(q)(u_{\rm ref} - u) + \eta_{\rm ref} - \eta \\
&= A_m(r_{\rm ref} - r) + \omega(q)\big(\mathcal{F}_q \circ (\mathcal{M}_q - \mathcal{I}) + \mathcal{I}\big)[u^{sync}_{\rm ref} - u^{sync}] \\
&\quad + (\mathcal{D}_q + \mathcal{I})[\eta_{\rm ref} - \eta] + \big(\mathcal{D}_q \circ \mathcal{A}_l + k(\mathcal{D}_q + \mathcal{I}) \circ \mathcal{M}_q\big)[\tilde{r}]. \qquad (6.117)
\end{aligned}$$

This and the definitions of u^{sync} in (6.14), u_{ref}^{sync} in (6.30), and the map $\mathcal{H}_q$ in (6.72) lead to

$$r_{\text{ref}} - r = \mathcal{H}_q \circ (\mathcal{D}_q + \mathcal{I})[\eta_{\text{ref}} - \eta] + \mathcal{H}_q \circ \big(\mathcal{D}_q \circ \mathcal{A}_l + k(\mathcal{D}_q + \mathcal{I}) \circ \mathcal{M}_q\big)[\tilde{r}]. \tag{6.118}$$

Hence, taking into account (6.113), we obtain

$$\begin{aligned}
&\|r_{\text{ref}} - r\|_{\mathcal{L}_\infty} \\
&\quad \leq \|\mathcal{H}_q \circ (\mathcal{D}_q + \mathcal{I})\|_{\mathcal{L}_1} \|\eta_{\text{ref}} - \eta\|_{\mathcal{L}_\infty} + \|\mathcal{H}_q \circ \big(\mathcal{D}_q \circ \mathcal{A}_l + k(\mathcal{D}_q + \mathcal{I}) \circ \mathcal{M}_q\big)\|_{\mathcal{L}_1} \|\tilde{r}\|_{\mathcal{L}_\infty} \\
&\quad \leq b_1 L \|r_{\text{ref}} - r\|_{\mathcal{L}_\infty} + b_2 \|\tilde{r}\|_{\mathcal{L}_\infty},
\end{aligned} \tag{6.119}$$

where $b_2 \triangleq \|\mathcal{H}_q \circ \big(\mathcal{D}_q \circ \mathcal{A}_l + k(\mathcal{D}_q + \mathcal{I}) \circ \mathcal{M}_q\big)\|_{\mathcal{L}_1}$. It follows from the stability condition in (6.80) that $b_1 L < 1$. Hence, solving for $\|r_{\text{ref}} - r\|_{\mathcal{L}_\infty}$ in (6.119) results in

$$\|r_{\text{ref}} - r\|_{\mathcal{L}_\infty} \leq \frac{b_2}{1 - b_1 L} \nu. \tag{6.120}$$

Similarly, the expression in (6.116) yields

$$\|u_{\text{ref}} - u\|_{\mathcal{L}_\infty} \leq b_3 \|r_{\text{ref}} - r\|_{\mathcal{L}_\infty} + b_4 \|\tilde{r}\|_{\mathcal{L}_\infty} \leq \Big(\frac{b_2 b_3}{1 - b_1 L} + b_4\Big)\nu \tag{6.121}$$

with $b_3 = b_{\mathcal{F}} L + \|\big(\mathcal{F}_q \circ (\mathcal{M}_q - \mathcal{I}) + \mathcal{I}\big)\|_{\mathcal{L}_1} \big(\|A_d \otimes \mathbb{I}_n\| + \|D \otimes \mathbb{I}_n\|\big)$ and $b_4 = \|\mathcal{F}_q \circ \mathcal{A}_l + k(\mathcal{F}_q \circ \mathcal{M}_q + \mathcal{I})\|_{\mathcal{L}_1}$. The claim follows by choosing ν and Γ such that the right-hand side of (6.120) is strictly less than 1. □

Here, the bound on $\tilde{r}$ implies that the size of the estimation error can be made arbitrarily small by increasing the adaptive gain. The bounds on $r_{\text{ref}} - r$ and $u_{\text{ref}} - u$ indicate that at high adaptive gain, the proposed control network and its control signals behave almost identically to the nonadaptive reference system and its control signal, respectively. In addition, the control inputs only contain low-frequency signals, since all high-frequency components that may be induced by the high adaptive gains are blocked by the low-pass filters. Thus, the use

of high values of the adaptive gains significantly improves adaptation, while guaranteeing bounded deviation from a nonadaptive reference system. Furthermore, since r_{ref} converges to a neighborhood of zero, so does r. The size of the neighborhood is inversely proportional to the filter bandwidth k. Consequently, the joint angles of the manipulators synchronize while tracking the common desired trajectories.

6.8 Alternate controller design

As discussed in Remark 6.3 at the end of Section 6.6, the use of a Lyapunov-Krasovskii functional results in a condition for A_m and k in (6.70) for exponential stability of the map $\mathcal{H}_q$. However, (6.70) and (6.80) are mutually exclusive, i.e., no combination k and A_m satisfies both conditions. This can be traced back to the dependence of η on A_m.

In this section, we discuss an alternative design of the control input such that $A_{m,i}r_i$ is actively generated by the control input, as opposed to $A_{m,i}r_i$ being part of η_i. Substitution of the first equation in (6.1) into the time derivative of (6.2) yields

$$\dot{r}_i = \underbrace{M_{ai}^{-1}(q_i)}_{\omega_i(q_i)} u_i + \underbrace{M_{ai}^{-1}(q_i)\big(- M_{pi}(q_i)\ddot{q}_p - N_{ai}(q_i,\dot{q}_i) + D_{ai}\big) - \ddot{q}_d + r_i + \dot{q}_d - q_{a,i} + q_d - \dot{q}_d}_{\eta_i}, \tag{6.122}$$

where η_i no longer depends on $A_{m,i}$. Consider the control input

$$u_i = A_{m,i}r_i + u_i^{ad} + u_i^{sync}. \tag{6.123}$$

It is obvious that $A_{m,i}r_i$ is now actively generated by the control input u_i of each robot. The other control components remain unchanged.

The reference system is then re-designed to reflect this change as follows

$$\dot{r}_{\rm ref} = \omega(q)u_{\rm ref} + \eta_{\rm ref}, \quad r_{\rm ref}(t) = r_0 \ \forall t \in [-T, 0] \tag{6.124}$$

$$u_{\rm ref} = A_m r_{\rm ref} + \mathcal{F}_q[\eta_{\rm ref}] + \big(\mathcal{F}_q \circ (\mathcal{M}_q - \mathcal{I}) + \mathcal{I}\big)[u_{\rm ref}^{sync}], \quad u_{\rm ref}(0) = 0 \tag{6.125}$$

where $\dot{q}_{\rm a,ref}$ and $u_{\rm ref}^{sync}(t)$ are governed by (6.27) and (6.30). Substitution of (6.125) into (6.124) yields

$$\dot{r}_{\rm ref} = A_\omega(q)z + \omega(q)\big(\mathcal{F}_q \circ (\mathcal{M}_q - \mathcal{I}) + \mathcal{I}\big)[u_{\rm ref}^{sync}] + (\mathcal{D}_q + \mathcal{I})[\eta_{\rm ref}], \tag{6.126}$$

where $A_\omega(q) \triangleq \omega(q)A_m$. Notice that if we replace $A_\omega(q)$ by A_m in (6.126) then (6.126) has the same form as (6.39) with $y = (\mathcal{D}_q + \mathcal{I})[\eta_{\rm ref}]$. The map $\mathcal{H}_q$ is then defined by (6.43), where Φ_{11} is the corresponding component of the fundamental solution matrix of the equation obtained by replacing A_m by $A_\omega(q)$ in (6.42). By using the Lyapunov-Krasovskii functional in (6.65), with $P = \mathbb{I}$ and the same Q, and performing the same analysis that follows, we arrive at the two stability conditions in (6.69) and (6.70). The inequality in (6.69) implies the same condition on k as before. The difference is that in (6.70),

$$A_{11}^\top + A_{11} = A_\omega^\top(q) + A_\omega(q) + (D \otimes \mathbb{I}_n)\omega(q) + \omega(q)(D \otimes \mathbb{I}_n).$$

The challenge now is how to make $A_\omega^\top(q) + A_\omega(q)$ sufficiently negative definite to satisfy (6.70) by changing A_m. Note that the sum of a Hurwitz matrix and its transpose may have positive eigenvalues. With the choice of $A_m = \text{diag}[a_i \otimes \mathbb{I}_n]$, the matrix $A_\omega(q) \triangleq \omega(q)\text{diag}[a_i \otimes \mathbb{I}_n]$ is symmetric, i.e.

$$A_\omega^\top(q) + A_\omega(q) = 2\omega(q)\text{diag}[a_i \otimes \mathbb{I}_n]. \tag{6.127}$$

In this case, by designing a_i more negative, we make $A_\omega^\top(q) + A_\omega(q)$ more negative definite,

and eventually satisfy (6.70). Since there is no other stability condition that involve both A_m and k, there is no potential conflict in this design. The rest of the analysis follows accordingly.

The main limitation of this controller design is that $A_m = \text{diag}[a_i \otimes \mathbb{I}_n]$. This means all degrees of freedom of the i^{th} manipulator have the same base-line feedback a_i.

6.9 Simulation results

We restrict attention in this section to a team of four typical pick-and-place manipulators operating on a ship in a high sea state, sketched in Fig. 6.2. Each manipulator has a 2-DOF shoulder joint at A_i and a 1-DOF elbow joint at B_i. Let $d_{A,i}$ be the displacement of A_i relative to the ship's center of mass along the w_1-direction. The physical parameters and initial conditions are listed in Table 6.1. The links' moment of inertia matrices are computed based on their assumed cylindrical geometry and homogeneous mass distribution.

Table 6.1: Physical parameters and initial conditions

i	$m_{1,2}$	$l_{1,2}$	$q_0^\top$	d_A
1	11, 6, 5.5	0.60, 0.50	[2 -0.2 -2]	-3
2	12, 8, 5	0.55, 0.55	[-2 -0.7 2]	5
3	9, 7.5, 6	0.65, 0.40	[0.4 2 -0.6]	6
4	10, 7, 6.5	0.50, 0.45	[-1 -2 0.9]	-4

The ship motions are assumed to be described by the rolling angle ϕ_p and the displacements x_p and z_p of its center of mass relative to the inertial reference frame along $\mathbf{w}_1$ and $\mathbf{w}_3$, respectively. These motions are unactuated and driven by the unknown influence of surface winds, waves, and ocean currents, here assumed to equal

$$D_{pp}^\top(t) = \left[2.5 \times 10^7 \sin(0.5t)\ 3 \times 10^5 \sin(0.5t)\ -3 \times 10^5 \cos(0.5t)\right].$$

The mass and moment of inertia about the $\mathbf{w}_2$ axis of the platform are modeled as $m_{\text{ship}} =$

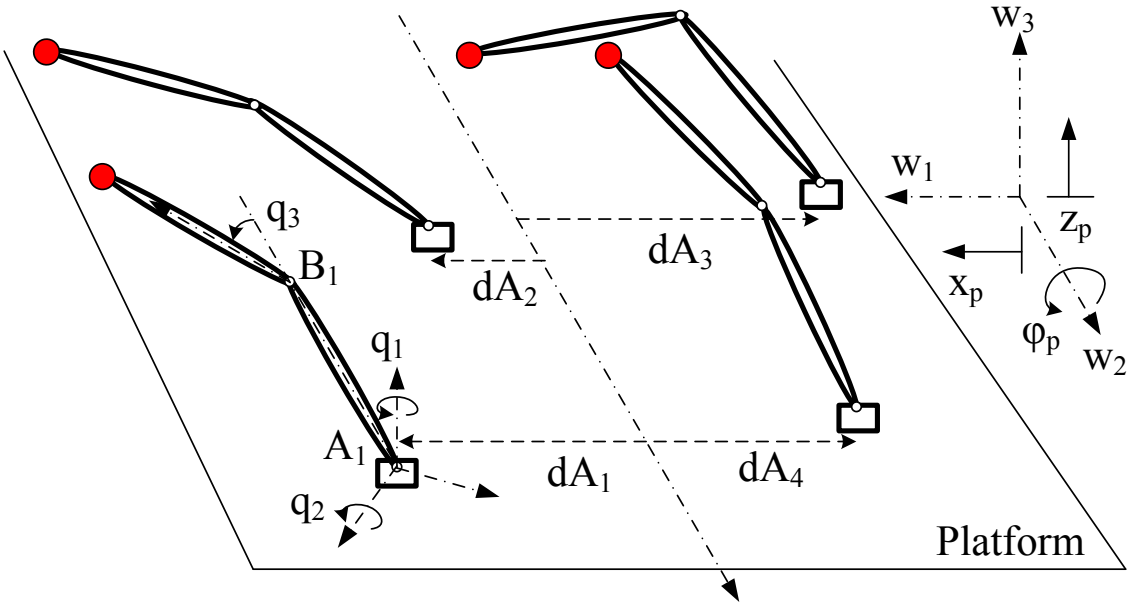

Figure 6.2: A team of 3-DOF manipulators with different configurations mounted on a dynamic platform with uncertain dynamics.

0.9×10^5 and $I_{\text{ship}} = 1.2 \times 10^5$, respectively. We use a linear spring-mass-damper to describe the dynamic interaction between the sea and the ship with effective stiffness and damping coefficient for the corresponding degrees of freedom given by $K_\phi = 10^7$ and $C_\phi = 10^8$, $K_x = 3.2 \times 10^5$, $C_x = 1.8 \times 10^5$, $K_z = 2.8 \times 10^5$ and $C_z = 2.2 \times 10^5$. A typical ship motion can be found in Figure 2.3. The peak-to-peak amplitudes of the ship's displacement are approximately 2 (m) in both the horizontal and vertical directions, and 63 degrees in the rolling angle ϕ_p. These motions contribute large unknown time-varying inertias and nonlinearity to the manipulator dynamics.

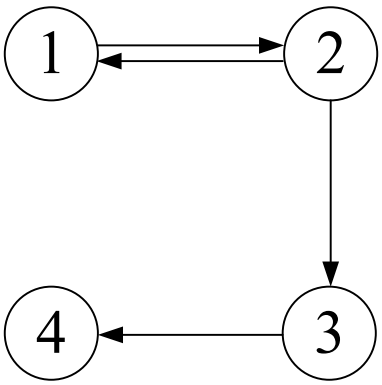

Figure 6.3: A connected graph topology

The network communication topology is depicted in Fig. 6.3(a), which is a simple connected directed graph. To explore the control scheme's robustness to time delay, a *communication delay* of 1 s is introduced in every communication path. The desired trajectory is set to $q_d^\top(t) = [\sin 1.2t \quad \sin 0.8t \quad \cos t]$. The adaptive gain Γ is set to 10^5 and $\lambda = 1$ for all robots. The tracking response characteristics are governed by the design matrices $A_{m,i} = -\text{diag}(15, 20, 10)$. The filter bandwidth is set to 20 (Hz).

Figure 6.4 shows the manipulators' response to the proposed control actuation. As seen in the bottom panel, the control signals are smooth and clean, in spite of the communication delay, as well as the use of high-rate adaptive estimation to accommodate nonlinearity and model uncertainty while retaining small prediction errors. The system responses quickly converge to synchronized trajectories despite the delays and the large inertia and nonlinearity added due to the unmodeled dynamics of the platform. Additional simulation shows that an increase in the filter bandwidth results in improved synchronization performance. However, better tracking is achieved with a trade-off in the system robustness. This is consistent with the theory discussed in this chapter.

6.10 Summary

We have designed an adaptive control scheme for tracking synchronization of a manipulator network operating on a platform, whose dynamics are influenced by environmental factors. The controller is composed of an adaptive part, which is designed along the framework presented in Chapter 2, and a synchronization part. The Razumikhin theorem is used to show the delay-independent stability of the proposed network controller in the presence of communication delays. The Lyapunov-Krasovskii functional offers an alternative analysis method. However, this approach leads to a potential conflict among the stability conditions. A modification to the controller for eliminating this conflict is also presented and discussed. Simulation results demonstrate that the manipulators' joint angles synchronize while tracking

a common desired trajectory despite starting from different initial conditions.

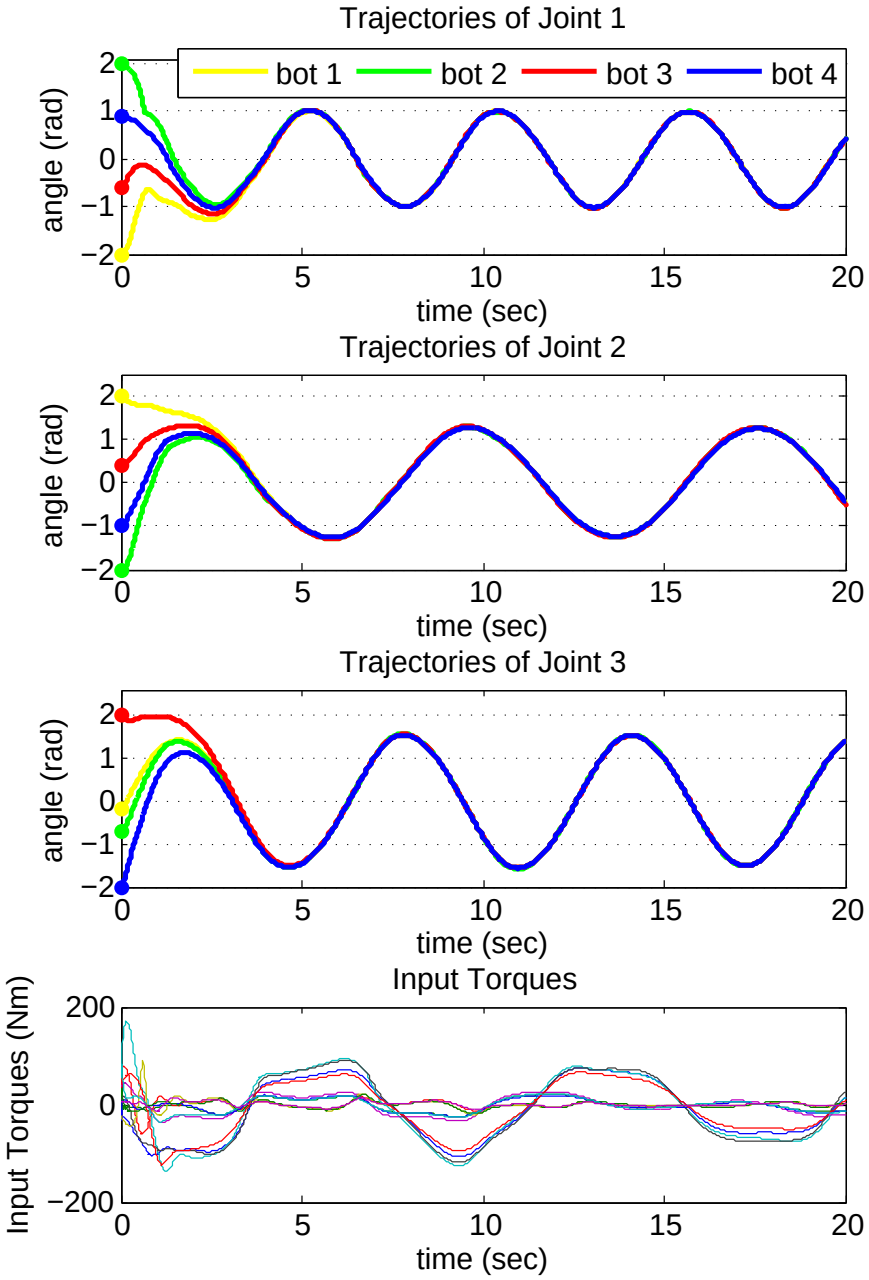

Figure 6.4: Synchronization performance of the proposed controller with a communication delay of 1 s.

CHAPTER 7

CONSENSUS

In this chapter, we propose modifications to the control scheme for tracking synchronization in Chapter 6 to solve a consensus problem for manipulators mounted on a dynamic platform. When there is no desired trajectory, the sliding variable in (6.2) is defined without q_d. The proposed controller in Chapter 6 then drives the manipulators' joint angles to zero. This is the case of zero consensus for identical robots studied in [25]. In this chapter, we redefine the sliding variable to allow the control framework from Chapter 6 to solve a non-trivial consensus problem for non-identical manipulators operating on a dynamic platform which has unmodeled dynamics and unknown environmental disturbances.

Specifically, redefine the kinematic variable as follows:

$$r_i(t) = \dot{q}_{a,i}(t) - \sum_{j \in \mathcal{S}_i} \big(q_{a,j}(t-T) - q_{a,i}(t)\big). \tag{7.1}$$

One of the control objectives is to drive r_i to 0, in which case equation (7.1) becomes a consensus algorithm. As before, the equations of motion are given in (6.7), with identical assumptions on η_i, and with $\zeta_i^\top \triangleq \left[r_i^\top, \chi_i^\top\right]$ and

$$\chi_i^\top(t) = [q_{a,i}^\top(t), ..., q_{a,j}^\top(t-T), ..., \dot{q}_{a,j}^\top(t-T), ..., q_p^\top(t), \dot{q}_p^\top(t), \ddot{q}_p^\top(t)],\ j \in \mathcal{S}_i. \tag{7.2}$$

Next, let the control input $u_i = u_i^{ad}$. The rest of the control components remain identical to (6.20), (6.21) and (6.24), where $\hat{\theta}_i(t)$ and $\hat{\sigma}_i(t)$ are also governed by the identical projection-based laws in (6.22) and (6.23).

7.1 Nonadaptive reference system

Consider the nonadaptive collective reference system

$$\dot{r}_{\rm ref} = A_m r_{\rm ref} + \omega(q) u_{\rm ref} + \eta(t, \zeta_{\rm ref}), \quad r_{\rm ref}(0) = r_0 \tag{7.3}$$

$$\dot{u}_{\rm ref} = -k \left(\omega(q) u_{\rm ref} + \eta\big(t, \zeta_{\rm ref}\big) \right), \quad u_{\rm ref}(0) = 0, \tag{7.4}$$

where $\zeta_{\rm ref}^{\top} = [r_{\rm ref}^{\top}, \chi_{\rm ref}^{\top}]$ with $\chi_{\rm ref}^{\top}(t) = [q_{\rm a,ref}^{\top}(t), q_{\rm a,ref}^{\top}(t-T), \dot{q}_{\rm a,ref}^{\top}(t-T), q_p^{\top}(t), \dot{q}_p^{\top}(t), \ddot{q}_p^{\top}(t)]$. In addition,

$$r_{\rm ref}(t) = \dot{q}_{\rm a,ref}(t) + (D \otimes \mathbb{I}_n) q_{\rm a,ref} - (A_d \otimes \mathbb{I}_n) q_{\rm a,ref}(t-T) \tag{7.5}$$

and $q_{\rm a,ref}(t) = q_a(0), \ \forall t \in [-T, 0]$.

The homogeneous equation of (7.5)

$$\dot{q}_{\rm a,ref}(t) + (D \otimes \mathbb{I}_n) q_{\rm a,ref}(t) - (A_d \otimes \mathbb{I}_n) q_{\rm a,ref}(t-T) = 0, \tag{7.6}$$

where D and A_d denote the degree matrix and the adjacency matrix of the network topology, respectively, has been studied extensively in the literature. In particular, a delay-dependent stability condition based on a linear matrix inequality is derived in [126]. In addition, the consensus of (7.5) can be reached independently of the delay for a strongly connected graph [86, 96, 10], and even for unbounded time-varying delays under certain conditions [79]. Consequently, assuming a strongly connected network, asymptotic stability of the homogeneous system (7.6) to a consensus state is guaranteed. Therefore, it follows from Proposition 2.5 of [116] that the nonhomogeneous linear DDE (7.5) is input-to-state stable. Hence, there exists Q_1 and Q_2, where $Q_2 = 0$ when $q_{\rm a,ref}(0) = 0$, such that (cf. (6.34))

$$\|q_{\rm a,ref}\|_{\mathcal{L}_\infty} \leq Q_1 \|r_{\rm ref}\|_{\mathcal{L}_\infty} + Q_2. \tag{7.7}$$

As in Chapter 6, we assume that q_p, $\dot{q}_p$ and $\ddot{q}_p$ are a priori bounded trajectories. It follows from the definition of χ_{ref} and (7.7) that

$$\begin{aligned}
\|\chi_{\text{ref}}\|_{\mathcal{L}_\infty} &\leq \max\{\|q_{\text{a,ref}}\|_{\mathcal{L}_\infty}, \|q_{\text{a,ref}}(t-T)\|_{\mathcal{L}_\infty}, \|\dot{q}_{\text{a,ref}}(t-T)\|_{\mathcal{L}_\infty}, \|q_p\|_{\mathcal{L}_\infty}, \|\dot{q}_p\|_{\mathcal{L}_\infty}, \|\ddot{q}_p\|_{\mathcal{L}_\infty}\} \\
&\leq \|q_{\text{a,ref}}\|_{\mathcal{L}_\infty} + \|\dot{q}_{\text{a,ref}}\|_{\mathcal{L}_\infty} + \max\{\|q_p\|_{\mathcal{L}_\infty}, \|\dot{q}_p\|_{\mathcal{L}_\infty}, \|\ddot{q}_p\|_{\mathcal{L}_\infty}\} \\
&\leq \big(Q_1\|r_{\text{ref}}\|_{\mathcal{L}_\infty} + Q_2\big) + \max\{\|q_p\|_{\mathcal{L}_\infty}, \|\dot{q}_p\|_{\mathcal{L}_\infty}, \|\ddot{q}_p\|_{\mathcal{L}_\infty}\} \\
&\quad + \|r_{\text{ref}}\|_{\mathcal{L}_\infty} + \Big(\|D\otimes\mathbb{I}_n\| + \|A_d\otimes\mathbb{I}_n\|\Big)\Big(Q_1\|r_{\text{ref}}\|_{\mathcal{L}_\infty} + Q_2\Big) \\
&= \underbrace{\Big(Q_1 + 1 + \big(\|D\otimes\mathbb{I}_n\| + \|A_d\otimes\mathbb{I}_n\|\big)Q_1\Big)}_{R_1}\|r_{\text{ref}}\|_{\mathcal{L}_\infty} \\
&\quad + \underbrace{\big(1 + \|D\otimes\mathbb{I}_n\| + \|A_d\otimes\mathbb{I}_n\|\big)Q_2 + \max\{\|q_p\|_{\mathcal{L}_\infty}, \|\dot{q}_p\|_{\mathcal{L}_\infty}, \|\ddot{q}_p\|_{\mathcal{L}_\infty}\}}_{R_2} \\
&= R_1\|r_{\text{ref}}\|_{\mathcal{L}_\infty} + R_2. \qquad (7.8)
\end{aligned}$$

Hence, we get

$$\|\zeta_{\text{ref}}\|_{\mathcal{L}_\infty} \leq \max\{\|r_{\text{ref}}\|_{\mathcal{L}_\infty}, \|\chi_{\text{ref}}\|_{\mathcal{L}_\infty}\} \leq \max\{\|r_{\text{ref}}\|_{\mathcal{L}_\infty}, R_1\|r_{\text{ref}}\|_{\mathcal{L}_\infty} + R_2\}. \qquad (7.9)$$

Let $\mathcal{I}$ be the identity map and $\mathcal{H}$ be the linear input-output map corresponding to the transfer function $(s\mathbb{I}_{Nn} - A_m)^{-1}$. It follows that

$$r_{\text{ref}}(t) = \big(\mathcal{H}\circ(\mathcal{I}+\mathcal{D}_q)\big)[\eta(t,\zeta_{\text{ref}}(t))] + \mathcal{H}[r(0)\delta(t)], \qquad (7.10)$$

where $b_1 \triangleq \sup_q \|\mathcal{H}\circ(\mathcal{I}+\mathcal{D}_q)\|_{\mathcal{L}_1} < \infty$ and $\rho_{\text{ic}} \triangleq \|\mathcal{H}[r(0)\delta(t)]\|_{\mathcal{L}_\infty} < \infty$. By replacing $\mathcal{H}_q$ by $\mathcal{H}$ in the analysis in Section 6.6, it follows that $b_1 \to 0$ uniformly in q as $k \to \infty$. Hence, there exists a K, such that the *stability condition*

$$b_1 < \frac{\rho_{\text{ref}} - \rho_{\text{ic}}}{L_{\rho_{\text{ref}}}\rho_{\text{ref}} + Z} \qquad (7.11)$$

is satisfied for some $\rho_{\text{ref}} > \rho_{\text{ic}}$ provided that $k > K$. Here, $Z \triangleq \max_i\{Z_i\}$, and

$$L \triangleq \frac{\bar{\rho}}{\rho_{\text{ref}}} \max_i\{d_i(\bar{\rho})\} \max\{1, R_1\}, \text{ with } \bar{\rho} \triangleq \max\{\rho_{\text{ref}} + 1, R_1(\rho_{\text{ref}} + 1) + R_2\}. \tag{7.12}$$

Unlike the analysis for tracking synchronization, here, the term $\max\{1, R_1\}$ appears in (7.12) because R_1 might be any positive number which is not known.

Theorem 7.1. *Suppose k satisfies the stability condition* (7.11) *for some $\rho_{\text{ref}} > \rho_{\text{ic}}$. Then, $\|r_{\text{ref}}(0)\|_\infty < \rho_{\text{ref}}$ implies that $\|r_{\text{ref}}\|_{\mathcal{L}_\infty} < \rho_{\text{ref}}$ and $\|u_{\text{ref}}\|_{\mathcal{L}_\infty} < \infty$.*

Proof. Suppose that $\|r_{\text{ref}}\|_{\mathcal{L}_\infty} \geq \rho_{\text{ref}}$. Then $\|r_0\|_\infty < \rho_{\text{ref}}$ implies that there exists a τ, such that

$$\|r_{\text{ref}}\|_\infty < \rho_{\text{ref}}, \quad \forall t \in [0, \tau), \quad \text{and} \quad \|r_{\text{ref},\tau}\|_{\mathcal{L}_\infty} = \|r_{\text{ref}}(\tau)\|_\infty = \rho_{\text{ref}}. \tag{7.13}$$

This, (7.9) and (7.12) lead to

$$\|\zeta_{\text{ref},\tau}\|_{\mathcal{L}_\infty} \leq \max\{\rho_{\text{ref}}, R_1\rho_{\text{ref}} + R_2\} < \max\{\rho_{\text{ref}} + 1, R_1(\rho_{\text{ref}} + 1) + R_2\} = \bar{\rho}. \tag{7.14}$$

Consequently, it follows from (2.19) and (7.12) that (similar to (6.91))

$$\|\eta_{\text{ref},\tau}\|_{\mathcal{L}_\infty} \leq \max_i\{\bar{\rho} d_i(\bar{\rho}) + Z_i\} \leq \rho_{\text{ref}} L + Z. \tag{7.15}$$

Using (7.10), (7.11) and (7.15) we obtain

$$\|r_{\text{ref},\tau}\|_{\mathcal{L}_\infty} \leq \|\mathcal{H} \circ (\mathcal{D}_q + \mathcal{I})\|_{\mathcal{L}_1} \|\eta_\tau\|_{\mathcal{L}_\infty} + \|\mathcal{H}[r_0\delta(t)]\|_{\mathcal{L}_\infty} \leq b_1(\rho_{\text{ref}} L + Z) + \rho_{\text{ic}} < \rho_{\text{ref}}, \tag{7.16}$$

contradicting the equality in (7.13). Thus $\|r_{\text{ref}}\|_{\mathcal{L}_\infty} < \rho_{\text{ref}}$. The claim that $\|u_{\text{ref}}\|_{\mathcal{L}_\infty} < \infty$ immediately follows by applying this result to (7.4). □

7.2 Transient performance bounds

The following theorem shows that the collective state and control input of the proposed consensus control system follow those of the nonadaptive reference system closely. This and Theorem 7.1 indicate the stability of the proposed control system.

Theorem 7.2. *Suppose that the condition in* (7.11) *is satisfied. Then, for* $\nu \ll 1$*, there exist* θ_b*,* σ_b *and* $C > 0$*, such that if* $\Gamma\nu^2 \geq C$*, it follows that* $\|\tilde{r}\|_{\mathcal{L}_\infty} \leq \nu$*, and the norms* $\|r_{\rm ref} - r\|_{\mathcal{L}_\infty}$ *and* $\|u_{\rm ref} - u\|_{\mathcal{L}_\infty}$ *are both* $\mathcal{O}(\nu)$.■

Proof. Suppose that $\nu > 0$ is given. Since $\|r_{\rm ref}(0) - r(0)\|_\infty = 0 < 1$ and $\|u_{\rm ref}(0) - u(0)\|_\infty = 0$, it follows by continuity that there exists a $\tau > 0$, $\tau > 0$, such that $\|(r_{\rm ref} - r)_\tau\|_{\mathcal{L}_\infty} < 1$ and $\|(u_{\rm ref} - u)_\tau\|_{\mathcal{L}_\infty} < \infty$. Theorem 7.1 implies that

$$\|r_\tau\|_{\mathcal{L}_\infty} < \rho_{\rm ref} + 1, \quad \|u_\tau\|_{\mathcal{L}_\infty} < \infty. \tag{7.17}$$

First, it follows from the Lyapunov analysis in Theorem 6.2 that there exists a $C > 0$ (independent of τ), such that

$$\|\tilde{r}_\tau\|_{\mathcal{L}_\infty} \leq \sqrt{C/\Gamma}, \tag{7.18}$$

which does not exceed ν provided that $\Gamma\nu^2 \geq C$.

It follows from (7.5) that

$$r_{\rm ref} - r = \big(\dot{q}_{\rm a,ref} - \dot{q}_a\big) + (D \otimes \mathbb{I}_n)(q_{\rm a,ref} - q_a) - (A_d \otimes \mathbb{I}_n)\big(q_{\rm a,ref}(t-T) - q_a(t-T)\big). \tag{7.19}$$

By the same arguments that lead to (7.7), we get

$$\|(q_{\rm a,ref} - q_a)_\tau\|_{\mathcal{L}_\infty} \leq Q_1 \|(r_{\rm ref} - r)_\tau\|_{\mathcal{L}_\infty}. \tag{7.20}$$

Here, $Q_2 = 0$ because $q_{\mathrm{a,ref}}(0) - q_a(0) = 0$. This and the definitions

$$\chi_{\mathrm{ref}}^\top(t) = \big[q_{\mathrm{a,ref}}^\top(t), q_{\mathrm{a,ref}}^\top(t-T), \dot{q}_{\mathrm{a,ref}}^\top(t-T), q_p^\top(t), \dot{q}_p^\top(t), \ddot{q}_p^\top(t)\big] \tag{7.21}$$

$$\chi^\top(t) = \big[q_a^\top(t), q_a^\top(t-T), \dot{q}_a^\top(t-T), q_p^\top(t), \dot{q}_p^\top(t), \ddot{q}_p^\top(t)\big] \tag{7.22}$$

imply

$$\begin{aligned}
\|(\chi_{\mathrm{ref}} - \chi)_\tau\|_{\mathcal{L}_\infty} &\leq \max\{\|(q_{\mathrm{a,ref}} - q_a)_\tau\|_{\mathcal{L}_\infty}, \|\big(q_{\mathrm{a,ref}}(t-T) - q_a(t-T)\big)_\tau\|_{\mathcal{L}_\infty}, \\
&\qquad\qquad \|\big(\dot{q}_{\mathrm{a,ref}}(t-T) - \dot{q}_a(t-T)\big)_\tau\|_{\mathcal{L}_\infty}\} \\
&\leq \|(q_{\mathrm{a,ref}} - q_a)_\tau\|_{\mathcal{L}_\infty} + \|(\dot{q}_{\mathrm{a,ref}} - \dot{q}_a)_\tau\|_{\mathcal{L}_\infty} \\
&\leq (Q_1+1)\|(r_{\mathrm{ref}} - r)_\tau\|_{\mathcal{L}_\infty} + \Big(\|D \otimes \mathbb{I}_n\| + \|A_d \otimes \mathbb{I}_n\|\Big) Q_1 \|(r_{\mathrm{ref}} - r)_\tau\|_{\mathcal{L}_\infty} \\
&= \underbrace{\Big(Q_1 + 1 + \big(\|D \otimes \mathbb{I}_n\| + \|A_d \otimes \mathbb{I}_n\|\big) Q_1\Big)}_{R_1} \|(r_{\mathrm{ref}} - r)_\tau\|_{\mathcal{L}_\infty} \\
&= R_1 \|(r_{\mathrm{ref}} - r)_\tau\|_{\mathcal{L}_\infty}.
\end{aligned} \tag{7.23}$$

Hence, the definitions of $\zeta_{\mathrm{ref}}^\top = [r_{\mathrm{ref}}^\top, \chi_{\mathrm{ref}}^\top]$ and $\zeta^\top = [r^\top, \chi^\top]$ lead to

$$\|(\zeta_{\mathrm{ref}} - \zeta)_\tau\|_{\mathcal{L}_\infty} \leq \max\{1, R_1\} \|(r_{\mathrm{ref}} - r)_\tau\|_{\mathcal{L}_\infty}. \tag{7.24}$$

The inequalities in (2.19) and (7.24) lead to

$$\|(\eta_{\mathrm{ref}} - \eta)_\tau\|_{\mathcal{L}_\infty} \leq \max_i \big\{d_i(\bar{\rho})\big\} \max\{1, R_1\} \|(r_{\mathrm{ref}} - r)_\tau\|_{\mathcal{L}_\infty} < L \|(r_{\mathrm{ref}} - r)_\tau\|_{\mathcal{L}_\infty}. \tag{7.25}$$

Equations (6.7), (6.20), (6.24), (7.3) and (7.4) imply that

$$\dot{r}_{\mathrm{ref}} - \dot{r} = A_m(r_{\mathrm{ref}} - r) + \omega(q)(u_{\mathrm{ref}} - u) + \eta_{\mathrm{ref}} - \eta, \tag{7.26}$$

where

$$u_{\text{ref}} - u = \mathcal{F}_q[\eta_{\text{ref}} - \eta] + \big(\mathcal{F}_q \circ \mathcal{A}_l + k(\mathcal{F}_q \circ \mathcal{M}_q + \mathcal{I})\big)[\tilde{r}], \tag{7.27}$$

which can be obtain by following the analysis in (6.116). By substituting (7.27) into (7.26), we get

$$\dot{r}_{\text{ref}} - \dot{r} = A_m(r_{\text{ref}} - r) + (\mathcal{D}_q + \mathcal{I})[\eta_{\text{ref}} - \eta] + \big(\mathcal{D}_q \circ \mathcal{A}_l + k(\mathcal{D}_q + \mathcal{I}) \circ \mathcal{M}_q\big)[\tilde{r}] \tag{7.28}$$

$$\Leftrightarrow r_{\text{ref}} - r = \mathcal{H} \circ (\mathcal{D}_q + \mathcal{I})[\eta_{\text{ref}} - \eta] + \mathcal{H} \circ \big(\mathcal{D}_q \circ \mathcal{A}_l + k(\mathcal{D}_q + \mathcal{I}) \circ \mathcal{M}_q\big)[\tilde{r}]. \tag{7.29}$$

Hence, taking into account (7.25), we obtain

$$\begin{aligned}
&\|(r_{\text{ref}} - r)_\tau\|_{\mathcal{L}_\infty} \\
&\quad \leq \|\mathcal{H} \circ (\mathcal{D}_q + \mathcal{I})\|_{\mathcal{L}_1} \|(\eta_{\text{ref}} - \eta)_\tau\|_{\mathcal{L}_\infty} + \|\mathcal{H} \circ \big(\mathcal{D}_q \circ \mathcal{A}_l + k(\mathcal{D}_q + \mathcal{I}) \circ \mathcal{M}_q\big)\|_{\mathcal{L}_1} \|\tilde{r}_\tau\|_{\mathcal{L}_\infty} \\
&\quad \leq b_1 L \|(r_{\text{ref}} - r)_\tau\|_{\mathcal{L}_\infty} + b_2 \|\tilde{r}_\tau\|_{\mathcal{L}_\infty},
\end{aligned} \tag{7.30}$$

where $b_2 \triangleq \|\mathcal{H} \circ \big(\mathcal{D}_q \circ \mathcal{A}_l + k(\mathcal{D}_q + \mathcal{I}) \circ \mathcal{M}_q\big)\|_{\mathcal{L}_1}$. It follows from the stability condition in (7.11) that $1 - b_1 L > 0$. Hence, solving for $\|(r_{\text{ref}} - r)_\tau\|_{\mathcal{L}_\infty}$ in (7.30) results in

$$\|(r_{\text{ref}} - r)_\tau\|_{\mathcal{L}_\infty} \leq \frac{b_2}{1 - b_1 L} \nu. \tag{7.31}$$

Similarly, the expression in (7.27) yields

$$\|(u_{\text{ref}} - u)_\tau\|_{\mathcal{L}_\infty} \leq b_3 \|(r_{\text{ref}} - r)_\tau\|_{\mathcal{L}_\infty} + b_4 \|\tilde{r}_\tau\|_{\mathcal{L}_\infty} \leq \Big(\frac{b_2 b_3}{1 - b_1 L} + b_4\Big)\nu, \tag{7.32}$$

with $b_3 = b_{\mathcal{F}} L$ and $b_4 = \|\mathcal{F}_q \circ \mathcal{A}_l + k(\mathcal{F}_q \circ \mathcal{M}_q + \mathcal{I})\|_{\mathcal{L}_1}$. The claim follows by choosing ν and Γ such that the right-hand side of (7.31) is strictly less than 1. □

From (6.7) and (7.1) we obtain

$$\dot{q}_{a,i} = \sum_{j \in \mathcal{S}_i} \big(q_{a,j}(t-T) - q_{a,i}\big) + b_i, \tag{7.33}$$

where the bias $b_i(t)$ is obtained from

$$b_i(s) = (s\mathbb{I}_n - A_{m,i})^{-1} \left(\bar{\eta}_i(s) - \frac{k}{s+k}\hat{\eta} + r_{i,0}\right), \tag{7.34}$$

where $\bar{\eta}_i(t) = \omega\big(q(t)\big)u(t) - u(t) + \eta(t)$.

Since the state and the control input are bounded according to Theorem 2, the bias term b_i is always bounded. Moreover, its size can be controlled by the value of the filter bandwidth k. In particular, we have $\frac{k}{s+k} \to 1$ when $k \to \infty$. Hence, in this case, it follows from (7.34) that $b_i \to 0$ as $t \to \infty$ since $\hat{\eta} \to \bar{\eta}$ due to the action of the fast adaptation. Consequently, in the absence of the delay T, (7.33) will become the standard consensus algorithm. In this case, let l be a left eigenvector of the Laplacian L corresponding to the zero eigenvalue. Also denote by $\alpha^k \in \mathbb{R}^n$ the consensus value to which the k-th joints of all manipulators converge. It follows from (7.33) that $\dot{q}^k = -Lq^k$, where q^k is the column vector containing the k-th joint angles of all robots. Also, let q_0^k be the initial condition of q^k. By following the analysis in [110], the formula for the consensus value of the k-th joints of all manipulators can be derived as: $\alpha^k = \big(l^\top q_0^k\big) \,/\, \big(l^\top \mathbf{1}_N\big)$.

In order to maintain a smooth control signal and system robustness, we employ small values for the filter bandwidth k in (6.20). As a result, the biases b_i are non-zero but bounded, and their size is controllable by changing k. In addition, it follows from [110] that these biases do not affect the stability analysis of (7.33). In this case, however, the consensus value is biased from the average value mentioned in the last paragraph due to the presence of the bias term b^k. In the presence of the delay T, the consensus algorithm results in a collective DDE whose homogeneous equation is given in (7.6). As analyzed in the discussion below this equation, the delay-independent stability of (7.33) in the presence of the bias term is

established given the strong connectivity of the network.

7.3 Leader-follower consensus

In the absence of a leader, the control scheme in the last section drives the robots' angles to their respective consensus values. These values depend on the initial conditions, the communication delays and the bias terms, therefore are very difficult to predict. In this section, we design an algorithm that allows for controlling the consensus value, as well as driving the consensus of the robots in a time-varying manner in the presence of a leader.

Suppose that in the network, only the N^{th} robot knows the assigned tasks or the desired trajectories. The rest have to follow the leader in a consensus manner. To achieve this, we modify the consensus variable of the leader as follows

$$r_N = \dot{q}_{a,N} - \sum_{j \in \mathcal{S}_N} \big(q_{a,j}(t-T) - q_{a,N}\big) - c\big(q_d - q_{a,N}\big), \tag{7.35}$$

where c is the leader's tracking gain, which decides how fast the leader's joint angles converge to the desired trajectories. The kinematic variables in (7.1) for the other robots, as well as the control components for all robots, remain unchanged.

In terms of the robots' joint angles, the consensus algorithm becomes

$$\begin{cases} \dot{q}_{a,i} = \sum\limits_{j \in \mathcal{S}_i} \big(q_{a,j}(t-T) - q_{a,i}\big) + b_i, \ i = 1, ..., N-1 \\ \dot{q}_{a,N} = \sum\limits_{j \in \mathcal{S}_N} \big(q_{a,j}(t-T) - q_{a,N}\big) + c\big(q_d - q_{a,N}\big) + b_N \end{cases} \tag{7.36}$$

where the bias terms b_i are bounded and their size is inversely proportional to the filter bandwidth k as discussed in the last section. It follows from the analysis in [86] that $q_{a,i} \to q_d$ when q_d is constant. The numerical experiments in the next section will illustrate that when q_d varies with time, the robots will follow the leader closely despite the communication delays. However, there is a lag between their motions and those of the leader due to the

delays as well as the nature of the consensus algorithm.

7.4 Numerical Results

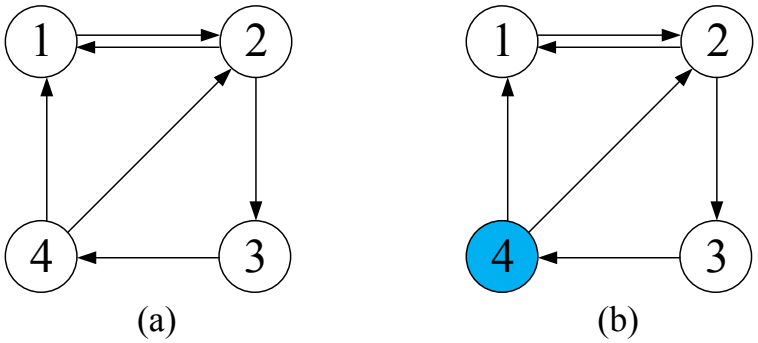

Figure 7.1: Network topology: (a) An unbalanced and strongly connected graph; (b) An unbalanced and strongly connected graph with node 4 as the leader.

In the case when a common desired trajectory is not available, the consensus controller is implemented for a strongly connected and unbalanced network as shown in Fig. 7.1(a). The identical control parameters and delays as in the case of synchronization are used here. The left eigenvector of the zero eigenvalue of the corresponding Laplacian matrix equals $l^\top = [0.209\ 0.417\ 0.626\ 0.626]$. The system response is shown in Fig. 7.2. Despite the delays and the unknown dynamics of the platform, the controller successfully compensates for the nonlinearities and uncertainties and drives the manipulators to a consensus configuration, $\alpha^\top = [0.1503\ -0.2134\ -0.0892]$. When the filter bandwidth of u_i^{ad} in (6.20) is increased, this consensus configuration gets closer to the values computed by $\alpha^k = \left(l^\top q_0^k\right) / \left(l^\top \mathbf{1}_N\right)$, i.e. $[0.3222\ -0.4222\ -0.1778]$. The deviation between these two sets of values stems from the bias b^k. In theory, the bias b^k does not converge to a constant. Nonetheless, the size of the neighborhood in which it varies is so small that it appears in Fig. 7.2 that the joint angles approximately approach a constant value.

In the case of leader-follower consensus, the network topology is given in Fig. 7.1(b). Robot 4 is the leader, who knows the desired trajectory. The other three manipulators, who do not have access to the information about the desired trajectory, are tasked to follow

robot 4 in a consensus manner using the formulation proposed in Section 7.3. All control parameters remain unchanged. Figure 7.3 illustrates the result when the desired trajectory is constant, in particular $q_d = [1\ 1.2\ 1.5]$, with a communication delay of 1 s. We can see here that the joint angles of the robots follow those of the leader, which converge to the respective desired values. These values no longer depend on the initial conditions and the delays, but are controlled by q_d. Figure 7.4 illustrates the result when the consensus values vary in time, in particular $q_d^\top(t) = [\sin 0.2t \quad \sin 0.2t \quad \cos 0.2t]$. The communication delay is set to 0.5 s. The data shows that the followers' angles closely track the motions of the leader, though there is a phase gap and tracking error between the leader and the other robots. This observation may be traced to the presence of the delay, and the fact that the followers have no knowledge of the desired trajectory, and have to observe the leader to figure out how to move.

Other numerical experiments also show that when either the desired trajectory varies faster or the delay is increased, the phase lag and the tracking error get larger. An intriguing observation is that the motions of robot 1 and robot 2 converge without any lag and tracking error between them despite the initial mismatch. This phenomenon is accounted for by the nature of the connection between these: they have full access to the motion measurements of each other. Furthermore, when all the followers receive the leader's motion data, the lag among the followers' motions vanishes and they converge to each other.

7.5 Summary

Consensus of manipulators has been studied in the literature only for the case of fixed-base robots (except for the preliminary version of the work in Chapters 6 and 7 in [101]). This chapter has proposed a robust adaptive controller that allows a team of manipulators mounted on an underactuated dynamic platform operating in a challenging environment to reach a consensus configuration in the absence of a common desired trajectory. The control

scheme was formulated without assuming detailed knowledge about the system model. This framework ensures a predictable transient response with smooth and implementable control signals, while maintaining the system robustness to communication delay. In addition, constant as well as time varying consensus configurations of the manipulators are reached in the presence of communication delay and the unmodeled platform dynamics disturbed by unknown environmental factors. The theoretical analysis in this chapter considers the performance of the control design. The numerical results demonstrate the successful application of a partial parameterization of the nonlinearity that extends the adaptive control of a single manipulator in Chapter 2 to the cooperative control of a team of manipulators on a moving platform. Similar to Chapter 2, the theoretical analysis in Chapters 6 and 7 is restricted to systems where the unactuated motions of the platform are assumed to be a priori bounded despite being influenced by the manipulators' dynamics.

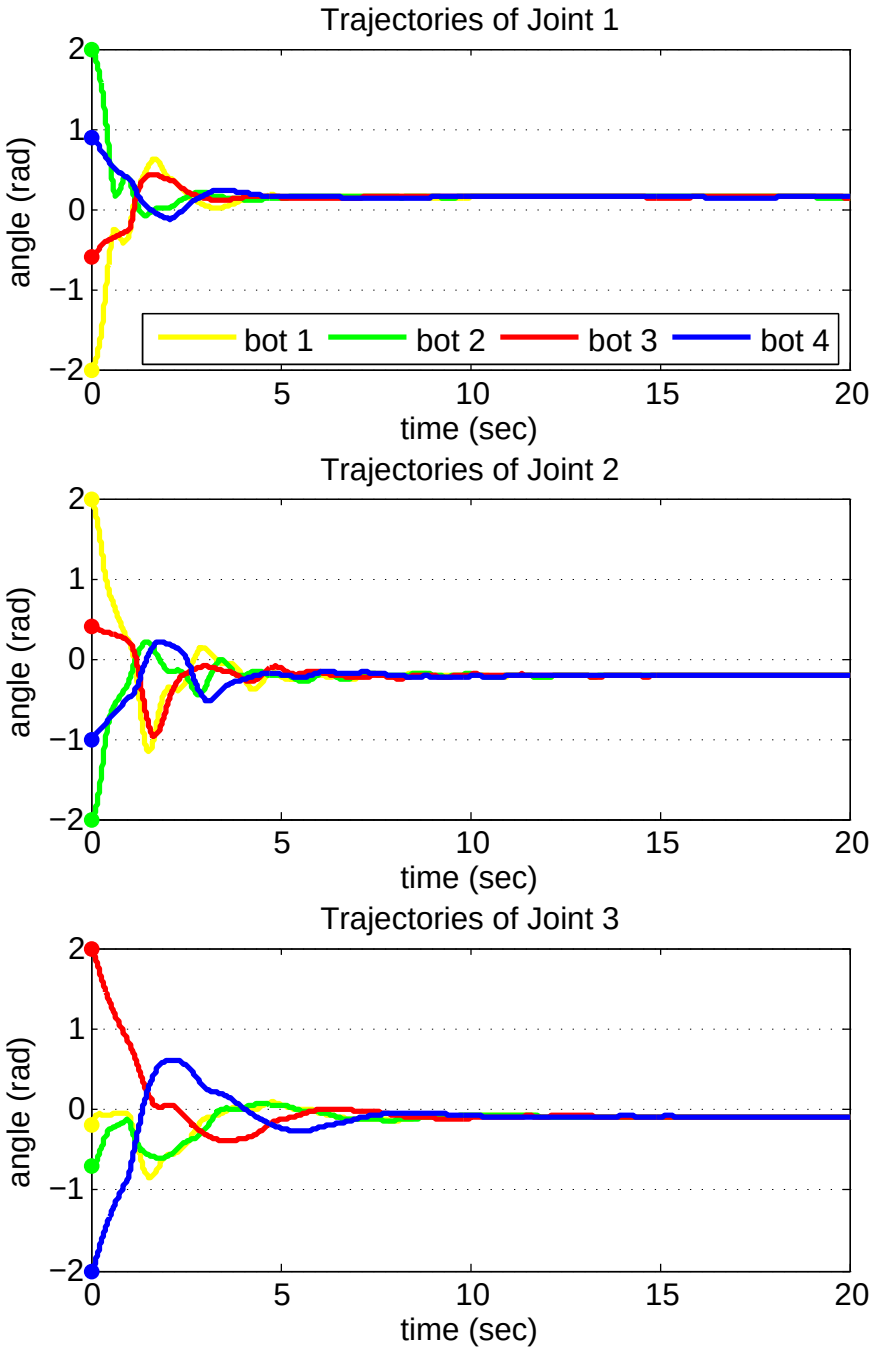

Figure 7.2: All robots converge to a consensus configuration with a communication delay of 1 s when a common desired trajectory is not available.

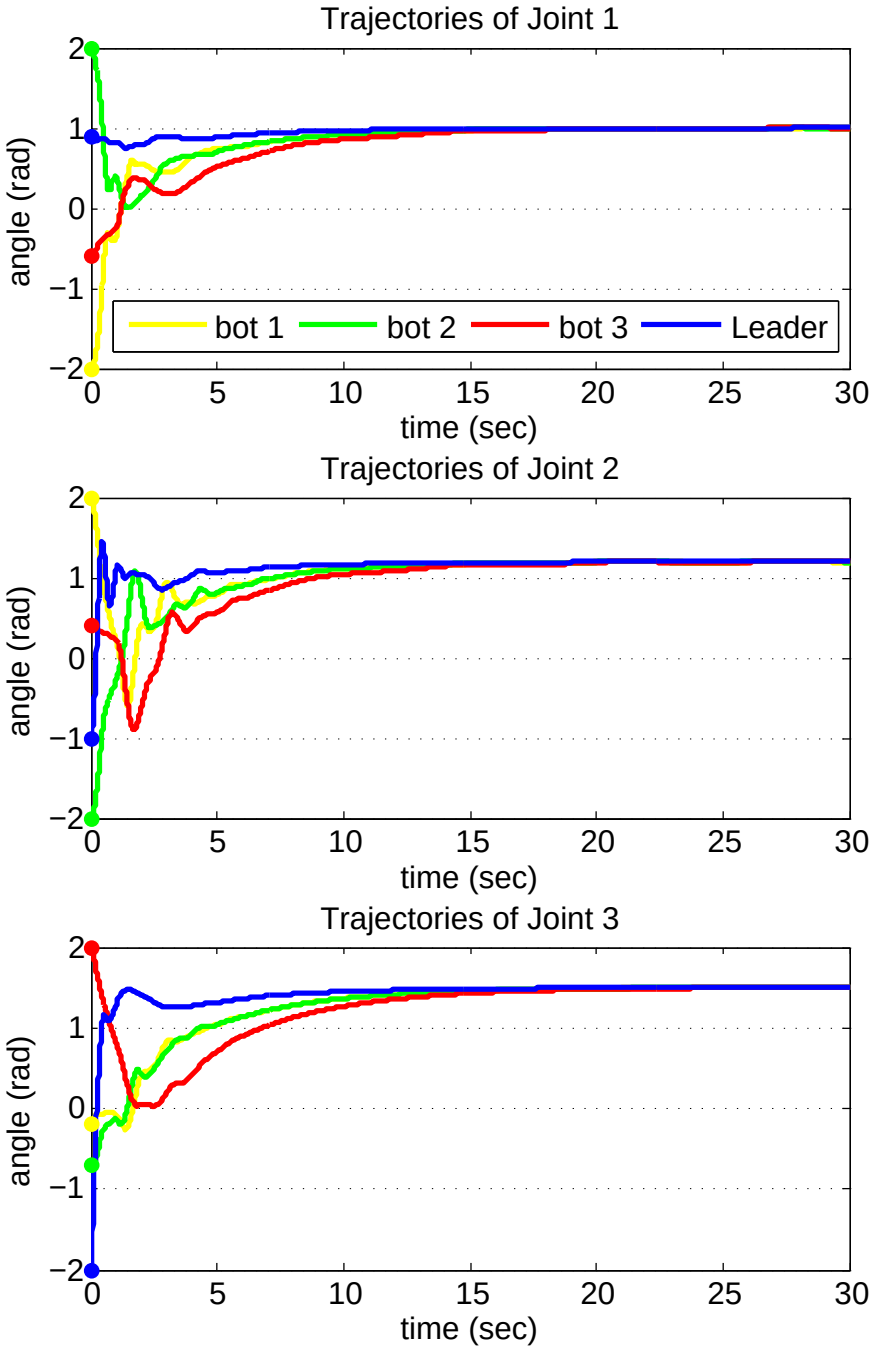

Figure 7.3: The robots converge to consensus values controlled by q_d using the leader-follower scheme with a communication delay of 1 s .

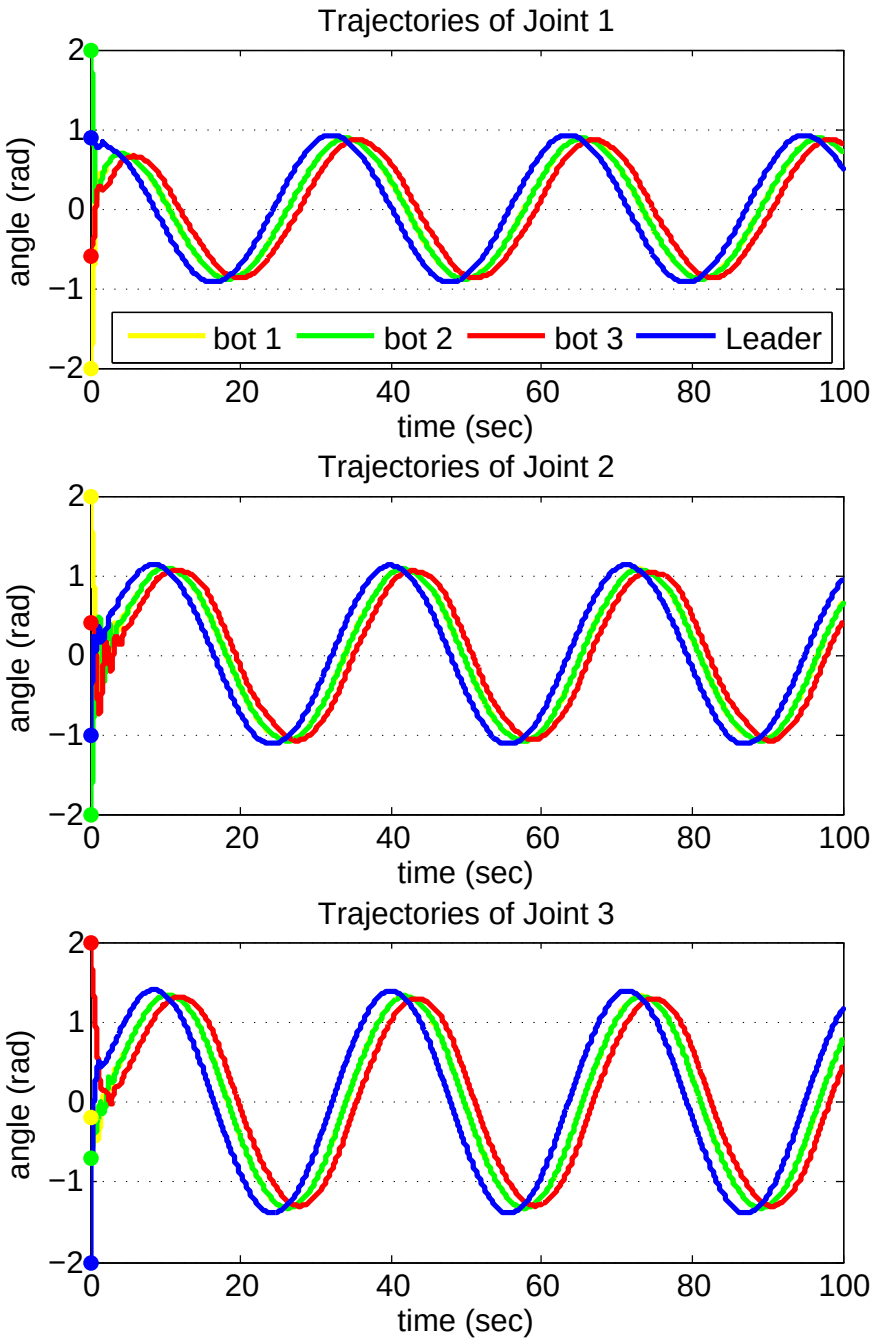

Figure 7.4: The followers'motions track the leader's motions which converge to time-varying consensus values controlled by q_d with a communication delay of 0.5 s.

CHAPTER 8

CONCLUSION

This dissertation has studied the stability and robustness of an adaptive control framework for underactuated Lagrangian systems and robotic networks. Chapter 2 presented an adaptive control framework for a manipulator, operating on an underactuated platform whose dynamics are influenced by environmental factors, for examples a ship in high sea state, an offshore platform, or a ground-based vehicle moving across a rough terrain. Inspired by the $\mathcal{L}_1$ control paradigm [61], the framework uses a filter in the control input of a model reference adaptive controller to improve the system robustness. In the analysis, the characteristics of the controller were represented by two decoupled indicators. First, the adaptive gain determined the rate of adaptation, as well as the deviation between the system output and an ideal response. Second, the filter bandwidth determined the deviation of the ideal response from an exponential decay to 0, as well as the system's ability to tolerate input delay.

The sensitivity of the control scheme to time delays in the control loop, which is an indicator of robustness, was studied using computational tools in Chapter 3. In particular, an LTI system was proposed in order to derive a conservative lower bound on the critical time delay for a static reference input in the limit of large estimation gains. In addition, a numerical method based on techniques of parameter continuation was proposed for quantifying the robustness against time delay of the system's performance for a given static reference input. Specifically, the method tracked the critical time delay at which local stability is lost in a Hopf bifurcation.

In a further study of the framework presented in Chapter 2, theoretical analysis was used in Chapters 4 and 5 to investigate the delay robustness of adaptive controllers designed for

a class of systems with unknown nonlinearities. Specifically, the nonlinear systems were assumed to have constant input-gain matrices in Chapter 4, while the input-gain matrices were time-varying and state-dependent in Chapter 5. The analysis showed that the controllers have positive lower bounds for their time-delay margin. In particular, if the input delay is below a critical value, the state and control input of the adaptive control system follow those of a nonadaptive, robust reference system closely. The analysis in Chapter 4 also suggested a way to compute this lower bound for the delay robustness using a Padé approximant.

The control framework was extended to the context of cooperative control of multiple robots in Chapters 6 and 7. In particular, these chapters presented the analysis of the synchronization and consensus problems of networked manipulators operating on an underactuated dynamic platform in the presence of communication delays. The proposed formulation does not require detailed information about the system model. The theoretical analysis based on input-output maps of functional differential equations showed that the adaptive control system's behavior matches closely that of a nonadaptive reference system. The tracking-synchronization objective was achieved despite the effect of communication delays, and the unknown dynamics of the platform. When there was no common desired trajectory, the modified controller drove all robots to a consensus configuration. In addition, a leader-follower scheme was proposed that allows for the control of the constant and time-varying consensus values.

The theoretical analysis presented in Chapters 2, 6 and 7 is restricted to systems where the platform's unactuated degrees of freedom and their first and second derivatives are bounded a priori. These a priori bounds result in the bounds on the actuated system state and control input derived in the respective chapters. In an actual mechanism, however, the response of the unactuated degrees of freedom clearly depends on the actuated system state and control input. In general, the resultant time-varying functions may not satisfy the a priori bounds. Nonetheless, in practice, it may be possible to overcome this problem by purposely designing the platform, e.g., its inertia, stiffness and damping properties such that the unactuated

degrees of freedom are robust to the actuated dynamics. Clearly, this is expected of a platform whose passive properties dominate any coupling from the manipulators. This issue will be further addressed in future work.

The control framework used throughout this dissertation was designed to control moving-base manipulators in joint-space. It is of interest to extend the framework to control moving-base manipulators in task-space, for example by defining the sliding variable r in terms of the cartesian coordinates of the end-effector and their derivatives. In the context of networked manipulators, solving task-space control problems allows for performing cooperative task for manipulators on a common platform even when they have different number of degrees of freedom or different kinematic structure. Task-space control also suggests opportunities for research in cooperative networks of human operators interacting with robotic manipulators on different mobile platforms.

To do this, the Jacobian matrix that relates joint-space coordinates to task-space configurations would need to be taken into account, but the resultant differential equation for r would include an input gain matrix that might not be symmetric or positive definite. This poses a challenge because the successful performance of the control framework designed in this dissertation assumes a positive definite input gain. In addition, an adaptive law would likely be needed to estimate the uncertain Jacobian matrix of each manipulator. Moreover, control in task-space would require measurements of the motion of the platform as well as the motion of the end-effector, which is usually inferred from the output of a visual sensor such as a camera. This raises another research question: How does camera space fit into the control framework to provide useful information?

Finally, we note that the heuristic approach in Chapter 4 underestimates the time-delay margin. A less conservative estimate might be attainable using numerical optimization, e.g., methods of parameter continuation. Moreover, since there is no *a priori* reason to expect transient performance bounds for all delays below the linear instability threshold ϵ_{us}, it is intriguing to note the close agreement between ϵ_{us} and the time-delay margin estimated

from forward simulation. In addition, though the existence of a theoretical lower bound for the time delay margin of a class of nonlinear systems with time and state dependent input gain is addressed in Chapter 5, a method for quantifying this lower bound remains to be investigated.

REFERENCES

[1] A. Abdessameud, I.G. Polushin and A. Tayebi, Adaptive synchronization of networked Lagrangian systems with irregular communication delays, in: Proceeding of IEEE Conf. Decision and Control, 2012, pp. 5936-5941.

[2] A. Abdessameud, I.G. Polushin, A. Tayebi, Synchronization of Lagrangian Systems with Irregular Communication Delays, IEEE Trans. Automatic Control 59(1) (2014) 187–193.

[3] S. Abiko, K. Yoshida, Adaptive reaction control for space robotic applications with dynamic model uncertainty, Advanced Robotics 24(8–9) (2010) 1099-1126.

[4] V. Andaluz, R. Carelli, L. Salinas, J. M. Toibero, F. Roberti, Visual control with adaptive dynamical compensation for 3D target tracking by mobile manipulators, Mechatronics 22(4) (2012) 499-502.

[5] R. Anderson, M.W. Spong, Bilateral control of teleoperators with time delay, IEEE Trans. Automatic Control 34(5) (1989) 494–501.

[6] A. Anokhin, L. Berezansky, E. Braverman, Exponential Stability of Linear Delay Impulsive Differential Equations, Journal of Mathematical Analysis and Applications 193(3) (1995) 923–941.

[7] G. Antonelli, F. Caccavale, S. Chiaverini, Adaptive tracking control of underwater vehicle-manipulator systems based on the virtual decomposition approach, IEEE Transactions on Robotics and Automation 20(3) (2004) 594-602.

[8] G. Antonelli, Underwater Robots: Control of vehicle manipulator systems, New York: Springer-Verlag, 2006.

[9] M. Asadpour, B. van den Bergh, D. Giustiniano, K. Hummel, S. Pollin, B. Plattner, Micro aerial vehicle networks: an experimental analysis of challenges and opportunities, IEEE Communications Magazine 52(7) (2014) 141–149.

[10] F.M. Atay, The consensus problem in networks with transmission delays, Phil. Trans. Royal Society A 371 (2013) 20120460.

[11] J. Baeten, K. Donne, S. Boedrij, W. Beckers, E. Claesen, Autonomous fruit picking machine: A robotic apple harvester, Springer Tracks in Advanced Robotics 42 (2008) 531-539.

[12] M. Bennehar, A. Chemori, F. Pierrot, $\mathcal{L}_1$ Adaptive Control of Parallel Kinematic Manipulators: Design and Real-Time Experiments, in Proc. IEEE Conf. Robotics and Automation, 2015.

[13] R. Berenstein, O.B. Shahar, A. Shapiro, Y. Edan, Grape clusters and foliage detection algorithms for autonomous selective vineyard sprayer, Intelligent Service Robotics 3(4) (2010) 233–243.

[14] M. Bergerman, E. van Henten, J. Billingsley, J. Reid, D. Mingcong, IEEE Robotics and Automation Society Technical Committee on Agricultural Robotics and Automation, IEEE Robotics & Automation Magazine 20(2) (2013) 20–23.

[15] H. Berghuis, H. Nijmeijer, A passivity approach to controller-observer design for robots, IEEE Transactions on Robotics and Automation 9(6) (1993) 740-754.

[16] R. Bhatia, Matrix analysis, Springer-Verlag, 1997.

[17] J. Billingsley, A. Visala, M. Dunn, Robotics in agriculture and forestry, in: Siciliano B, Khatib O (eds) Springer handbook of robotics, Chap 46. Springer, Berlin, pp. 1065-1077

[18] M. Boukattaya, M. Jallouli, T. Damak, On trajectory tracking control for nonholonomic mobile manipulators with dynamic uncertainties and external torque disturbances, Robotics and Autonomous Systems 60 (2012) 1640-1647.

[19] R.W. Brockett, Asymptotic stability and feedback stabilization, Differential geometric control theory (R.W. Brockett, R.S. Millmann, H.J. Sussmann eds.) (1983) 181-191.

[20] C. Cao, N. Hovakimyan, Stability Margins of $\mathcal{L}_1$ Adaptive Control Architecture, IEEE Trans. Automatic Control 55(2) (2010) 480–487.

[21] F.A.A. Cheein, R. Carelli, Agricultural Robotics: Unmanned Robotic Service Units in Agricultural Tasks, IEEE Industrial Electronics Magazine 7(3) (2013) 48–58.

[22] N. Chopra, M.W. Spong, Passivity-based control of multi-agent systems, Advances in Robot Control: From Everyday Physics to Human-Like Movements, S. Kawamura and M. Svinin, Eds. New York: Springer-Verlag, pp. 107-134, 2006.

[23] J. Chung, S. Velinsky, R. Hess, Interaction control of a redundant mobile manipulator, The International Journal of Robotics Research 17(12) (1998) 1302-1309.

[24] S.J. Chung, J.J.E. Slotine, Cooperative Robot Control and Synchronization of Lagrangian Systems, in: Proc. IEEE Conf. Decision and Control, 2007, pp. 2504–2509.

[25] S.J. Chung, J.J.E. Slotine, Cooperative robot control and concurrent synchronization of Lagrangian systems, IEEE Trans. Robotics 25(3) (2009) 686-700.

[26] P. Coelho, U. Nunes, Path-following control of mobile robots in presence of uncertainties, IEEE Trans. Robotics 21(2) (2005) 252–261.

[27] T.H. Cormen, C.E. Leiserson, R.L. Rivest, C. Stein, Introduction to Algorithms, Second Edition, MIT Press and McGrawHill, 2001.

[28] J.J. Craig, P. Hsu, S.S. Sastry, adaptive control of mechanical manipulators, J. Robotics Research 6(2) (1987) 16–28.

[29] J.M. Daly, Y. Ma, S.L. Waslander, Coordinated landing of a quadrotor on a skid-steered ground vehicle in the presence of time delays, in: Proc. IEEE/RSJ Conf. Intelligent Robots and Systems, pp. 4961–4966, 2011.

[30] W. Dong, On trajectory and force tracking control of constrained mobile manipulators with parameter uncertainty, Automatica 38(9) (2002) 1475–1484.

[31] A. Dorobantu, P. Seiler, G.J. Balas, Time-Delay Margin Analysis for an Adaptive Controller, J. Guidance, Control, and Dynamics 35(5) (2012) 1418-1425.

[32] S. Dubowsky, D.T. DesForges, The application of model reference adaptive control to robotic manipulators, Journal of Dynamic Systems, Measurement and Control 101 (1979) 193–200.

[33] Y. Edan, D. Rogozin, T. Flash, G.E. Miles, Robotic melon harvesting, IEEE Trans. on Robotics and Automation 16(6) (2000) 831–835.

[34] K. Engelborghs, T. Luzyanina, D. Roose, Numerical bifurcation analysis of delay differential equations using DDE-BIFTOOL, ACM Trans. Math. Software 28(1) (2002) 1-21.

[35] I. Fantoni, R. Lozano, Non-linear control for underactuated mechanical systems, London:Springer-Verlag, 2002.

[36] R. Fierro, F. L. Lewis, Control of a nonholonomic mobile robot using neural networks, IEEE Transactions on Neural Networks 9(4) (1998) 589–600.

[37] M.M. Foglia, G. Reina, Agricultural robot for radicchio harvesting, J. Field Robotics 23 (2006) 363-377.

[38] T.I. Fossen, S.I. Sagatun, Adaptive control of nonlinear systems: A case study of underwater robotic systems, Journal of Robotic System 8 (1991) 393-412.

[39] M. French, Adaptive Control and Robustness in the Gap Metric, IEEE Trans. Automatic Control 53(2) (2008) 461-478.

[40] E. Fridman, Introduction to Time-Delay Systems: Analysis and Control, Birkhauser, 2014.

[41] P.J. From, V. Duindam, J. T. Gravdahl, S. Sastry, Modeling and motion planning for mechanisms on a non-inertial base, in: Proc. IEEE Conf. Robotics and Automation, 2009, pp. 3320–3326.

[42] P.J. From, J.T. Gravdahl, P. Abbeel, On the influence of ship motion prediction accuracy on motion planning and control of robotic manipulators on seaborne platforms, in: Proc. IEEE Conf. Robotics and Automation, 2010, pp. 5281–5288.

[43] P.J. From, V. Duindam, K.Y. Pettersen, J.T. Gravdahl, S. Sastry, Singularity-free dynamic equations of vehicle-manipulator systems, Simulation Modelling Practice and Theory 18(6) (2010) 712–731.

[44] P.J. From, J.T. Gravdahl, T. Lillehagen, P. Abbeel, Motion planning and control of robotic manipulators on seaborne platforms, Control Engineering Practice 19(8) (2011) 809–819.

[45] T.T. Georgiou, M.C. Smith, "Robustness analysis of nonlinear feedback systems: An input-output approach," IEEE Trans. Automatic Control 42(9) (1997) 1200–1221.

[46] I.G. Gravalos, D.E. Moshou, S.J. Loutridis, T.A. Gialamas, D.L. Kateris, Z.T. Tsiropoulos, P.I. Xyradakis, Design of a pipeline sensor-based platform for soil water content monitoring, Biosystems Engineering 113(1) (2012) 1–10.

[47] K. Gu, S. Niculescu, Survey on recent results in the stability and control of time-delay systems, ASME J. Dynamic Systems, Measurement and Control 125(1) (2003) 158-165.

[48] J. Hale, *Theory of Functional differential equations*, Springer-Verlag, 1977.

[49] B. Herisse, T. Hamel, R. Mahony, F.-X. Russotto, Landing a VTOL unmanned aerial vehicle on a moving platform using optical flow, IEEE Trans. Robotics 28(1) (2012) 77–89.

[50] S. Hayashi, K. Ganno, Y. Ishii, I. Tanaka, Robotic harvesting system for eggplants, Japan Agricultural Research Quarterly 36(3) (2002) 163–168.

[51] S. Hayashi, K. Shigematsu, S. Yamamoto, K. Kobayashi, Y. Kohno, J. Kamata, M. Kurita, Evaluation of a strawberry-harvesting robot in a field test, Biosystems Engineering 105(2) (2010) 160-171.

[52] J.D. Hernandez, J. Barrientos, J. del Cerro, A. Barrientos, D. Sanz, Moisture measurement in crops using spherical robots, Industrial Robot 40(1) (2013) 59–66.

[53] E.J. van Henten, J. Hemming, B.A.J. van Tuijl, J.G. Kornet, J. Meuleman, J. Bontsema, E.A. van Os, An Autonomous Robot for Harvesting Cucumbers in Greenhouses, Autonomous Robots 13(3) (2002) 241–258.

[54] E.J. Van Henten, J. Hemming, B.A.J. Van Tuijl, J.G. Kornet, J. Bontsema, Collision-free Motion Planning for a Cucumber Picking Robot, Biosystems Engineering 86(2) (2003) 135–144.

[55] E.J. Van Henten, B.A.J. Van Tuijl, J. Hemming, J.G. Kornet, J. Bontsema, E.A. van Os, Field Test of an Autonomous Cucumber Picking Robot, Biosystems Engineering 86(3) (2003) 305–313.

[56] E.J. van Henten, B.A.J. Van Tuijl, G.-J. Hoogakker, M.J. Van Der Weerd, J. Hemming, J.G. Kornet, J. Bontsema, An Autonomous Robot for De-leafing Cucumber Plants grown in a High-wire Cultivation System, Biosystems Engineering 94(3) (2006) 317–323.

[57] E.J. van Henten, L.G. van Willigenburg, D. Vant Slot, Optimal design of a cucumber harvesting robot, Computers and Electronics in Agriculture 65 (2009) 247-257.

[58] E.J. Van Henten, E.J. Schenk, L.G. van Willigenburg, J. Meuleman, P. Barreiro, Collision-free inverse kinematics of the redundant seven-link manipulator used in a cucumber picking robot, Biosystems Engineering 106(2) (2010) 112-124.

[59] W.K. Ho, K. W. Lim, W. Xu, Optimal Gain and Phase Margin Tuning for PID Controllers, Automatica 34(8) (1998) 1009-1014.

[60] R. Horowitz, M. Tomizuka, An adaptive control scheme for mechanical manipulators - compensation of nonlinearity and decoupling control, Journal of Dynamic Systems, Measurement, and Control 108 (1986) 127–136.

[61] N. Hovakimyan, C. Cao, $\mathcal{L}_1$ adaptive control theory: guaranteed robustness with fast adaptation, Philadelphia, PA: SIAM, 2010.

[62] Z.H. Ismail, M.W. Dunnigan, Tracking control scheme for an underwater vehicle-manipulator system with single and multiple sub-regions and sub-task objectives, IET Control Theory & Applications 5(5) (2011) 721-735.

[63] J. Jang, Adaptive control design with guaranteed margins for nonlinear plants, Ph.D. Thesis, Massachusetts Institute of Technology, 2008.

[64] H.S. Jeong, C.W. Lee, Time delay control with state feedback for azimuth motion of the frictionless positioning device, IEEE/ASME Trans. Mechatronics 2(3) (1997) 161-168.

[65] D. Johnson, D. Naffin, J. Puhalla, J. Sanchez, C. Wellington, Development and Implementation of a Team of Robotic Tractors for Autonomous Peat Moss Harvesting, Journal of Field Robotics 26(6-7) (2009) 549–571.

[66] M. Kacira, P. Ling, T. Short, Machine Vision Extracted Plant Movement for Early Detection of Plant Water Stress, Trans. the American Society of Agricultural Engineers 45(4) (2002) 1147–1153.

[67] H. Kajita, K. Kosuge, Force control of a water-surface robot utilizing vehicle restoring force, Advanced Robotics 12(6) (1997) 651-662.

[68] H.K. Khalil, J.W. Grizzle, Nonlinear systems, Prentice Hall, 2002.

[69] V.B. Kolmanovskii, V.R. Nosov, Stability of Functional Differential Equations, Academic Press, New York, 1986.

[70] R. Lamm, D. Slaughter, D. Giles, Precision Weed Control System for Cotton, Transactions of the ASABE 45(1) (2002) 231-238.

[71] E. Lavretsky, T.E. Gibson, Projection Operator in Adaptive Systems, arXiv:1112.4232v6 [nlin.AO] (2011).

[72] E. Lavretsky, K.A. Wise, Robust and Adaptive Control, Springer-Verlag London, 2013.

[73] W. Lee, D. Slaughter, D. Giles, Robotic Weed Control Systems for Tomatoes, Precision Agriculture 1 (1999) 95–113.

[74] D. Lee, M.W. Spong, Passive Bilateral Teleoperation With Constant Time Delay, IEEE Trans. Robotics 22(2) (2006) 269–281.

[75] D. Lee, A. Franchi, H.I. Son, C. Ha, H.H. Bulthoff, P.R. Giordano, Semiautonomous Haptic Teleoperation Control Architecture of Multiple Unmanned Aerial Vehicles, IEEE/ASME Trans. Mechatronics 18(4) (2013) 1334–1345.

[76] F.L. Lewis, D.M. Dawson, C.T. Abdallah, Robot manipulator control: theory and practice, Marcel Dekker, 2004.

[77] Z. Li, Y. Kang, Dynamic Coupling Switching Control Incorporating Support Vector Machines for Wheeled Mobile Manipulators with Hybrid Joints, Automatica 46(5) (2010) 785–958.

[78] Z. Li, Y. Zhang, Robust adaptive motion/force control for wheeled inverted pendulums, Automatica 46(8) (2010) 1346-1353.

[79] X. Liu, W. Lu and T. Chen, Consensus of Multi-Agent Systems With Unbounded Time-Varying Delays, IEEE Trans. Automatic Control 55(10) (2010) 2396–2401.

[80] Y. Liu and N. Chopra, Controlled Synchronization of Heterogeneous Robotic Manipulators in the Task Space, IEEE Trans. Robotics 28(1) (2012) 268–275.

[81] Y. Liu, H. Yu, A survey of underactuated mechanical systems, IET Control Theory & Applications 7(7) (2013) 1–53.

[82] Y.C. Liu, N. Chopra, Control of semi-autonomous teleoperation system with time delays, Automatica 49(6) (2013) 1553–1565.

[83] Y. Liu, N. Chopra, Synchronization of Networked Mechanical Systems With Communication Delays and Human Input, J. Dynamic Systems, Measurement, and Control 135(4) (2013) 041004.

[84] W. Lohmiller, J.J.E. Slotine, On contraction analysis for nonlinear systems, Automatica 34(6) (1998) 683–696.

[85] L.J. Love, J.F. Jansen, F.G. Pin, On the modeling of robots operating on ships, in: Proc. IEEE Conf. Robotics and Automation 2004, pp. 2436–2443.

[86] J. Lu, D.W.C. Ho and J. Kurths, Consensus over directed static networks with arbitrary finite communication delays, Physical Review E 80 (2009) 066121.

[87] R.C. Luo, K.L. Su, S.H. Shen, K.H. Tsai, Networked intelligent robots through the Internet: issues and opportunities, Proceedings of the IEEE 91(3) (2003) 371–382.

[88] D. Maalouf, A. Chemori, V. Creuze, $\mathcal{L}_1$ Adaptive depth and pitch control of an underwater vehicle with real-time experiments, Ocean Engineering 98(1) (2015) 66–77.

[89] T. Madani, B. Daachi, A. Benallegue, Adaptive variable structure controller of redundant robots with mobile/fixed obstacles avoidance, Robotics and Autonomous Systems 61(6) (2013) 555-564.

[90] M. Matsutani, Robust adaptive flight control systems in the presence of time delay, Ph.D. Thesis, Massachusetts Institute of Technology, 2013.

[91] A. Mazur, Hybrid adaptive control laws solving a path following problem for nonholonomic mobile manipulators, International Journal of Control 77(15) (2004) 1297-1306.

[92] A. Meijering, H. Hogeveen, C. de Koning, Automatic Milking: A Better Understanding, Wageningen Academic Publishers, Wageningen, 2004.

[93] K. Melhem, W. Wang, Global output tracking control of flexible joint robots via factorization of the manipulator mass matrix, IEEE Trans. Robotics 25(2) (2009) 428–437.

[94] N. Michael, M. Schwager, V. Kumar, D. Rus, An experimental study of time scales and stability in networked multirobot systems, Experimental Robotics, O. Khatib, V. Kumar, G. Pappas (Eds.), Springer Berlin Heidelberg, 2014.

[95] S.J. Moorehead, C.K. Wellington, B.J. Gilmore, C. Vallespi, Automating orchards: A system of autonomous tractors for orchard maintenance, in: Proc. IEEE Conf. Intelligent Robots and Systems, 2012.

[96] L. Moreau, Stability of continuous-time distributed consensus algorithms, in: Proc. IEEE Conf. Decision and Control, 2004, pp. 3998–4003.

[97] R. Murray, Z. Li, S. Sastry, A Mathematical Introduction to Robotic Manipulation, Boca Raton, FL: CRC, 1994.

[98] M. Naghnaeian, P.G. Voulgaris, N. Hovakimyan, On robustness of $\mathcal{L}_1$ adaptive control with time varying perturbations & filter design, in: Proc. American Control Conf., 2012, pp. 1937–1942.

[99] K.D. Nguyen, H. Dankowicz, N. Hovakimyan, Marginal stability in $\mathcal{L}_1$-adaptive control of manipulators, in: Proc. 9th Conf. Multibody Systems, Nonlinear Dynamics, and Control, 2013, DETC2013-12744.

[100] K.D. Nguyen, H. Dankowicz, Robust Adaptive Control of Manipulators, IDEALS UIUC, January, 2014, https://www.ideals.illinois.edu/handle/2142/46993.

[101] K.D. Nguyen and H. Dankowicz, Synchronization and Consensus of a Robot Network on an Underactuated Dynamic Platform, in: Proc. IEEE/RSJ Conf. Intelligent Robots and Systems, 2014, pp. 117–122.

[102] K.D. Nguyen and H. Dankowicz, Adaptive Control of Underactuated Robots with Unmodeled Dynamics, Robotics and Autonomous Systems 64 (2015) 84–99.

[103] K.D. Nguyen, Y. Li and H. Dankowicz, Delay Robustness of an Adaptive Controller for Systems with Unknown Nonlinearities, under review.

[104] N.T. Nguyen, E. Summers, On Time Delay Margin Estimation for Adaptive Control and Robust Modification Adaptive Laws, in: Proc. AIAA Guidance, Navigation, and Control Conf., 2011, AIAA 2011–6438.

[105] S. Nicosia, P. Tomei, Model reference adaptive control algorithms for industrial robots, Automatica 20(5) (1984) 635–644.

[106] S.I. Niculescu, Delay Effects on Stability: A Robust Control Approach, New York: Springer-Verlag, 2001.

[107] G. Niemeyer, J.J.E. Slotine, Stable adaptive teleoperation, IEEE Journal of Oceanic Engineering 16(1) (1991) 152–162.

[108] S.R. Oh, S. K. Agrawal, Cable suspended planar robots with redundant cables: Controllers with positive tensions, IEEE Tran. Robotics 21(3) (2005) 457-465.

[109] R. Olfati-Saber, R.M. Murray, Consensus problems in networks of agents with switching topology and time-delays, IEEE Trans. Automatic Control 49(9) (2004) 1520–1533.

[110] R. Olfati-Saber, J.A. Fax, R.M. Murray, Consensus and cooperation in networked multi-agent systems, Proceedings of the IEEE 95(1) (2007) 215-233.

[111] G. Oriolo, Y. Nakamura, Control of mechanical systems with second-order nonholonomic constraints: Underactuated manipulators, in: Proc. IEEE Conf. Decision and Control, 1991, pp. 2398-2403.

[112] R. Ortega, M. Spong, Adaptive motion control of rigid robots: A tutorial, Automatica 25(6) (1989) 877–888.

[113] R. Ortega, A.J. van de Schaft, B. Maschke, G. Escobar, Interconnection and damping assignment passivity-based control of port-controlled Hamiltonian systems, Automatica 38(4) (2002) 585–596.

[114] O. Parlaktuna, M. Ozkan, Adaptive control of free-floating space manipulators using dynamically equivalent manipulator model, Robotics and Autonomous Systems 46(3) (2004) 185–193.

[115] M. Pastell, H. Takko, H. Grohn, M. Hautala, V. Poikalainen, J. Praks, I. Veermae, M. Kujala, J. Ahokas, Assessing cows welfare: weighing the cow in a milking robot Biosystems Engineering, 93 (2005) 81-87.

[116] P. Pepe, Z.P. Jiang, A Lyapunov-Krasovskii methodology for ISS and iISS of time-delay systems, Systems & Control Letters 55(12) (2006) 1006-1014.

[117] Q.C. Pham and J.J.E. Slotine, Stable concurrent synchronization in dynamic system networks, Neural Networks 20(1) (2007) 62–77.

[118] K. Pfeiffer, M. Bengel and A. Bubeck, Offshore robotics - Survey, implementation, outlook,in: Proc. Conf. Intelligent Robots and Systems, 2011, pp. 241–246.

[119] W. Ren, R.W. Beard and E. Atkins, Information consensus in multivehicle cooperative control: collective group behavior through local interaction, IEEE Control Systems Magazine 27(2) (2007) 71-82.

[120] M. Reyhanoglu, A.J. van der Schaft, N.H. McClamroch, I. Kolmanovsky, Dynamics and control of a class of underactuated mechanical systems, IEEE Transactions on Automatic Control 44(9) (1999) 1663-1671.

[121] J.P. Richard, Time-delay systems: an overview of some recent advances and open problems, Automatica 39(10) (2003) 1667–1694.

[122] A. Rodriguez-Angeles and H. Nijmeijer, Mutual synchronization of robots via estimated sate feedback: a cooperative approach, IEEE Trans. Control Systems Technology 12(4) (2004) 542–554.

[123] A.J. Scarfe, R.C. Flemmer, H.H. Bakker, C.L. Flemmer, Development of an autonomous kiwifruit picking robot, in: Proc. Conf. Autonomous Robots and Agents, 2009, pp. 380–384.

[124] C. Secchi, A. Franchi, H.H. Bulthoff, P.R. Giordano, Bilateral teleoperation of a group of UAVs with communication delays and switching topology, IEEE Conf. Robotics and Automation, 2012, pp. 4307–4314.

[125] A.I. Setiawan, T. Furukawa, A. Preston, A low-cost gripper for an apple picking robot, in: Proc. Conf. Robotics and Automation, 2004, pp. 4448–4453.

[126] A. Seuret, D.V. Dimarogonas, K.H. Johansson, Consensus under communication delays, in: Proc. Conf. IEEE Conf. Decision and Control, pp. 4922–4927, 2008.

[127] J.R. Silvester, Determinants of block matrices, The Mathematical Gazette 84(501) (2000) 460-467.

[128] E. Slawinki, V.A. Mut, J.F. Postigo, Teleoperation of Mobile Robots With Time-Varying Delay, IEEE Tran. Robotics 23(5) (2007) 1071–1082.

[129] D.C. Slaughter, D.K. Giles, D. Downey, Autonomous robotic weed control systems: A review, Computers and Electronics in Agriculture 61(1) (2008) 63–78,

[130] J.J.E. Slotine, W. Li, On the adaptive control of robot manipulators, International Journal of Robotics Research 6(3) (1987) 49-59.

[131] J.J.E. Slotine, W. Li, Adaptive manipulator control: A case study, IEEE Trans. Automatic Control 33(11) (1988) 995–1003.

[132] G. Stepan, Delay-Differential Equation Models for Machine Tool Chatter, Dynamics and Chaos in Manufacturing Process, F.C. Moon, (Ed.), New York, 1998, pp. 165-192.

[133] D. Story, M. Kacira, C. Kubota, A. Akoglu, L. An, Lettuce calcium deficiency detection with machine vision computed plant features in controlled environments, Computers and Electronics in Agriculture 74 (2010) 238–243.

[134] H. Su , G. Chen , X. Wang, Z. Lin, Adaptive second-order consensus of networked mobile agents with nonlinear dynamics, Automatica 47(2) (2011) 368–375.

[135] H.S. Wall, *Analytic Theory of Continued Fractions*, New York: Van Nostrand, 1948.

[136] W. Wang and J.J.E. Slotine, On partial contraction analysis for coupled nonlinear oscillators, Biological Cybernetics 92(1) (2005) 38–53.

[137] H. Wang, Y. Xie, Passivity based adaptive Jacobian tracking for free-floating space manipulators without using spacecraft acceleration, Automatica 45(6) (2009) 1510-1517.

[138] H. Wang, On the recursive adaptive control for free-floating space manipulators, Journal of Intelligent & Robotic Systems 66(4) (2012) 443-461.

[139] H. Wang, Passivity based synchronization for networked robotic systems with uncertain kinematics and dynamics, Automatica 49(3) (2013) 755–761.

[140] H. Wang, Task-Space Synchronization of Networked Robotic Systems With Uncertain Kinematics and Dynamics, IEEE Trans. Automatic Control 58(12) (2013) 3169–3174.

[141] H. Wang, Flocking of networked uncertain Euler-Lagrange systems on directed graphs, Automatica 49(9) (2013) 2774–2779.

[142] H. Wang, Consensus of networked mechanical systems with communication delays: A unified framework, IEEE Trans. Automatic Control 59(6) (2013) 1571–1576.

[143] L. Weiss, On the controllability of delay–differential equations, SIAM Journal of Control 5(4) (1967) 575-587.

[144] J.N Wilson, Guidance of agricultural vehicles a historical perspective, Computers and Electronics in Agriculture 25(12) (2000) 3-9.

[145] C.M. Wronka, M.W. Dunnigan, Derivation and analysis of a dynamic model of a robotic manipulator on a moving base, Robotics and Autonomous Systems 59(10) (2011) 758-769.

[146] C. Yang, Z. Li, J. Li, Trajectory Planning and Optimized Adaptive Control for a Class of Wheeled Inverted Pendulum Vehicle Models, IEEE Transactions on Cybernetics 43(1) (2013) 24–36.

[147] K. Youcef-Toumi, S. Reddy, Dynamic analysis anf control of high speed and high precision active magnetic bearings, ASME J. Dynamic Systems, Measurement and Control 14(4) (1992) 544-555.

[148] E. Zergeroglu, D.M. Dawson, I. Walker, and P. Setlur, Nonlinear tracking control of kinematically redundant robot manipulators, IEEE/ASME Trans. Mechatronics 9(1) (2004) 129–132.

[149] D.A. Zhao, J. Lv, W. Ji, Y. Zhang, Y. Chen, Design and control of an apple harvesting robot, Biosystems Engineering 110(2) (2011) 112–122.

[150] G. Zhong, Y. Kobayashi, Y. Hoshino, T. Emaru, System modeling and tracking control of mobile manipulator subjected to dynamic interaction and uncertainty, Nonlinear Dynamics 73(1-2) (2013) 167-182.

[151] R.B. Zmood, The euclidean space controllability of control systems with delay, SIAM Journal Control 12 (1974) 609-623